UNIVERSITAT DE BARCELONA

Development and application of *in-vitro* assays for the study of the biological activity of pharmaceutical products

Mariona Cañellas Santos

UNIVERSITAT DE BARCELONA

FACULTAT DE FARMÀCIA I CIÈNCIES DE L'ALIMENTACIÓ

Development and application of *in-vitro* assays for the study of the biological activity of pharmaceutical products

Mariona Cañellas Santos

Biotechnology Ph.D. program of Universitat de Barcelona

July 2022

FACULTAT DE FARMÀCIA I CIÈNCIES DE L'ALIMENTACIÓ

DOCTORAT EN BIOTECNOLOGIA

Development and application of *in-vitro* assays for the study of the biological activity of pharmaceutical products

Memòria presentada per Mariona Cañellas Santos per optar al títol de doctor per la universitat de Barcelona

Treball realitzat sota la direcció de la doctora Elisabet Rosell i Vives i del doctor Carlos Julián Ciudad Gómez

Elisabet Rosell i Vives
Directora

Carlos Julián Ciudad Gómez
Director / Tutor

Mariona Cañellas Santos
Setembre 2022

Aquest projecte d'investigació s'ha elaborat en col·laboració amb l'empresa Laboratorios Reig Jofre en el pla de doctorats industrials, convocatòria DI 2018.

Responsable del projecte en la empresa: Alicia Ortega Bonet

AGRAÏMENTS

Aquesta tesi doctoral s'ha realitzat gràcies al finançament de les següents institucions i empreses:

- Ajut de Doctorat Industrial concedit per l'Agència de Gestió d'Ajuts Universitaris i de Recerca (AGAUR) del Departament d'Empresa i Coneixement de la Generalitat de Catalunya (2018 DI 072)
- Departament d'Innovació, Universitats i Empresa de la Generalitat de Catalunya
- Laboratorios Reig Jofre, Sant Joan Despí, Barcelona
- Universitat de Barcelona

Vull començar donant les gràcies a totes aquelles persones que han fet possible el desenvolupament d'aquest projecte de doctorat industrial entre Reig Jofre i la Universitat de Barcelona. Aquesta experiència m'ha servit per créixer personalment i laboralment, i estic molt agraïda a tota la gent que ha fet possible que gaudís d'aquesta oportunitat.

A la Dra. Elisabet Rossell, et vull agrair molt especialment la oportunitat que em vas donar, ja des del moment de les pràctiques del màster, per començar en aquest projecte. Moltes gràcies també pel teu suport i ajuda durant aquests anys, aconsellant-me sempre tant encertadament, tant en la tesi com en altres aspectes de la meva experiència a Reig.

Al Dr. Carles Ciudad, moltíssimes gràcies per tota l'ajuda que m'has donat durant el desenvolupament de la tesi. Has fet que tot fos molt fàcil tot i les dificultats que suposa conciliar entre universitat i empresa durant un doctorat industrial. M'has ajudat sempre que ho he necessitat, m'has donat bons consells i tu, juntament amb la resta de membres del grup, m'heu fet sentir com una més sempre que he vingut a la UB, tot i haver passat poc temps al laboratori.

A tots els meus companys que han anat passant pel laboratori durant els últims 5 anys, us vull donar les gràcies per fer que aquesta experiència fos molt més fàcil, ajudant-me amb la feina sempre que ho he necessitat i compartint xerrades i riures que han fet que els moments durs ho fossin menys.

A la resta de persones de Reig Jofre amb qui he tingut la oportunitat de treballar durant aquest temps, moltes gràcies per tot el que m'heu ensenyat i totes les eines que m'heu donat per poder enfrontar-me millor a futurs reptes.

Ana i Esther, durant els últims anys hem tingut moments de veure'ns més i de veure'ns menys, però sempre hi heu sigut, disposades a buscar temps per una caminada acompanyada d'una conversa llarga, una cervesa/xampú/vermut o, fins i tot, quan han quadrat les nostres ocupades agendes, un viatge. M'ha anat molt bé comptar amb vosaltres per estones de desconnexió i riures durant aquests anys.

Marina, Miki, Marta, Mariona, Carla, Josep i Adri, heu estat la meva alegria dels dijous. Des de que ens vam trobar ja fa 9 anys, els nostres sopars, escapades pels diferents punts de la geografia catalana, i fins i tot, algun viatget una mica més lluny, han sigut un gran suport emocional. Començant per la carrera i acabant pel doctorat, sense vosaltres tot això hagués sigut molt més dur. Moltes gràcies!

Mercè i Júlies, sou la millor recompensa que m'emporto de la decisió que vaig prendre fa anys d'apuntar-me a castells. Tot i que cap de les quatre siguem especialment conegudes per suar camisa, des d'aquell moment sé que puc comptar amb vosaltres. En els últims anys hem tingut moments d'estar més repartides pel món, però tot i això, mai han faltat ni moments ni excuses per trobar-nos, sempre a punt per comentar un bon cotilleo, per donar els millors consells a les altres o simplement per ajudar-nos a desconnectar. Moltes gràcies per tot!

Avi, Padrina, moltes gràcies pel vostre suport durant la tesi, pel vostre amor incondicional i per ser els meus models a seguir. Jo de gran vull ser com vosaltres! Gràcies per ensenyar-me que sempre és bon moment per seguir fent el que a un li agrada, que l'edat és només un número i per fer que tothom em recordi sempre la bona genètica que tinc. És un orgull poder presumir d'avis allà on vaig.

Àvia, no podràs llegir això però igualment vull donar-te les gràcies per tots els anys que vam poder gaudir de tu. Estic segura que t'hauria agradat acompanyar-me durant la tesi i vull dir-te que t'he trobat a faltar. Una abraçada molt gran allà on siguis.

Papes, moltes gràcies per ser-hi sempre, per estar disposats a ajudar-me sempre fent-m'ho tot més fàcil, per aguantar totes els meus drames i moments d'estrès, per no deixar-me anar mai de la mà i per lluitar sempre al meu costat. Es una sort tenir-vos i saber que mai estaré sola perquè sempre us tindré amb mi.

Joana, ets la persona amb la qui més he compartit i amb la que sé que sempre puc comptar. Una estona amb tu em serveix per arreglar gairebé qualsevol problema. Gràcies pels riures, per ser frikis juntes, pels nostres jocs que ningú no entén i pels nostres atacs de bogeria després de

menjar. Ets la millor germana que em podria haver tocat. Núria, moltes gràcies a tu també per fer-la tant feliç i per convertir-te en una més de la família. Moltes gràcies a les dues per les estones que hem compartit. Maya, gràcies per ser la meva nebodeta de 4 potes i treure'm a passejar de tant en tant.

Per últim, Víctor, segurament ets la persona que ha patit més aquesta tesi després de mi. Moltes gràcies per tot el suport i els ànims que mai m'han faltat en els moments durs. Moltes gràcies també per la paciència, per escoltar-me sempre que ho he necessitat i per aguantar-me en moments en que no m'aguantava ni jo. Moltes gràcies per demostrar-me sempre que soc important i que puc comptar amb tu. Vull enfrontar-me a tots els reptes i viure totes les aventures al teu costat.

Us estimo molt a tots!

Mariona

SUMMARY

This industrial Ph.D. thesis aimed to illustrate the presence of the cell-based bioassays throughout the whole life of a drug product and to demonstrate its importance for a complete characterization of a pharmaceutical product, ensuring its quality, effectiveness, and safety. To do so, the assays performed for the analysis of three different products under study in Reig Jofre were analysed to illustrate the importance of this assays to guarantee the obtention of high-quality products in the pharmaceutical industry.

In the first place, the candidates to be used as active ingredients for a cream to treat acne outbreaks were analysed. The first step taken was to characterize the impact of an infection produced by heat inactivated *Cutibacterium acnes*, associated with acne, in the HaCaT cell line. To do so, the modification of the expression of the toll like receptors 2 and 4, and the inflammatory response caused in response to the activation of these two receptors in the infection, were evaluated. After that, the anti-inflammatory capacity of a *Camellia sinensis* plant extract, a *Morinda citrifolia* plant extract and a combination of both, achieving a reduction of the inflammatory response caused by *Cutibacterium acnes*, was illustrated.

In the second place, different analysis for the demonstration of biosimilarity and for the evaluation of the potency of a new thrombopoietin receptor agonist biosimilar, under development at Reig Jofre, for the treatment of immune thrombocytopenia were performed. The first thing done was to demonstrate equivalent receptor binding between the reference material product and the biosimilar to the thrombopoietin receptor, using a biacore analysis. The second step performed was to develop two assays for the evaluation of the potency of the thrombopoietin receptor agonist biosimilar based on two modified cell lines to overexpress in their membranes the thrombopoietin receptor. All the assays performed for the demonstration of the adequate responsiveness of the cell line to the stimulation with the biosimilar, the steps taken for the optimization process of the two bioassays and the validation exercises for the demonstration of adequate linearity, precision, accuracy, selectivity, and robustness of the two developed assays are presented in this industrial Ph.D. thesis. The bioassays developed have been used for the demonstration of biosimilarity of the new Reig Jofre product, for the demonstration of batch-to-batch equivalency and of the stability of the product and for the evaluation of the impact of manufacturing modifications in the final product obtained.

Finally, the cytotoxicity produced by a cream for scabies treatment, based on disulfiram and benzyl benzoate as active ingredients, which is already in the marked, was characterized,

illustrating the importance of continuing evaluating the products after their launching to the marked to gain new information, which may be useful to find new possibilities for the product. For the characterization of the cytotoxicity occurring after the application of the treatment, a cytotoxicity assay was performed to evaluate the effect of the different cream components on HEK001, a keratinocytes cell line, and, after that, a microarray analysis was performed to provided information on the cellular signalling pathways affected after the 24 h treatment with the cream.

Altogether, the analysis presented for the evaluation of different drug products' biological activities at different stages of the drug development process illustrate the essentiality of this kind of assays to ensure the production of high-quality products for patients' treatment.

INDEX

ABREVIATIONS LIST

- 4PL: 4-parameter logistic model
- AC: agarose conjugate
- ADME: absorption, distribution, metabolism, and excretion
- ADP: adenosine diphosphate
- αhIgG(Fc): anti-human Fc immunoglobulin G
- BB: benzyl benzoate
- BCL2: B-cell lymphoma 2
- BSA: bovine serum albumin
- BVES: blood Vessel Epicardial Substance
- C: *Camellia sinensis* extract
- *C. acnes*: *Cutibacterium acnes*
- cAMP: cyclic adenosine monophosphate
- CCK8: cell counting kit 8
- CD: cluster of differentiation
- cDNA: complementary desoxyribonucleic acid
- C:Q (1:1): *Camellia sinensis* extract / *Morinda citrifolia* extract ratio 1:1
- CTD: common technical document
- CXCL1: chemokine ligand 1
- DAPI: 4',6-diamidino-2-phenylindole
- D: disulfiram
- DNA: desoxyribonucleic acid
- DP: drug product
- DS: drug substance
- DTT: dithiothreitol
- EC_{50}: half maximal effective concentration
- ECM: extracellular matrix
- EGF: epidermal growth factor
- EMA: European medicines agency
- EPO: erythropoietin
- FBS: fetal bovine serum
- Fc region: fragment crystallizable region
- FDA: Food and Drug Administration
- GABA: gamma-aminobutyric acid

- GM-CSF: granulocyte-macrophage colony-stimulating factor
- GMP: good manufacturing practices
- GP: glycoprotein
- hEGF: human epidermal growth factor
- HEK001: human epidermal keratinocyte 001
- hMPL: human MPL
- HSC: hematopoietic stem cells
- ICH: international council for harmonization
- IgG: immunoglobulin G
- Iκβ: inhibitor of nuclear factor kappa-beta
- IKK: inhibitor of nuclear factor kappa-beta kinase
- IL: interleukin
- IRAK: Interleukin-1 receptor-associated kinase 1
- ITP: immune thrombocytopenia
- JAK: janus kinase
- KSFM: keratinocytes serum free medium
- Luc: Luciferase
- mAb: monoclonal antibody
- MAL: myelin and lymphocyte
- MAP: mitogen-activated protein
- MAPK: mitogen-activated protein kinase
- MCB: master cell bank
- ICH: international council for harmonization
- mRNA: messenger ribonucleic acid
- MW: molecular weight
- MyD88: myeloid differentiation primary response 88
- NADP: nicotinamide adenine dinucleotide phosphate
- NADPH: reduced nicotinamide adenine dinucleotide phosphate
- NF-κβ: nuclear factor kappa-light-chain-enhancer of activated B cells
- OD: optical density
- PAMP: pathogen associated molecular pattern
- PBS: phosphate-buffered saline
- PCNA: proliferating cell nuclear antigen
- PDGF: platelet-derived growth factor
- PE: phycoerythrin

- PEG-rHuMGDF: pegylated megakaryocyte growth and development factor
- PFA: paraformaldehyde
- PI3K: phosphoinositide 3-kinase
- PI(3,5)P2: phosphatidylinositol 3,5-bisphosphate
- PIC/S: pharmaceutical inspection and co-operation scheme
- PMDA: pharmaceutical and medical devices agency
- RQ: relative quantification
- PRR: pattern recognition receptor
- Q: *Morinda citrifolia* extract
- qPCR: quantitative polymerase chain reaction
- q.s.: quantum sufficit (as much as suffices)
- RhTPO: recombinant human thrombopoietin
- RJF: Reig Jofre
- RLU: relative luminescence units
- RMP: reference material product
- RNA: ribonucleic acid
- RT-PCR: real time polymerase chain reaction
- RSD: relative standard deviation
- RT: room temperature
- Shc: SH2-containing domain
- SOP: system operator procedure
- SPR: surface plasmon resonance
- STAT: signal transducer and activator of transcription
- STAT5-RE: STAT5 response element
- TLR: toll like receptor
- TNFα: tumor necrosis factor alpha
- TPO: thrombopoietin
- TPO-RA: thrombopoietin receptor agonists
- TRAF6: TNF receptor associated factors 6
- TYK: tyrosine kinase
- WCB: working cell bank
- WST-8: water-soluble tetrazolium 8

1. GENERAL INTRODUCTION

1.1. INTRODUCTION TO THE PHARMACEUTICAL INDUSTRY

The pharmaceutical industry carries out activities for the discovery, development, production, and delivery to the market of drugs or other pharmaceutical products, useful for the diagnosis, cure, or mitigation of the symptomatology of the patients receiving these products. Additionally, pharmaceutical companies ensure determined quality standard for the products developed, guarantying its efficacy and safety.

Laboratories Reig Jofre, hereafter RJF, is one of the many pharmaceutical companies that compromise with the generation of high-quality pharmaceutical specialities for consumers.

1.1.1. REIG JOFRE LABORATORIES

The projects discussed in this dissertation have been developed under RJF initiative. RFJ is a Catalan pharmaceutical company that has been working in the pharmaceutical context since its foundation in 1929. Its business activities are focused on the development of pharmaceutical technologies, such as antibiotics and lyophilized injectables, which suppose the 48 % of its total sales, the development of specialty pharma care, focused on dermatology, osteoarticular and gynaecological health, representing the 29 % of its total sales, and the development of nutritional supplements for weight control, beauty, and stress & sleep disorders, among others, that represent the 23 % of its total sales. Apart from the production of pharmaceutical products of its own, RJF also offers specialized production services for third parties (1).

RJF accounts with more than 1,100 employees, distributed among its 4 production centres, 1 in Barcelona, 2 in Toledo and 1 in Malmo (Sweden), orientated to the distribution and manufacturing of the pharmaceutical products. Additionally, RJF directly sales to 7 countries and has more than 130 business partners around the globe, located in more than 70 countries (1).

During the last decade, RJF has shown special interest in its introduction to the development and manufacturing of biological products, which present growing positive perspectives in the future of medicine. Accordingly, the interest of the company in the development of methods for the characterization and evaluation of these new products has also expanded.

1.2. DEVELOPMENT PROCES OF A PHARMACEUTICAL PRODUCT

According to the definition provided by the food and drug administration, a **drug** is a product which is intended for use in the diagnosis, cure, mitigation, treatment, or prevention of disease. Additionally, FDA defines a **drug product** as the final dosage form of a pharmaceutical product, the **drug substance** as the active pharmaceutical ingredient in a drug product, and the **excipients** as the inactive ingredients associated with the drug substance in the drug product (2,3).

The journey for developing a new drug product and launching it into the market is typically long and challenging and requires a high investment of time and monetary costs. The average time required to get one pharmaceutical new product into the market is 12 years (4). Despite this, enormous differences can be observed depending on the therapeutic area (5). In terms of economic expenses, the average cost of getting a drug product into the market is around 1,000,000,000 € (6).

The drug development process can be divided in different stages which can be seen as a funnel with a huge number of compounds at the beginning, from which, luckily, one gets into the market (Figure 1) (7).

The steps generally included in a development process of a new pharmaceutical product are the following:

- **New medical need definition and target identification and validation:** the development of a new pharmaceutical entity starts when an unreasoned medical necessity is identified. After this, it is necessary to identify a molecular structure within the organism, which is important for the disease, known as target, and to demonstrate the capability of impacting on the disease outcome by the modulation of this target (8).

- **Hit discovery:** the second step is to identify compounds capable of interacting with the identified target. This process is usually performed by the evaluation of huge compound libraries, using high throughput screening (HTS) analysis techniques (9).

- **Assay development:** together with the hit discovery phase, it is important to develop an assay useful for determining the affinity of the candidate for the target and to tests the candidate's potency. Nowadays, most assays are based on stable cell lines which overexpress the molecule of interest for the candidates to interact with (10). During the initial phases of the development this assay is going to be used to identify the most

promising candidates and to test their evolution trough the different optimization steps, while in the most advanced steps in the drug development process and after the launching of the product to the market, this assay is going to be used to for the validation of new batches, for proving batch-to-batch consistency, for stability controls and for the evaluation of any changes produced on the manufacturing process.

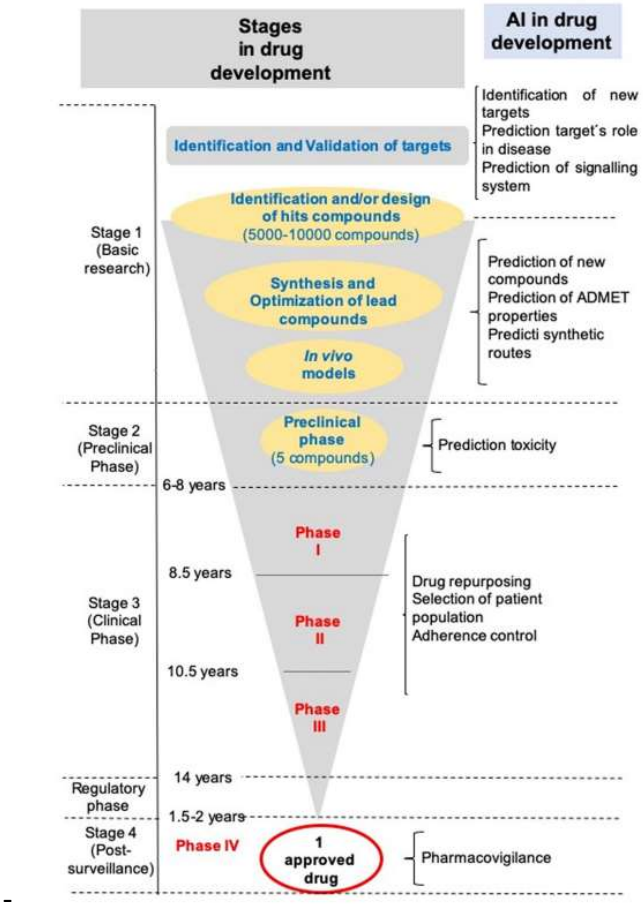

- *Figure 1: Drug development process* (7).

- **Hit to lead and lead optimization phases:** several steps are performed for the generation of the leads, which consist of the selection of the best compounds among all selected hits. Firstly, dose response curves are generated for each hit to select the ones with a best binding profile to the target. Secondly, an assay for the detection of the functional response of the best hits selected in the first step are performed. The hits identified as the most potent and selective are optimized to improve its absorption,

distribution, metabolism, and excretion (ADME) profile, for the generation of the leads (10). The optimization process continues for the leads obtained to improve their potency, specificity, selectivity, and safety characteristics. Additionally, the productivity and purification costs of the candidates are also evaluated for the selection of the best lead which will become the preclinical development candidate (11).

- **Preclinical drug development:** the preclinical development candidate is generally tested in a rodent and in a non-rodent species through different studies for the determination of the therapeutic window and for the evaluation of the toxicity of the new pharmacological candidate and its metabolites. Additionally, studies for the determination of genotoxicity and teratogenesis are also performed (9,10).

- **Clinical drug development:** If the candidates prove sufficient efficacy and safety during preclinical evaluation, authorization for starting clinical development is granted. The economic cost of failure once the clinical drug development phase is reached is huge. Because of this, it is important to develop good preclinical testing to fail fast and cheap. The phases included in clinical testing are the following:

    - **Phase I:** it is usually performed on a small group of healthy volunteers, and it is the first contact of the product with the human organism. Because of this, the main purposes of Phase I studies are the assessment of safety and the evaluation of the pharmacokinetic (ADME) and the pharmacodynamic profile of the product (8).
    - **Phase II:** it is performed in a small group of patients, and additionally to continue evaluating safety, the effectivity of the product is assessed (8).
    - **Phase III:** it is the last phase before the product commercialization, and it evaluates the safety and effectivity of the candidate in a large group of patients. It usually involves several hospitals of diverse geographical areas (8).
    - **Phase IV:** it occurs when the product gets to the market and it includes the whole population receiving the treatment, and it is used for continuing evaluating the safety of the product with a larger number of treated subjects (8).
    - **Pharmacovigilance:** is the discipline responsible to continue monitoring the less common adverse reactions, the interaction with other drugs, etc during the whole life of a pharmaceutical product (12).

- **Regulatory phase:** the developer of a new pharmaceutical candidate shall submit all the documentation regarding the new candidate to the corresponding authorities, from the identification of the medical need to phase III studies results. Among other documentation, all the information generated during de drug discovery and development process must be presented in a standardized form, the Common Technical Document (CTD) (Figure 2) (9).

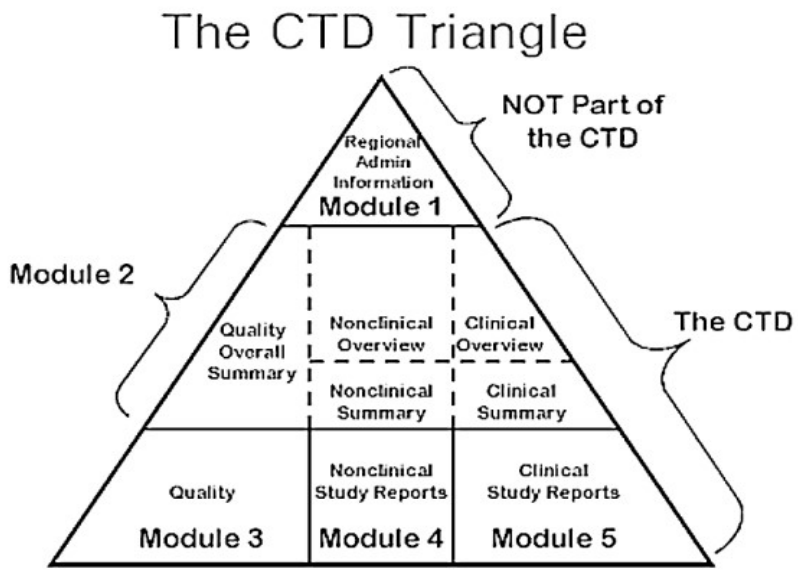

Figure 2: The Common Technical Document (9).

In parallel with the development and optimization of the new compound structure and its formulation, it is essential to develop adequate methodologies for the evaluation of this new pharmaceutical product, to be able to identify any change occurring in the product or in its functioning, which may have a critical impact in the quality. The information regarding all the assays to be performed to ensure the quality of the product under development must also be submitted to the registration organ.

Additionally, the manufacturing method of the product shall also be parametrically described and presented with the documentation required for the authorities. The impact of any change required in the production method should be reported and its impact in the quality of the final product must be evaluated.

1.2.1. Sources of new drug candidates

Regarding the sources of the molecules necessary for starting the drug development process, there are three main groups of compounds suitable to be used for the development of a new drug product. Those are:

- **Natural sources compounds**, which are compounds which have directly been obtained from nature, for example, from a biological source such as plants and microorganisms or from a mineral source (9). This type of products has been widely used historically and they have proven its effectiveness for the treatment of several medical conditions, as they present a great variability in terms of structure and mechanism of action. On the other hand, this kind of products are difficult to purify, and this makes its therapeutic range harder to determine (13), what limits their use in the development of new pharmaceuticals.

- **Small chemical molecules**, which are chemical synthesis compounds of typically less than 500 Daltons which are registered in libraries of molecules and that can be easily used for high throughput screening (13). The main disadvantage of this type of molecules is that they can interact with a limited number of biological processes, since most of these compounds interact with a reduced number of receptor families, including nuclear receptors, G-protein coupled receptors and ion channels (14).

- **Biologics**, which are biotechnological products synthesized in living cell through the modification of their complex natural metabolically pathways allowing the generation of new products, including recombinant proteins, hormones, monoclonal antibodies, gene therapies, cellular therapies, growth factors… (15,16) Biologics are large and complex molecules, what make their characterization highly difficult. Additionally, they usually are less stable than chemical drugs, which result in stricter monitorization requirements for their storage conditions. This, together with their complex manufacturing process, to which any small variation can result in a modification in the final product obtained, makes them very expensive products. On the other hand, biologics have demonstrated to be capable of affecting on biological processes considered “undruggable”, which offers promising perspective to new therapeutic opportunities (13).

1.2.2. Generics and Biosimilars

After the discovery of a new pharmaceutical product, designated as reference material, the discoverer has a time in which the product is protected by a patent or as intellectual property to recover the economic investment made during the process of development. After this period other laboratories can start to develop generics or biosimilars to the reference product, which is a cheaper and faster alternative to the development of a new drug product.

Generics are products formulated with the same active ingredients, but possibly with different excipients, as the reference material. To register a product as a generic to a pre-registered pharmaceutical formula, the posology and the specifications need to be equivalent to the ones for the reference material. The quality attributes required for generics are the same as for any other pharmaceutical products, but neither preclinical nor clinical studies are required, as the demonstration of bioequivalence for the generic product, together with the knowledge gained during the development of the reference material can be used for efficacy and safety verification (17).

Biosimilars are biotechnological products developed to present equivalent biological activity, efficacy, and safety to an original biological product. Despite this, the high complexity of biologics and its production process, make the exact replication of the reference product impossible. Because of this, even though the scientific knowledge generated during the reference product development can be used, biosimilars are controled under its own development process and full quality dossier is required for registration (18,19). A biosimilar is a biological product which, even though it might present minor differences related with its production process, is highly similar with a priorly authorized biological product in terms of composition, both for the active substance, efficacy, and safety (18,20).

Considering the high complexity of biologics and biosimilars, to prove biosimilarity, the generic approach, which only requires the demonstration of bioequivalence, that is the demonstration of equivalent availability of the product after administration, is not sufficient, and the demonstration of equivalent effect produced by the same dose is also required. Additionally, the demonstration of similarity in the manufacturing process is also desirable as, as mentioned before, changes occurring during the manufacturing or storage of a biological product may cause dramatic changes in the final product obtained. Finally, purity and impurities profiles of the biosimilar and the reference material should be compared, considering the specific degradation pathways and the post-transcriptional modifications specifically expected for the product. The

submission of a full quality dossier is required, and this should be supplemented with the demonstration of biosimilar comparability, where any differences identified shall be reported and properly justified (18,21).

1.2.3. Drug repositioning

Another alternative to the expensive process of new drug development is drug repositioning. Drug repositioning consists in rescuing existing pharmaceutical products or drug candidates that did not get to the market, for a different medical purpose (22). Even though most of the drug repositioning past achievements occurred serendipitously and without a strategy supporting them, nowadays, pharmaceutical companies may opt for this approach as it supposes a cheaper alternative to traditional drug development, and it presents a reduced risk of failure due to the existence of previous information regarding the drug substance itself and its possible adverse effects (23). It is also a good alternative for those pharmaceuticals with a patent expiration date near or already completed, as finding them a new medical use may allow the generation of a new patent, increasing the economic benefits obtained for that product.

1.3. CELL-BASED BIOASSAYS

With the increase of the complexity of the new molecules used for drug development, the necessity of developing assays capable of predicting the molecules mechanism of action also increased. Additionally, the aim of reducing the number of animals required for preclinical drug testing also observed an upward trend.

Cell-based bioassays allow for the determination of the biological activity elicited by a pharmaceutical product, mimicking the drugs mechanism of action within the organism if the adequate cell line is used, and they are a good alternative to the use of animals in the pharmaceutical industry. Cell-based bioassays have a greater variability that the traditional physicochemical techniques, as they use living organisms, the cell, as reagents, but they offer as advantage that they provide essential information about the effect that a drug will have within the organism. This has special importance when talking about biologics and biosimilars, but cell-based bioassays can also provide useful information about the mechanism of action and the adverse effects associated with chemical synthesis products.

In this dissertation, the importance of cell-based bioassays in the whole life of a drug product is evidenced through the analysis of the information provided by this kind of assays for three products of RJF that are in different stages of a pharmaceutical product life. Cell-based assays can be used for:

- The **characterization of new candidates** during the drug development for the selection of those with the most desirable characteristics for the final product. This is exemplified in chapter 1, were the anti-inflammatory characteristics of different plant extract candidates for the development of an anti-acneic cream are evaluated.

- The **assessment of the required quality attributes** of a manufactured drug product, both during development and after the commercialization of the product. During drug development, cell-based bioassays can be used for the comparison of different formulation option, for the determination of the product's stability and for the verification of the manufacturing method suitability and the evaluation of the impact of any modification occurring in it. After commercialization, cell-based bioassays are used for the demonstration of batch-to-batch consistency and for the confirmation of the product's stability during its whole self-life (9). This is exemplified in chapter 2, were two cell-based bioassays for the evaluation of the potency of a biosimilar product are developed.

- The **generation of new information about drugs already in the market** for the prediction of non-expected adverse effects or for drug repositioning. This is exemplified in chapter 3, were the mechanisms of cytotoxicity of an already commercial cream for the treatment of scabies are evaluated in perspective of a possible future market expansion or drug repositioning.

1.4. REGULATORY FRAMEWORK

One of the most critical aspects of the drug development process is the insurance of quality and safety to be maintained through the whole development and production process, as medical products are first necessity products that can be used to heal the organism but that may also be subject to severe adverse effects if not properly controlled. To guaranty the patients' safety, all the processes occurring in a pharmaceutical industry are highly regulated.

After the thalidomide tragedy in 1960-1961, the evidence of the necessity for the establishment of properly defined regulatory requirements for proper drug products testing before those to be launched to the market. The Good Manufacturing Practices (GMP) are a compendium of requirements, that were firstly proposed by the government of the United States in 1963, which establish the essentials for the production, packaging, and distribution of medicines and medical products, and define the minimum requirements in terms of safety, physicochemical and biological activity qualities for the products (24,25).

According to GMPs, all the procedures required for the production and the assessment of the quality of the pharmaceutical products must be parametrically defined in system operator procedures (SOPs), which must have been defined during the product's development process, together with the acceptance criteria limits for every step. Additionally, every task performed must be traceable, ensuring that every step is registered for its revision in the future. The personnel responsible for carrying on any procedure must be correctly qualified according to its position. The equipment required for the performance of the manufacturing and the testing of the products must be qualified and calibrated, and the personnel must be provided with proper personal protection equipment. The existence of risk management documentation is also essential. All the procedures and documentation generated shall be closely monitored by the quality assurance department of the company, which has as main responsibilities the insurance of the GMP compliance in all company's areas and the application of preventive and correction actions in case of any deviation being detected (24,25).

All these requirements ensure the production of high-quality manufacturing products, and therefore, GMP compliance shall be seen as an insurance for the maintenance of patients' health and the prevention of future litigations for the company, instead of seeing it as a regulatory burden.

GMP compliance is essential for the production and commercialization of pharmaceuticals in the main markets around the globe, the compliance of the demanded regulatory requirements is controlled by multiple agencies, including the European Medicines Agency (EMA), the United Kingdom Medicines and Health Care Products regulatory agency (MHRA), Pharmaceutical Inspection and Co-operation Scheme (PIC/S), the United States Food and Drug Administration (FDA) and the Japanese Pharmaceutical and Medical Devices Agency (PMDA).

Considering the elevated number of agencies controlling the compliance of the regulatory requirements for pharmaceutical industry, and harmonization of the it became necessary to

prevent de request of duplicated studies and to facilitate pharmaceuticals access to more than one market. The unification of the regulatory requirements was defined and compiled during the International Council for Harmonization of Technical Requirements for Pharmaceuticals for Human Use (ICH) (26).

As the GMPs and ICHs evolve for the inclusion of the most advanced medicines and medical products, it is important to be updated to the most recent version of the guidelines to ensure the adequate compliance of the requirements.

2. OBJECTIVES

This industrial Ph.D. thesis aimed to demonstrate the importance of cell-based bioassays in the pharmaceutical industry, and that they have a crucial role in all the parts of a pharmaceutical product self-life.

This main objective was achieved through the analysis of the cell-based assays performed on three RJF products, found in different stages of the drug development process, which were used as an example of the importance of cell-based bioassays in the pharmaceutical industry. The specific objectives for the characterization of the different products were:

- To analyse the effect of an infection with inactivated *C. acnes* on the HaCaT cell line and evaluate the anti-inflammatory profile of a *Camellia sinensis* and a *Morinda citrifolia* plant extracts and of a combination of both, to study their potential as active ingredients of a cream for acne treatment.

- To develop and validate two potency assays, one based on a proliferation assay for the determination of the late response, and one based on a reporter gene assay for the determination of the early response, for the assessment of the potency of a TPO-RA biosimilar being developed in RJF.

- To characterize the cytotoxic response elicited in the skin by the treatment with an already commercial disulfiram / benzyl benzoate cream.

3. MATERIALS

The reagents used in the realization of the different analysis described in this industrial Ph.D. thesis are summarized in Table 1.

Table 1: Reagents.

Reagent	Reference	Brand	Use
DMEM High Glucose	11500596	Fisher Scientific, Hampton, USA	Cell culture
RPMI 1640 Medium, Glutamax Supplement	12027599	Fisher Scientific, Hampton, USA	Cell culture
Keratinocyte Serum Free Medium	11510366	Fisher Scientific, Hampton, USA	Cell culture
FBS Heat inactivated.	11550356	Fisher Scientific, Hampton, USA	Cell culture
Penicillin / Streptomycin	11548876	Fisher Scientific, Hampton, USA	Cell culture
Sodium Pyruvate	12539059	Fisher Scientific, Hampton, USA	Cell culture
IL-3	10670154	Fisher Scientific, Hampton, USA	Cell culture
GM-CSF	215-GM-010	R&D Systems, Minneapolis, USA	Cell culture
Puromycin	A1113803	ThermoFisher, Waltham, USA	Cell culture
Blasticidin S	12172530	Fisher Scientific, Hampton, USA	Cell culture

Reagent	Reference	Brand	Use
Hygromycin B	10453982	Fisher Scientific, Hampton, USA	Cell culture
Human Recombinant Epidermal Growth Factor (EGF 1-53)	10134762	Fisher Scientific, Hampton, USA	Cell culture
Glutamax	11574466	Fisher Scientific, Hampton, USA	Cell culture
Trypsin-EDTA 0.25%	11580626	Fisher Scientific, Hampton, USA	Cell culture
Trypan blue	11538886	Fisher Scientific, Hampton, USA	Cell culture
PBS pH 7.4	11503387	Fisher Scientific, Hampton, USA	General use
Cultibacterium acnes	0170L	TISELAB, Cornella de Llobregat, Spain	Cell treatment
Benzil Benzoate	Kingly gifted by Bioglan AB (Malmö, Sweden)		Cell treatment
Disulfiram	Kingly gifted by Bioglan AB (Malmö, Sweden)		Cell treatment
D / BB cream	Kingly gifted by Bioglan AB (Malmö, Sweden)		Cell treatment
Cell Counting Kit-8	96992-19	Sigma-Aldrich, Sant Louis, USA	Cytotoxicity / Proliferation assay
Rneasy Mini Kit	74104	WERFEN, Barcelona, Spain	qPCR
iScript RT-PCR Supermix 100	170-8841	Bio-Rad, Hercules, USA	qPCR

Reagent	Reference	Brand	Use
LightCycler 480 Probes Master	4887301001	Roche, Basel, Switzerland	qPCR
Nucelase Free Water	J71786	Fisher Scientific, Hampton, USA	qPCR
Hs00174103_m1 (IL-8) Hs00174128_m1 (TNFα) Hs00174131_m1 (IL6) Hs00236937_m1 (CXCL1) Hs02786624_g1 (GADPH)	4331182	ThermoFisher, Waltham, USA	qPCR
Antibody anti-TLR2	565349	Becton Dickenson, Franklin Lakes, USA	Flow cytometry
Antibody anti-TLR4	564251	Becton Dickenson, Franklin Lakes, USA	Flow cytometry
Anti-CD110 antibody	562416	Becton Dickenson, Franklin Lakes, USA	Flow cytometry
PE Mouse IgG1, κ Isotype Control	554680	Becton Dickenson, Franklin Lakes, USA	Flow cytometry
Anti-IgG2b antibody (isotype control)	562305	Becton Dickenson, Franklin Lakes, USA	Flow cytometry
DAPI solution 1 mg / mL	62248	ThermoFisher, Waltham, USA	Flow cytometry / NF-κβ Translocation assay
BSA Fraction V IgG Free	15755993	Fisher Scientific, Hampton, USA	Flow cytometry / NF-κβ Translocation assay
16% Formaldehyde (w/v), Methanol-free	11586711	Fisher Scientific, Hampton, USA	NF-κβ Translocation assay
Triton™ X-100	T8787	Sigma-Aldrich, Sant Louis, USA	NF-κβ Translocation assay
Tween-20	P2287	Sigma-Aldrich, Sant Louis, USA	NF-κβ Translocation assay / Western blot

Reagent	Reference	Brand	Use
Anti-NFκB p65 Antibody (F-6) Alexa Fluor® 488	sc-8008 AF488	Santa Cruz Biotechnology, Inc., Dallas, USA	NF-κβ Translocation assay
Biacore amine coupling kit	BR100050	GE-Healthcare, Uppsala, Sweden	Biacore
Biacore CM5 optical sensor chip	BR100012	GE-Healthcare, Uppsala, Sweden	Biacore
Biacore human antibody caprure kit	BR100893	GE-Healthcare, Uppsala, Sweden	Biacore
Lysis Buffer	87787	ThermoFisher, Waltham, USA	Western blot
Phosphatase and protease inhibitor	78442	ThermoFisher, Waltham, USA	Western blot
Anti-STAT5 (A-9) AC antibody	sc-74442-AC	Santa Cruz Biotechnology, Inc., Dallas, USA	Western blot
Sample Buffer	1610747	Bio-Rad, Hercules, USA	Western blot
DTT	646563	Sigma-Aldrich, Sant Louis, USA	Western blot
4–15% Mini-PROTEAN® TGX™ Precast Protein Gels	4561083	Bio-Rad, Hercules, USA	Western blot
Running Buffer	LC2675	ThermoFisher, Waltham, USA	Western blot
Nitrocellulose Blotting Membrane	GE10600001	Sigma-Aldrich, Sant Louis, USA	Western blot
Transfer Buffer	LC3675	ThermoFisher, Waltham, USA	Western blot

Reagent	Reference	Brand	Use
Antibody anti-STAT5	sc-74442	Santa Cruz Biotechnology, Inc., Dallas, USA	Western blot
Antibody anti-p-TYR	sc-508	Santa Cruz Biotechnology, Inc., Dallas, USA	Western blot
Antibody anti-α-tubulin	T8203	Sigma-Aldrich, Sant Louis, USA	Western blot
Antibody Anti-Mouse IgG (γ-chain specific) − Alkaline Phosphatase	A3438	Sigma-Aldrich, Sant Louis, USA	Western blot
Novex AP Chromogenic Substrate (BCIP/NBT)	WP20001	Invitrogen, Waltham, USA	Western blot
Bio-Glo™ Luciferase Assay System	G7940	Promega, Madison, USA	Reporter gene assay
Cell Titer Glo®	G7570	Promega, Madison, USA	Cytotoxicity assay

The equipment used in the realization of the different analysis described in this industrial Ph.D. thesis are summarized in Table 2.

Table 2: Equipment.

Equipment	Brand	Use
Biological safety cabinet Bio II Advance	Azvil Telstar, S.L.U., Terrassa, Spain	General Use
CO_2 incubator	ThermoFisher, Waltham, USA	General Use
Thermostatic bath	VWR International, Radnor, USA	General Use
Inverted Microscope	ThermoFisher, Waltham, USA	General Use
Centrifuge	VWR International, Radnor, USA	General Use
Gallios Cytometer	Beckman Coulter, Brea, USA	Flow cytometry
Victor 2030	Perkin Elmer, Waltham, USA	Cytotoxicity / Potency assays
Lightcycler 480®	Roche, Basel, Switzerland	qPCR
NanoDrop Lite	ThermoFisher, Waltham, USA	qPCR / immunoprecipitation / micorarrays
PxE Thermal Cycler	ThermoFisher, Waltham, USA	qPCR / microarrays
Spectral confocal microscope Leica TCS-SPE	Leica Microsystems, Wetzlar, Germany	NF-κβ Translocation assay
ChemiDoc ™ MP Imaging System	Bio-Rad, Hercules, USA	Western Blot

4. METHODS

4.1. CELL LINES

4.1.1. HaCaT

The transformed immortal keratinocyte HaCaT cell line was kindly gifted by the Department of Biochemistry and Molecular Biomedicine of the Faculty of Biology of the Universitat de Barcelona. A cell bank was generated and maintained in liquid nitrogen at the RJF facilities. The bank was tested against mycoplasma and other microorganisms.

After thawing, the cells were cultured for two weeks before to its use, to guarantee the integrity of the cells and their correct growth. The cells were grown in monolayer on solid support, at 37ºC in a humified atmosphere with 5 % CO_2, and maintained in DMEM media supplemented with 10 % FBS and 1 % Penicillin / Streptomycin antibiotic, from here HaCaT medium.

4.1.2. BA/F3-hMPL

4.1.2.1. Cell line development

The cell line development was outsourced to GenScript, a biotechnological company with high experience in developing recombinant stable cell lines using its platform of lentiviral-based expression cassette.

The first step taken for GenScript was the subcloning of the target gene, the human thrombopoietin receptor gene, into Lenti-EF1a-puro vector, property of GenScript. This vector uses EF1 promoter as the target for the hMPL gene insertion and includes puromycin resistance gen for cell selection after transfection. After that, the plasmid vector was subcloned into a lentivirus.

In the second place, the viral vector generated was used for the Ba/F3 cell line infection. The resulting cell line, named BA/F3-hMPL, grew in selective medium with puromycin and under the stimulation of the cytokine IL3 and expressed in its membrane the receptor of human thrombopoietin.

To ensure the generation of a fully transduced population of cells the cell pools produced were screened with puromycin. The single-cell-derived stable clones were obtained by limiting dilution. After that, the target gene expression in the resulting stable pool cells was determined by qPCR. Based on the hMPL gene sequence (see ANNEX I) the following Forward and Reverse primers were designed:

- Forward primer → CCCAAGAACTCCACTGGTCC
- Reverse primer → TGCTTTGGTCCATCTTGCCA

For the performance of the qPCR, for each reaction, 10 µL of SYBER Green, 0.8 µL of forward primer at 10 µM, 0.8 µL of reverse primer at 10 µM, 0.4 µL of ROX Dye, 4 µL of DNA template and 4 µL of Mili-Q water were used. After the preparation of the samples, 40 cycles of increasing the temperature to 95ºC for denaturation of the two strands of DNA, decreasing the temperature to 60ºC for annealing of the primers to the template, and increasing it to 72ºC for the elongation of the primers, were performed. Fluorescence signals were acquired for the quantification of hMPL expression.

The two best clones obtained, based on receptor expression levels, were selected. Two cryovials containing 1 x 10^7 cells for each clone and supplied to RJF.

4.1.2.2. Thawing and maintenance

For cell expansion, a cells cryovial was thawed with thawing medium, consisting of RPMI media supplemented with 10 % FBS, 1 % Sodium Pyruvate and 3 ng / mL IL-3. The cells were maintained in culture, not exceeding passage 30, and were generally subcultured three times a week. After thawing, the complete medium supplemented with the selection antibiotic was used. The compete medium consisted of RPMI media supplemented with 10 % FBS, 1 % Sodium Pyruvate, 3 ng / mL IL-3 and 1.5 ng / mL Puromycin.

For the performance of the assays, the selection antibiotic and the growth factor IL-3 were eliminated from the media was performed, as it could have an interference in the assays results.

4.1.2.3. Master Cell Bank and Working Cell Bank establishment

When developing a cell-based assay to evaluate any of the parameters required to ensure the quality of a pharmaceutical product it is important to ensure enough cell availability to cover the complete self-life of the product (27). To guarantee this, after the reception of the two clones provided by GenScript, one cryovial of each clone was thawed, maintained, and expanded under defined conditions to passage 14. Then, the cells were preserved in multiple cryovials to generate the Master Cell Bank. After the generation of the MCBs, one cryovial of each clone was thawed, maintained, and expanded under defined conditions to passage 18. Then the cells were preserved in multiple cryovials to generate the Working Cell Bank.

After the establishment of the MCBs and the WCBs at RJF, the cell banks were characterised to ensure absence of mycoplasma, sterility, viability after freezing and the expression of the receptor of interest. Every time that a new WCB was required a comparison of it with the WCB in use was made in addition to the characterization of the bank.

The MCB ensures the availability of cell through the whole self-life of the product, while the WCB is the one used for the performance of the assays.

4.1.3. TF1 - Stat5 - Luc 2P – TPO-R

4.1.3.1. Cell line development

The cell line development was outsourced to Promega, a specialized manufacturer of multiple biotechnological products and with experience in the field of development of recombinant stable cell lines.

The first step taken for Promega was the introduction of its already developed transfection vector based on Luc2P/STAT5-RE/Hygro in the TF-1 cell line. The resulting cell line expressed the Luciferase reporter gene under the regulation of STAT5 promoter. For the selection of those cells which had successfully incorporated the vector the selection antibiotic hygromycin was used.

Secondly, Promega developed an expression vector encoding for the TPO receptor together with the gen of resistance to blasticidin and used it for the transfection of TF-1 cells stably expressing STAT5-Luc2P reporter gene.

The resulting cell line, named TF1 - Stat5 - Luc 2P - TPOR, grow in selective medium with hygromycin and blasticidin and under the stimulation of the cytokine GM-CSF, and expresses in its membrane the receptor of human thrombopoietin.

To ensure the generation of a fully transduced population of cells, the cell pools produced were screened with blasticidin and hygromycin. The single-cell-derived stable clones were obtained by limiting dilution.

After the selection of the satisfactorily transfected clones, those were assessed in front of a thrombopoietin analogue to determine the induction of the STAT5-Luc2P reporter in response to TPO-R activation. The best two clones, based on relative luminescence units' induction, were selected, and delivered to RJF in form of two cryovials containing 1 x 10^7 cells for each clone.

4.1.3.2. Thawing and maintenance

For cell expansion, a cells cryovial was thawed with thawing medium, consisting of RPMI media supplemented with 10 % FBS and 2 ng / mL GM-CSF. The cells were maintained in culture, not exceeding passage 30, and were generally subcultured three times a week. After thawing, the complete medium supplemented with the selection antibiotics was used. The compete medium consisted of RPMI media supplemented with 10 % FBS, 2 ng / mL GM-CSF, 200 µg / mL hygromycin B and 10 µ g / mL blasticidin.

For the performance of the assays, the selection antibiotics, and the growth factor GM- CSF were eliminated from the medium, as it could have an interference in the assays results.

4.1.3.3. Master Cell Bank and Working Cell Bank establishment

To guarantee cell availability, after the reception of the two clones provided by Promega, one cryovial of each clone was thawed, maintained, and expanded under defined conditions to passage 13. Then, the cells were preserved in multiple cryovials to generate the Master Cell Bank. After the generation of the MCBs, one cryovial of each clone was thawed, maintained, and

expanded under defined conditions to passage 21. Then the cells were preserved in multiple cryovials to generate the Working Cell Bank.

After the establishment of the MCBs and the WCBs at RJF, the cell banks were characterised to ensure absence of mycoplasma, sterility, viability after freezing and the expression of the receptor of interest. Every time that a new WCB was required a comparison of it with the WCB in use was made in addition to the characterization of the bank.

4.1.4. HEK001

The HEK001 (human epidermal keratinocyte 001) cell line, obtained from ATCC®, CRL2404™, was used. A MCB and a posterior WCB were generated and maintained in liquid nitrogen at RJF before the beginning of the assays. The banks were tested against mycoplasma and other microorganisms for suitability control.

The cells were maintained for at least two weeks after the thawing of the WCB cryovials, before its use in the performance of any assays. The cells were maintained growing in monolayer on a solid support, at 37ºC in a humified atmosphere with 5 % CO_2 in KSFM supplemented with 1% Glutamax and 5 ng/ml hEGF.

4.2. CYTOTOXICITY ASSAY OF THE PLANT EXTRACTS ON HaCaT CELL LINE

24 hours before the assay, nine 96-well clear flat bottom culture treated polystyrene microplate were seeded with 10,000 HaCaT cells / well in 100 µL of medium, equivalent to half of the desired final volume for each well. Only the central 60 wells of the plates were used for the assay. The rest of the wells were filled with PBS. The plates were incubated at 37ºC in a humified atmosphere with 5 % CO_2.

The following day, cells were treated with the plant extracts. 3 plates were incubated with the *Camellia sinensis* extract (C), 3 plates were incubated with the *Morinda citrifolia* extract (Q) and 3 plates were incubated with a preparation consisting in a Ratio 1:1 of the two extracts (C:Q (1:1)). 10 concentrations of the corresponding extract were assessed in each plate in sextuplicate. The concentrations tested were the following: 2.000, 1.500, 1.000, 0.750, 0.500, 0.250, 0.125, 0.063, 0.031 and 0.000 %. The dilutions were prepared at twice the desired

concentration and the same volume used to seed the cells was loaded into the plates, thereby making a ½ dilution on the plate. After treatment, the plates were incubated for 24 h at 37ºC in humidified atmosphere with 5 % CO_2.

	1	2	3	4	5	6	7	8	9	10	11	12
A	PBS	PBS	PBS	PBS	PBS	PBS	PBS	PBS	PBS	PBS	PBS	PBS
B	PBS	2.000%	1.500%	1.000%	0.750%	0.500%	0.250%	0.125%	0.063%	0.031%	0.000%	PBS
C	PBS	2.000%	1.500%	1.000%	0.750%	0.500%	0.250%	0.125%	0.063%	0.031%	0.000%	PBS
D	PBS	2.000%	1.500%	1.000%	0.750%	0.500%	0.250%	0.125%	0.063%	0.031%	0.000%	PBS
E	PBS	2.000%	1.500%	1.000%	0.750%	0.500%	0.250%	0.125%	0.063%	0.031%	0.000%	PBS
F	PBS	2.000%	1.500%	1.000%	0.750%	0.500%	0.250%	0.125%	0.063%	0.031%	0.000%	PBS
G	PBS	2.000%	1.500%	1.000%	0.750%	0.500%	0.250%	0.125%	0.063%	0.031%	0.000%	PBS
H	PBS	PBS	PBS	PBS	PBS	PBS	PBS	PBS	PBS	PBS	PBS	PBS

Figure 3: Plate layout.

After 24 hours of incubation, the cells were added with the CCK8 reagent in a volume equivalent to 10 % of the final volume in the wells, that was 20 µL of CCK8 reagent, and incubated for 3.5 h before reading the absorbance at 450 nm. CCK8 is a reagent based on tetrazolium salt (WST-8 [2-(2-methoxy-4-nitrophenyl)-3-(4-nitrophenyl)-5-(2,4-disulfophenyl)-2H-tetrazolium, monosodium salt]) which in the presence of an electron mediator is reduced by dehydrogenase generating an orange-coloured product, formazan, in an amount directly proportional to the viable cells number (Figure 4 and Figure 5) (28).

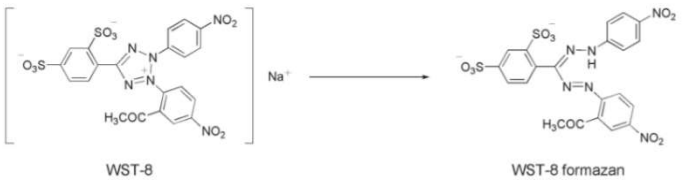

Figure 4: WST-8 reduction to WST-8 formazan (28).

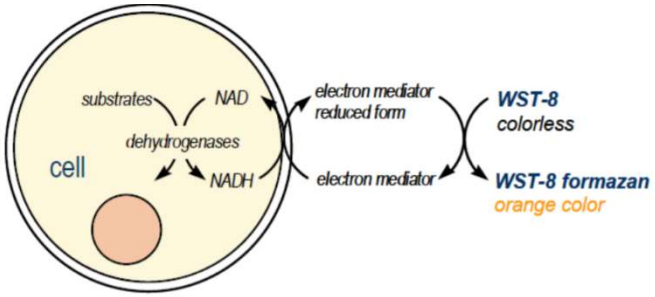

Figure 5: Cell viability detection with CCK8 (28).

With the results obtained, the percentage of cell viability was calculated with respect to the 0 concentration, corresponding to the negative control, according to the following formula:

$$\%\ survival = \frac{OD\ Sample}{OD\ Control}\ x\ 100$$

4.3. EVALUATION OF THE EXPRESSION OF PROTEINS IN THE CELL MEMBRANE BY FLOW CYTOMETRY

For each flow cytometry performed, 6 samples were used. For each sample, 5 x 10^5 cells were loaded in an Eppendorf tub. The cell suspensions were centrifuged at 800 x g, and the supernatants were eliminated by aspiration. The pellets were washed two times with the cytometry buffer (PBS, 5% BSA, 0.5% sodium azide). Then the pellets were resuspended in 100 µL of the cytometry buffer and the labellers were added as appropriate, using two samples for each condition, and labelling them with nothing, the isotype control antibody, or the antibody for the detection of the protein of interest. The samples were incubated for 30 min protected from light. The cell suspensions were centrifuged at 800 x g, and the supernatants were eliminated by aspiration. The pellets were washed two times with the cytometry buffer and then resuspended in 500 µL of the cytometry buffer and labelled with DAPI at a final concentration of 8 µg / mL. The flow cytometry acquisition was performed using a Gallios Cytometer (Beckman Coulter).

4.4. EVALUATION OF THE PLANT EXTRACTS ANTI-INFLAMMATORY EFFICACY ON HaCaT CELL LINE AFTER THE STIMULATION WITH *C. acnes* BY qPCR

24 h before cell treatment, 5 wells of three different 6-well plates were seeded with 500,000 HaCaT cells on HaCaT medium. Each of the plates was seeded with cells originating from a different expansion from cells originating from the thawing of a single cryovial. Plates were incubated at 37ºC in humidified atmosphere with 5 % CO_2. After 24 hours, the following conditions were tested on each of the plates:

- Negative control (untreated cells).
- Cells treated with *C. acnes* 10 bact. / cell for 6 h.

- Cells treated with *C. acnes* 10 bact. / cell + C at 0.25% for 6 h.
- Cells treated with *C. acnes* 10 bact. / cell + Q at 0.25% for 6 h.
- Cells treated with *C. acnes* 10 bact. / cell + C:Q 1:1 at 0.25 % for 6 h.

After the treatment, a lysate of the cells was obtained and the RNA from the samples was extracted using the Rneasy Mini Kit, according with suppliers' instructions. The mRNA obtained was quantified using the NanoDrop Lite.

For the generation of the cDNA, a preparation for each sample was made with sufficient sample volume to have 1 µg of mRNA. The volume was adjusted to 16 µL with nuclease free water. 4 µL of iScript RT-PCR Supermix were added to each preparation and the samples were placed in the thermocycler for the reverse transcription of mRNA to cDNA. At the end of the process, cDNA originates was contained in a volume of 20 µL was obtained. Each sample was brought to a final volume of 100 µL to reach the working concentration of approximately 10 ng / µL.

After the obtention of the cDNA a qPCR was performed to determine the expression of 3 inflammatory mediators, an interleukin, IL-8, a cytokine, TNFα, and a chemokine, CXCL1. For the performance of the qPCR, for each reaction, 10 µL of LightCycler 480 Probes Master, containing the FastStart Taq DNA Polymerase, the reaction buffer, the deoxyribonucleotide mix, and 6.4 mM $MgCl_2$, 5 µL of Nuclease Free Water, 1 µL of the corresponding TaqMan Gene Expression assays mix, consisting of a pair of the selected gene unlabelled primers and a fluorescent labelled TaqMan probe, and finally 4 µL of the corresponding sample. After the preparation of the samples, 40 cycles of increasing the temperature to 95 ºC for denaturation of the two strands of DNA, decreasing the temperature to 60 ºC for annealing of the primers to the template, and increasing it to 72 ºC for the elongation of the primers, were performed. Fluorescence signals were acquired for the quantification of the inflammatory mediators' expression. One qPCR plate (Figure 6) was used for each biological triplicate.

	A	B	C	D	E	F	G	H	I	J	K	L
1	M1 - GADPH	M1 - GADPH	M1 - GADPH	M1 -TNFα	M1 -TNFα	M1 -TNFα	M1 - IL8	M1 - IL8	M1 - IL8	M1 - IL6	M1 - IL6	M1 - IL6
2	M2 - GADPH	M2 - GADPH	M2 - GADPH	M2 -TNFα	M2 -TNFα	M2 -TNFα	M2 -IL8	M2 -IL8	M2 -IL8	M2 -IL6	M2 -IL6	M2 -IL6
3	M3 - GADPH	M3 - GADPH	M3 - GADPH	M3 -TNFα	M3 -TNFα	M3 -TNFα	M3 -IL8	M3 -IL8	M3 -IL8	M3 -IL6	M3 -IL6	M3 -IL6
4	M4- GADPH	M94- GADPH	M94- GADPH	M4 -TNFα	M4 -TNFα	M4 -TNFα	M4 -IL8	M4 -IL8	M4 -IL8	M4 -IL6	M4 -IL6	M4 -IL6
5	M5 - GADPH	M5 - GADPH	M5 - GADPH	M5 -TNFα	M5 -TNFα	M5 -TNFα	M5 -IL8	M5 -IL8	M5 -IL8	M5 -IL6	M5 -IL6	M5 -IL6
6	M1 -CXCL1	M1 -CXCL1	M1 -CXCL1	M2 -CXCL1	M2 -CXCL1	M2 -CXCL1	M3 -CXCL1	M3 -CXCL1	M3 -CCL20	M4 -CXCL1	M4 -CXCL1	M4 -CXCL1
7	M5 -CXCL1	M5 -CXCL1	M5 -CXCL1									
8												

M1	**CELLS (Ctrl)**
M2	**Cells + *C. acnes***
M3	**Cells + *C. acnes* + C (0.25%)**
M4	**Cells + C. acnes + Q (0.25%)**
M5	**Cells + *C. acnes* + C:Q (1:1) (0.25%)**

Figure 6: qPCR plate layout.

4.5. EVALUATION OF THE TRANSLOCATION TO NUCLEUS OF NF-κβ AFTER THE STIMULATION WITH *C. acnes* ON HaCaT CELL LINE

24 h before cell treatment 5 wells of a 6-well plate, in which a glass cover slip had been placed at the bottom, were seeded with 500,000 cells on HaCaT medium and the plates were incubated at 37ºC in humidified atmosphere with 5 % CO_2. After 24 hours, the following conditions were tested:

- Negative control (untreated cells).
- Cells treated with *C. acnes* 10 bact. / cell for 1 h.
- Cells treated with *C. acnes* 10 bact. / cell + C at 0.25 % for 1 h.
- Cells treated with *C. acnes* 10 bact. / cell + Q at 0.25 % for 1 h.
- Cells treated with *C. acnes* 10 bact. / cell + C:Q 1:1 at 0.25 % for 1 h.

After the corresponding incubation time, cells were washed with PBS and fixated with a solution of diluted PFA at 4 % for 10 min at RT. Then the cells were washed 3 times with PBS and then incubated with a solution 0.2 % Triton X-100 in PBS for 15 min at RT for cell permeabilization. After that, the cells were incubated in a solution of 3 % BSA, 0.1 % Tween-20 in PBS for 30 min at RT for blocking.

For staining, the samples were incubated with the antibody anti-NFκB p65, conjugated with Alexa Fluor® 488, diluted 1 / 50 in blocking solution, for 1 h at RT, protected from light. After that, 5 washes of 5 minutes with PBS were performed and posteriorly, the cells were incubated for 10 min with a solution of DAPI at a concentration of 1 µg / mL, diluted in PBS. Finally, the cells were washed 2 times with PBS for the elimination of the exceeding DAPI.

The glass cover slips were taken from the bottom of the wells and mounted on microscope slides with MOWIOL mounting medium. The slides were maintained overnight at RT for MOWIOL drying and then the samples were visualized using confocal microscopy for image capturing.

The images were analysed using the Software image-J for channel merging and for the evaluation in the cell nuclei of the green and blue fluorescence intensities, and the ratio between them. This analysis allowed a semi-quantitative evaluation of the translocation of NF-κB produced in each condition. For the analysis, a line was drawn across each of the assessed nuclei to determine the blue and green fluorescence at each of the pixels forming the line. The total fluorescence of each colour for the whole line, and the graph representing both fluorescence intensities were evaluated.

4.6. COMPARISON OF THE RECEPTOR BINDING PROFILES BETWEEN THE TPO-RA RMP AND ITS BIOSIMILAR BY BIACORE

In the first place, the anti-human IgG(Fc) monoclonal antibody provided with the "Biacore human antibody capture kit" was covalently coupled to the surface of a CM5 sensor chip following the kit protocol. Then, the reference TPO-RA was passed over the αhIgG(Fc) mAb sensor chip surface in a serial dilution range between 155 ng / mL and 2.4 ng / mL, to stablish a linear relationship between TPO-RA concentration and its binding with the αhIgG(Fc) mAb sensor chip. The analyte flow applied was of 30 µL / min and the concentration report point was seated at 320 seconds after injection time.

In the second place, the TPO-R was coupled to a CM5 sensor chip surface, through amine coupling (Figure 7), at a TPO-R immobilization on the surface of the sensor chip of 824 RU. Amine coupling consists in the activation of the carboxyl groups present on the surface of the chip for the generation of ester groups which will be able to interact with amine groups in the ligand, producing the attachment of the ligand to the sensor chip surface.

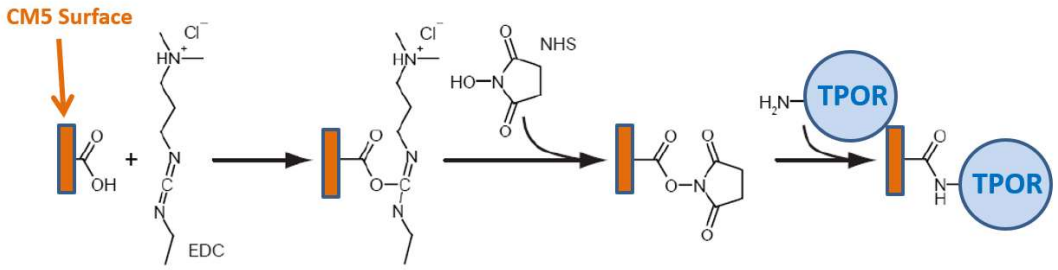

Figure 7: TPO-R coupling to the CM5 sensor chip surface

After that, the TPO-RA reference material was applied as analyte in a serial dilution range between 1,235 ng / mL and 0.3 ng / mL, to detect the sensitive linear range of the logarithmic dose response curve. The analyte flow applied was of 30 µL / min and the concentration report points were set at 320 seconds and 340 seconds after injection time.

To investigate the capability of the biacore system to detect differences in the potency a set of serial dilutions parting from 80 % (320 µg / mL), 100 % (400 µg / mL) and 125 % (500 µg / mL) concentrations of the TPO-RA reference material were assessed.

Finally, 3 batches of RJF biosimilar DS and 3 batches of RJF biosimilar DP were assessed in front of 3 batches of the reference material product, to determine if they presented a similar behaviour.

For the analysis of the results sensorgrams were analyzed by mathematical curve fitting using BiaEvaluation 4.1 software. Sensorgram fitting was carried out by applying a Langmuir 1:1 and a bivalent analyte algorithm, respectively.

4.7. EVALUATION OF THE THROMBOPOIETIN RECEPTOR RESPONSIVENESS TO STIMULATION IN BA/F3-HMPL AND IN TF1 - STAT5 - LUC 2P – TPO-R SELECTED CLONES

Two WB, one for the identification of total STAT5 in the sample and another for the identification of phosphorylated STAT5 after the treatment with thrombopoietin analogue were performed. 24h before the treatment 4 T25 flasks were seeded with $5x10^6$ cells in 5 mL of cell medium (RPMI; 10% FBS) and incubated at 37ºC in humidified atmosphere with 5 % CO_2. After 24 h, medium was removed by aspiration and replaced with 5 mL of fresh medium. Cells in each flask were treated with 100 ng / mL of TPO-RA for 0 min, 5 min, 10 min or 30 min. After the treatment cells were centrifuged at 800 x g, the supernatant was eliminated by aspiration and the pellet was frozen in dry ice for 10 seconds. The pellet was washed with ice cold PBS and the incubated with 600 µL of lysis buffer supplemented with 10 µL / mL of a phosphatase and protease inhibitor for 5 minutes on ice. The cell lysate was centrifuged for 10 min at 13000 x g for the elimination of cell debris. The supernatant was transferred to a new Eppendorf tube. Once the cell lysates were obtained, the protein concentration of each sample was determined through the measurement of absorbance 280 nm using nanodrop. Sufficient lysate volume of each sample to have 12,000 µg of total protein was separated and incubated with 50 µL of anti-STAT5 (A-9) AC antibody to make the conjugation with agarose. The samples were incubated over night at 4ºC with gentle agitation. The rest of the lysate volume was conserved at 4ºC.

One day after the samples conjugated with agarose were centrifuged at 800 x g for 60 s for immunoprecipitation of STAT5. The supernatant was eliminated by aspiration and the pellet was resuspended by adding 26 µL H_20 Mili-Q, 10 µL Sample Buffer and 4 µL of DTT.

The cell lysates were used to prepared by mixing 26 µL of Sample, 10 µL of Sample Buffer and 4 µL of DTT. The samples prepared were heated ad 95ºC for denaturation and then temperate 5

min at RT. One polyacrylamide gel was loaded with the samples prepared form the cell lysate and the other gel was loaded with the samples resulting from immunoprecipitation.

The gels were run for 30 min at 200 V. After the separation of the proteins through electrophoresis, the proteins were transferred to a nitrocellulose membrane by electroblotting using a 0.31 A current for 30 min. After the transference, the membranes were incubated in blocking solution (PBS, 0.1 % Tween-20) for 2h. Once blocked, the membrane with the proteins from the cell lysate was incubated with the primary antibody anti-STAT5 and the membrane with STAT5 from immunoprecipitation was incubated with the primary antibody anti-p-TYR. The antibodies were diluted in blocking solution 1 / 200, achieving a final concentration of 1 µg / mL. The membranes were incubated overnight at 4ºC with gentle agitation.

After the overnight incubation, the membrane with proteins from the cell lysate was washed for 15 min at RT with TPBS 0.1 % and then the membrane and then incubated for 1 h at RT in gentle agitation, with the primary antibody anti-α-tubulin, diluted 1 / 2,000 achieving a final concentration of 1 µg / mL. After that, the two membranes, the one with the proteins from the cell lysate and the one with STAT5 from immunoprecipitation were washed 3 times for 15 min at RT with TPBS 0.1 %. The membranes were incubated for 45 min at RT in gentle agitation with the Anti-Mouse IgG (γ-chain specific) conjugated with Alkaline Phosphatase secondary antibody, diluted 1 / 20,000, and then washed 3 times for 15 min at RT with TPBS 0.1 % and one time with PBS. The membranes were revealed with Novex AP Chromogenic Substrate (BCIP / NBT) and the images were captured with ChemiDoc ™ MP Imaging System.

4.8. BA/F3-HMPL PROLIFERATION ASSAY DEVELOPMENT AND OPTIMIZATION OF THE ASSAY CONDITIONS

For all the assays performed, 96-well clear flat bottom culture treated polystyrene microplate were loaded with the desired number of cells in 125 µL of medium, equivalent to half of the desired final volume for each well. Only the central 60 wells of the plates were used for the assay. The rest of the wells were filled with PBS. The plates were incubated at 37ºC in humidified atmosphere with 5 % CO_2. 3 hours after plating the cells, the corresponding stimulus were loaded into each well. The dilutions were prepared at twice the desired concentration and the same volume used to seed the cells was loaded into the plates, thereby making a ½ dilution on

the plate. After treatment, the plates were placed at the incubator at 37ºC in humidified atmosphere with 5 % CO_2.

For the determination of the cell proliferation the CCK8 reagent was added to the wells in a volume equivalent to 10 % of the final volume, that was 25 µL of CCK8 reagent and incubated for 3.5 h before reading the absorbance at 450 nm.

The results were analysed using the software UNISTATS and a 4-parameter logistic model, a regression model often used to analyse assays which follows a sigmoidal shape curve, useful for characterizing bioassays, as they are often only linear across a specific range of concentrations.

Due to the intrinsic variability of cell-based assays, to be able to compare results obtained in different assays, the absolute potency measurement is not adequate, and the results must be presented as relative to a Standard, with biological behaviour similar or identical to the Test sample, loaded in the same plate, for which a Potency of 100 % is assumed (29,30). For the calculation of the relative potency one complete dilutions curve is loaded for the standard and another complete dilution curve for the test sample, then both curves are superposed and the horizontal displacement between them is calculated to determine the relative potency of the sample. When data is introduced in the UNISTAT software indicating that one of the preparations must be used as standard and the other one as sample, UNISTAT gives a result in form of percentage, indicating the relative potency of the Sample compared with the Standard.

4.9. TF1 - STAT5 - LUC 2P - TPOR REPORTER GENE ASSAY DEVELOPMENT AND OPTIMIZATION OF THE ASSAY CONDITIONS

For all the assays performed, 96-well clear flat bottom culture treated white polystyrene microplates were loaded with the desired number of cells in 50 µL of medium, equivalent to half of the desired final volume for each well. Only the central 60 wells of the plates were used for the assay. The rest of the wells were filled with PBS. The plates were incubated at 37ºC in humidified atmosphere with 5 % CO_2 overnight. The day after plating the cells, the corresponding stimulus were loaded into each well. The dilutions were prepared at twice the desired concentration and the same volume used to seed the cells was loaded into the plates, thereby making a ½ dilution on the plate. After treatment, the plates were placed at the incubator at 37ºC in humidified atmosphere with 5 % CO_2.

For the determination of the cell proliferation 50 µL of Bio-Glo™ Luciferase Assay System reagent was added to each well and incubated for 10 min. Then luminometry was measured. Bio-Glo™ Luciferase Assay System includes in its composition a luciferase substate, which after being metabolized by the luciferase (Figure 8) produced in the sample as the reporter gene emits light in a directly proportional way to the gene of interest expression (31).

The results were analysed using the software UNISTATS and a 4PL model.

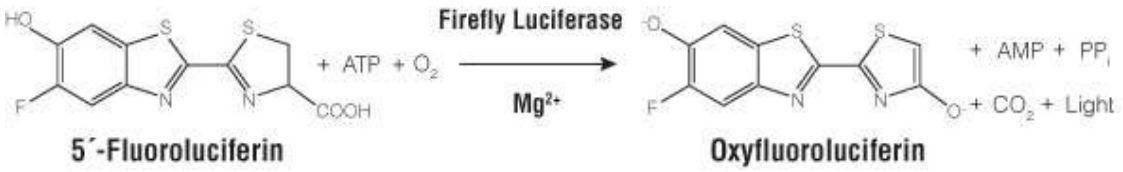

Figure 8: 5'-Fluoroluciferin oxidation to Oxyfluoroluciferin (31).

4.10. BA/F3-HMPL PROLIFERATION ASSAY AND TF1 - STAT5 - LUC 2P - TPOR REPORTER GENE ASSAY VALIDATIONS

Linearity, accuracy, precision, specificity, and robustness of the methods were evaluated.

Linearity was investigated after the calculation of relative potencies of curves diluted at 60 %, 80 %, 100 %, 120 % and 140 % in front of a control (100 %). For each concentration level, three 96-well plates were used. The corresponding assay was performed for each one of the plates. For the assessment of the results, the relative potencies obtained were represented against concentration to determine the linearity of the method. To consider the method as linear a $R^2 \geq 0.95$ had to be obtained.

For the analysis of the methods precision, the variability between the results obtained for 9 assays was analysed. For each assay, one preparation of STD and one preparation of Test solution at 100 % were prepared and loaded into a plate. For the assessment of the results, the % RSD of the relative potencies obtained was calculated. For the method precision to comply with acceptance criteria % RSD had to be lower than 20 %.

For the analysis of the intermediate precision, day-to-day precision and analyst-to-analyst-precision were evaluated. To analyse this, the variability between the results obtained for 12

assays performed by two different analysts in 3 independent days was analysed. Analyst 1 performed 3 independent assays on day 1, on day 2 and on day 3, and analyst 2 performed 3 independent assays on day 2. For each assay, one preparation of STD and one preparation of Test solution at 100 % was prepared and loaded into a plate. For the assessment of the results, the % RSD of the relative potencies obtained was calculated. For the method precision to comply with acceptance criteria % RSD had to be lower than 30 %.

To evaluate accuracy, the relative potencies obtained for the analysis of curves diluted at 80 %, 100 %, and 120% in front of a control (100 %) were studied. For each concentration level, three assays were performed. For the assessment of the results, the relative potency was calculated for each assay and the percentage of the recovery for each dilution curve was calculated using the following formula:

$$Recovery = \frac{Relative\ EC50\ real}{Relative\ EC50\ expected}\ x\ 100$$

To consider accuracy as adequate, the % of the recovery of each dilution curve had to be between 70 % and 130 %.

To assess selectivity, 3 plates were loaded with an STD curve (100 %) and a Tests solution curve prepared using the DP excipients buffer. For the assessment of the results the response generated for the excipients buffer dilutions curve was evaluated. For the selectivity of the method to be considered as adequate, no response had to be observed for the buffer of excipients and the OD values obtained at each concentration level had to be equivalent to the OD values reported in cells treated with a 0 ng / mL concentration.

In the case of the BA/F3-hMPL proliferation assay, for the assessment of the robustness of the method, the impact of a small modification in the incubation time of the plates after the application of the CCK8 was assessed. To do so, the absorbance 450 nm of 9 plates, loaded with a STD (100 %) and a Test sample (100 %) dilutions curve, was read 3 h; 3.5 h and 4 h after the application of the CCK8. For the assessment of the results, the relative potencies obtained at each incubation time were compared through the evaluation of % RSD and through an analysis ANOVA comparing the 3 CCK8 incubation times under study.

In the case of the TF1 - Stat5 - Luc 2P - TPOR reporter gene assay validation, for the analysis of the robustness of the assay, the impact of a small modification in the incubation time of the plates after the application of the stimuli and after the application of Bio-Glo™ Luciferase Assay System were assessed. To do so, 3 independent preparations of Standard and Test Sample dilution curves at 100 % were loaded in 3 plates each. From the 3 plates loaded with the same combination of STD and Test Sample, one plate was incubated for 5:30 h, the second one was incubated for 6 h, and the last one was incubated for 6:30 h. Luminescence of each of the 9 plates used was read at 10 min and at 25 min after the addition of Bio-Glo™ Luciferase Assay System in the wells. For the assessment of the results, the comparison of the results obtained at the different incubation times, through the evaluation of % RSD and through an ANOVA analysis comparing the different groups under study, was performed.

4.11. CYTOTOXICITY ASSAY OF THE D / BB CREAM AND ITS COMPONENTS ON HEK001 CELL LINE

24h before the assay, four 96-well clear flat bottom culture treated white polystyrene microplates were seeded 10,000 cells / well in 50 µL of KSFM supplemented with 1% Glutamax, from here HEK001 assay media, and incubated at 37ºC in humidified atmosphere with 5 % CO_2. Only the central 60 wells of the plates were used for the assay. The rest of the wells were filled with PBS. After the incubation, the cells were treated with 10 concentrations of each product under assessment, using 1 plate for each condition. The concentrations tested for BB tested were 5,000.00, 1,666.67, 555.56, 185.19, 61.73, 20.58, 6.86, 2.29, 0.76, 0.25 and 0.00 µM while the concentrations tested for D were 33.36, 22.24, 14.83, 9,88, 6.59, 4.39, 2.93, 1.95 1.30 and 0.00 µM, as BB is much more concentrated in the final product than disulfiram. The concentrations tested for D / BB cream were for the active ingredients (D / BB) to be 32.10 / 504.76, 21.40 / 336.51, 14.27 / 224.34, 9.51 / 149.56, 6.34 / 99.76, 4.23 / 66.47, 2.82 / 44.31, 1.88 / 29.54, 0.94 / 14.77, and 0.00 µM / 0.00 µM. Finally, the placebo, composed by the matrix of excipients, was assessed, prepared equivalently to D / BB cream. The dilution curve was prepared on HEK001 medium at twice the desired concentration and loaded into the plates in sextuplicate, using the same volume used to seed the cells, thereby making a ½ dilution on the plate. After treatment, the plates were incubated for 24 h at 37ºC in humidified atmosphere with 5 % CO_2.

For the determination of the cell viability, after a 24 h incubation of the cells with the compounds, 100 µL of CellTiter-Glo® reagent were added to each well and incubated for 10 min. Then, luminescence in each well was measured using the luminometer Victor x3.

CellTiter-Glo® reagent mechanism of action is based on the metabolization of Luciferin to Oxyluciferin, a light emitting compound, depending on the ATP presence in the sample, which is directly related with the number of viable cells (Figure 9).

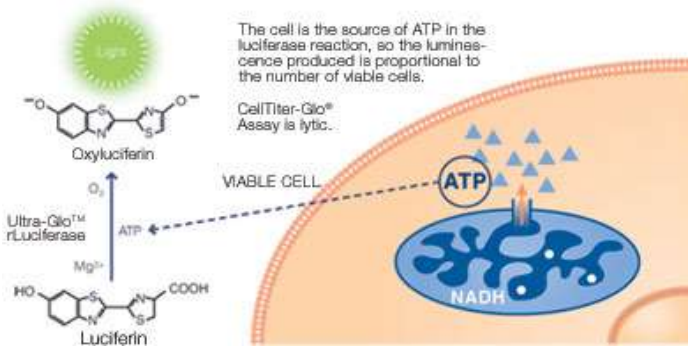

Figure 9: CellTiter-Glo® reagent mechanism of action (32).

4.12. EVALUATION OF THE IMPACT OF THE TREATMENT WITH THE D / BB CREM ON HEK001 GENE EXPRESSION THROUGH A TRANSCRIPTOMIC MICROARRAY ANALYSIS

24 h before the performance of the assay, 6 wells of a 6-well plates were seeded with 250,000 cells on HEK001 assay medium. The plate was incubated at 37ºC in humidified atmosphere with 5 % CO_2. The day after, the medium of the wells was removed and replaced with fresh HEK001 assay medium in 3 of the wells and a solution of with the combination of 6.59 µM of D and 99.77 µM BB, diluted on HEK001 assay medium, in the other 3 wells. The plate was incubated at 37ºC in humidified atmosphere with 5 % CO_2 for 24 h.

After the treatment, the cells were lysate and the RNA from the samples was extracted using the Rneasy Mini Kit, according with suppliers' instructions. The mRNA obtained was quantified using the NanoDrop Lite and the samples were prepared to achieve a final concentration of 500 ng in 5 µL. The samples were then delivered to Genomics core facility of the Institut d'Investigacions Biomèdiques August Pi i Sunyer (IDIBAPS) for the microarray analysis using a

Clariom_S_Human transcriptomic array (Afimetrix) for the analysis of the cell transcriptome through the evaluation of 21,448 probe sets.

After the obtention of the results, gene expression data from the different samples were compared using the software GeneSpring 14.9.1, applying a a one-way T-test and a stringent cut-off criterion of transcripts with fold change (FC)> 1.5 and p-value ≤ 0.05.

CHAPTER 1: PROVE OF CONCEPT ASSAYS FOR THE DEVELOPMENT OF AN ANTI-ACNEIC CREAM

5. INTRODUCTION TO CHAPTER 1

5.1. THE HUMAN SKIN

The human skin, with a mean extension between adult individuals of 1.8 m^2, is the largest organ in the body. It is the out covering of the rest of the organs and is responsible for the organism protection against external harm, including the immunological defence against pathogenic invasions (33). The skin of the face area corresponds to approximately a 4% of the total (34).

To fulfil its mission, the skin hosts a very specialized microbiome, which has a symbiotic relationship with the organism, and that is responsible for the preservation of the skin's homeostasis and for the prevention of the colonization of its surface by pathogenic microorganisms (35).

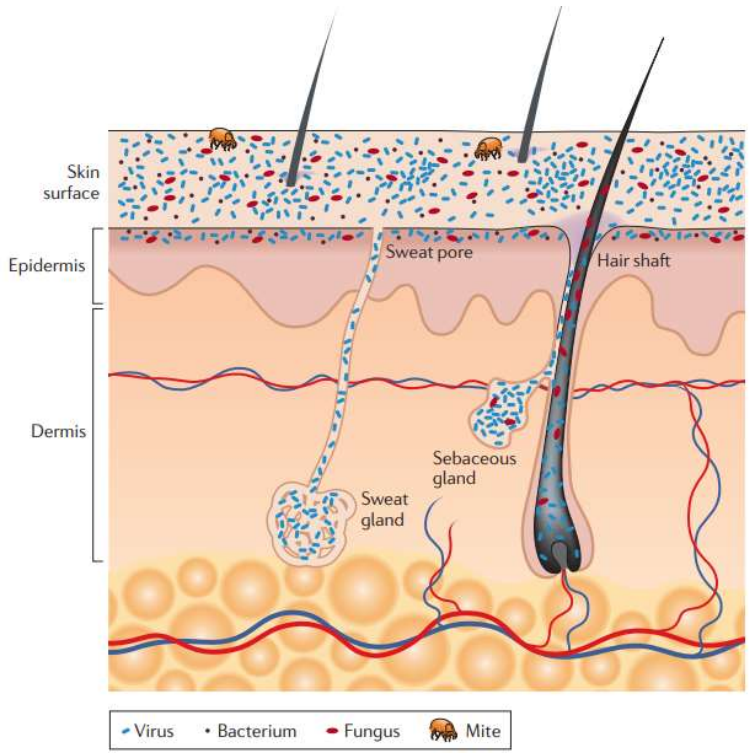

Figure 10: The skin structure (6).

The skin presents a high variety of structures, like hair follicles and diverse glands, which make it an irregular surface, presenting a diversity of environments suitable for the proliferation of specifically adapted microorganisms (36). Even though the microbiome presents variations depending on the host physical and environmental factors, the four phyla with a higher representation are *Actinobacteria*, *Firmicutes*, *Bacteroidetes* and *Proteobacteria*, from which around a 60 % belong to genera *Staphylococcus*, *Corynebacterium*, and *Cutibacterium* (33).

Despite the symbiotic relationship stablished between the organism and its microbiome, the loss of the balance between the microbes and the host may lead to the development of skin pathologies (37).

5.2. ACNE

One of the most characteristic skin diseases caused by a disruption of the microbiota is acne. It is a multifactorial chronic inflammatory disorder, which affects around 70 % of the population during adolescence and that may persist in adulthood. Despite the non-severity of the disease, it is associated with high physiological impact, which causes a reduction in life quality, due to the stigma associated with the appearance of visible lesions, mostly in the face but also in other regions reach in sebaceous follicles (38).

The development of acne is related with an excessive production of abnormal sebum, in the sebaceous glands, which are associated with the hair follicles, leading to the apparition of initial non-inflammatory lesions that may evolve to inflammatory lesions in form of papules, pustules, and cysts, in the pilosebaceous units in the skin (39,40).

The inflammation of the skin in acne is associated with the tissue damage caused by the obstruction and rupture of the ducts in the sebaceous gland, but also with the abnormal proliferation of the pilosebaceous microbiome, mainly of *Cutibacterium acnes*, which may also be related with the modifications in sebum composition and secretion by skin glands (41).

Pharmacological treatment of acne is usually reserved to moderate and severe cases, and its main objectives are the elimination of the active lesions and the prevention of the apparition of new ones (42). The two principal treatment options consist of retinoids, which aim to reduce the inflammatory response (43), and antibiotics, destined to prevent *C. acnes* proliferation (44). Usually, moderate cases are treated with a topical application of the drugs, while severe cases

or those showing resistance to topical treatment require oral intake for systemic treatment. Other anti-inflammatory products are also available, together with other non-drug alternatives for the alleviation of the symptomatology in the mild cases (45).

5.3. *Cutibacterium acnes*

Cutibacterium acnes is a gram-positive, anaerobic bacteria, and it is the main representative of the microbiome in the pilosebaceous unit. In a physiological situation, *C. acnes* is responsible for the degradation of the lipids and the hydrolysation of the triglycerides present in the skin sebum, generating free fatty acids which contribute to the maintenance of the acidic pH that difficult the colonization of the skin by noxious microorganisms. Despite this, in pathological conditions, when there is an excessive proliferation of microbiome, this bacterium contributes to the development of acne through an excessive synthesis of molecules with inflammatory potential (46,47).

5.4. INNATE IMMUNITY AND TLR

Innate immunity is the organisms first line of defence against pathogenic infections. The sensing of invading pathogens is made through the detection of highly conserved structures of the microbes, essential for the pathogens survival and not shared with the host's cells, which are denominated as pathogen associated molecular patterns (PAMPs). The receptors responsible for the detection of PAMPs are known as pattern recognition receptors (PRR) (48).

Toll-like receptors, a type I transmembrane receptors family, are the main representatives of PRRs. These receptors present an extracellular domain, reach in leucine residues, responsible for receptor-ligand interaction, and an intracellular Toll / IL-1 domain, responsible for downstream signalling. They are expressed in a high variety of cells, including skin cells, as keratinocytes, and cells of the immune system, where they are responsible for infections detection for the organism defence (49–51). The high conservation of PAMPs and the capability of TLRs of recognizing more than one ligand, added to its activation through homo- or heterodimerization, permitting the formation of different complexes, allows for a reduced number of TLRs to be sufficient for the detection of any pathogenic invasion (52).

The inflammatory response produced in acne is mediated through the detection of *C. acnes* PAMPs, mainly peptidoglycan and lipoteichoic acid, by TLR2 and TLR4 (Figure 11), which after its activation induce the NF-κβ canonical pathway and the consequent inflammatory molecules synthesis, which, at its turn, causes the recruitment of the immune system effector cells, that induce the inflammatory symptomatology in the corresponding skin area (53,54).

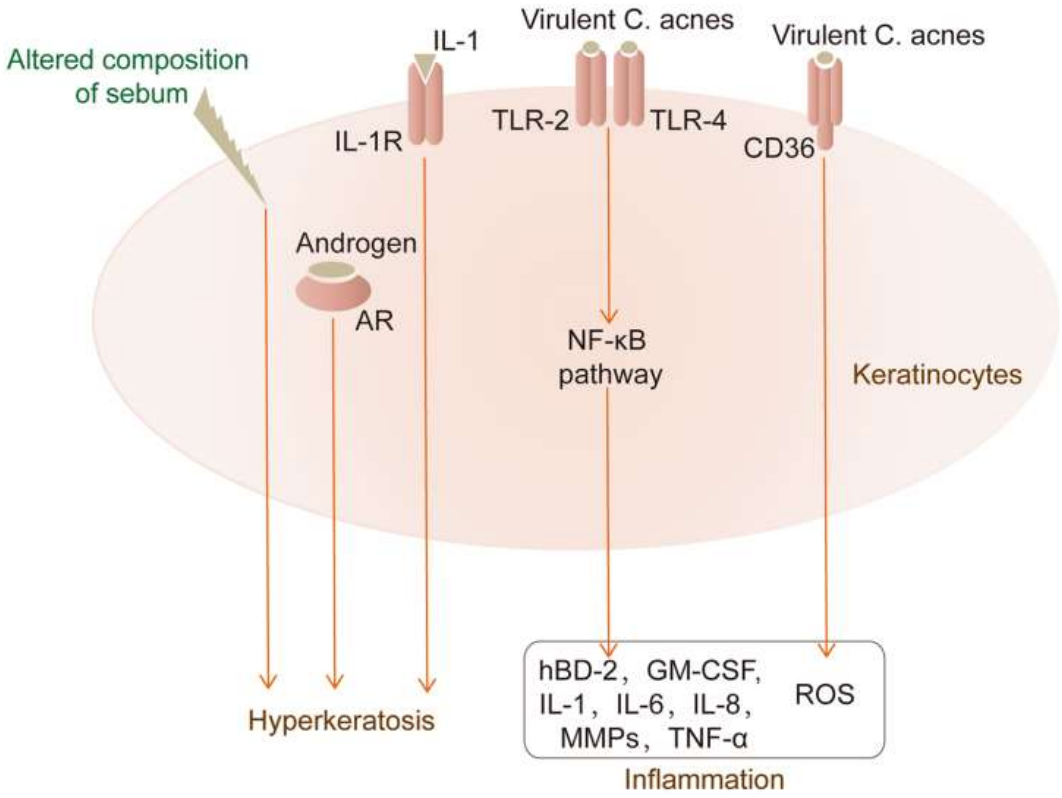

Figure 11: Inflammatory response caused by C. acnes infection (55).

5.4.1. Activation of the NF-κβ the canonical pathway in response to *C. acnes* and consequent inflammatory response

TLR2 and TLR4 share a common downstream signalling pathway. After the activation of the two receptors in response to *C. acnes*' PAMPs, the intracellular domain of the receptors induces the requitement of the adaptor protein MAL, which at its turn is responsible for the interaction with MyD88 protein. The consequent activation of IRAK through phosphorylation leads to the activation of TRAF6 and the IKK phosphorylation, facilitating Iκβ ubiquitination (56–58).

In absence of receptor activation, Iκβ is bound to NF-κβ and inhibits its translocation to the cell nucleus. After its ubiquitination, Iκβ is degraded by the 26S proteasome, freeing NF-κβ, which rapidly migrates to the cell nucleus (59). The NF-κβ can then directly bind to DNA in a sequence present in the promoter region of several genes involved in immune and inflammatory response, activating their transcription (60,61), and inducing inflammatory cytokines and chemokines secretion in the pilosebaceous unit and the consequent requitement of dendritic cells, macrophages, and neutrophils, among other immune system cells (58).

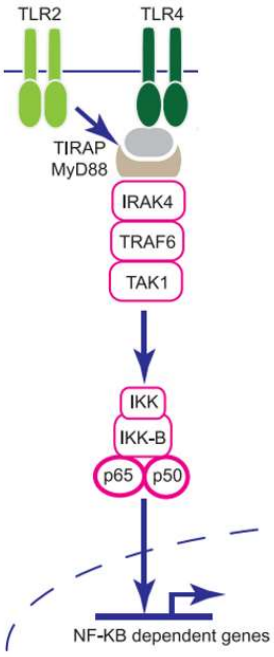

Figure 12: NF-κβ canonical pathway (62).

5.5. DEVELOPMENT OF AN ANTI-ACNEIC CREAM

RJF aims to develop an anti-acne cream for the treatment of acne episodes. The approach sought is to develop a plant-based treatment aimed to reduce the inflammatory response produced in acne, as it is the main source of the appearance of uncomfortable symptoms and acne lesions. Before the beginning of the development process, the company aims to demonstrate the anti-inflammatory capacity of two different plant extract candidates to be used as active ingredients of the cream.

5.5.1. *Camellia sinensis*

Camellia sinensis is the main plant species used to produce green tea, one of the most popular drinks worldwide (63,64) and, since antiquity, associated with health benefits (65). The main components of *Camellia sinensis* are polyphenols (90 % of the content), amino acids, theanine, proanthocyanins and caffeine (66). From these components, the polyphenol catechins are the principal mediators of the biological effects, and their consumption is associated with a reduction of the expression of inflammatory associated genes, an increase of the expression of antioxidative genes and with antimicrobial activity, among other health benefits (67–70).

The anti-inflammatory capacity of *Camellia sinensis* makes it an ideal candidate for the development of a treatment for acne outbreaks, as the inflammatory response generated is the main responsible for the appearance of lesions and pustules on the skin.

5.5.2. *Morinda citrifolia*

Morinda citrifolia is a tropical tree and it is one of the most common species of the *Morinda* genus. It has been part of the traditional medicine for over 2000 years (71) due to its association with beneficial health properties, including, among others, antibiotic, and anti-inflammatory properties (72–74). Apart from that, there is evidence suggesting that it can be also useful to prevent the formation of biofilms (75,76).

Morinda citrifolia properties make it an optimal candidate for the development of a possible acne treatment, not only because its anti-inflammatory properties which might be helpful for the improvement of the symptomatology, but also because its antibiotic and anti-biofilm formation properties, which can reduce the colonization of the pilosebaceous units by *C. acnes*.

6. RESULTS OF CHAPTER 1

6.1. CYTOTOXICITY ASSAY OF THE PLANT EXTRACTS ON HaCaT CELL LINE

A cytotoxicity assay was performed for the determination of the non-cytotoxic threshold of the compounds under assessment, for the determination of the working concentrations. The results obtained after the 24 h treatment with the different plant extracts are presented in Table 3, Table 4 and Table 5 while Figure 13 shows the graphic representation of the survival rates.

Table 3: OD values and % of survival after a 24 h treatment at different concentrations of the Camellia sinensis extract.

[C] %	OD P1	OD P2	OD P3	% survival plate 1	% survival plate 2	% survival plate 3	% survival Mean
2.00 %	0.705	0.709	0.715	84 %	83 %	84 %	**84 %**
1.50 %	0.669	0.730	0.735	80 %	86 %	86 %	**84 %**
1.00 %	0.678	0.696	0.711	81 %	82 %	83 %	**82 %**
0.75 %	0.681	0.708	0.726	81 %	83 %	85 %	**83 %**
0.50 %	0.703	0.746	0.762	84 %	88 %	89 %	**87 %**
0.25 %	0.802	0.819	0.833	96 %	96 %	98 %	**96 %**
0.13 %	0.830	0.844	0.852	99 %	99 %	100 %	**99 %**
0.06 %	0.831	0.844	0.852	99 %	99 %	100 %	**99 %**
0.03 %	0.821	0.848	0.857	98 %	99 %	100 %	**99 %**
0 %	0.838	0.852	0.854	100 %	100 %	100 %	**100 %**

Table 4: OD values and % of survival after a 24 h treatment at different concentrations of the C:Q (1:1) extract.

[Q] %	OD P1	OD P2	OD P3	% survival plate 1	% survival plate 2	% survival plate 3	% survival Mean
2.00 %	0.728	0.649	0.658	81%	74%	74%	**76%**
1.50 %	0.849	0.811	0.812	95%	92%	91%	**93%**
1.00 %	0.765	0.683	0.691	86%	77%	77%	**80%**
0.75 %	0.793	0.698	0.712	89%	79%	80%	**83%**
0.50 %	0.746	0.751	0.773	84%	85%	86%	**85%**
0.25 %	0.890	0.859	0.884	100%	97%	99%	**99%**
0.13 %	0.962	0.854	0.911	108%	97%	102%	**102%**
0.06 %	0.973	0.852	0.896	109%	97%	100%	**102%**
0.03 %	0.864	0.880	0.911	97%	100%	102%	**100%**
0 %	0.893	0.882	0.894	100%	100%	100%	**100%**

Table 5: OD values and % of survival after a 24 h treatment at different concentrations of the Camellia sinensis extract.

[C:Q (1:1)] %	OD P1	OD P2	OD P3	% survival plate 1	% survival plate 2	% survival plate 3	% survival Mean
2.00 %	0.805	0.732	0.711	94 %	86 %	84 %	**88 %**
1.50 %	0.929	0.868	0.840	109 %	102 %	99 %	**103 %**
1.00 %	0.847	0.794	0.746	99 %	94 %	88 %	**94 %**
0.75 %	0.826	0.767	0.719	97 %	91 %	85 %	**91 %**
0.50 %	0.818	0.755	0.698	96 %	89 %	82 %	**89 %**
0.25 %	0.825	0.768	0.713	97 %	91 %	84 %	**90 %**
0.13 %	0.983	0.930	0.877	115 %	110 %	103 %	**109 %**
0.06 %	0.957	0.917	0.889	112 %	108 %	105 %	**108 %**
0.03 %	0.897	0.873	0.854	105 %	103 %	100 %	**103 %**
0 %	0.854	0.847	0.850	100 %	100 %	100 %	**100 %**

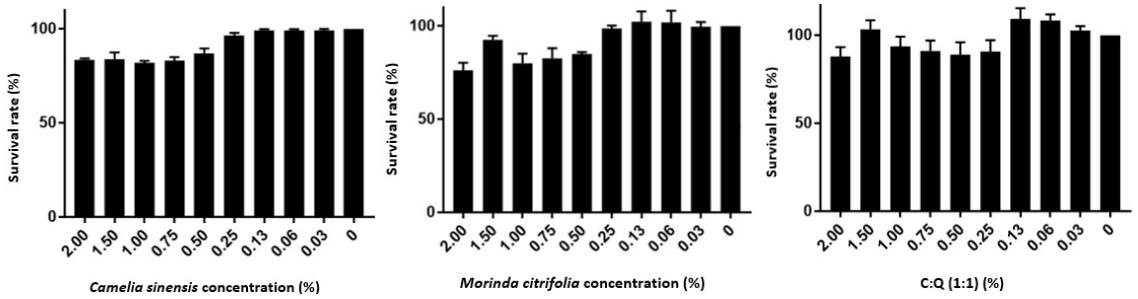

Figure 13: Bar graphs representing the % of survival after a 24 h treatment at different concentrations of the Camellia sinensis, Morinda citrifolia or C:Q (1:1) extracts.

The analysis of the presented results showed that, for both the *Camellia sinensis* and the *Morinda citrifolia* extracts, the highest concentration that did not present significant differences in cell survival compared with the control, is the 0.25 % concentration. In the case of the C:Q (1:1) extract, none of the concentrations tested showed a significant difference in cell survival compared with the control.

Based on these results, the concentration of 0.25 % was established as the optimal working concentration because it was the highest concentration at which the cell survival was not diminished for any of the plant extracts tested. In the case of the C:Q (1:1) extract a 0.25 % concentration refers to a solution prepared with a 0.25 % of the *Camellia sinensis extract* and 0.25 % *Morinda citrifolia* extract.

6.2. EVALUATION OF THE EXPRESSION OF THE TLR2 AND TLR4 RECEPTORS ON HaCaT CELL LINE BY FLOW CYTOMETRY

TLR2 and TLR4 are responsible for the recognition of *C. acnes* (77), and the triggering of the consequent inflammatory response, during an acne episode. The expression of TLR2 and TLR4 in the HaCaT cell line was evaluated trough a flow cytometry assay, under basal conditions and after the stimulation with *C. acnes*.

Flow cytometry is an analytical methodology which can be used for the characterization of cell populations. The technic is based on the injection of the sample fluid into the cytometer in a one cell at a time flow. Cells are then illuminated with a laser. The light scattered after the interaction with the cell, give information about cell characteristics. Apart from that, the cells can be marked fluorescent labels which, after its excitation by the laser beam, emit at a concrete wavelength, giving information about cell components. Flow cytometry technic allows the analysis of thousands of cells in a short period of time, which makes its use helpful for the analysis of whole cell populations (78).

The results presented in Table 6 and in Figure 14 proved that the HaCaT cell line express the two receptors responsible for *C. acnes* recognition. The results also demonstrated that a 48-h treatment with *C. acnes* increases the expression of both TLR2 and TLR4, providing evidence of the interaction of the bacteria with the two receptors.

Table 6: Tabulated results of the TLR2 and TLR4 expression

Sample	**TLR2 Expression**	**Relative expression of TLR2 (Compared with the basal expression)**
Non treated cells (Basal)	77 %	**100%**
Cells treated with *C. acnes* 10 bact./cell	93 %	**121%**
Sample	**TLR4 Expression**	**Relative expression of TLR4 (Compared with the basal expression)**
Non treated cells (Basal)	37 %	**100%**
Cells treated with *C. acnes* 10 bact./cell	59 %	**159%**

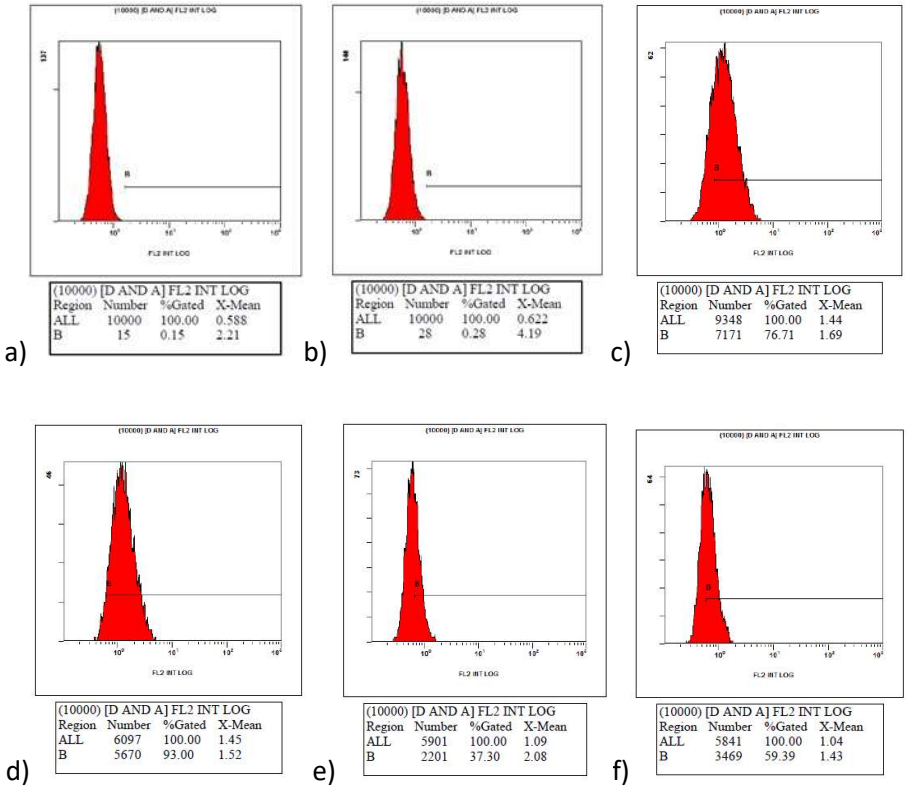

Figure 14: Cytometry histograms: a) DAPI control; b) Isotype control; c) TLR2 expression in basal conditions; d) TLR2 expression after the stimulation with C. acnes 10 bact. / cell; e) TLR4 expression in basal conditions; f) TLR4 expression after the stimulation with C. acnes 10 bact. / cell

6.3. EVALUATION OF THE PLANT EXTRACTS ANTI-INFLAMMATORY EFFICACY ON HaCaT CELL LINE AFTER THE STIMULATION WITH *C. acnes* BY qPCR

To determine the anti-inflammatory capacity of C, Q, and C:Q (1:1) in an infection caused by *C. acnes*, the extracts were tested at a concentration of 0.25 % on cells in which the inflammatory response had been induced by stimulation with *C. acnes* to study if there was a reduction in the production of inflammatory mediators in relation with cells stimulated with *C. acnes* and not treated. The evaluation of the expression of the inflammatory mediators was performed by qPCR. Biological triplicates were performed, using 3 independent expansions from cells originating from the thawing of a single cryovial.

The relative quantification results obtained for the inflammatory mediators evaluated, IL-8, TNFα and CXCL1, after the HaCaT cells stimulation with *C. acnes* and after the stimulation with *C. acnes* together with the treatment with the plant extracts under assessment are presented in Table 7.

Table 7: Relative quantification results for the expression of inflammatory mediators IL-8, TNFα and CXCL1

	RQ (Relative to negative control)								
	IL-8			TNFα			CXCL1		
	Rep. 1	Rep. 2	Rep. 3	Rep. 1	Rep. 2	Rep. 3	Rep. 1	Rep. 2	Rep. 3
Negative control (untreated cells)	1.0	1.0	1.0	1.0	1.0	1.0	1.0	1.0	1.0
Cells + *C. acnes*	4.2	3.3	2.7	3.6	3.0	3.3	2.7	4.5	1.5
Cells + C. acnes + C (0.25%)	1.4	2.0	1.1	1.7	1.3	1.5	1.2	3.0	0.8
Cells + C. acnes + Q (0.25%)	2.1	1.4	0.9	1.8	1.2	1.5	1.4	1.5	0.6
Cells + C. acnes + C:Q 1:1 (0.25%)	2.5	1.4	1.1	1.2	1.0	1.3	1.7	2.7	0.8

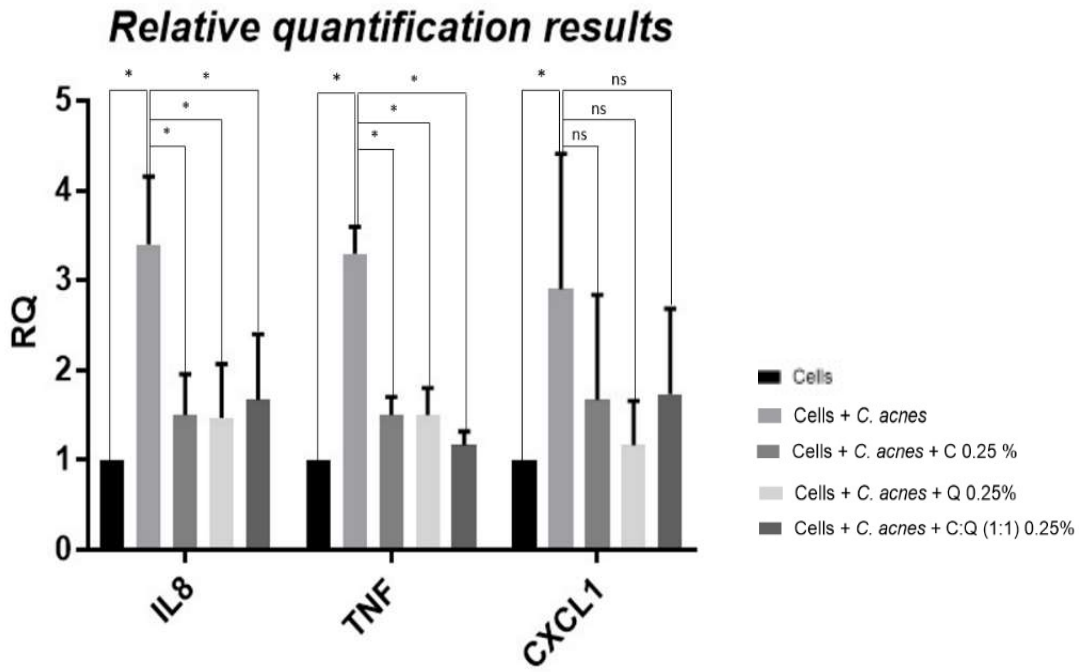

Figure 15: Graphic representation of the relative quantification results (RQ) obtained for the expression of inflammatory mediators IL-8, TNFα and CXCL1 after the HaCaT cells stimulation with C. acnes and after the stimulation with C. acnes and the treatment with the Camellia sinensis extract at 0.25%, the Morinda citrifolia extract at 0.25% or the C:Q (1:1) extract at 0.25%

The graphic representation of the results and its statistical analysis by ANOVA (Figure 15), show that there are statistically significative differences between the expression of all three evaluated inflammatory mediators between the negative control, consisting in cells without any treatment, and the positive control, consisting in the HaCaT cells stimulated with *C. acnes*. On

the other hand, all three treatments a significative reduction in the expression of the inflammatory mediators IL-8 and TNFα is observed, but none of the treatments achieve to significatively reduce the expression of CXCL1, even though a tendency can be observed.

Posteriorly, a pos-hoc analysis of the results was performed using Fisher Pairwise Comparison. In this statistical analysis, the different experimental conditions are grouped using letters, which indicate if there exist significative differences between the treatments. The treatments not sharing a letter present significative differences between them.

In the case of IL-8 (Table 8), it can be observed that all three treatments were grouped together with the negative control (letter A), indicating that the treatments achieved a reduction of IL-8 expression to the basal level, and the positive control was grouped separately (letter B), showing that the stimulation with *C. acnes* increased significatively the expression of this cytokine.

Table 8: Fisher Pairwise Comparisons for IL-8 expression. Grouping Information Using the Fisher Method and 95% Confidence. Means that do not share a letter are significantly different

Condition	N	Mean	Grouping	
Negative control (untreated cells)	3	1.00	**A**	
Cells + *C. acnes* + C (0.25%)	3	1.52	**A**	
Cells + *C. acnes* + Q (0.25%)	3	1.50	**A**	
Cells + *C. acnes* + C:Q 1:1 (0.25%)	3	1.66	**A**	
Cells + *C. acnes*	3	3.39		**B**

For TNFα (Table 9), there was also a significant reduction of TNFα expression with all three treatments, but only the treatment with C:Q (1:1) achieved to recover the negative control expression levels (letter A). Despite this, the treatments with C and Q extracts (letter B) presented significative differences with the positive control (letter C), indicating that they also caused a significative reduction of TNFα expression. It has also to be considered that the reduction caused by the treatment with C:Q (1:1) was not sufficient to be significatively different to the one achieved with the other two treatments.

Table 9: Fisher Pairwise Comparisons for TNFα expression. Grouping Information Using the Fisher Method and 95% Confidence. Means that do not share a letter are significantly different

Condition	N	Mean	Grouping		
Negative control (untreated cells)	3	1.00	**A**		
Cells + *C. acnes* + C (0.25%)	3	1.52		**B**	
Cells + *C. acnes* + Q (0.25%)	3	1.50		**B**	
Cells + *C. acnes* + C:Q 1:1 (0.25%)	3	1.18	**A**	**B**	
Cells + *C. acnes*	3	3.31			**C**

Finally, in the case of CXCL1 (Table 10), only the negative control (letter A) and the positive control (letter B) presented significant differences between them. The three treatments were shown to be in an intermediate situation (group AB) which indicated that there was a tendency of reducing the expression of the chemokine after the stimulation with *C. acnes*, but this reduction was not sufficient to be significative. This tendency might become a significant difference with an increase of the amount of analysis performed.

Table 10: Fisher Pairwise Comparisons for CXCL1 expression. Grouping Information Using the Fisher Method and 95% Confidence. Means that do not share a letter are significantly different.

Condition	N	Mean	Grouping	
Negative control (untreated cells)	3	1.00	**A**	
Cells + *C. acnes* + C (0.25%)	3	1.69	**A**	**B**
Cells + *C. acnes* + Q (0.25%)	3	1.16	**A**	**B**
Cells + *C. acnes* + C:Q 1:1 (0.25%)	3	1.75	**A**	**B**
Cells + *C. acnes*	3	2.89		**B**

6.4. EVALUATION OF THE TRANSLOCATION TO NUCLEUS OF NF-κβ AFTER THE STIMULATION WITH *C. acnes* ON HaCaT CELL LINE

As a final step for the evaluation of the C, Q, and C:Q (1:1) capacity to inhibit the inflammatory response, an assay was designed to evaluate the induction of NF-κβ transcription factor translocation to nucleus after the stimulation of the HaCaT cells with *C. acnes* and the inhibition of this translocation caused by a treatment with C, Q, and C:Q (1:1) extracts at 0.25%

concentration, as the activation of the NF-κβ canonical pathway is one of the principal mediators of the inflammatory reaction caused by the over proliferation of *C. acnes*.

Figure 16 shows the images obtained with the Leica TCS-SPE confocal microscope, located in the advanced microscopy service in the Diagonal Campus of Universitat de Barcelona. In the images, it can be observed how the cells without treatment presented a perfectly defined nucleus, stained with DAPI and shown in blue, in which no green fluorescence was observed. On the other hand, cells stimulated with *C. acnes* showed a high presence of NF-κβ, stained with Alexa Fluor® 488 and shown in green, in the cell nuclei. Finally, the cells stimulated with *C. acnes* and treated with the plant extracts of *Camellia sinensis*, *Morinda citrifolia* or C:Q (1:1), presented a greater amount of green fluorescence in the nuclei compared with the control cells, but it was clearly inferior to the amount observed in the cells stimulated with *C. acnes* and without treatment.

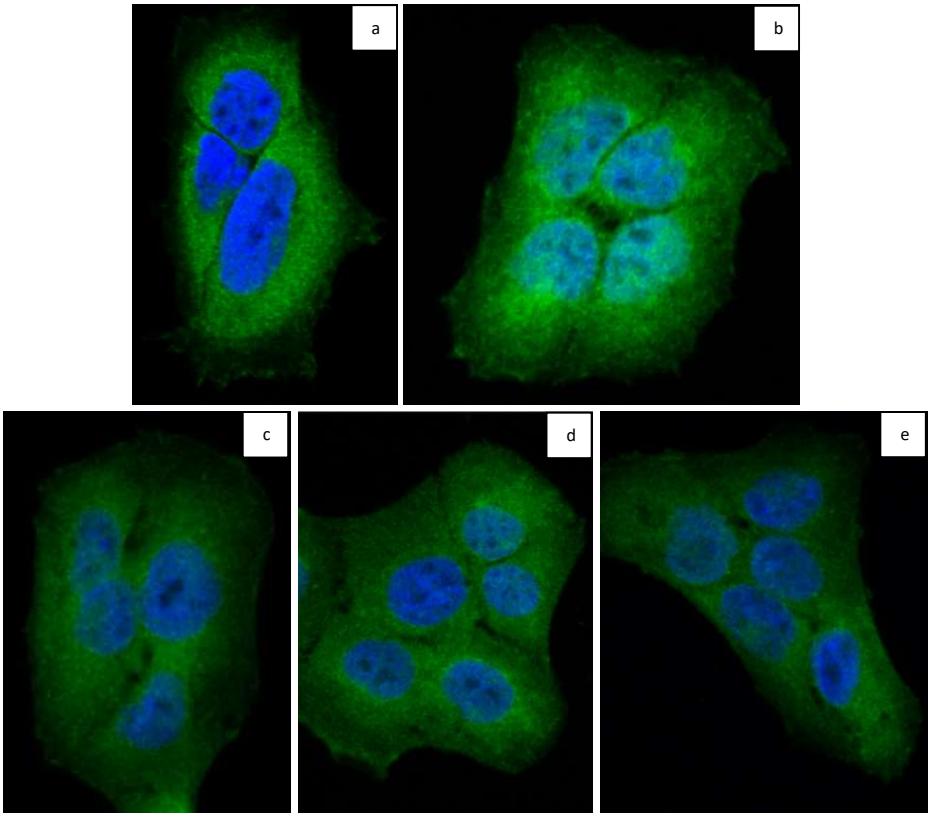

Figure 16: Leica TCS-SPE confocal microscope images. a) Negative control (untreated cells); b) Cells + C. acnes 1h; c) Cells + C. acnes + Camellia sinensis 1h; d) Cells + C. acnes + Morinda citrifolia 1h; e) Cells + C. acnes + C:Q (1:1) 1h.

The analysis of the blue and green fluorescence intensities obtained for 6 cell nuclei of each condition can be observed in Table 11, while Figure 17 shows an example of the fluorescence profiles obtained in each case. The results presented show how, in the case of the control cells, the blue fluorescence in the nucleus was much higher than the green fluorescence, while in the case of the cells stimulated with *C. acnes*, the intensity of both fluorescences were practically equivalent. The cells stimulated with *C. acnes* and treated with one of the plant extracts under assessment, presented an intermediate situation, proving that the three candidates had an impact in the reduction of NF-κβ translocation to the cell nucleus, reducing the inflammatory response produced in a *C. acnes* infection.

Table 11: Intensity results obtained for the analysis of 6 nuclei of each condition.

Sample	Replicate	Green fluorescence intensity	Blue fluorescence intensity	Ratio Blue/Green	Mean Ratio
CTRL	1	3,421	31,971	9.3	**7.1**
	2	6,412	28,383	4.4	
	3	5,484	34,158	6.2	
	4	4,956	37,684	7.6	
	5	4,610	37,047	8.0	
	6	5,016	35,006	7.0	
C. acnes	1	9,409	14,414	1.5	**1.4**
	2	9,383	15,522	1.7	
	3	11,626	10,875	0.9	
	4	10,846	13,321	1.2	
	7	6,728	9,423	1.4	
	8	6,231	8,769	1.4	
***C. acnes* + C 0.25%**	1	10,959	30,536	2.8	**3.2**
	2	7,190	25,094	3.5	
	3	11,260	17,270	1.5	
	4	7,459	32,124	4.3	
	5	8,225	26,703	3.2	
	6	9,047	32,542	3.6	
***C. acnes* + Q 0.25%**	1	9,064	17,797	2.0	**3.6**
	2	6,057	25,040	4.1	
	3	7,763	25,273	3.3	
	4	5,699	23,973	4.2	
	5	5,301	26,310	5.0	
	6	5,511	15,766	2.9	
***C. acnes* + C:Q (1:1) 0.25%**	1	5,850	21,348	3.6	**3.9**
	2	4,924	33,831	6.9	
	3	9,779	22,485	2.3	
	4	9,086	26,776	2.9	
	5	5,476	18,968	3.5	
	6	3,828	15,056	3.9	

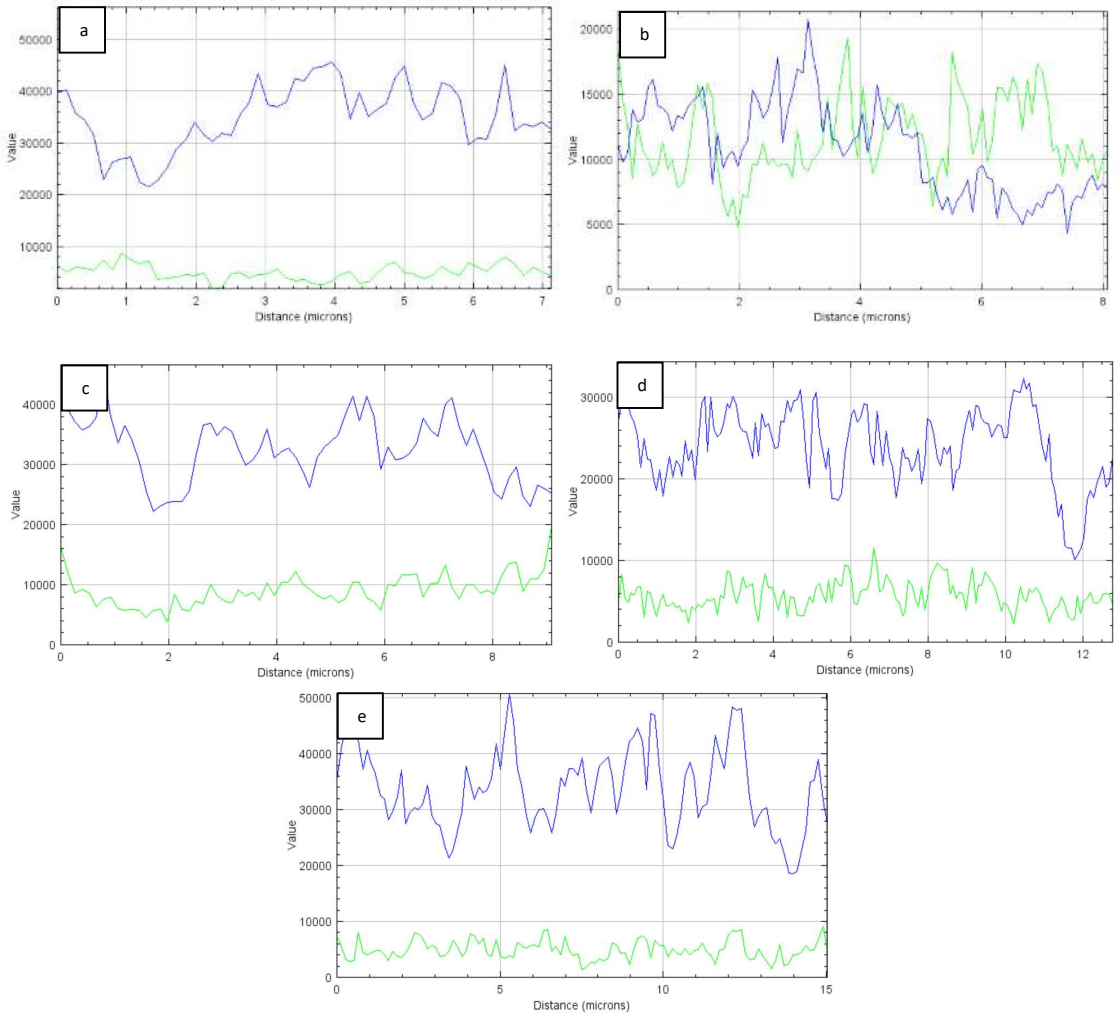

Figure 17: Analysis of the fluorescence profile in the cell nuclei. a) Negative control (untreated cells); b) Cells + C. acnes 1h; c) Cells + C. acnes + Camellia sinensis 1h; d) Cells + C. acnes + Morinda citrifolia 1h; e) Cells + C. acnes + C:Q (1:1) 1h.

8. DISCUSSION OF CHAPTER 1

The skin is the organism's first protection barrier against external harm, and it accounts with a specialized community of microorganisms, which prevent other microbes for its colonization, and specific cellular structures for the detection of pathogen associated molecules to trigger the corresponding innate immune response in case of microbial invasion (33,35). One of the main receptor families responsible for the detection of foreign pathogens are the TLRs (48).

The disruption of the equilibrium stablished between the microbiome and its host can cause the recognition of the symbiotic microorganisms as noxious, which may lead to the development of skin pathologies such as acne, one of the most common skin disorders, which is mediated though the over proliferation of *C. acnes* and the interaction of its PAMPs with TLR2 and TLR4, triggering an inflammatory reaction in the skin (41,48).

Inflammation is one of the main biological processes related with the symptomatology of diseases and, many times, the main cause of the adverse effects of pathologies. Because of that, a lot of research has been performed, focused on the discovery of new pharmaceutical products capable of modulating the inflammatory response produced in the organism (79). On the other hand, many of the products used for this purpose over the years, such as NSAIDs and corticosteroids, have been proved to cause severe adverse effects, which make its chronical use non recommended (80).

Considering that acne is not a sever pathology and adding to this the fact that the anti-inflammatory chemicals abuse is non-recommended, the recuperation of the use of traditional medicine, based on natural active ingredients, is a good option for consideration.

RJF aims to develop a skin cream, based on plant extracts as active ingredient, for the treatment of outbreaks of acne, which have an impact in the quality of life of the subjects suffering them due to the stigmatization related with the appearance of skin lesions. Plant extracts from medicinal plants, such as *Camellia sinensis* or *Morinda citrifolia*, contain molecules with known anti-inflammatory potential, which make them good candidates for the development of that new therapeutic product. Besides to the consideration of the two extracts separately, the efficacy of a combination of both was also evaluated.

HaCaT cell line was chosen as the study model since keratinocytes are, together with sebocytes, the main cells responsible for the triggering of the inflammatory response in the pilosebaceous units in consequence of *C. acnes* over proliferation sensing (55).

The assessment of the anti-inflammatory capacity of the two plant extracts separately and combined proved that the three candidates to be the active ingredient of the cream in development achieved a significant reduction for IL-8 and TNFα cytokines expression in an infection caused by *C. acnes*. These two cytokines are two important mediators of the inflammatory response triggered, and their reduction will probably relate with an improvement of the symptomatology. Additionally, even though its reduction was non-significant, a tendency in the decrease of the chemokine CXCL1 was also observed after the cells' treatment with the compounds. Chemokines are important recruiters of the immune cells in an inflammatory reaction, and its reduction is expected to also have a positive impact in an acne outbreak.

Added to the quantitative reduction in the chemokine expression caused by the three treatments tested, a qualitative decrease of the NF-κβ nuclear translocation after a *C. acnes* infection was also observed after the treatment of the cells with the plant extracts. NF-κβ in one of the main mediators of the inflammatory reaction in the organism and the blocking of this signalling pathway is expected to have a major effect on the reduction of the inflammatory response, probably on most inflammation mediators, additionally to the ones studied, as NF-κβ in implicated in the activation of their genes' transcription.

Even though a synergy in the anti-inflammatory efficacy of the two plant extracts is not evidently observed in the C:Q (1:1) treatment, as there is only an increased non-significant reduction in the case of TNFα, compared with the effect obtained with the two extracts separately, it would be interesting to include both compounds in the final product. This observation comes from the fact that, additionally to the anti-inflammatory effect, the extracts present other characteristics which might be attractive for the final product. There is evidence that *Camellia sinensis* presents antimicrobial and antioxidant properties (70), while *Morinda citrifolia* has antimicrobial effect and prevents the biofilms formation (75,76). As mentioned, the antimicrobial activity and the capacity of impeding the formation of biofilms are desirable as acne is characterized by an excessive proliferation of microbiome on human skin and these properties of the extracts would help to minimize this proliferation. On the other hand, the formation of reactive oxygen species is one of the consequences associated with the activation of the NF-κβ (81), and its presence contributes to an increment in the inflammatory response in the area, generating a positive feedback loop, negative for the progression of acne symptomatology. The antioxidant properties of *Camellia sinensis* may contribute to the interruption of this positive feedback loop, improving the symptoms on the skin.

With all this in mind, the next step will be to develop a cream for the treatment of acne that contains as active ingredients a combination of the extracts of *Camellia sinensis* and *Morinda citrifolia* in a ratio of 1 to 1. Once the final product is developed, proper bioassays for the testing of the efficacy and safety of the anti-acne cream will be required.

CHAPTER 2: DEVELOPMENT OF TWO *IN-VITRO* ASSAYS FOR THE ASSESSMENT OF THE POTENCY OF A ROMIPLOSTIM BIOSIMILAR

9. INTRODUCTION TO CHAPTER 2

9.1. IMMUNE THROMBOCYTOPENIA

Immune Thrombocytopenia is a bleeding disorder characterized for the presentation of a low platelet count, inferior to 100 x 10^9 platelets per litre of blood (82,83). It can appear in both children and adults, although the usual onset of the disease occurs during childhood, adolescence or in elderly (84). The disease can be presented as primary ITP if it is not associated with any other condition, or as secondary ITP if it has an underlying cause (85). Most of the ITP cases correspond to primary IPT, while only the 20% are secondary (82). The incidence of primary ITP oscillates between 2 and 4 cases per year per 100,000 people presenting a prevalence in the adult population around 9.5 cases per 100,000 people. The impact in women is slightly superior during adulthood, even though the prevalence of the disease equilibrates between men and women in the elderly (85–87).

9.1.1. Causes of Immune Thrombocytopenia

Most cases of primary ITP are mediated by two different mechanisms. In the first place, in around 60% of the patients suffering from primary ITP, the presence of pathologic anti-platelet IgG antibodies can be observed (88). These antibodies are mainly directed against GPIIb/IIa and GP1b/IX/V glycoproteins, abundant in the platelet surface (89), and contribute to the opsonization of the platelets marking them for their destruction (90) by splenic macrophages, clearing them from circulation (91). After the degradation of the platelets, macrophages present the derived peptides to CD4+ autoreactive T cells (91,92), which then interact with B cells, which become differentiated antiplatelet antibody producing cells (93). The pathologic ITP mechanism varies between different patients mainly depending on the antigenic determinant to which the autoreactive antibodies are targeted (94).

The second main cause of primary IPT, is the recognition of the glycoproteins expressed by the platelets also in megakaryocytes surface (95,96). The presence of autoantibodies directed to these proteins leads to megakaryocytes destruction which causes defective megakaryocytopoiesis (97), abnormal megakaryocytes apoptosis or reduced megakaryocytes growth (98,99). These mechanisms lead to an inhibition of the production of new platelets (90).

The development of secondary ITP is associated with the presence of underlying causes. The conditions most connected with secondary ITP are systemic autoimmune diseases, immunodeficiencies, infections and malignancies (87,100). Each disease presents different mechanisms which may lead to secondary ITP onset, but generally, the pathology of secondary ITP can be explained by the generation of cross-reactive antibodies, able to recognise platelets, developed as a consequence of a previous infection or vaccination (101,102), and by the existence of direct cytotoxicity against platelets or megakaryocytes due to the underlying pathology (103,104).

9.1.2. Symptomatology of Immune Thrombocytopenia

Even though one-third of ITP patients do not present symptoms (83), bleeding, derived from the thrombocytopenia is common. Bleeding symptoms occurring in mucous membranes, appearing in the form of bruising, petechiae and epistaxis, and the appearance of blisters in the oral cavity are the most observed (105), but in the most severe cases of the disease patients can also suffer from gastrointestinal, intracranial, or genitourinary haemorrhages (106,107). Bleeding symptoms are usually accompanied with fatigue and anaemia (108).

In the cases in which ITP becomes chronic, patients present a higher risk of suffering from thromboembolism (109). The risk of mortality appears to be approximately 1.5-fold superior in patients suffering from ITP than in the general population (110). The causes of death which present a higher impact in patients suffering from ITP are cardiovascular events, haemorrhages, infections, and blood related neoplasia (111).

All together, these symptoms contribute to poor quality of life scores for the patients suffering from ITP (112,113).

9.1.3. Diagnosis of Immune Thrombocytopenia

The diagnosis of ITP is mainly based in the analysis of the patient's clinical history and in a peripheral blood smear, in which a blood sample is examined under a microscope to evaluate the blood cell count. Tests for the evaluation of the existence of underlying diseases which could be related with secondary ITP are also recommended, along with an analysis of the patient's antiglobulins (114,115).

9.1.4. Treatment of Immune Thrombocytopenia

The first line management for primary ITP has been for many years the immunosuppression for the reduction of the production of anti-platelet auto-antibodies with a treatment with Prednisone in a dose of 1mg/kg/day during between 2 and 4 weeks (116,117). This treatment is highly effective in most of the patients, but it commonly associates with severe adverse effects (118).

Splenectomy has been for long the procedure of choice for second line management of the disease, as the removal of the spleen decreases platelet destruction as it has a role in the elimination of platelets marked, and in the production of anti-platelet antibodies (114). However, there is recent evidence suggesting that patients that undergo splenectomy present a higher risk of suffering from infection, thrombosis, haemorrhage, venous thromboembolism, and pulmonary hypertension, together with a high risk of immediate complications directly derived from the surgery (119,120).

More recent approaches investigated the benefits of alternative treatments, as for example the treatment with dexamethasone or rituximab (117), but, even though these treatments, presented better remission rates than the ones obtained for prednisolone, (121–123) they do not achieve remission rates as good as the ones obtained with splenectomy (124).

New approaches for ITP treatment, using thrombopoietin receptor agonists, which aim to increase the platelet number instead of seeking for the prevention of platelet destruction, present new opportunities for the patients (125).

The treatment of secondary IPT is usually focused on the treatment of the underlying cause, despite this, the most severe cases require specific treatment for the thrombocytopenia to control the platelet number (82).

9.2. THROMBOPOIETIN

In 1958, the existence of a growth factor responsible for causing an increase in platelet synthesis was firstly proposed by Professor Endre Kelemen. The term used to describe this substance was thrombopoietin (TPO) (126). In the following years, many efforts were made to purify this hematopoietic growth factor, but it was not until 1994 when several research groups achieved, almost at the same time, the purification the hormone (127–131). Following this achievement, the structure of the protein was elucidated.

TPO is produced in the form of a precursor which consists in a 353 amino acids peptide (132). After its secretion, the pre-protein suffers several modifications, including the elimination of the 21 amino acids forming the secretory leader sequences and a posterior glycosylation (133), which leads to the formation of a two-domain glycoprotein, composed by 332 amino acids (134), which is the mature TPO.

The TPO amino-terminal domain consists in the first 153 amino acids in the protein sequence, and it contains an EPO-like domain formed by a four alpha helixes bundle, which presents high homology with human erythropoietin binding domain (134). This domain is the one responsible for the protein binding to its receptor (127), concretely through the residues Arg10, Lys14 and Arg17, located in the first α-helix, and His133, Gln132, Lys138 and Phe141, located in the fourth α-helix (135,136). Despite the high similarities between TPO and EPO the specificity of each of these two proteins for its receptor is high and they do not compete for each other receptor binding (137).

The TPO carboxy-terminal domain is found between amino acids 154 and 332 of the sequence (58) and it is responsible for conferring stability to the molecule (139), thanks to the addition to its carbons of multiple N- and O- residues during the glycosylation of the molecule (140,141). The carboxy-terminal domain is also important for the correct folding of the protein, due to its function as chaperone (142,143).

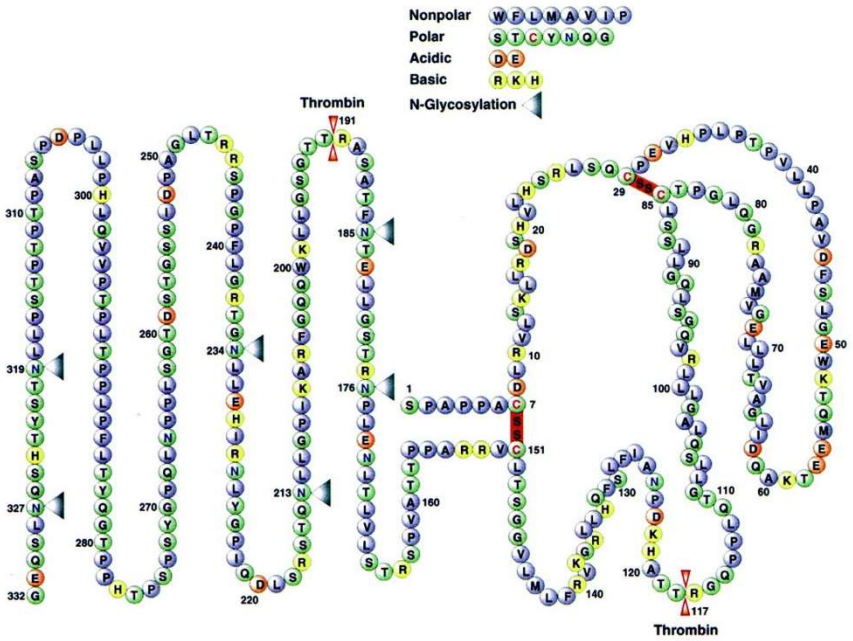

Figure 18: TPO structure (144).

TPO is produced mainly by the liver, specifically by the parenchymal cells, and delivered to the blood flow directly from hepatocytes with no previous storage. In physiologic conditions TPO liver production is constant (145). Secondary sites of TPO production, with a much lower production rate, are the kidneys and the bone marrow (146).

9.3. THROMBOPOIETIN RECEPTOR

The action of TPO is mediated though the binding of the hormone to its receptor, the thrombopoietin receptor (TPO-R), also known as c-Mpl, as it is encoded by the myeloproliferative leukaemia virus oncogene (147). TPO-R expression occurs mainly in the hematopoietic cells, including megakaryocytes, platelets, and hematopoietic stem cells. The TPO-R is formed by a sequence of 635 amino acids, and it presents three distinguished domains, the extracellular domain, the transmembrane domain, and the cytoplasmic domain (148).

The domain responsible for the binding of TPO is the extracellular domain. It is formed by two cytokine receptor homology modules, each formed at its turn by two fibronectin-III-like domains, each of which consists in seven antiparallel β-strands piling to form a β-sandwich. TPO binds to the region formed in the connection between the two fibronectin-III-like domains in ECD (149,150).

The transmembrane domain of the TPO-R presents a helical structure and it is responsible for fixing the receptor to the cell membrane and it also has an important role in determining the state of activation of the receptor (150), as it presents residues and regions both in the C-terminal and the N-terminal of the domain, which change of conformation after TPO binding allowing the dimerization and activation of the TPO-R (151). The orientation of the transmembrane domain residues in absence of TPO is responsible for the prevention of the constitutive activation of the receptor (152,153).

The cytoplasmatic domain does not present a defined secondary structure (146) and it is responsible for the intracellular signalling after TPO binding.

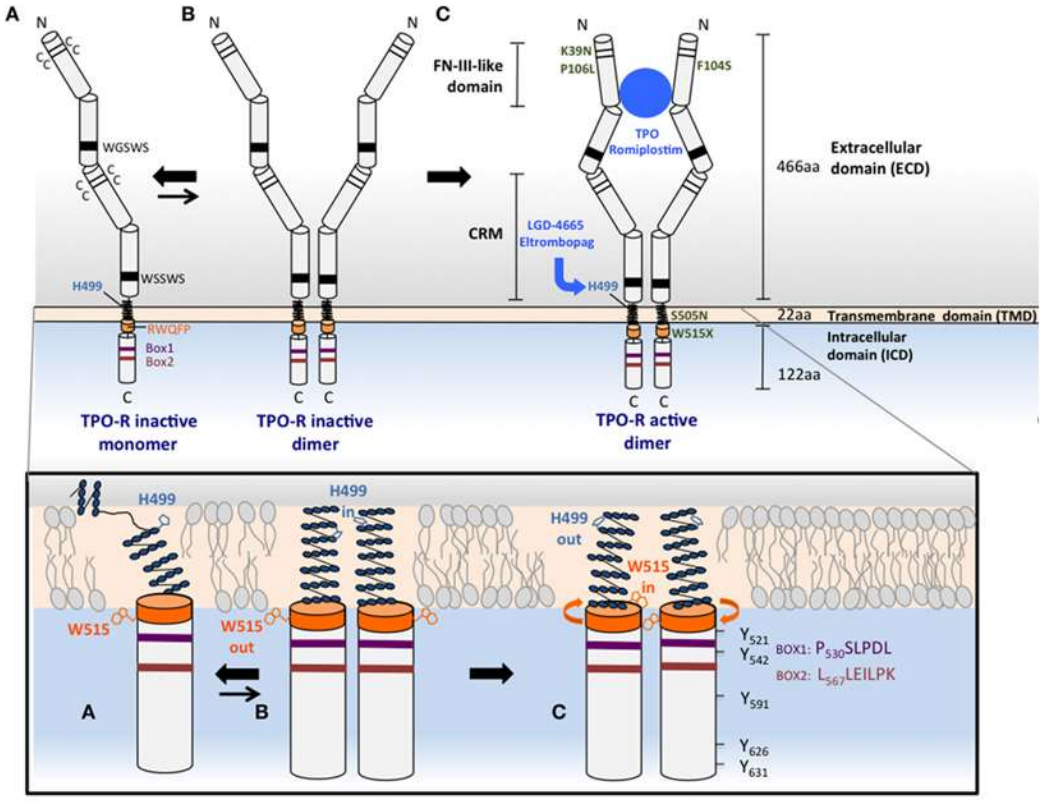

Figure 19: TPO-R structure. A) TPO-R inactive monomer; B) TPO-R inactive dimer; and C) TPO-R active dimer (148).

9.4. THROMBOPOIETIN – THROMBOPOIETIN RECEPTOR BINDING

When thrombopoietin binds its receptor in the most distal CRH of the two CRH present in the receptor's extracellular region, it produces a change of receptors conformation which causes the activation of JAK, JAK2 and TYK2 kinases (154), which are united with the TPO-R cytoplasmatic portion. These kinases are responsible for the phosphorylation of the receptor in five tyrosine residues (Y521, Y542, Y591, Y626, and Y631) present in the intracellular domain (148). The phosphorylation of Y521 an Y591 activates negative feedback pathways (155) as it induces the receptor internalization (156) and its destruction trough lysosomal digestion and ubiquitin mediated proteasomal degradation (157). On the other hand, the phosphorylation of Y626 and Y631 induces the activation of the MAPK signalling pathway, important for cell maturation, trough the phosphorylation of Shc adaptor protein (158,159). Additionally, TPO binding with its receptor is also responsible for activation of the kinase pathways PI3K/AKT and Raf/MAP, which are important pathways involved in cell survival (160).

Finally, the kinases associated with the receptor also cause the phosphorylation of STAT1, 3 and 5 transcription factors, initiating the signalling cascade for the transduction of the signal to the cell nucleus and the induction of cell proliferation (161).

9.5. THROMBOPOIETIN BIOLOGICAL ACTIVITY

The two main roles of TPO are the conservation of the HSC and the induction of platelet formation. The activation of anti-apoptotic pathways after the activation of TPO-R by its union with TPO it important for the HSC survival, ensuring the maintenance of the hematopoietic stem cells and precursors reservoir (162). In the second place, TPO is responsible for the generation of megakaryocytes from HSC. Additionally, it has been shown to play a role in the early maturation of the stem cells into other hematopoietic linages (163). The activation MAPK signalling pathway induces megakaryocytic maturation into polyploid cells by the initiation of endomitosis, which consists in the repetitive duplication of the genetic material with no cell division occurring between the different DNA replication cycles (164).

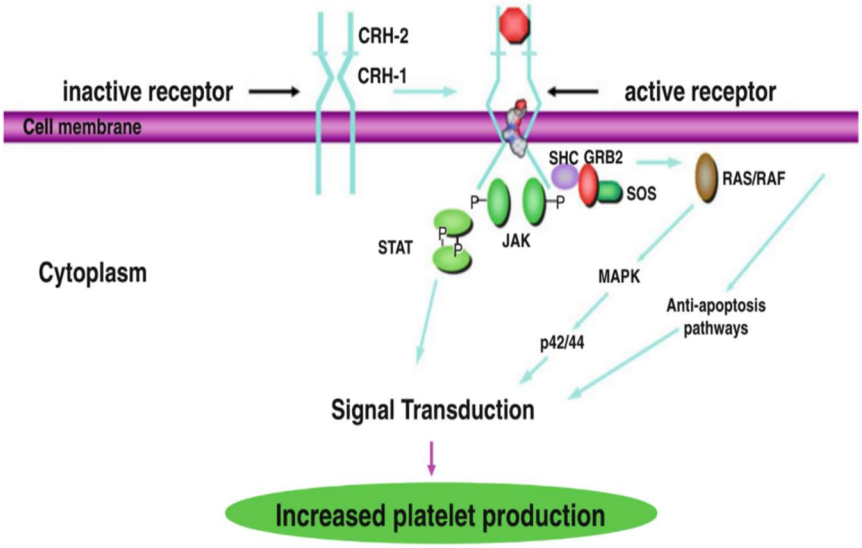

Figure 20: Thrombopoietin receptor activation signaling cascade

9.6. REGULATION OF THROMBOPOIETIN AVAILABILITY

As mentioned, TPO shows a continuous production which makes the existence of mechanisms for the regulation of its availability in blood essential. TPO availableness presents a directly proportional relationship between the platelet blood counts and the TPO removal from blood. Platelets present TPO receptor in its surface which internalize and degrade TPO after its binding, therefore at lower platelet amounts there is less TPO elimination and consequently there is more of it available for platelet production induction. When platelet counts are high the invers situation occurs (165).

9.7. NEW APPROACHES FOR ITP TREATMENT

9.7.1. First generation thrombopoietic drugs

Shortly after the cloning on TPO, the first generation of thrombopoietic drugs appear. The two products included in this group of drugs, which achieved clinical trials stage in its development, were RhTPO, a recombinant human thrombopoietin identical to the endogenous form, and PEG-rHuMGDF, a truncated form of recombinant TPO, consisting in the 163 amino terminal amino acids conjugated with polyethylene glycol through a process denominated pegylation (166).

Both products were able to induce an increase of the platelet counts after its administration to subjects suffering from chemotherapy related thrombocytopenia. Despite this a significant number of the subjects involved in the clinical trial for PEG-rHuMGDF developed antibodies against the drug, which cross-reacted with endogenous TPO, inducing a worsening of the pre-existing thrombocytopenia days after the initiation of the treatment (133).

The detection of this adverse effect produced by PEG-rHuMGDF caused the discontinuity of all the clinical trials involving products related with a recombinant form of TPO.

9.7.2. Second generation thrombopoietic drugs

After the failure of the first generation thrombopoietic drugs the efforts were focused on the discovery of products with no homology with endogenous TPO but capable of inducing thrombopoiesis. The result of these efforts was the discovery of two novel drugs which were approved in 2008 by the FDA for the treatment of ITP in those cases in which the first line treatments were failing (167,168).

The first one of this two drugs was romiplostim. It was developed after the identification of a short peptide, formed by a sequence of 14 amino acids (ARAALWQRLTPGEI), capable of binding with the TPO-R. To increase the stability and the self-life in the organism, the final molecule was developed by conjugating the peptide with the human IgG1 Fc region. The dimerization of the peptide was necessary for the achievement of a biological activity equivalent to the one obtained with endogenous TPO. The final molecule consisted in two dimers, each of which formed by two identical chains, united through disulphide bonds, bound to the human IgG1 Fc region (Figure 21) (169).

Romiplostim acts as a TPO agonist through its high affinity union with the TPO-R which induces the activation of the same signalling pathways and cellular responses as TPO, increasing the platelet counts due to a stimulated production and a maximized platelet and platelet precursors survival (170).

During clinical trials and after, no significant adverse effects were detected. Apart from that, even though some patients presented antibodies against TPO and romiplostim, its presence did not show an impact neither in efficacy nor in safety of the developing drug, as those antibodies did not show neutralizing activity (171,172).

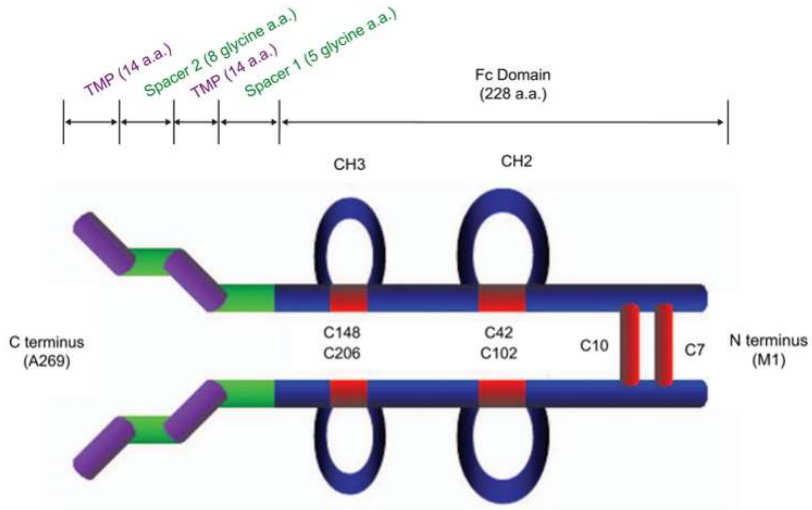

Figure 21: Romiplostim structure (167).

The second product developed was eltrombopag, which is a small molecule that conducts its effect through its interaction with the transmembrane domain of the TPO receptor, producing a modification of the receptor conformation, activating it. Even though eltombopag does not bind the receptor through the TPO binding site, its effect is specific on the TPO-R and the signalling cascade, and the cellular response produced by the drug is identical to the one observed for TPO (168).

Clinical trials showed the capability of eltrombopag of rising platelet representation in blood without the induction of severe adverse effects. The positive effect was maintained after ending the treatment (168).

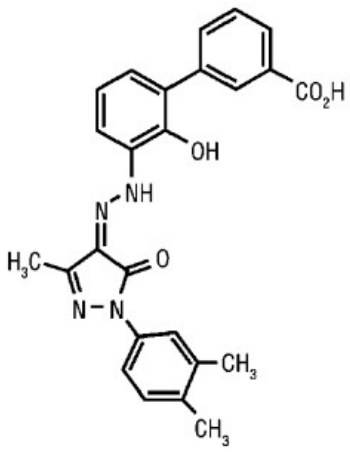

Figure 22: Eltrombopag structure (168).

9.8. DEVELOPMENT OF A ROMIPLOSTIM BIOSIMILAR IN RJF

RJF aims to develop a drug product intended to be a biosimilar to the reference product romiplostim, licensed and commercialized by Amgen under the trade name Nplate®.

For the development of the RJF biosimilar, three initial batches where manufactured based on the available information on the reference material product. Then, these three batches were compared with the reference product in a head-to-head study and optimized from there until the obtention of the final drug substance and drug product formula. Even though the reference product is presented in 3 different strengths, 125 µg, 250 µg and 500 µg, the strategy for product development was to start with the development of a 500-µg product with the possibility of moving to the other two strengths if desirable.

The steps taken for the assessment of RJF biosimilar quality aspects relate with the TPO-RA binding with TPO-R and with the biological activity of the product are discussed further in this thesis. The physicochemical characteristics of the product were assessed in a different department of the company and therefore not included.

9.8.1. Binding analysis by Biacore

Biacore systems are based on the surface plasmon resonance, which is an optical event that occurs in a layer of conducting material, commonly gold, placed between two media of distinct refractive indices. When a light beam with a concrete wavelength impact on the conducting material in the correct angle, produces the excitation of the plasmons in the surface, what causes a drop in the reflected light intensity (Figure 23)(173).

This phenomenon can be used to study molecular interactions as, for example, the ones occurring between a receptor and its ligand. The technique is based on the attachment of one of the two interacting components, denominated ligand, to the surface of a chip, then, the other component, denominated analyte, is injected in a constant and non-turbulent flow which passes over the chip. The interaction between the ligand and the analyte causes changes in mass on the sensor chip surface which modifies the refractive index of the surface (174).

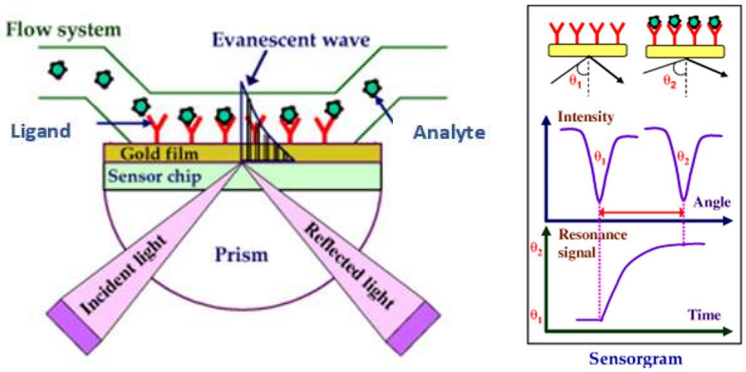

Figure 23: SPR technique principle (175).

These changes are registered in real time, creating a sensorgram which can be studied for the evaluation of the molecular interaction of the two compounds. Different stages of the interaction can be identified (Figure 24). When the injection of the analyte in solution starts, the binding of the analyte with the ligand produces an increase of the response, which is denominated the association phase. After saturation, an equilibrium between association and dissociation is achieved. After finishing the injection, the separation of the two molecules occurs, producing a decrease of the response, which corresponds with the dissociation phase. If dissociation is not complete, regeneration, which consists in a forced dissociation of the analyte from the ligand, is required to return to basal conditions. The analysis of the generated data using an adequate model permits the determination of the association and dissociation constants (176).

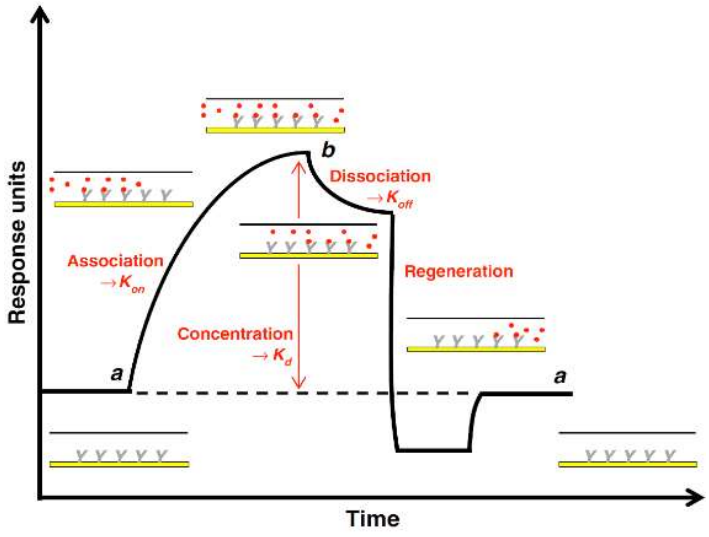

Figure 24: Sensorgram phases scheme (176)

9.8.2. Potency assays development

Potency is defined as the as the quantitative determination of the biological activity of a substance. Potency is related with therapeutic efficacy, and, because of this, its evaluation is essential for grating the quality attributes of the final pharmaceutical product (177).

The assessment of the biological function of an active ingredient and/or the final pharmaceutical product are evaluated though potency assays, which should be able to demonstrate that the final product presents the desired biological activity. The potency assays are also used for the confirmation of batch-to-batch consistency and for the detection of any loss of activity of the product during its self-life (178).

Before starting to develop a potency assay it is important to decide the information desired to obtain at the end of the treatment period (179). Depending on the type of response that wants to be measured the assays can be classified in different types:

- Early response assays: the assay endpoint occurs minutes after the application of the stimuli. An example of this type of assays would be a phosphorylation assay.
- Intermediate response assays: the assay endpoint occurs hours after the application of the stimuli. An example of this type of assays would be the study of changes in the gene expression.
- Late response assays: the assay endpoint occurs days after the application of the stimuli. An example of this type of assays would be a proliferation assay.

The advantages of using early or intermediate response assays are that they are less time-consuming and that, since a reasonably immediate effect is measured, the effect detected is more specific to the action of the drug. The main disadvantage is the fact that it is not possible to know if this first effect measured will end up causing a final effect in the cell, that is, the phosphorylation of the receptor may not end in cell division.

On the other hand, late-response assays have the advantage that they give information about the final effect produced by the product of interest, but they have the disadvantages that they require a longer assay time and that they are more likely to be affected by nonspecific effects.

Considering all of this, the ideal scenario, whenever possible, is to carry out an assay of each type to guarantee that the drug produces a specific response and that it leads to the desired

final effect. In the cases of the romiplostim biosimilar, two independent assays, a proliferation assay, and a gen-reporter assay, were developed.

9.8.3. Methods validation

Method validation consists in the process of demonstrating by the generation of documented evidence that the characteristics of an analytical procedure satisfy the necessities of its intended purpose. Method validation has the objective of assuring that the results which are going to be generated during methods use are reliable by proving that the method is linear, accurate, precise, specific, and robust within the range in which the samples will be analysed. The performance of an analytical method validation is required whenever a new method is developed but also when major modifications are made in the analysis technic or in the product formula, to guarantee the goodness of the procedure for the generation of adequate results (180).

The linearity of an analytical method is described as the capability of the procedure of providing a directly proportional response to the concentration of the sample being analysed within a defined sample's concentration range (180). The analysis of linearity allows the determination of the range where there is a linear dependency between de concentrations applied, and the response obtained, which is the maximum and minimum concentrations at which it is acceptable to work.

Precision indicates the closeness of agreement between a series of results obtained for a determined amount of analysis of a homogeneous test sample and under equivalent assay conditions. The analysis of precision determines the variability of the assay method. The precision of the method studies the variability intrinsic to the procedure, also known as repeatability, and it is determined by the repeated analysis of a unique sample under the exact same conditions. The intermediate precision studies not only repeatability but also reproducibility, and it considers causes of variability other than the method itself (180).

The accuracy of a method evaluates the similarity between the expected result of an assay, being this expected value the known potency of the reference product, and the experimental result (180).

Selectivity is defined as the method's capability of measuring the substance of interest without interference of the rest of compounds which might be present in the mixture, as for example, impurities, substances of degradation or the excipients matrix (180).

Robustness shows the capacity of the method to persist unaltered despite the occurrence of minor alterations in the procedure parameters (180).

10. RESULTS OF CHAPTER 2

10.1. COMPARISON OF THE RECEPTOR BINDING PROFILES BETWEEN THE TPO-RA RMP AND ITS BIOSIMILAR BY BIACORE

10.1.1. Determination of the active concentration of the samples

To determine the active concentration of the samples being analysed, a biacore system was designed to analyse test samples capacity to bind to αhIgG(Fc) mAb via their Fcγ fusion parts, irrespective of their TPO-R target binding potency. The correct quantification of the concentration of the products under assessment was essential to ensure that the differences obtained in the following assays were due to changes in the potency and not related with differences in the concentrations.

To do so, it was necessary to prove that there was a linear relationship between TPO-RA concentration and its binding with the αhIgG(Fc) mAb sensor chip. With this purpose, the reference TPO-RA was injected over the αhIgG(Fc) mAb sensor chip surface in a serial dilution range between 155 ng / mL and 2.4 ng / mL. The sensorgram obtained for the assay is presented in Figure 25 and the relative units results obtained at 320 report point after injection are presented in Table 12.

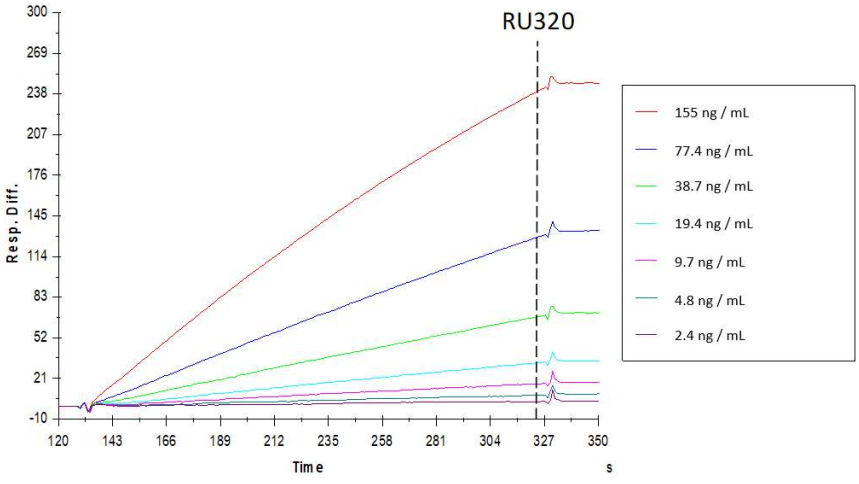

Figure 25: Serial Analyte Dilution Sensorgram for the the demonstration of a linear relationship between TPO-RA concentration and its binding with the αhIgG(Fc) mAb sensor chip.

Table 12: Relative units results obtained at 320 report point after injection for the demonstration of a linear relationship between TPO-RA concentration and its binding with the αhIgG(Fc) mAb sensor chip.

TPO-RA (ng / mL)	RU320
155.0	235.6
77.4	125.9
38.7	66.5
19.4	32.1
9.7	16.5
4.8	7.9
2.4	3.3

The representation of the relative unit values obtained from the sensorgram (Figure 26) showed a linear relationship between the TPO-RA concentration and the binding with the αhIgG(Fc) mAb sensor chip, which proved the suitability of the method for the determination of the active concentration of TPO-RA in the samples to be analysed.

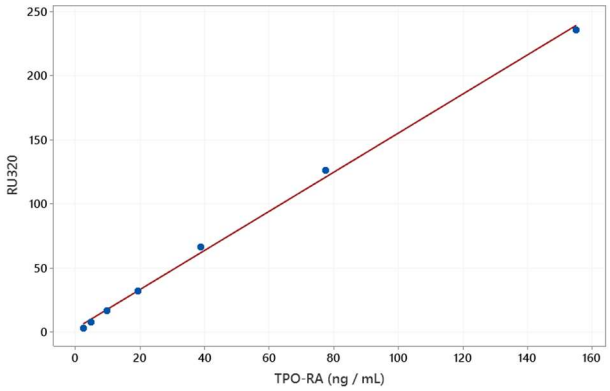

Figure 26: Representation of the 320 relative unit results obtained from the sensorgrams for the demonstration of a linear relationship between TPO-RA concentration and its binding with the αhIgG(Fc) mAb sensor chip.

10.1.2. Thrombopoietin-Thrombopoietin receptor binding characterization

To characterize the interaction occurring between TPO-R and TPO-RA, the first step taken was the determination of the linear range of the dose response curve. In SPR based assays dose response curves are derived from serial analyte dilution sensorgram plots by setting report points at defined sensorgram positions and plotting bound response units against sample concentration. Serial dilution sensorgrams were generated after the application of the reference

material in a serial dilution range between 1,235 ng / mL and 0.3 ng / mL. The report points after the injection time at 320 seconds, representative for equilibrium phase, and at 340 seconds, representative for the dissociation phase, were studied.

Figure 27 presents the sensorgrams obtained for the different dilutions of the TPO-RA tested, while Table 13 presents de relative unit values obtained at 320 and 340 seconds after the injection time.

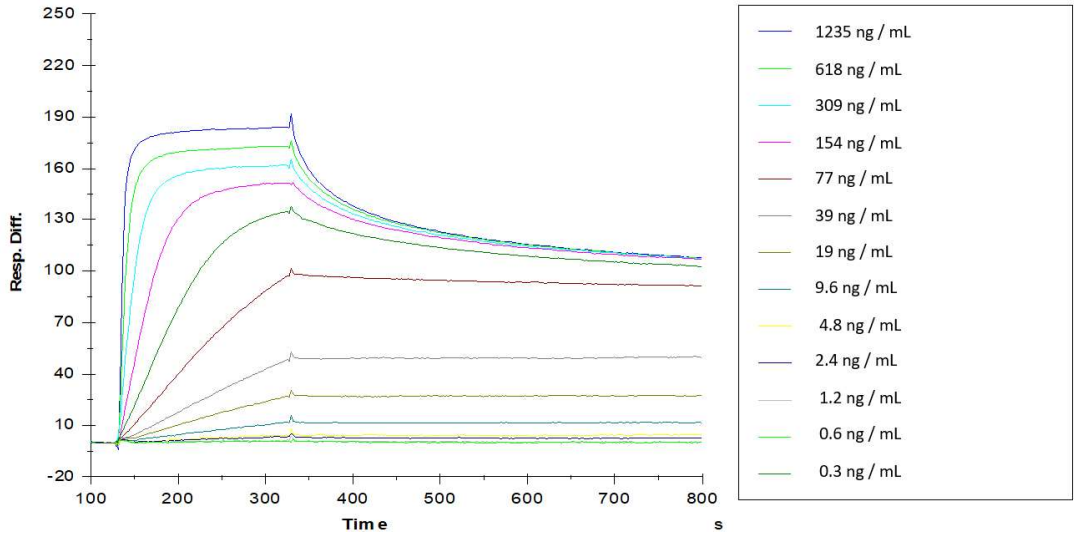

Figure 27: Serial Analyte Dilution Sensorgram for the determination of the linear range of the curve.

Table 13: Relative units results obtained at 320 and 340 report points after injection for the determination of the linear range of the curve.

TPO-RA (ng / mL)	RU320	RU340
1235.0	183.7	166.8
618.0	172.7	159.9
309.0	162.0	153.1
154.0	150.8	145.1
77.0	133.7	130.2
39.0	94.3	97.7
19.0	46.7	49.0
9.6	26.1	22.1
4.8	11.5	11.9
2.4	4.3	4.3
1.2	3.2	3.3
0.6	1.2	1.1
0.3	0.9	0.7

The representation of the 320 and 340 relative unit values obtained for the analysis of the sensorgram allows for the drawing of a dose response curve for the binding between the TPO and the TPO-RA and the calculation of the EC_{50}. Based on the results presented in Figure 28, the sensitive linear range of the logarithmic dose response curve can be seated between 10 and 100 ng / mL and the EC_{50}s obtained for the analysis of the results at 320 and 340 seconds after the injection were 37.6 ng / mL and 31.5 ng / mL, respectively.

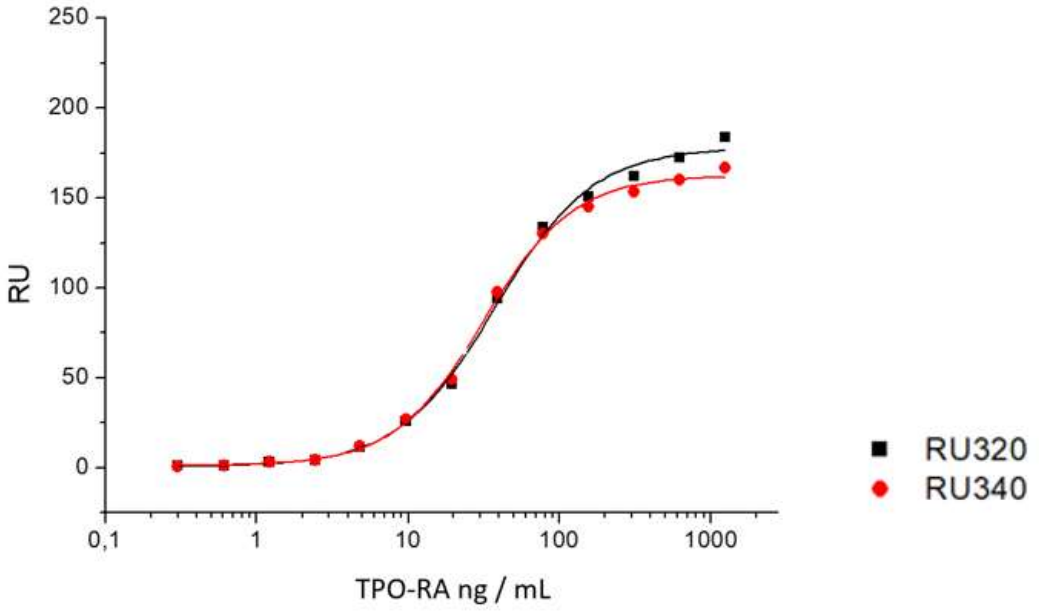

Figure 28: Representation of the 320 and 340 relative unit results obtained from the sensorgrams for the determination of the linear range of the curve.

To determine the capability of the system to discriminate between differences in the potencies of the compounds under assessment, dose response curves were generated on 824 RU TPO-R sensor chip surface density by applying serial analyte dilution curves prepared with the TPO-RA reference material corresponding to 80 %, 100 % and 120 % relative concentration. The report point at 340 seconds after the injection time was studied.

Figure 29, Figure 30 and Figure 31 show the sensorgrams obtained for the 3 dilution curves prepared, and Table 14 presents de relative unit values obtained at 340 seconds after the injection time.

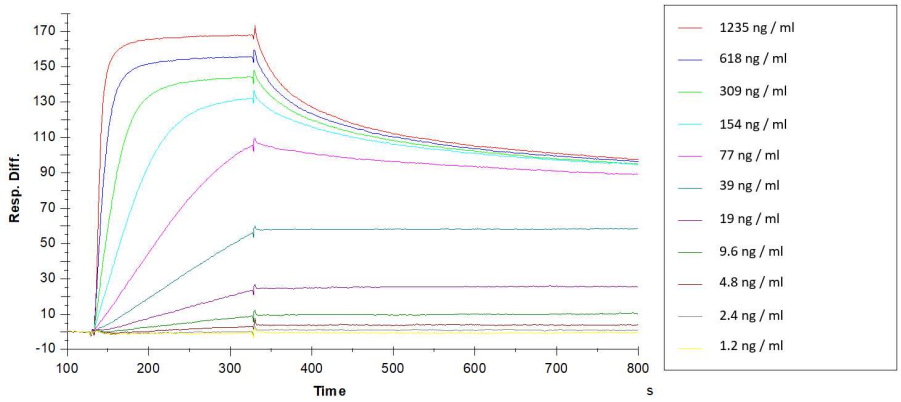

Figure 29: Serial Analyte Dilution Sensorgram ("100 % Potency") for the assessment of the accuracy of the method.

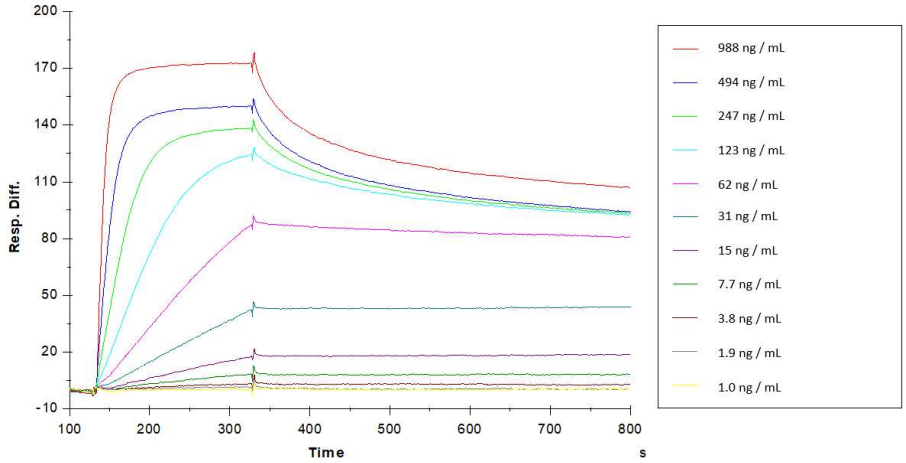

Figure 30: Serial Analyte Dilution Sensorgram ("80 % Potency") for the assessment of the accuracy of the method.

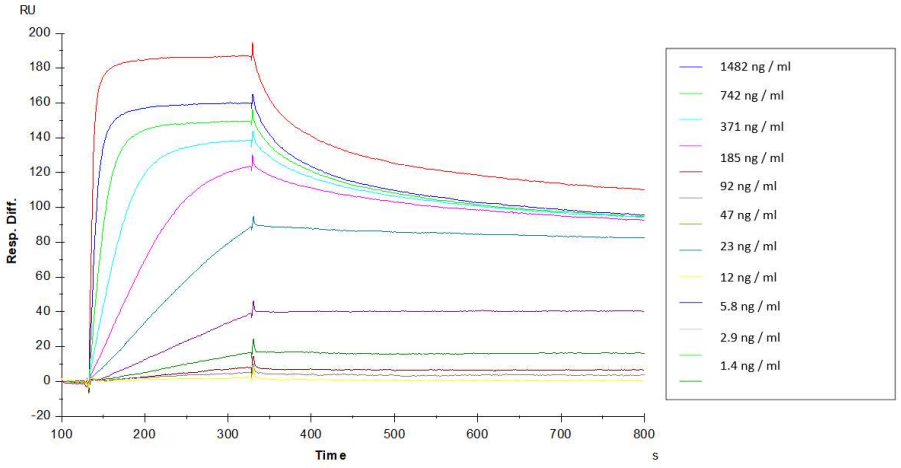

Figure 31: Serial Analyte Dilution Sensorgram ("120 % Potency") for the assessment of the accuracy of the method.

Table 14: Relative units results obtained at 320 and 340 report points after injection for the assessment of the accuracy of the method.

TPO-RA (ng / mL) (equivalent [ ] in 80% / equivalent [ ] in 120%)	Analyte serial dilution curve at 100%	Analyte serial dilution curve at 80%	Analyte serial dilution curve at 120%
1235 (988 / 1482)	157.1	162.9	172.1
618 (494 / 742)	147.2	142.2	149.6
309 (247 / 371)	138.6	133.6	141.9
154 (123 / 185)	129.1	122.6	133.4
77 (62 / 92)	106.0	88.3	121.3
39 (31 / 47)	57.5	43.4	89.6
19 (15 / 23)	24.6	18.3	40
9.6 (7.7 / 12)	9.5	8.6	17.2
4.8 (3.8 / 5.8)	4.1	3.7	7.5
2.4 (1.9 / 2.9)	0.9	1.6	5
1.2 (0.96 / 1.4)	0.9	0.5	1.9

The 340 relative unit values obtained for the analysis of the sensorgram were represented (Figure 32) and the EC_{50} of the 3 curves were calculated. The EC_{50} obtained for the curve corresponding to the sample at 100 % was 48.9 ng / mL, the one obtained for the sample at 80 % was 60.8 ng / mL and the one obtained for the sample at 120 % was 38.5 ng / mL. Relative to the 100 % potency sample, the EC_{50} value of the 80 % potency sample was 24 % higher, which indicates that the sample was 24 % less potent, and the ED_{50} value of the 120 % potency sample was 21 % lower, which indicates that the sample was 21 % more potent. With this results, it was determined that the method was suficiently accurate to detect differences in the interacction between the TPO-R and the analyte under analysis.

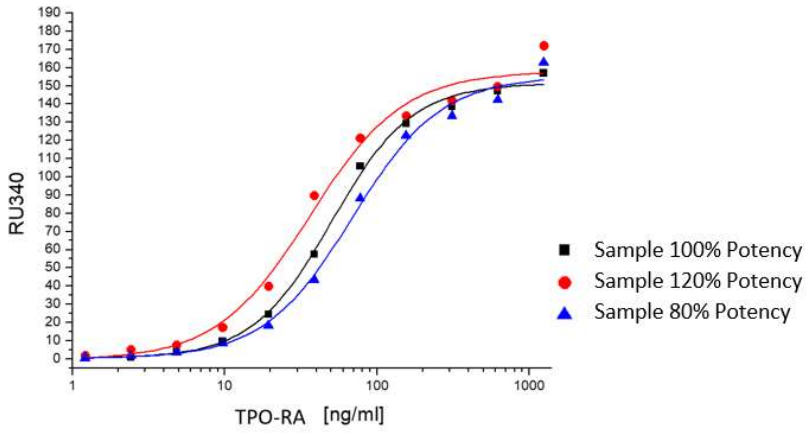

Figure 32: Representation of the 340 relative unit results obtained from the sensorgrams of the analyte serial dilutions at potency 100 %, 80 % and 120 % for the determination of the accuracy of the method.

10.1.3. Comparison between the reference material product and the biosimilar

Finally, after proving the adequacy of the biacore system to discriminate between differences in the potency, three batches of RJF TPO-RA biosimilar DS and three batches of RJF TPO-RA biosimilar DP were assessed. The results obtained were compared with the results of three batches of the reference material product to demonstrate similarity. Each sample was assessed twice, and the mean values obtained were used for the comparison.

For the analysis, all 9 samples were treated assuming its theorical concentration as correct. After the obtention of the EC_{50} of the samples, the results were corrected by the concentration obtained for each sample when assessed on the αhIgG(Fc) mAb sensor chip. The results presented in Table 15 show that the 9 samples analysed are comparable in terms of potency after the correction for the relative active concentration, proving equivalence between RMP and the RJF TPO-RA biosimilar drug substance and drug product.

Table 15: Results comparison between 3 batches of RJF TPO-RA biosimilar DS and 3 batches of RJF TPO-RA biosimilar DP with the TPO-RA reference material product.

Sample	Result 1 (EC_{50} ng / mL)	Result 2 (EC_{50} ng / mL)	Mean (EC_{50} ng / mL)	Relative Potency % (To the mean of the RMP)	Active concentration ng / mL	Relative Active concentration % (To the mean of the RMP)	Corrected Relative Potency %
RMP 1	38.3	41.2	39.8	90	80.9	95	**95**
RMP 2	35.7	38.1	36.9	97	77.9	99	**98**
RMP 3	25.9	36.3	31.1	115	72.2	107	**108**
DS 1	31.9	28.1	30.0	120	65.2	118	**101**
DS 2	35.3	27.7	31.5	114	70.3	110	**104**
DS 3	28.8	32.8	30.8	117	63.3	122	**96**
DP 1	37.8	43.2	40.5	89	79.2	97	**91**
DP 2	29.9	24.3	27.1	133	63.6	121	**109**
DP 3	31.3	26.1	28.7	125	60.2	128	**98**

To demonstrate that the 9 samples present a similar behaviour in terms of association and dissociation with the TPO receptor the sensorgrams obtained for the concentration of 154 ng / mL of all samples were compared. The results obtained are presented in Figure 33 and demonstrate a similar behaviour in terms of affinity with the TPO-R for the 9 samples under study.

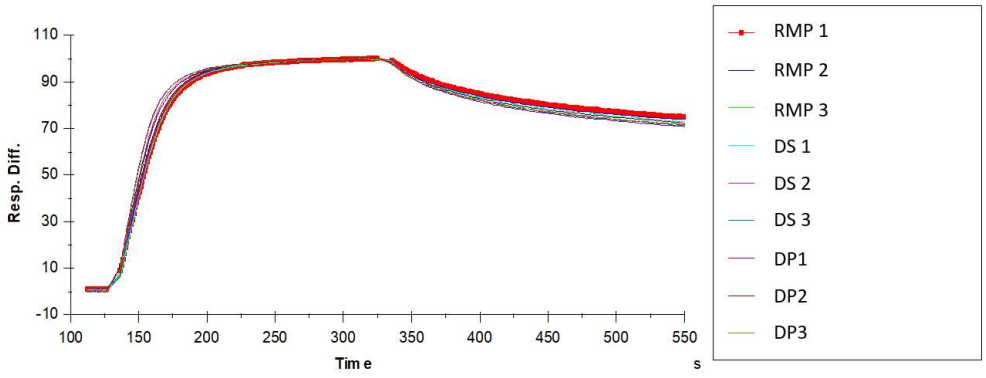

Figure 33: Superposition of the sensorgrams obtained for the concentration of 154 ng/mL for the 9 samples used in the similarity study.

10.2. DEVELOPMENT OF A POTENCY ASSAY BASED ON CELL PROLIFERATION

10.2.1. Cell line development

The first objective in the development of a cell proliferation bioassay capable of testing the potency of romiplostim biosimilar products was the development of a cell line intrinsically and stably expressing a functional human thrombopoietin receptor. The cell line of choice was the Ba/F3 cell line, which is a murine cell line, derived from BALB/c mouse strain, and dependent on IL-3 for its growth. The hMPL was introduced to the cell line by means of an infection with a lentivirus that had been transfected with a vector in which the TPO-R gene had ben subcloned.

The resulting cell line, named BA/F3-hMPL, grew in selective medium with puromycin and under the stimulation of the cytokine IL-3 and expressed in its membrane the receptor of human thrombopoietin which, after its activation through its union to TPO or to an analogue to this, induced cell proliferation. Cell proliferation measurement and quantification can be used for the determination of the potency of the products.

After the generation of single-cell-derived stable clones, the hMPL expression in the resulting cell clones was determined by qPCR for GeneScript to be able to select the two best clones obtained, based on receptor expression levels.

The results of relative expression of the transfected clones compared with non-transfected BA/F3 cell line are presented in Figure 34.

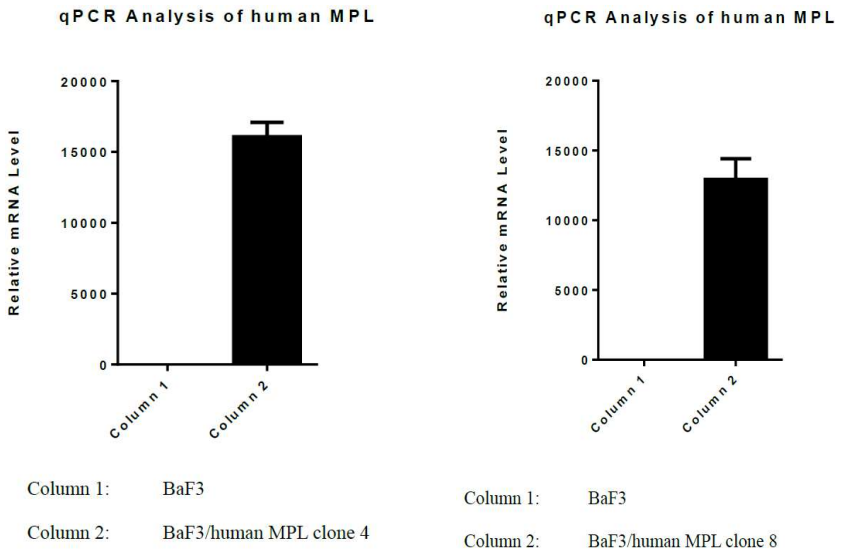

Figure 34: hMPL gene expression in BaF3/hMPL Clone 4 and Clone 8

After the identification of the best clones depending on its expression of the TPO-RA, two cryovials of cells for Clone 4 and 2 for Clone 8, containing 1 x 10^7 cells each, were supplied to RJF.

10.2.2. Evaluation of the thrombopoietin receptor expression in BA/F3-hMPL selected clones

The confirmation of the expression of the human MPL receptor in the BA/F3-hMPL selected clones cell membrane was performed before starting with the development of the cell proliferation potency bioassay. To do so, two flow cytometry assays, one just after thawing the cells and one three passages after thawing, were performed for each one of the two clones. The anti-CD110 antibody was used for the detection of the protein of interest, the TPO-RA.

The flow cytometry results obtained for BA/F3-hMPL Clone 4 and Clone 8 at passage 18, just after tawing, and at passage 21, after 1 passage with thawing medium and 2 passages with complete medium, are presented in Figure 35. The diagrams show the CD110 receptor expression for the selected clones at the two passages mentioned.

PASSAGE	BaF3/hMPL. Clone 4.	BaF3/hMPL. Clone 8.
CTRL DAPI	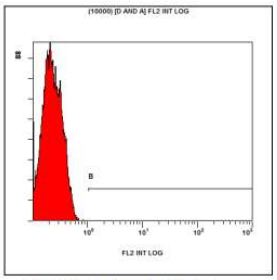 (10000) [D AND A] FL2 INT LOG Region Number %Gated X-Mean ALL 10000 100.00 0.251 B 4 0.04 1.4	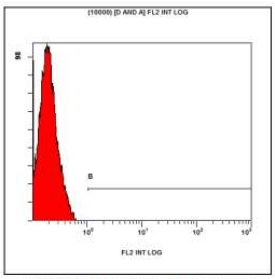 (10000) [D AND A] FL2 INT LOG Region Number %Gated X-Mean ALL 10000 100.00 0.214 B 0 0.00 0
CTRL ISOTYPE IgG2b	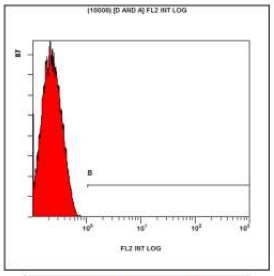 (10000) [D AND A] FL2 INT LOG Region Number %Gated X-Mean ALL 10000 100.00 0.252 B 4 0.04 1.17	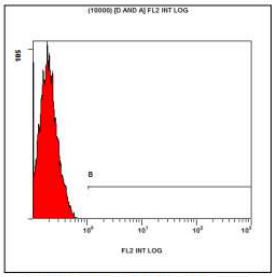 (10000) [D AND A] FL2 INT LOG Region Number %Gated X-Mean ALL 10000 100.00 0.215 B 3 0.03 2.83
PASSAGE 18 Just after thawing	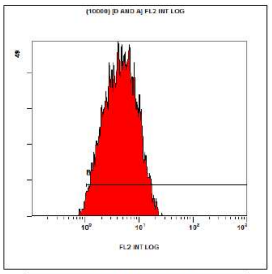 (10000) [D AND A] FL2 INT LOG Region Number %Gated X-Mean ALL 10000 100.00 5.73 B 9818 98.18 5.82	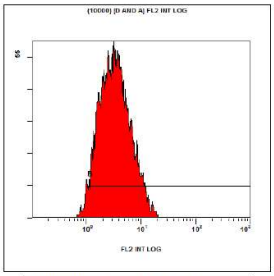 (10000) [D AND A] FL2 INT LOG Region Number %Gated X-Mean ALL 10000 100.00 4.24 B 9684 96.84 4.35
PASSAGE 21 Passage 3 post thawing	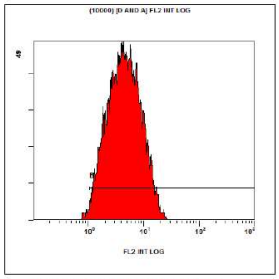 (10000) [D AND A] FL2 INT LOG Region Number %Gated X-Mean ALL 10000 100.00 5.57 B 9829 98.29 5.66	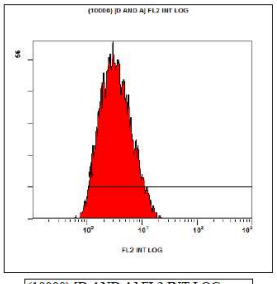 (10000) [D AND A] FL2 INT LOG Region Number %Gated X-Mean ALL 10000 100.00 4.26 B 9726 97.26 4.36

Figure 35: Cytometry diagrams for hMPL expression in Clone 4 and in Clone 8 at two different passages

The tabulated results for CD110 receptor expression are presented in Table 16.

Table 16: Receptor % of expression obtained for clone 4 and clone 8 at two different passages

Clone	Passage	hMPL % Expression
Clone 4	P18 (passage 0 post-thawing)	98%
Clone 4	P21 (passage 3 post-thawing)	98%
Clone 8	P18 (passage 0 post-thawing)	97%
Clone 8	P21 (passage 3 post-thawing)	97%

No differences could be observed in terms of expression neither between the two clones nor between the cell passages. Thus, both clones can be considered adequate for its purpose.

Even though both clones' suitability was demonstrated, the decision of using only one of the two clones for the development of the potency assay was made, to minimize potential differences between assays and increase comparability. Clone 4 was selected for this purpose.

10.2.3. Evaluation of the thrombopoietin receptor responsiveness to stimulation in BA/F3-hMPL selected clones

After the confirmation of the expression of hMPL receptor in the membrane of BA/F3-hMPL cell line, it was necessary to determine that this receptor was functional and capable of being activated through its binding with its ligand. The activation of the TPO receptor through its binding with thrombopoietin or with a thrombopoietin analogue induces the phosphorylation of the STAT5 kinase, what initiates the signalling cascade. The detection of the phosphorylation of STAT5 produced after the stimulation of BA/F3-hMPL cells with a thrombopoietin analogue was used for the confirmation of the presence of a functional TPO receptor in the cells.

To do so, the BA/F3-hMPL cell were treated with the biosimilar for 0, 5, 10 or 30 minutes. Then STAT5 and STAT5-P, through the detection of P-Tyr, were measured by means of WB technique. The samples were loaded as presented in Table 17:

Table 17: Samples loading sequence.

	LANE 1	LANE 2	LANE 3	LANE 4	LANE 5	LANE 6
SAMPLE	MW	0' TPO-RA (CTRL)	5' TPO-RA	10' TPO-RA	30' TPO-RA	MW

As it can be observed in Figure 36, two bands appear in each lane of image A. The first band presents a molecular weight of around 90 kDa and corresponds to STAT5 and the second band presents a molecular weight of approximately 50 kDa and corresponds to tubulin. In image B no band can be observed in lane 2, corresponding with the control, as TPO receptor was not activated and there was no phosphorylation of STAT5, so no phosphorylated tyrosine could be detected, in lanes 3, 4 and 5 a band can be observed at 90 kDa, indicating that the phosphorylation of STAT5 occurs as soon as 5 minutes after cellular stimulation with TPO-RA and that this phosphorylation is maintained for at least 30 minutes.

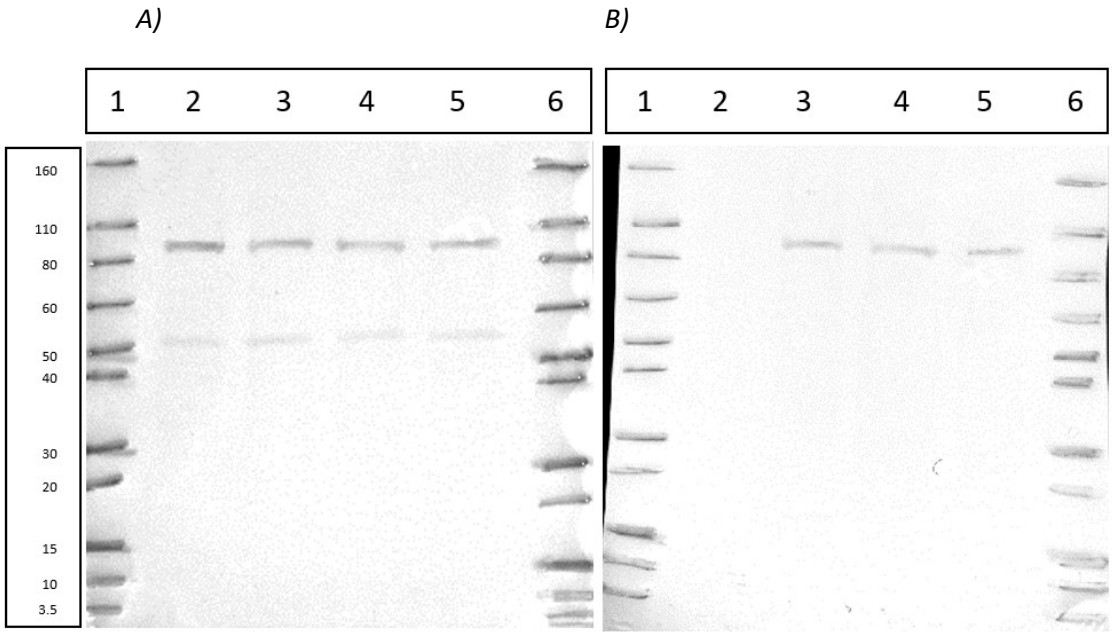

Figure 36: STAT5 phosphorylation after TPO agonist stimulation in BA/F3-hMPL cell line. A) Membrane transferred from a gel loaded with samples proceeding directly from cell lysate and reveled with a primary antibody anti-STAT5 and with a primary antibody anti-α-tubulin. B) Membrane transferred from a gel loaded with samples proceeding from immunoprecipitation of STAT5 (non-phosphorylated and phosphorylated) from the cell lysate, using an anti-STAT5 antibody conjugated with agarose, and reveled with a primary antibody anti-P-Tyr.

10.2.4. BA/F3-hMPL proliferation assay development and optimization of the assay conditions

The development of a bioassay for the determination of the potency of a pharmaceutical product requires a parametric definition of all the steps followed for the performance of the assay, meaning that all the steps undertaken need to be properly described and monitored.

To address the aim of developing a proliferation assay based on the BA/F3-hMPL cell line capable of determining the potency of romiplostim biosimilar DS, DP, DP intermediate samples and RMP samples, to identify batch-to-batch differences and detect if a loss of potency of the products occurs, a series of steps were taken for the determination of the most appropriate assay characteristics to guarantee the obtention of adequate results.

The first step taken was the determination of the most appropriate **working range**. To do so, a wide range of concentrations was applied to the cells to identify the linear range and the lower and upper asymptotes of the dose-response curve. The concentrations tested were: 2,000.0000, 666.4000, 222.0445, 73.9852, 24.6519, 8.2140, 2.7369, 0.9119, 0.3039, 0.1012, 0.0337, 0.0112, 0.0037, 0.0012, 0.0004 and 0.0001 ng / mL.

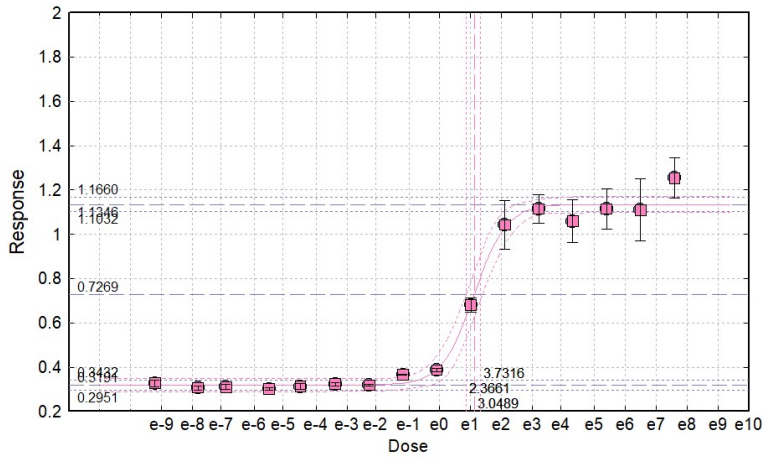

Figure 37: Dose-response graphs for the proliferation assay range determination. Doses in ng / mL.

The results presented in Figure 37 show that the most appropriate working range, in which the linear part of the curve and the lower and upper asymptotes are comprised, goes from dilution 4 (74.00 ng / mL) to dilution 11 (0.034 ng / mL) approximately. The results presented illustrate the need of adjusting the concentration levels to be tested to have more representation in the linear part of the curve. The adjustment of the dilutions curve is described in subsequent steps.

The aspects determined in the second place were the most adequate **cell number** to be used in the assays and the **incubation time of the plates after the application of the tested substance** to obtain consistent results. To do so, 3 assays were performed. In the first assay, 3 plates were seeded with a concentration of 1,000 cells / plates, 3 plates were seeded with a concentration of 2,000 cells / plate, 3 plates were seeded with a concentration of 4,000 cells / plate and 3 plates

were seeded with a concentration of 8,000 cells / plate. The cells in each plate were treated with 5 different concentrations of the compound: 9.00, 3.00, 1.00, 0.33 and 0.00 ng / mL. After the application of the stimuli one plate of each cell concentration was incubated for 72 h, one for 96 h and one for 120 h before the application of CCK8.

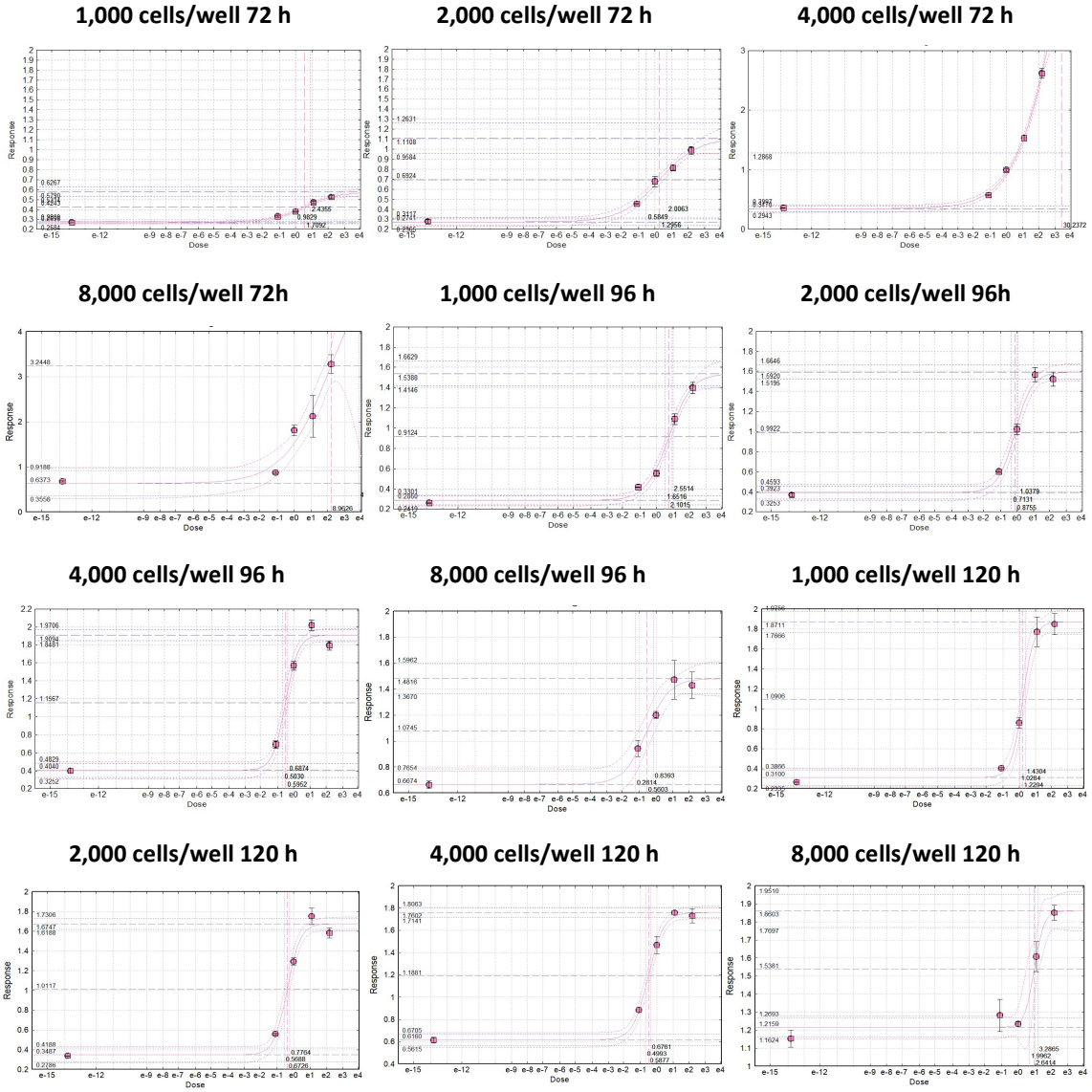

Figure 38: Dose-response graphs for the determination of cell number to be used in the proliferation assay and of the incubation time of the plates after the application of the tested substances (Assay 1). Doses in ng / mL.

The results presented in Figure 38 show that the best dose-response curves were obtained with the cell concentration between 2,000 cells / well and 4,000 cells / well. The optimal incubation time for the plates was found to be between 72 h and 96 h. Considering these results, a second assay

was performed, in which the conditions that obtained most promising results were assessed. In this assay 2 plates were seeded with a concentration of 1,500 cells / plate and 2 plates were seeded with a concentration of 3,000 cells / plate. The cells in each plate were treated with 7 different concentrations of the compound: 270.00, 2.70, 9.00, 3.00, 1.00, 0.33, 0.03 and 0.00 ng / mL. One plate of each cell concentration was incubated for 72 h and the other for 96 h.

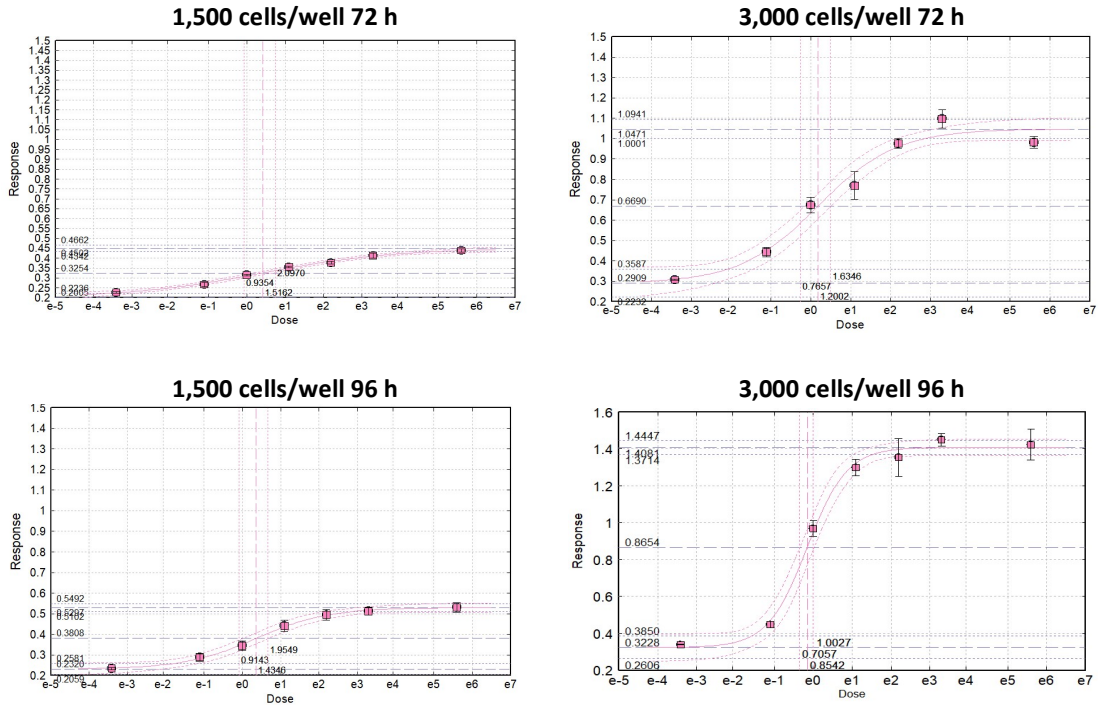

Figure 39: Dose-response graphs for the determination of cell number to be used in the proliferation assay and of the incubation time of the plates after the application of the tested substances (Assay 2). Doses in ng / mL.

Figure 39 shows that, although a curve was formed when a concentration of 1,500 cells / well was used, this curve was flat and did not allow for a correct estimation of the cell response to the compound. The results obtained with a cell concentration of 3,000 cells / well were adequate at both incubation times, 72 h and 96 h, but at 96 h there was a high accumulation of results at the upper asymptote which made it more adequate to use an incubation time of 72 h.

Considering the results obtained, the number of cells to be used in the ongoing assays was established at 3,000 cells / well and the incubation time of the plates after the application of the compounds was established at 72 h.

After having defined the working range, the cell number to be seeded per well and the incubation time of the plates after the application of the compounds, the **elimination of the FBS from the assay medium** was evaluated. FBS is an important component of most cell culture medium, and it is usually essential for cell growth. On the other hand, it is formed by many components which present a high batch-to-batch variability. Bioassays are sensitive methods which may be affected by this composition changes, leading to abnormal results. The aim of the assays described in this section was to test if it was possible to eliminate FBS from the assay medium to avoid this problem or, if it was not possible, to reduce the amount of FBS in the assay medium to minimize the impact of batch-to-batch variations.

To assess if it was possible to perform the assay without adding FBS in the assay medium, one plate was seeded with a concentration of 3,000 cells / plate, proceeding from cells in culture. Half of the plate, dividing it horizontally, was seeded with normal assay medium and the other with assay medium without FBS. Two independent dilution curves were prepared, one with normal assay medium and the other with assay medium without FBS. The cells were treated with 7 different concentrations of the compound: 270.00, 2.70, 9.00, 3.00, 1.00, 0.33, 0.03 and 0.00 ng / mL and the plates were incubated for 72 h before the addition of CCK8 detection reagent.

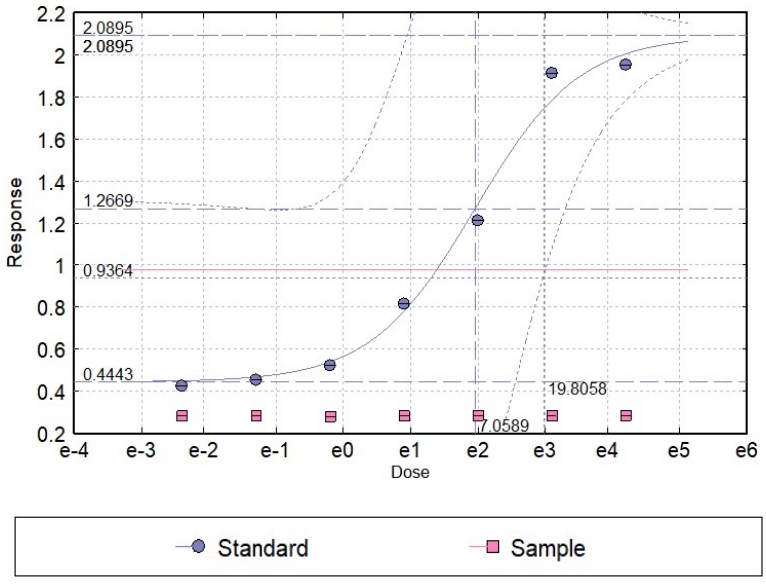

Figure 40: Dose-response graph for the comparison of using the 10 % FBS medium with the FBS free medium in the proliferation assay. Doses in ng / mL.

The results presented in Figure 40 show that the curve prepared with FBS free culture medium (curve in red) did not produce a response in the cells, providing evidence of the impossibility of eliminating the FBS from the culture medium for the performance of the assays.

After it was seen that the elimination of FBS from the assay medium was not possible, the viability of the **reduction of FBS from the assay medium** to 1 % was tested. To assess this, three plates were seeded with a concentration of 3,000 cells / plate. Half of the plate, dividing it horizontally, was seeded with normal assay medium and the other with assay medium with 1 % FBS. Two independent dilution curves were prepared, one with normal assay medium and the other with assay medium with 1 % FBS. The cells were treated with the 7 concentrations described for the previous assay and incubated for 72 h before the addition of CCK8 detection reagent.

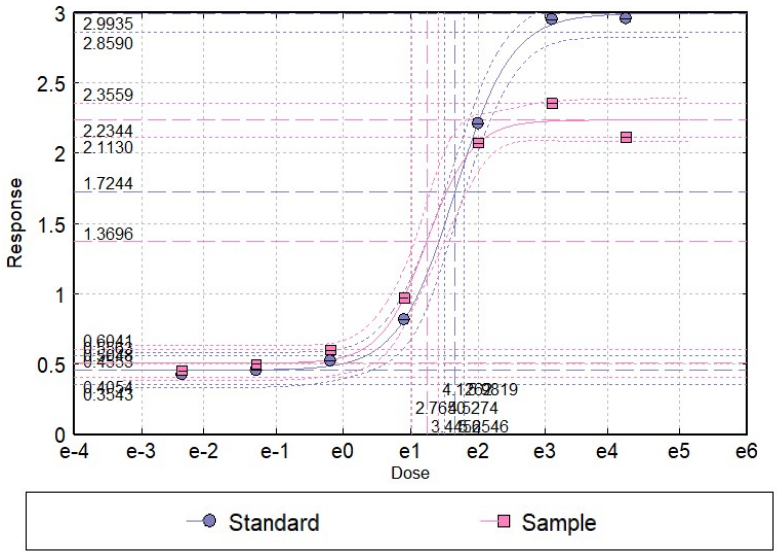

Figure 41: Dose-response graph for the comparison of using the 10% FBS medium with the 1% FBS medium in the proliferation assay. Doses in ng/mL.

The results presented in Figure 41 show that comparable curves in terms of behaviour were obtained when using assay medium containing 10 % or 1 % FBS. It can be observed that when cells were treated with the assay medium containing 1 % FBS (curve in red) the maximum response obtained was reduced compared with the one obtained when using 10 % FBS assay medium (curve in blue), but this has no impact in the shape of the curve. Considering this, in subsequent experiments, a reduction of the FBS in the assay medium to 1 % was applied as both

standard and sample dilution curves were going to be prepared with the same assay medium so no differences in the response would be observed.

In the fourth place, the **assessment of the capability of the cells of responding to the stimulation of the TPO receptor just after thawing** was performed. A first assay was performed using the conditions established in previous assays. In this assay, 3 plates were seeded with 3,000 cells / well in 1 % FBS medium. The cells were treated with 7 different concentrations of the compound: 270.00, 2.70, 9.00, 3.00, 1.00, 0.33, 0.03 and 0.00 ng / mL and the plates were incubated for 72 h before the addition of CCK8 detection reagent.

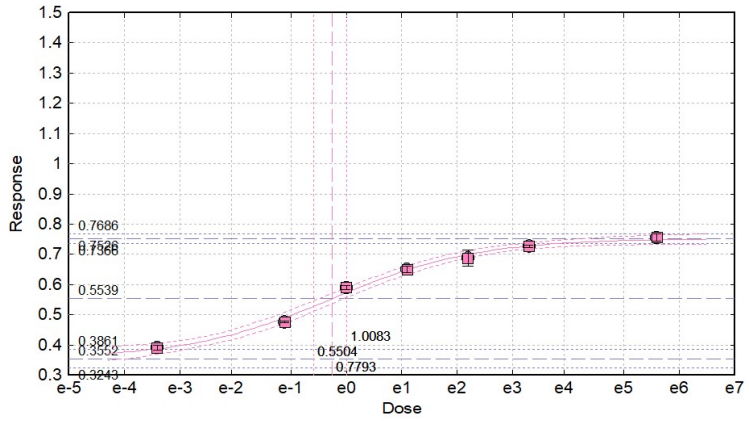

Figure 42: Representative dose-response graphs for the determination of the response capability of BA/F3-hMPL cell line used just after thawing when seeded at a concentration of 3,000 cells / well. Doses in ng / mL.

Figure 42 shows that BA/F3-hMPL cells were able to respond to the stimulation with the drug just after thawing even though the response obtained was lower than expected. To improve the response obtained from the cells, a second assay was performed, increasing the number of cells seeded in each well to test if it was possible to mitigate the low response capability of the cells. This second assay was performed using 5,000 cells / well instead of 3,000 cells / well seeded in 1 % FBS medium. A total of 3 plates were used in this assay. The cells were treated with 7 different concentrations of the compound: 270.00, 2.70, 9.00, 3.00, 1.00, 0.33, 0.03 and 0.00 ng / mL and the plates were incubated for 72 h before the addition of CCK8 detection reagent.

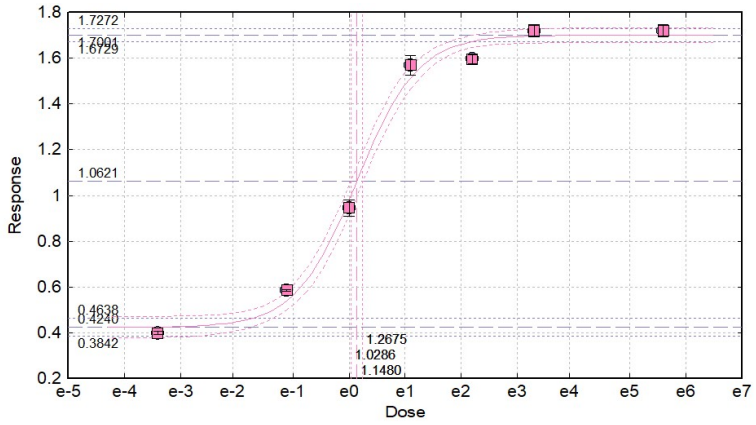

Figure 43: Representative dose-response graphs for the determination of the response capability of BA/F3-hMPL cell line used just after thawing when seeded at a concentration of 5000 cells / well. Doses in ng / mL.

Figure 43 shows that BA/F3-hMPL can be used as just after thawing and still give an adequate response to the stimulation with the drug, even though the cell concentration required for this was more elevated than the one required when using cells which had been previously cultured. The use of cells just after thawing (T&U cells) presents many benefits, since it reduces the cost of the assays as less material and time are required, and since it reduces the variability between assays as all the cells come from the same cellular expansion, minimizing the differences due to culture conditions. A cell bank, named **BA/F3-hMPL T&U cell bank**, ready for its thawing and resuspension in a defined medium volume for the generation of a cell suspension adequate for its use on the performance of the proliferation assay, was generated.

Finally, the **optimization of the dilutions curve** was performed. The aim of this optimization was to achieve a higher accumulation of points in the linear part of the curve. Apart from that, two extra dilution levels were added to the curve, passing from a 7 dilution levels curve to a 9 dilution levels dilution curve. After diverse optimization steps, the dilutions curve presented in Figure 44 was established. The concentration levels included in the optimized dilutions curve were 27.00, 2.70, 1.35, 0.90, 0.68, 0.45, 0.23, 0.11, 0.02 and 0.00 ng / mL.

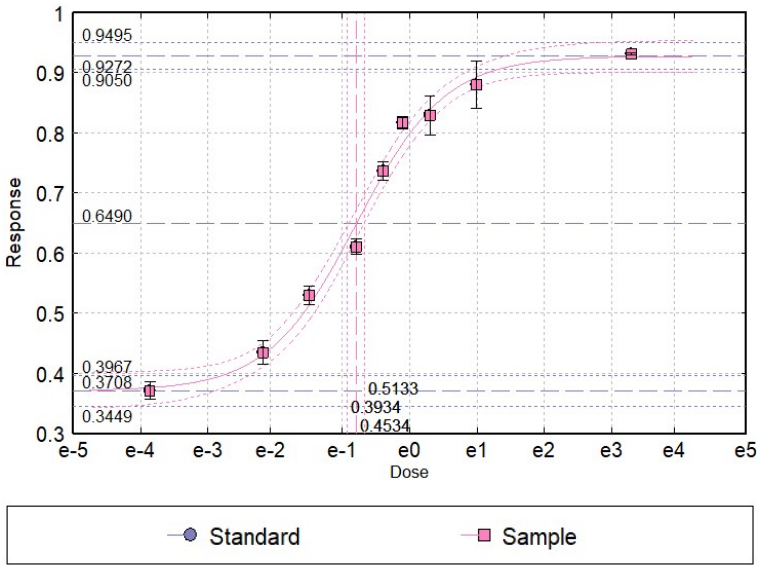

Figure 44: Dose-response graphs obtained after the optimization of the dilution levels to be used in the BA/F3-hMPL proliferation potency assay. Doses in ng / mL.

After the performance of multiple assays to determine the **optimal assay conditions** for the evaluation of the potency of the products included in the project by means of a proliferation assay based on BA/F3-hMPL, the following assay procedure was established:

- A vial of the BA/F3-hMPL T&U cell bank should be thawed just before the assay. The cell pellet is then resuspended in 1 % FBS assay medium (98 % RPMI, 1 % FBS, 1 % Sodium Pyruvate), to have a cell suspension with a concentration of 40,000 cells / mL.
- For plates seeding, 125 µL of the cell suspension prepared are pipetted into the central 60 wells of a 96 well plate. The rest of the wells are filled with 250 µL of PBS. After seeding, the plates are incubated for 3 h at 37ºC in a humified atmosphere with 5 % CO_2.
- For cell treatment, the cells must be treated with one dilution curve for the Standard and one for the Test Sample in each plate. The dilution curves need to be prepared as described in Table 18 and applied to the plates in a volume of 125 µL / well as shown in Figure 45, as the decision of loading the standard and the test sample dilution curve triplicates intercalated was made to minimize any possible effect related with the position in the plate. After treatment, plates are incubated for 72 h at 37ºC in a humified atmosphere with 5 % CO_2.

Table 18: STD and Test Sample dilution curves for BA/F3-hMPL proliferation assay

No.	Concentration (ng/mL)	Method of dilution		
		Standard / Test sample Solution		Cell Culture medium
		Pre-dilution	Sampling Volume (µL)	Sampling Volume (µL)
Stock	500,000.00	NA	NA	NA
A	5,000.00	Stock	15.0	1,485
B	500.00	A	100.0	900
C	54.00	B	432.0	3,568
S1 / T1	54.00	C	1,500.0	0
S2 / T2	5.40	C	150.0	1,350
S3 / T3	2.70	C	75.0	1,425
S4 / T4	1.80	C	50.0	1,450
S5 / T5	1.35	C	37.5	1,463
S6 / T6	0.90	C	25.0	1,475
S7 / T7	0.45	C	12.5	1,488
S8 / T8	0.23	C	12.5	2,988
S9 / T9	0.04	C	8.0	9,992
S10 / T10	0.00	C	0.0	1,500

	1	2	3	4	5	6	7	8	9	10	11	12
A	B	B	B	B	B	B	B	B	B	B	B	B
B	B	S1	S2	S3	S4	S5	S6	S7	S8	S9	S10	B
C	B	T1	T2	T3	T4	T5	T6	T7	T8	T9	T10	B
D	B	S1	S2	S3	S4	S5	S6	S7	S8	S9	S10	B
E	B	T1	T2	T3	T4	T5	T6	T7	T8	T9	T10	B
F	B	S1	S2	S3	S4	S5	S6	S7	S8	S9	S10	B
G	B	T1	T2	T3	T4	T5	T6	T7	T8	T9	T10	B
H	B	B	B	B	B	B	B	B	B	B	B	B

B	PBS	S1-S10	STD dilution curve	T1-T10	Test sample dilution curve

Figure 45: BA/F3-hMPL proliferation assay plate design

- For cell proliferation measurement, 25 µL of CCK8 detection reagent are added to each well. The plates are incubated for 3.5 h at 37ºC in a humified atmosphere with 5 % CO_2. Then absorbance at OD 450 nm is recorded.

10.2.5. BA/F3-hMPL proliferation assay validation

After de optimization of the method and the definition of the final conditions, the BA/F3-hMPL proliferation assay was validated. The validation exercise consisted in 42 plates, described in Table 19, in which range, linearity, accuracy, method precision, intermediate precision,

selectivity, and robustness of the assay was evaluated. In some cases, one plate was used for the assessment of more than one parameter.

Table 19: Proliferation assay validation. Summary of the plates.

Plate id.	Test compounds	Day	Analyst	CCK8 incubation time	Parameters assessed
PLATE 1, 2, 3	STD 100% Sample 60%	1	1	3.5h	Linearity
PLATE 4, 5, 6	STD 100% Sample 80%	1	1	3.5h	Linearity and accuracy
PLATE 7, 8, 9	STD 100% Sample 100%	1	1	3.5h	Linearity, accuracy, and intermediate precision
PLATE 10, 11, 12	STD 100% Sample 120%	1	1	3.5h	Linearity and accuracy
PLATE 13, 14, 15	STD 100% Sample 140%	1	1	3.5h	Linearity
PLATE 16, 17, 18	STD 100% Sample 100%	2	1	3.5h	Method Precision and intermediate precision
PLATE 19, 20, 21	STD 100% Sample 100%	2	1	3.5h	Method Precision
PLATE 22, 23, 24	STD 100% Sample 100%	2	1	3.5h	Method Precision
PLATE 25, 26, 27	STD 100% Sample 100%	2	2	3.5h	Intermediate precision
PLATE 28, 29, 30	STD 100% Sample 100%	3	1	3.5h	Intermediate precision
PLATE 31, 32, 33	STD 100% Excipients	4	1	3.5h	Selectivity
PLATE 34, 35, 36, 37, 38, 39, 40, 41, 42	STD 100% Sample 100%	5	1	3h, 3.5h, 4h	Robustness

10.2.5.2. BA/F3-hMPL proliferation assay linearity

Linearity was assessed trough the representation of the relative potencies obtained against the concentration applied in the plates. The range covered in the assessment of linearity went from 60 % to 140 % of the standard's curve concentration. For each concentration level tested, a dilutions curve consisting in 10 concentration levels was used. The concentrations tested in the dilutions curve at 60 % were 16.20, 1.62, 0.81, 0.54, 0.41, 0.27, 0.14, 0.07, 0.01 and 0.00 ng / mL. The concentrations tested in the dilutions curve at 80 % were 21.60, 2.16, 1.08, 0.72, 0.54, 0.36, 0.18, 0.09, 0.02 and 0.00 ng / mL. The concentrations tested in the dilutions curve at 100 % and in the standard's dilutions curve were 27.00, 2.70, 1.35, 0.90, 0.68, 0.45, 0.23, 0.11, 0.02 and 0.00 ng / mL. The concentrations tested in the dilutions curve at 120 % were 32.40, 3.24, 1.62, 1.08, 0.81, 0.54, 0.27, 0.14, 0.03 and 0.00 ng / mL. The concentrations tested in the dilutions curve at 140 % were 37.80, 3.78, 1.86, 1.26, 0.95, 0.63, 0.32, 0.16, 0.03 and 0.00 ng / mL. Three independent assays were performed for each concentration level. All the dilution curves were prepared by the same analyst and on the same day.

The results obtained for the linearity plates performed during the validation are presented in Table 20.

Table 20: Proliferation assay validation. Linearity results.

Plate Id.	Conc. Level (%)	Relative potency (%)	Mean (%)	% RSD
Plate 1	**60%**	60%	62%	10%
Plate 2		70%		
Plate 3		55%		
Plate 4	**80%**	83%	80%	4%
Plate 5		76%		
Plate 6		81%		
Plate 7	**100%**	111%	110%	2%
Plate 8		111%		
Plate 9		107%		
Plate 10	**120%**	106%	114%	7%
Plate 11		125%		
Plate 12		110%		
Plate 13	**140%**	161%	154%	3%
Plate 14		148%		
Plate 15		153%		
Correlation coefficient		**0.9532**		

Figure 46 shows the representation of the calculated potencies against the theorical values. The results presented illustrated moderate differences in the relative potencies obtained for the triplicates, these differences were related with the inherent variability of the assay. The results presented show a linear relationship between the concentrations applied and the relative responses obtained for the complete tested range.

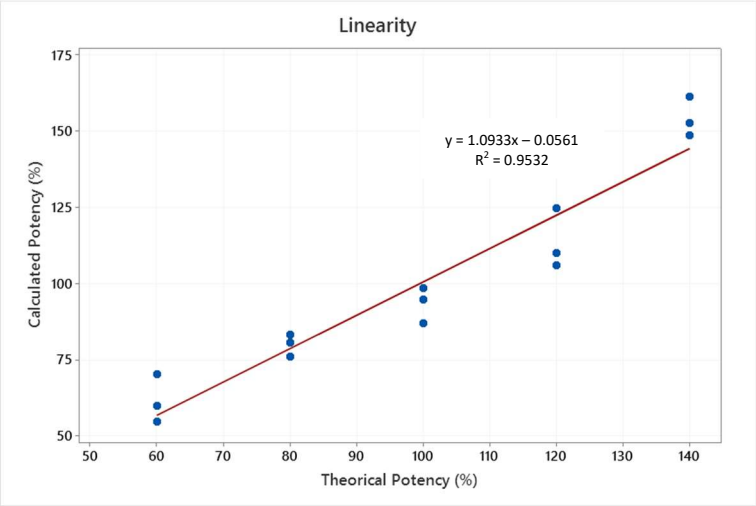

Figure 46: Proliferation assay validation. Linearity results.

The evaluation of the residuals plot, presented in Figure 47, showed that no tendency in the distribution of the results through the different concentrations evaluated.

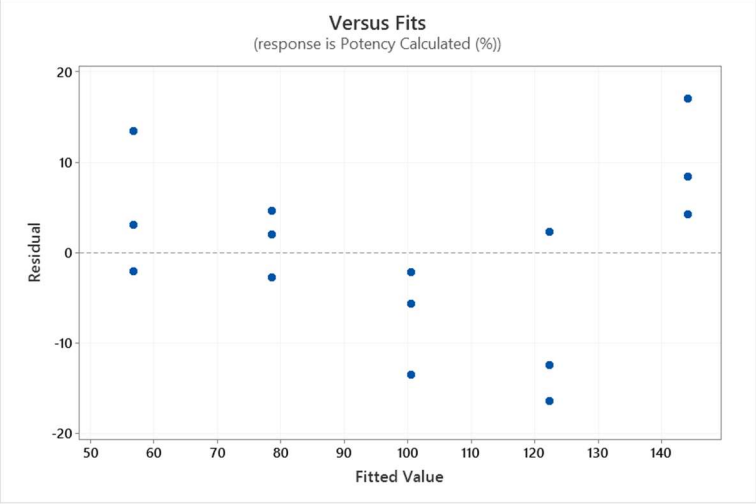

Figure 47: Linearity residuals plot.

10.2.5.3. BA/F3-hMPL proliferation assay precision

10.2.5.3.1. BA/F3-hMPL proliferation assay method precision

Precision of the method or method repeatability was assessed trough the analysis of a unique sample 9 independent times. Each assay consisted in one plate in which a standard curve at 100 % and a sample curve at 100 % were loaded. The concentrations tested for the standard and the sample were 27.00, 2.70, 1.35, 0.90, 0.68, 0.45, 0.23, 0.11, 0.02 and 0.00 ng / mL. The 9 dilution curves for the standard and the 9 for the sample were prepared for the same analyst in the same day. The relative potencies obtained for the sample in each assay and de % RSD obtained are presented in Table 21.

Table 21: Proliferation assay validation. Method precision results.

Plates id.	Analyst	Day	Relative Potency	Average (%)	% RSD
Plate 16	Analyst 1	Day 2	111%	103%	**5%**
Plate 17			111%		
Plate 18			107%		
Plate 19			96%		
Plate 20			97%		
Plate 21			97%		
Plate 22			105%		
Plate 23			103%		
Plate 24			102%		

The results showed that the % RSD between the results obtained for the 9 independent assays of a unique test sample was below the threshold established (% RSD < 20 %). Therefore, the precision of the method was considered adequate for its intended purpose.

10.2.5.3.2. BA/F3-hMPL proliferation assay Intermediate precision

Intermediate precision or method reproducibility was assessed trough the analysis of a unique sample 12 independent times in 3 different days and by 2 different analysts. Each assay consisted in one plate in which a standard curve at 100 % and a sample curve at 100 % were

loaded. The concentrations tested for the standard and the sample were the ones indicated in section 10.2.5.1 for concentration level 100 %.

For the analysis of the intermediate precision between analysts (Table 22), analyst 1 prepared 3 dilution curves for the standard and the 3 for the sample, which were loaded in pairs in 3 independent plates. The same day, analyst 2 performed the exact same procedure.

For the analysis of the intermediate precision between days (Table 23), analyst 1 prepared 3 dilution curves for the standard and the 3 for the sample, which were loaded in pairs in 3 independent plates. The same exact procedure was performed for 3 consecutive days.

Table 22: Proliferation assay validation. Intermediate precision between analysts results.

Plates id.	Analyst	Day	Relative Potency	Average (%)	% RSD
Plate 16	Analyst 1	Day 2	111%	110%	2%
Plate 17	Analyst 1		111%		
Plate 18	Analyst 1		107%		
Plate 25	Analyst 2		115%	**117%**	**6%**
Plate 26	Analyst 2		127%		
Plate 27	Analyst 2		110%		
Intermediate precision (Analysts)				**113%**	**3%**

Table 23: Proliferation assay validation. Intermediate precision between days results.

Plates id.	Analyst	Day	Relative Potency	Average (%)	% RSD
Plate 7	Analyst 1	Day 1	87%	93%	5%
Plate 8		Day 1	98%		
Plate 9		Day 1	95%		
Plate 16		Day 2	111%	110%	2%
Plate 17		Day 2	111%		
Plate 18		Day 2	107%		
Plate 28		Day 3	103%	104%	1%
Plate 29		Day 3	105%		
Plate 30		Day 3	105%		
Intermediate precision (Days)				**102%**	**7%**

The results presented showed that there were not remarkable differences in the results obtained for plates prepared by different analysts or in different days, as the % RSD between the results obtained was below the threshold established for intermediate precision (% RSD < 30%). Therefore, the intermediate precision was considered adequate for the performance of the potency assay.

10.2.5.4. BA/F3-hMPL proliferation assay Accuracy

For the evaluation of the accuracy of the method three different dilution curves with a 20 % shift between them where evaluated. The concentrations tested in the dilutions curve at test sample 80 %, standards and test sample at 100 %, and test sample at 120 % were the ones indicated in section 10.2.5.1. Three independent assays were performed for each concentration level. All the dilution curves were prepared by the same analyst and on the same day. After the performance of the proliferation potency assay the percentage of recovery was calculated using the relative potency obtained and the theorical value. The results obtained for the recoveries are presented in Table 24.

Table 24: Proliferation assay validation. Accuracy results.

Plate Id.	Conc. Level (%)	Relative potency (%)	Recovery (%)	Average (%)	% RSD
Plate 4	80%	83%	104%	100%	4%
Plate 5		76%	95%		
Plate 6		81%	101%		
Plate 7	100%	111%	111%	110%	2%
Plate 8		111%	111%		
Plate 9		107%	107%		
Plate 10	120%	106%	88%	95%	7%
Plate 11		125%	104%		
Plate 12		110%	92%		
Accuracy				**101%**	**6%**

As it can be observed in the results presented, the recoveries obtained for all the plates assessed fitted the acceptance criteria established, as all the recoveries fitted between 70 % and 130 %. Apart from that, no tendency in the recoveries depending on the level of concentrations of the

dilutions curve was observed. With these considerations, it was possible to determined that the method presented an accuracy compatible with its use as a potency assay.

10.2.5.5. BA/F3-hMPL proliferation assay Selectivity

To assess selectivity, 3 plates were loaded with an STD curve prepared at 100 % and a test sample solution curve prepared using the DP excipients buffer. The response generated for the excipients buffer dilutions curve after the performance of the cell proliferation potency assay was evaluated (Figure 48).

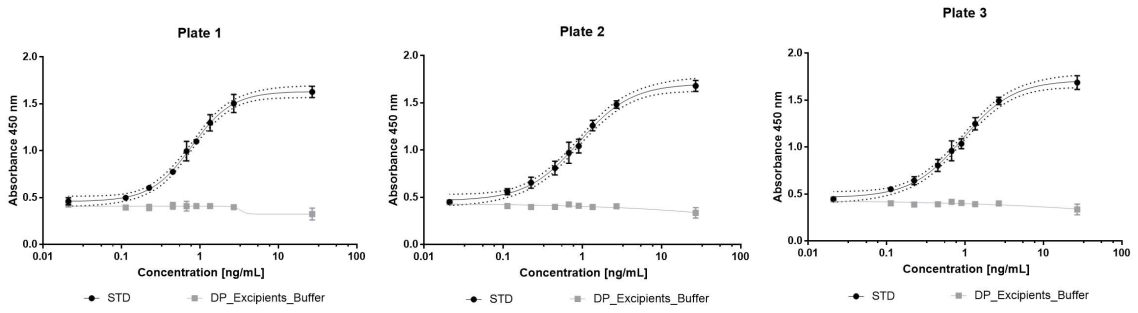

Figure 48: Proliferation assay validation. Selectivity results.

It can be observed in the graphic that no response was obtained when the dilution curve was prepared using the DP buffer of excipients.

On the other hand, the OD values obtained for the different concentrations of romiplostim biosimilar excipients buffer were compared with the OD values obtained for cells without treatment (Table 25). The results showed that no remarkable differences between the OD values obtained at the different concentration levels.

Table 25: OD values obtained for the assessment of selectivity in the cell proliferation potency assay.

Concentration (ng/mL)	27.00	2.70	1.35	0.90	0.68	0.45	0.23	0.11	0.02	0.00	
OD values Plate 31	0.362	0.402	0.442	0.401	0.446	0.429	0.424	0.400	0.399	0.465	Selectivity
	0.251	0.387	0.397	0.409	0.430	0.435	0.399	0.410	0.431	0.472	
	0.359	0.405	0.389	0.417	0.349	0.372	0.359	0.370	0.459	0.394	
OD values Plate 32	0.367	0.403	0.389	0.399	0.441	0.403	0.405	0.395	0.443	0.480	
	0.368	0.391	0.386	0.398	0.409	0.387	0.379	0.409	0.433	0.490	
	0.271	0.420	0.414	0.431	0.423	0.406	0.408	0.418	0.470	0.461	
OD values Plate 33	0.364	0.394	0.384	0.392	0.427	0.390	0.391	0.391	0.438	0.479	
	0.371	0.382	0.376	0.392	0.403	0.380	0.370	0.397	0.427	0.491	
	0.270	0.421	0.414	0.430	0.422	0.401	0.404	0.412	0.466	0.457	
Average (%)	0.331	0.401	0.399	0.408	0.417	0.400	0.393	0.400	0.441	0.465	**0.406**
% RSD	15%	3%	5%	4%	7%	5%	5%	3%	5%	6%	**2%**

Table 26 shows the composition of the excipients buffer of romiplostim biosimilar DP and DS. It can be observed that the buffer of excipients of the DS presents the exact same components that the DP excipients buffer but at half the concentration, which means that when the assay is performed on DS samples the excipients are going to be diluted to half the concentration. Considering this, it can be determined that if no interference of the components of the excipient's matrix is observed for romiplostim biosimilar DP excipients buffer, no interference is going to occurred for romiplostim biosimilar DS excipients buffer.

Table 26: DP excipients buffer and DS excipients buffer composition.

Component	DP Excipients Buffer	DS Excipients Buffer
D-Mannitol	4% w/v	2% w/v
Sucrose	2% w/v	1% w/v
L-Histidine	10 mM	5 mM
Polysorbate 20	0.004% w/v	0.002% w/v
HCl	q.s. pH 5.0	q.s. pH 5.0
Water for injections	q.s.	q.s.

All in all, the results presented showed the selectivity of the assay method for the active substance in romiplostim biosimilar products.

10.2.5.6. BA/F3-hMPL proliferation assay Robustness

Robustness was assessed through the reading of the absorbance at 450 nm in 9 plates 3.0 h; 3.5 h and 4.0 h after the application of CCK8 detection reagent. The plates had been loaded with a standard curve at 100 % and a sample curve at 100 %. The concentrations tested for the standard and the sample were the ones indicated in section 10.2.5.1 for concentration level 100 %.

The results presented in Table 27 show the differences in the results observed for the different incubation times with CCK8.

Table 27: Proliferation assay validation. Robustness results.

Plate Id.	CCK8 incubation time (h)	Relative potency (%)	Average (%)	% RSD
Plate 34	3	99%	102%	5%
Plate 34	3.5	109%		
Plate 34	4	97%		
Plate 35	3	112%	108%	2%
Plate 35	3.5	107%		
Plate 35	4	106%		
Plate 36	3	98%	100%	1%
Plate 36	3.5	100%		
Plate 36	4	101%		
Plate 37	3	102%	102%	0%
Plate 37	3.5	102%		
Plate 37	4	103%		
Plate 38	3	106%	106%	2%
Plate 38	3.5	108%		
Plate 38	4	104%		
Plate 39	3	89%	88%	1%
Plate 39	3.5	87%		
Plate 39	4	87%		
Plate 40	3	93%	91%	3%
Plate 40	3.5	93%		
Plate 40	4	88%		
Plate 41	3	108%	104%	3%
Plate 41	3.5	102%		
Plate 41	4	101%		
Plate 42	3	87%	87%	1%
Plate 42	3.5	85%		
Plate 42	4	88%		

The results showed that the % RSD observed between the different incubation times was equivalent, as no major changes could be observed in the relative potencies obtained at different incubation times with CCK8 detection reagent.

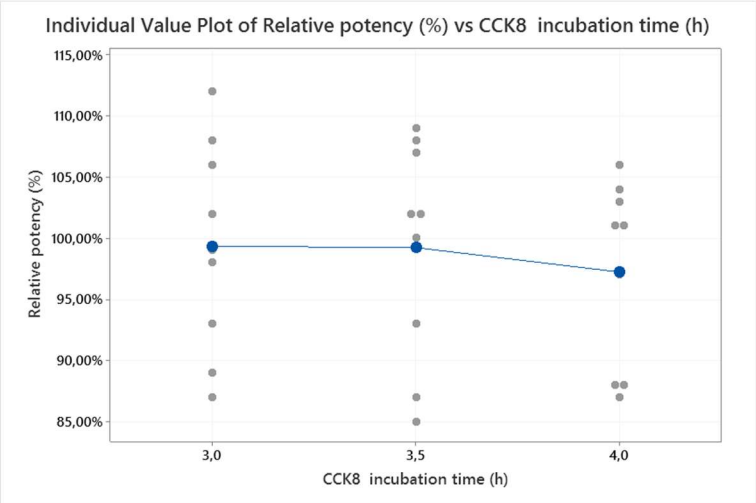

Figure 49: Proliferation assay validation. Results distribution for the different CCK8 incubation times

A p-value of 0.836 was obtained for the ANOVA analysis of the results, showing with 95 % confidence that there were no significant differences between the results obtained after 3.0 h, 3.5 h or 4.0 h of incubation with CCK8 detection reagent. Apart from that, the results presented in Figure 49 illustrate that there was no tendency in the distribution of the results for any of the incubation times.

Analysed all together, the results presented proved that the assay is robust for CCK8 incubation time 3.5 h ± 30 min.

10.2.5.7. Summary of the cell proliferation potency assay validation results

Table 28: Proliferation assay validation. Results summary.

Parameters	Acceptance criteria	Results		Complies / No Complies
Specificity	No response observed	No response observed		Complies
Linearity	$R^2 \geq 0.95$	$R^2 = 0.95$		Complies
Method Precision	% RSD ≤ 20 %	% RSD = 5 %		Complies
Intermediate Precision	% RSD ≤ 30 %	Analysts	% RSD = 3 %	Complies
		Days	% RSD = 7 %	Complies
Accuracy	Recovery between 70 % - 130 %	Plate 4	Recovery 104 %	Complies
		Plate 5	Recovery 95 %	Complies
		Plate 6	Recovery 101 %	Complies
		Plate 7	Recovery 111 %	Complies
		Plate 8	Recovery 111 %	Complies
		Plate 9	Recovery 107 %	Complies
		Plate 10	Recovery 88 %	Complies
		Plate 11	Recovery 104 %	Complies
		Plate 12	Recovery 92 %	Complies
Robustness	P-Value > 0.05	p = 0.836		Complies

10.3. DEVELOPMENT OF A POTENCY ASSAY BASED ON A REPORTER GENE

10.3.1. TF1 - Stat5 - Luc 2P - TPOR cell line development

The first objective in the development of a potency gene reporter-based bioassay capable of testing the potency of romiplostim biosimilar products was the development of a cell line intrinsically and stably expressing a functional human thrombopoietin receptor. The cell line of choice for the expression of TPO-R was the TF-1 cell line, which is a human cell line, derived from human erythroleukemia, which is dependent on GM-CSF for its growth. The TPO-R gen was

introduced into the TF-1 cells by means of a Promega's already developed expression vector based on Luc2P/STAT5-RE/Hygro.

The resulting cell line, named TF1 - Stat5 - Luc 2P - TPOR, grew in selective medium with hygromycin and blasticidin and under the stimulation of the cytokine GM-CSF, and expressed in its membrane the receptor of human thrombopoietin which, after its activation through its union to TPO or to an analogue, activated a signalling cascade which triggered the transcription of STAT5 and, therefore, also of luciferase through STAT5 response element (STAT5-RE). The addition of the luciferase substrate, after the appropriate incubation time, triggered the substrate oxidation generating light, which could be measured, allowing for the quantification of the luciferase gene transcription, which was, in turn, proportional to the activation of the thrombopoietin receptor (Figure 50).

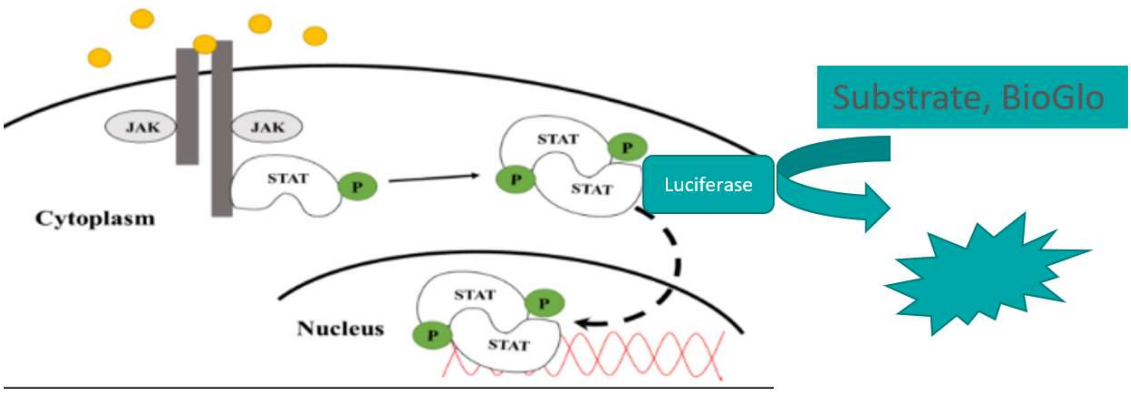

Figure 50: Schema of the principle of the potency assay based on a reporter gene under development.

After the generation of single-cell-derived stable clones, Promega determined the responsiveness of the generated clones to stimulation with TPO for the selection of the two best clones obtained. The responsiveness of the clones was determined based on the relative luminescence unit's induction produced by TPO stimulation.

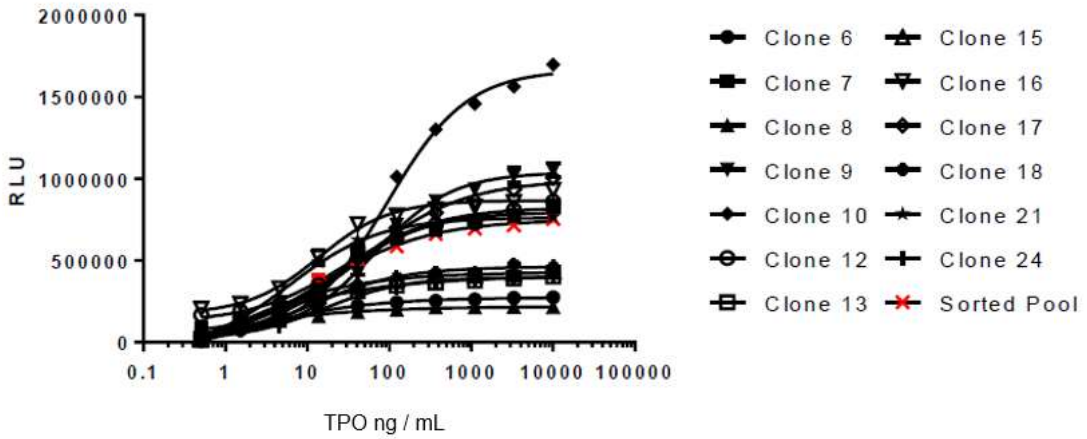

Figure 51: Responsiveness of the survival single-cell-derived stable clones to TPO stimulation

After the identification of the best clones, two cryovials of cells for Clone 9 and two for Clone 10, containing 1 x 10^7 cells each, were supplied to RJF.

10.3.2. Evaluation of the thrombopoietin receptor expression in the TF1 - Stat5 - Luc 2P - TPOR selected clones

Two flow cytometry were performed to confirm the correct expression of the TOPR in the two clones obtained from Promega. The flow cytometry results obtained for TF1 - Stat5 - Luc 2P - TPOR Clone 9 and Clone 10 at passage 21, just after tawing, and at passage 24, after 1 passage without the selection antibiotics and 2 passages with blasticidin S and hygromycin B, are presented in Figure 52. The anti-CD110 antibody was used for the detection of the protein of interest, the TPO-R.

The diagrams show the CD110 receptor expression for the selected clones at the two passages mentioned.

PASSAGE	Clone 9	Clone 10
CTRL DAPI	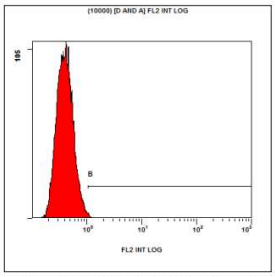 (10000) [D AND A] FL2 INT LOG Region Number %Gated X-Mean ALL 10000 100.00 0.427 B 68 0.68 1.18	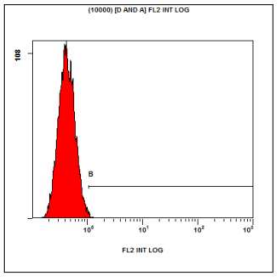 (10000) [D AND A] FL2 INT LOG Region Number %Gated X-Mean ALL 10000 100.00 0.463 B 119 1.19 1.9
CTRL ISOTYPE IgG2b	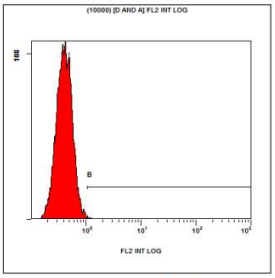 (10000) [D AND A] FL2 INT LOG Region Number %Gated X-Mean ALL 10000 100.00 0.429 B 70 0.70 1.25	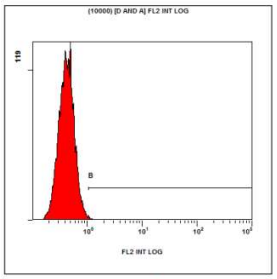 (10000) [D AND A] FL2 INT LOG Region Number %Gated X-Mean ALL 10000 100.00 0.447 B 84 0.84 1.43
PASSAGE 21 Just after thawing	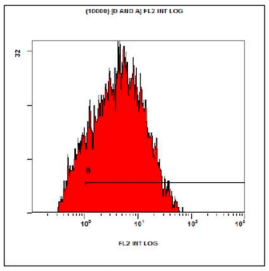 (10000) [D AND A] FL2 INT LOG Region Number %Gated X-Mean ALL 10000 100.00 8.4 B 8575 85.75 9.68	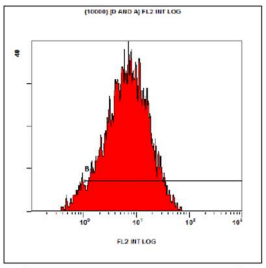 (10000) [D AND A] FL2 INT LOG Region Number %Gated X-Mean ALL 10000 100.00 10.5 B 9362 93.62 11.1
PASSAGE 24 Passage 3 post thawing	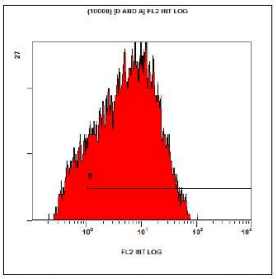 (10000) [D AND A] FL2 INT LOG Region Number %Gated X-Mean ALL 10000 100.00 11.1 B 8531 85.31 12.9	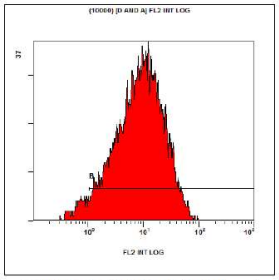 (10000) [D AND A] FL2 INT LOG Region Number %Gated X-Mean ALL 10000 100.00 13.7 B 9400 94.00 14.5

Figure 52: Cytometry diagrams for hMPL expression in TF1 - Stat5 - Luc 2P - TPOR Clone 9 and in Clone 10 at two different passages

The tabulated results for CD110 receptor expression are presented in Table 29.

Table 29: Receptor % of expression obtained for TF1 - Stat5 - Luc 2P - TPOR Clone 9 and Clone 10 at two different passages

Clone	Passage	hMPL % Expression
Clone 9	P21 (passage 0 post-thawing)	86%
Clone 9	P24 (passage 3 post-thawing)	85%
Clone 10	P21 (passage 0 post-thawing)	94%
Clone 10	P24 (passage 3 post-thawing)	94%

No differences were observed in terms of expression between the cell passages. Clone 10 presented approximately a 10% higher expression than Clone 9. Considering this, the decision of working with Clone 10 for the development of the assay was made.

10.3.3. Evaluation of the thrombopoietin receptor responsiveness to stimulation in TF1 - Stat5 - Luc 2P – TPO-R

Equivalently to the observations made for BA/F3-hMPL cell line, it was also confirmed that TF1 - Stat5 - Luc 2P – TPO-R cell line presents a functional TPO-R, capable of responding to the stimulation with TPO-RA. The phosphorylation kinetics is also comparable to the one observed for the TPO receptor in BA/F3-hMPL cell line as STAT5 phosphorylation occurs 5 minutes after the treatment and is maintained for a minimum of 30 minutes (Figure 53).

The samples were loaded as presented in Table 30Table 17:

Table 30: Samples loading sequence.

	LANE 1	LANE 2	LANE 3	LANE 4	LANE 5	LANE 6
SAMPLE	MW	0' TPO-RA (CTRL)	5' TPO-RA	10' TPO-RA	30' TPO-RA	MW

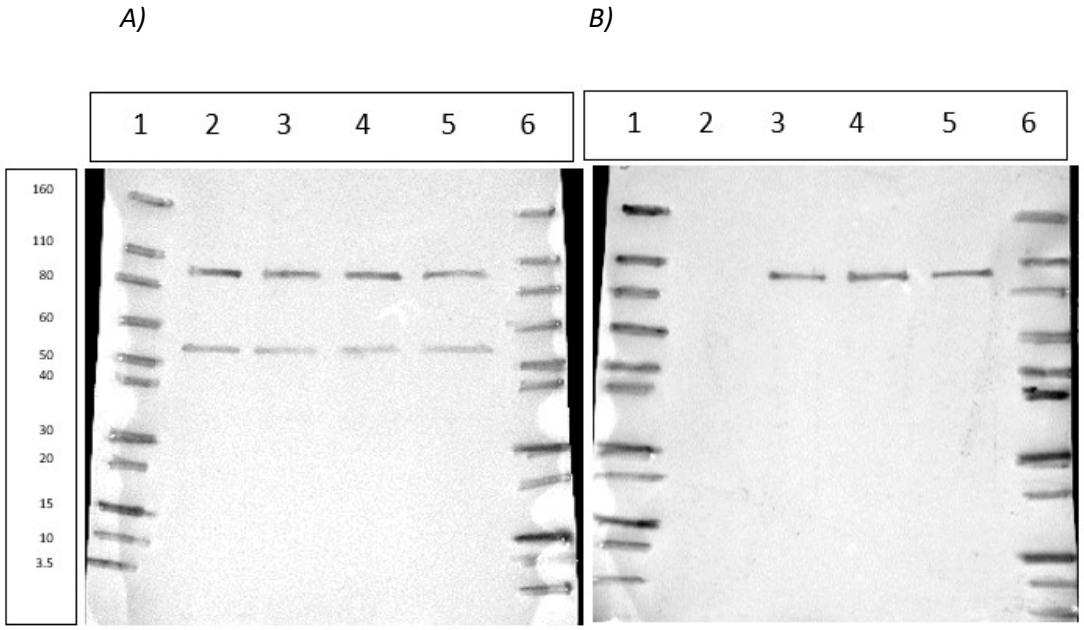

Figure 53: STAT5 phosphorylation after TPO agonist stimulation in TF1 - Stat5 - Luc 2P – TPO-R cells. A) Membrane transferred from a gel loaded with samples proceeding directly from cell lysate and reveled with a primary antibody anti-STAT5 and with a primary antibody anti-α-tubulin. B) Membrane transferred from a gel loaded with samples proceeding from immunoprecipitation of STAT5 (non-phosphorylated and phosphorylated) from the cell lysate, using an anti-STAT5 antibody conjugated with agarose, and reveled with a primary antibody anti-P-Tyr.

10.3.4. TF1 - Stat5 - Luc 2P - TPOR reporter gene assay development and optimization of the assay conditions

For the determination of the optimal TF1 - Stat5 - Luc 2P - TPOR reporter gene assay conditions, the first step taken was the determination of the most appropriate **working range**. To do so, an assay was performed seeding 30,000 cells in 50 µL of medium and a wide range of concentrations was applied to the cells to identify the linear range and the lower and upper asymptotes of the dose-response curve. The concentrations tested were: 1,000.00, 500.00, 250.00, 125.00, 62.50, 31.30, 15.60,7.81, 3.91, 1.95, 0.98, 0.49, 0.24, 0.12, 0.06, 0.03, 0.02, 0.01 and 0.00 ng / mL.

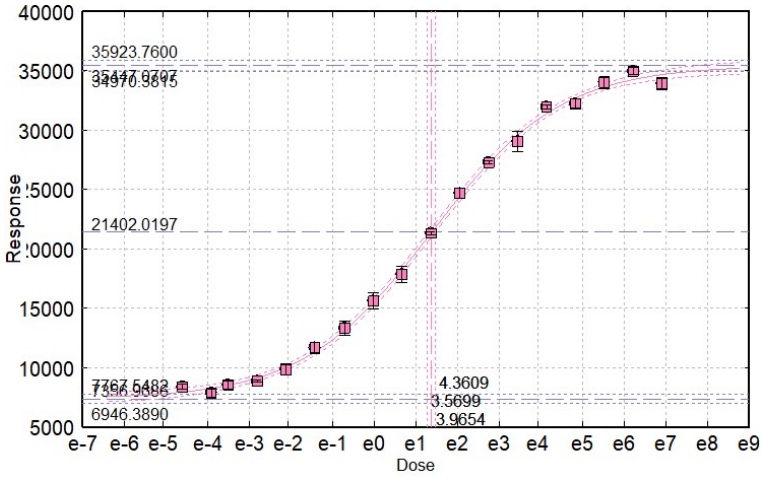

Figure 54: Dose-response graphs for the reporter gene assay range determination. Doses in ng/mL.

The results presented in Figure 54 show that the whole range tested was necessary to be able to observe both the upper and the lower asymptotes of the sigmoidal curve, therefore the appropriate range to work with was comprised between dilution 1 (1,000 ng / mL) and dilution 18 (0.01 ng / mL). Even though the whole range evaluated was considered important for the curve to present the desired shape, it was determined that a reduction of the number of concentration levels to be assessed in each assay could be reduced to 9, allowing the loading of two complete curves on the plates to be able to test the standard and the sample on the same plate. Therefore, to cover the full range and ensure a correct formation of both asymptotes, it was decided to work with a 9-points curve in which a 1 / 10 dilution was made between dilutions 1 and 2 and between dilutions 9 and 10, and a dilution 1 / 3 was made between the rest of dilutions. Considering this, the concentration levels which were decided to be included in the plates were: 1,000.00, 100.00, 33.33, 11.11, 3.70, 1.24, 0.41, 0.14, 0.01 and 0.00 ng / mL.

In the second place, the evaluation of the **cell number to be seeded** in each well to obtain consistent results was performed. The objective of developing a cellular assay based on a reporter gene was to have a quicker assay to determine the potency of the compound under evaluation. Protein synthesis in response to the activation of a membrane receptor is a fast process, which causes that no cell duplication occurs during the time course of the assay. It was decided to seed a relatively large number of cells in each well. During the set-up of the method, various cellular concentrations were tested, and equivalent results were obtained for all of them. Considering this, it was decided to maintain initial conditions tested, seeding 30,000 cells / well in 50 µL of medium.

Regarding the **incubation time** of the plates after the application of the compounds, an incubation time of 6 h and an overnight incubation time of approximately 16 h were assessed. An assay was performed using the conditions established in previous assays. In this assay, 2 plates were seeded with 30,000 cells/well. The cells were treated with the following concentrations of the compound: 1,000.00, 100.00, 33.33, 11.11, 3.70, 1.24, 0.41, 0.14, 0.01 and 0.00 ng / mL. Then, one of the plates was incubated for 6 h and the other for 16 h after which Bio-Glo™ Luciferase Assay System was added to the wells to quantify luciferase synthesis.

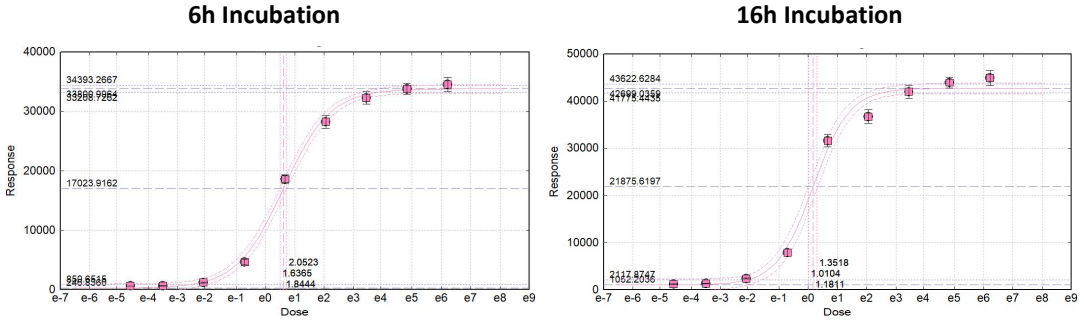

Figure 55: Dose-response graphs obtained for 6h and 16h incubation times with the test compound in the reporter gene assay. Doses in ng/mL.

The results presented in Figure 55 showed that the dose-response curves obtained at the two different incubation times assessed had an equivalent shape, nevertheless, the distribution of the points in the dose-response curve obtained for the plate incubated 6 h after the application of the compounds presented a more balanced distribution of the points in the curve than the plate incubated 16 h. Apart from that, a shorter incubation time was preferable, as it let to the faster obtention of results. Considering all, an incubation time of 6 h after the application of the compounds was established.

Finally, the testing of the **capability of the TF1 - Stat5 - Luc 2P - TPOR cell line of responding to the stimulation with the compound just after thawing** was assessed. An assay was performed seeding 3 plates with 30,000 cells / well. The cells were treated with 1,000.00, 100.00, 33.33, 11.11, 3.70, 1.24, 0.41, 0.14, 0.01 and 0.00 ng/mL of the compound and then incubated for 6 h before the detection of luciferase synthesis with Bio-Glo™ Luciferase Assay System.

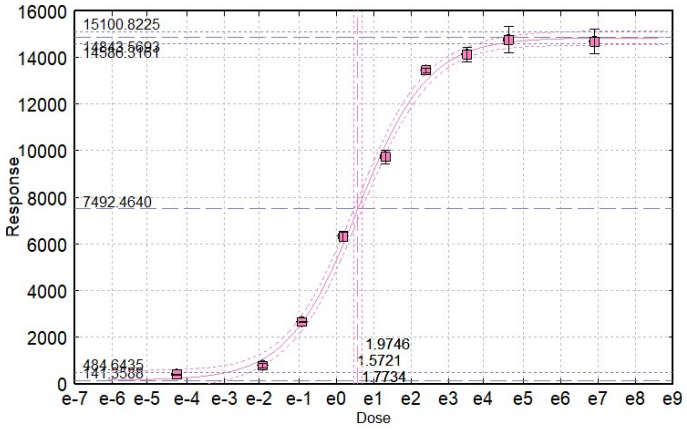

Figure 56: Representative dose-response graph of the results obtained for TF1 - Stat5 - Luc 2P - TPOR cells, used as T&U. Doses in ng/mL.

Figure 56 illustrates the capability of TF1 - Stat5 - Luc 2P - TPOR cells of responding to the thrombopoietin agonists immediately after thawing, as the dose-response curve obtained behaves equivalently to the one obtained when using cells in culture. As mentioned before, the use of T&U cells is desirable as it eliminates the variability due to cell maintenance, and as it is less time and material requiring. Because of this, the use of TF1 - Stat5 - Luc 2P - TPOR T&U cells was established and a **TF1 - Stat5 - Luc 2P – TPOR T&U cell bank** was created.

After the performance of the assays required for the set-up of the method, the following **assay procedure** was determined:

- A vial of the TF1 - Stat5 - Luc 2P - TPOR T&U cell bank should be thawed just before the assay and a cell suspension with a concentration of 600,000 cells / mL is prepared, using a predefined resuspension volume of the TF1 - Stat5 - Luc 2P - TPOR reporter gene assay medium (90 % RPMI, 10 % FBS).
- For plates seeding, 50 µL of the cell suspension prepared are pipetted into the central 60 wells of a 96 well plate. The rest of the wells are filled with 100 µL of PBS. After seeding, the plates are going to be incubated at 37ºC in a humified atmosphere with 5 % CO_2 overnight.
- For cell treatment, the cells are treated with one dilution curve for the Standard and one for the Test Sample in each plate. The dilution curves are prepared as described in Table 31 and applied to the plates in a volume of 50 µL / well as shown in Figure 57. The plates are incubated at 37ºC in a humified atmosphere with 5 % CO_2 for 6 h.

Table 31: Optimized dilutions curve for STD and Test Sample

No.	Concentration (ng/mL)	Method of dilution		
		Standard / Test sample Solution		Cell Culture medium
		Pre-dilution	Sampling Volume (µL)	Sampling Volume (µL)
Stock	500000.00	NA	NA	Na
A	5000.00	Stock	15	1,485
B	2000.00	A	800	1,200
C	20.00	B	20	1,980
S1 / T1	2000.00	B	1,500	0
S2 / T2	200.00	B	150	1,350
S3 / T3	67.00	B	50	1,450
S4 / T4	22.00	B	17	1,483
S5 / T5	7.40	C	555	945
S6 / T6	2.50	C	188	1,312
S7 / T7	0.82	C	62	1,438
S8 / T8	0.27	C	20	1,480
S9 / T9	0.03	C	11	6,989
S10 / T10	0.00	C	0	1,500

	1	2	3	4	5	6	7	8	9	10	11	12
A	B	B	B	B	B	B	B	B	B	B	B	B
B	B	S1	S2	S3	S4	S5	S6	S7	S8	S9	S10	B
C	B	T1	T2	T3	T4	T5	T6	T7	T8	T9	T10	B
D	B	S1	S2	S3	S4	S5	S6	S7	S8	S9	S10	B
E	B	T1	T2	T3	T4	T5	T6	T7	T8	T9	T10	B
F	B	S1	S2	S3	S4	S5	S6	S7	S8	S9	S10	B
G	B	T1	T2	T3	T4	T5	T6	T7	T8	T9	T10	B
H	B	B	B	B	B	B	B	B	B	B	B	B

B	PBS	S1-S10	STD dilution curve	T1-T10	Test sample dilution curve

Figure 57: TF1 - Stat5 - Luc 2P - TPOR reporter gene assay plate design

- For luciferase expression measurement, 50 µL of Bio-Glo™ Luciferase Assay System detection reagent is added to each well. The plates are incubated for 10 min and then luminescence emitted by each well is recorded.

10.3.5. TF1 - Stat5 - Luc 2P - TPOR reporter gene assay validation

The TF1 - Stat5 - Luc 2P - TPOR reporter gene validation exercise consisted in 42 plates, described in Table 32, in which range, linearity, accuracy, method precision, intermediate precision, selectivity, and robustness of the assay was evaluated. In some cases, one plate was used for the assessment of more than one parameter.

Table 32: Reporter gene assay validation. Summary of the plates.

Plate	Test compounds	Day	Analyst	Plate incubation time	Bio-Glo incubation time	Parameters assessed
PLATE 1, 2, 3	STD 100% Sample 60%	1	1	6h	10 min	Linearity
PLATE 4, 5, 6	STD 100% Sample 80%	1	1	6h	10 min	Linearity and accuracy
PLATE 7, 8, 9	STD 100% Sample 100%	1	1	6h	10 min	Linearity, accuracy, and intermediate precision
PLATE 10, 11, 12	STD 100% Sample 120%	1	1	6h	10 min	Linearity and accuracy
PLATE 13, 14, 15	STD 100% Sample 140%	1	1	6h	10 min	Linearity
PLATE 16, 17, 18	STD 100% Sample 100%	2	1	6h	10 min	Method Precision and intermediate precision
PLATE 19, 20, 21	STD 100% Sample 100%	2	1	6h	10 min	Method Precision
PLATE 22, 23, 24	STD 100% Sample 100%	2	1	6h	10 min	Method Precision
PLATE 25, 26, 27	STD 100% Sample 100%	2	2	6h	10 min	Intermediate precision
PLATE 28, 29, 30	STD 100% Sample 100%	3	2	6h	10 min	Intermediate precision
PLATE 31, 32, 33	STD 100% Excipients buffer	4	1	6h	10 min	Selectivity
PLATE 34	STD 100% (prep 1) Sample 100% (prep 1)	5	1	5:30h	10 min 25 min	Robustness
PLATE 35	STD 100% (prep 1) Sample 100% (prep 1)	5	1	6h	10 min 25 min	Robustness
PLATE 36	STD 100% (prep 1) Sample 100% (prep 1)	5	1	6:30h	10 min 25 min	Robustness
PLATE 37	STD 100% (prep 2) Sample 100% (prep 2)	5	1	5:30h	10 min 25 min	Robustness
PLATE 38	STD 100% (prep 2) Sample 100% (prep 2)	5	1	6h	10 min 25 min	Robustness
PLATE 39	STD 100% (prep 2) Sample 100% (prep 2)	5	1	6:30h	10 min 25 min	Robustness
PLATE 40	STD 100% (prep 3) Sample 100% (prep 3)	5	1	5:30h	10 min 25 min	Robustness
PLATE 41	STD 100% (prep 3) Sample 100% (prep 3)	5	1	6h	10 min 25 min	Robustness
PLATE 42	STD 100% (prep 3) Sample 100% (prep 3)	5	1	6:30h	10 min 25 min	Robustness

10.3.5.1. TF1 - Stat5 - Luc 2P - TPOR reporter gene Linearity

Linearity was assessed trough the representation of the relative potencies obtained against the concentration applied in the plates. The range covered in the assessment of linearity went from 60 % to 140 % of the standard's curve concentration. The concentrations tested in the dilutions curve at 60 % were 600.00, 60.00, 20.01, 6.66, 2.22, 0.75, 0.25, 0.08, 0.01 and 0.00 ng / mL. The concentrations tested in the dilutions curve at 80 % were 800.00, 80.00, 26.68, 8.88, 2.96, 1.00 0.33, 0.11, 0.01 and 0.00 ng / mL. The concentrations tested in the dilutions curve at 100 %, and in the standard's dilutions curve were 1,000.00, 100.00, 33.35, 11.10, 3.70, 1.25, 0.41, 0.14, 0.02 and 0.00 ng / mL. The concentrations tested in the dilutions curve at 120% were 1200, 120, 40.02, 13.32, 4.44,1.50, 0.49,0.16 0.02 and 0.00 ng / mL. The concentrations tested in the dilutions curve at 140% were 1400.00, 140.00, 46.69, 15.54, 5.18, 1.75, 0.57, 0.19, 0.02 and 0.00 ng / mL.

The results obtained for the linearity plates performed during the validation are presented in Table 33.

Table 33: Reporter gene assay validation. Linearity results.

Plate Id.	Conc. Level (%)	Relative potency	Mean (%)	% RSD
Plate 1	**60%**	62%	63%	2%
Plate 2		62%		
Plate 3		65%		
Plate 4	**80%**	70%	72%	4%
Plate 5		71%		
Plate 6		76%		
Plate 7	**100%**	101%	99%	5%
Plate 8		92%		
Plate 9		105%		
Plate 10	**120%**	128%	115%	9%
Plate 11		102%		
Plate 12		114%		
Plate 13	**140%**	149%	152%	8%
Plate 14		139%		
Plate 15		168%		
Correlation coefficient		**0.9757**		

Figure 58 shows a directly proportional relationship between the concentrations applied to the plates and the results obtained, proving the linearity of the method through the whole evaluated range.

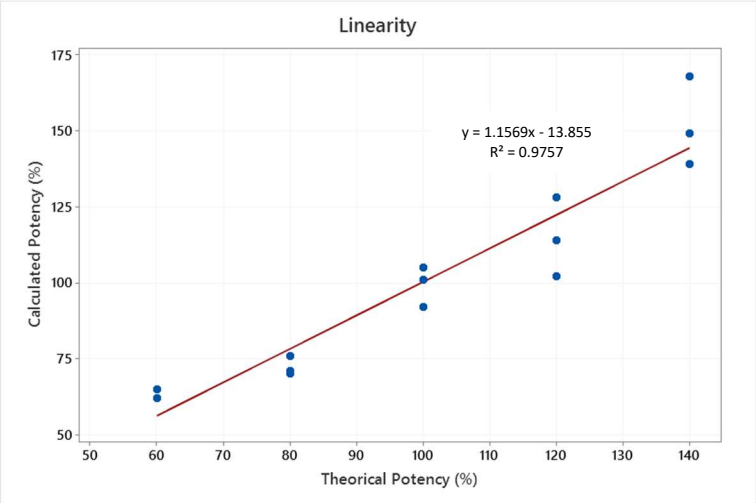

Figure 58: Reporter gen assay validation. Linearity results.

Figure 59 shows a random distribution of linearity results residuals, which indicates that there is no tendency in the results obtained.

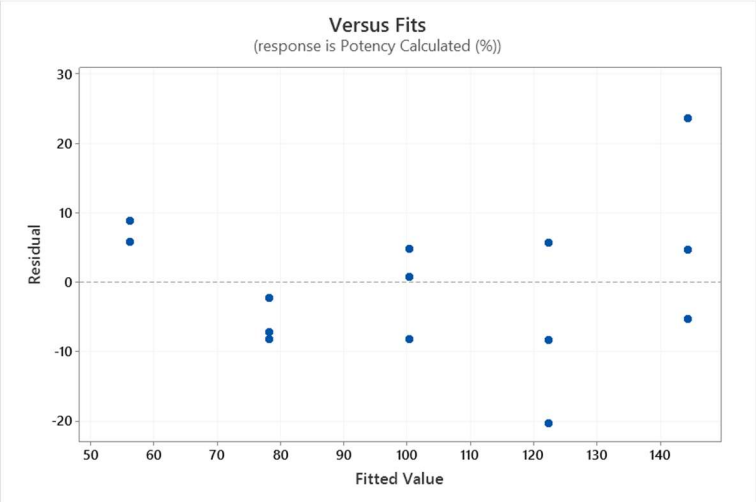

Figure 59: Reporter gen assay validation. Linearity residuals plot.

10.3.5.2. TF1 - Stat5 - Luc 2P - TPOR reporter gene Precision

10.3.5.2.1. TF1 - Stat5 - Luc 2P - TPOR reporter gene Method precision

Precision of the method was assessed trough the repeated analysis of a unique sample a total of 9. Each assay consisted in one plate in which a standard curve at 100 % and a sample curve at 100 % were loaded. The concentrations tested for the standard and the sample were the ones indicated in section 10.3.5.1 for concentration level 100 %.

The relative potencies obtained for the sample in each assay and de % RSD obtained are presented in Table 34.

Table 34: Reporter gene assay validation. Method precision results.

Plates id.	Analyst	Day	Relative Potency	Average (%)	% RSD
Plate 16	Analyst 1	Day 2	111%	102%	7%
Plate 17			109%		
Plate 18			108%		
Plate 19			107%		
Plate 20			103%		
Plate 21			103%		
Plate 22			92%		
Plate 23			93%		
Plate 24			91%		

The results presented a compliant % RSD between the 9 results obtained, as a % RSD < 20% was established as a threshold. Therefore, the precision of the method suitability was demonstrated.

10.3.5.2.2. TF1 - Stat5 - Luc 2P - TPOR reporter gene Intermediate precision

For the study of the intermediate precision, the analysis of the same sample was performed three times by each one of two independent analysts on the same day (Table 35) and 3 times by a single analyst each one of 3 independent days (Table 36). Each assay consisted in one plate in which a standard curve at 100 % and a sample curve at 100 % were loaded. The concentrations

tested for the standard and the sample were the ones indicated in section 10.3.5.1 for concentration level 100 %.

Table 35: Reporter gene assay validation. Intermediate precision between analysts results.

Plates id.	Analyst	Day	Relative Potency	Average (%)	% RSD
Plate 16	Analyst 1	Day 2	111%	109%	1%
Plate 17	Analyst 1		109%		
Plate 18	Analyst 1		108%		
Plate 25	Analyst 2		86%	90%	3%
Plate 26	Analyst 2		93%		
Plate 27	Analyst 2		90%		
Intermediate precision (Analysts)				**100%**	**10%**

Table 36: Reporter gene assay validation. Intermediate precision between days results.

Plates id.	Analyst	Day	Relative Potency	Average (%)	% RSD
Plate 7	Analyst 1	Day 1	101%	99%	5%
Plate 8		Day 1	92%		
Plate 9		Day 1	105%		
Plate 16		Day 2	111%	109%	1%
Plate 17		Day 2	109%		
Plate 18		Day 2	108%		
Plate 28		Day 3	102%	102%	0%
Plate 29		Day 3	102%		
Plate 30		Day 3	103%		
Intermediate precision (Days)				**104%**	**4%**

The results presented show that the performance of the assay by independent analysts or in different days was not a major cause of variability in the results obtained, as the % RSDs were in both cases kept lower than the 30 % established limit. This proves the adequacy of the intermediate precision of the method.

10.3.5.3. TF1 - Stat5 - Luc 2P - TPOR reporter gene Accuracy

The accuracy of the method was evaluated through the calculation of the recovery percentage of 3 preparations of each of 3 concentration levels, 80 %, 100 %, and 120 %. The concentrations tested in the dilutions curve at test sample 80 %, standards and test sample at 100 %, and test sample at 120 % were the ones indicated in section 10.3.5.1.

Table 37: Reporter gene assay validation. Accuracy results.

Plate Id.	Conc. Level (%)	Relative potency (%)	Recovery (%)	Average (%)	% RSD
Plate 4	80%	70%	87%	90%	4%
Plate 5		71%	88%		
Plate 6		76%	95%		
Plate 7	100%	101%	101%	99%	5%
Plate 8		92%	92%		
Plate 9		105%	105%		
Plate 10	120%	128%	106%	95%	9%
Plate 11		102%	85%		
Plate 12		114%	95%		
Accuracy				95%	4%

The recoveries obtained, as shown in Table 37, meet the requirements of recovery between 70 % and 130%. Additionally, no tendency was observed between the recoveries at the different dilution curve concentrations prepared. All in all, these results demonstrated that the method presented adequate accuracy for the determination of the potency of the product samples which testing is going to be required.

10.3.5.4. TF1 - Stat5 - Luc 2P - TPOR reporter gene Selectivity

For the assessment of methods selectivity, the preparation and loading in 3 plates of 3 STD dilutions curves and 3 DP excipients buffer dilutions curves, used as test samples was performed. Figure 60 shows the response generated for the STD in contrast with the DP excipients buffer.

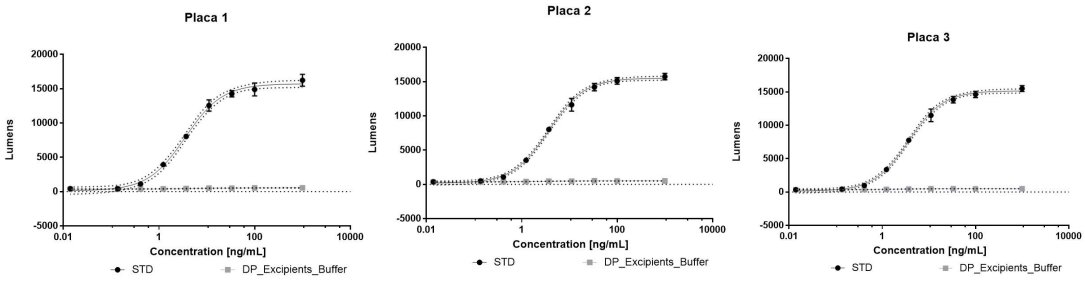

Figure 60: Reporter gene assay validation. Selectivity results.

It can be observed in the graphics that no response was obtained when the dilution curve was prepared using the DP buffer of excipients.

On the other hand, the OD values obtained for the different concentrations of romiplostim biosimilar excipients buffer were compared with the OD values obtained for cells without treatment (Table 38).

Table 38: OD values obtained for the assessment of selectivity in the reporter gene assay.

Concentration (ng/mL)	**1,000.00**	**100.00**	**33.35**	**11.11**	**3.70**	**1.25**	**0.41**	**0.14**	**0.02**	**0.00**	
Luminometry values Plate 31	648	624	520	508	436	404	402	358	382	406	Selectivity
	550	552	552	586	454	398	394	412	314	342	
	478	474	398	454	456	402	364	358	434	392	
Luminometry values Plate 32	532	500	568	468	522	468	374	350	328	388	
	518	506	564	500	452	378	388	354	320	436	
	472	470	482	440	410	418	404	376	404	422	
Luminometry values Plate 33	524	500	538	472	492	410	356	342	328	314	
	532	516	528	530	456	368	384	384	326	416	
	452	436	460	492	400	448	342	364	364	384	
Average	523	509	512	494	453	410	379	366	356	389	**439**
% RSD	10%	10%	10%	8%	8%	7%	5%	5%	11%	9%	**14%**

Even though a small tendency of obtaining higher luminometry values at higher product concentrations, these variations are not sufficient for causing differences in the results obtained as a high signal to noise ratio is observed.

As explained in the validation of the proliferation potency assay, the DS excipients buffer is equivalent to DP excipients buffer but at half the excipients concentration, which makes it adequate to assume that no interference is going to be observed for DS either.

With everything considered, the results presented show the methods selectivity in the determination of the products of interest potency, without interference of the excipients matrix.

10.3.5.5. TF1 - Stat5 - Luc 2P - TPOR reporter gene Robustness

TF1 - Stat5 - Luc 2P - TPOR reporter gene assay robustness was assessed through the reading of the luminescence of 9 plates, incubated for 5.5 h, 6.0 h or 6.5 h after the application of the stimuli, 10 min and 25 min after the application of the Bio-Glo™ Luciferase Assay System detection reagent. The plates had been loaded with a standard curve at 100 % and a sample curve at 100 %. The concentrations tested for the standard and the sample were the ones indicated in section 10.3.5.1 for concentration level 100 %.

To determine if there were differences in the results obtained caused by the different incubation times of the plates after the application of the stimuli the % RSD between the mean of the results obtained at the 3 incubation times was calculated (Table 39). Apart from that an ANOVA was performed to detect significant differences between the 3 groups.

Table 39: Reporter gene assay validation. Robustness results for the plates incubation time after the application of the stimuli.

Plate Id	Plate incubation time (h)	Relative potency (%)	Average (%)	% RSD
Plate 34	5.5	89%	92%	9%
Plate 37	5.5	103%		
Plate 40	5.5	83%		
Plate 35	6	117%	101%	11%
Plate 38	6	92%		
Plate 41	6	93%		
Plate 36	6.5	95%	88%	6%
Plate 39	6.5	88%		
Plate 42	6.5	82%		
Robustness			**94%**	**6%**

The results presented show that there were not important variations due to changes in the incubation time of the plates after the application of the stimuli in the evaluated times range.

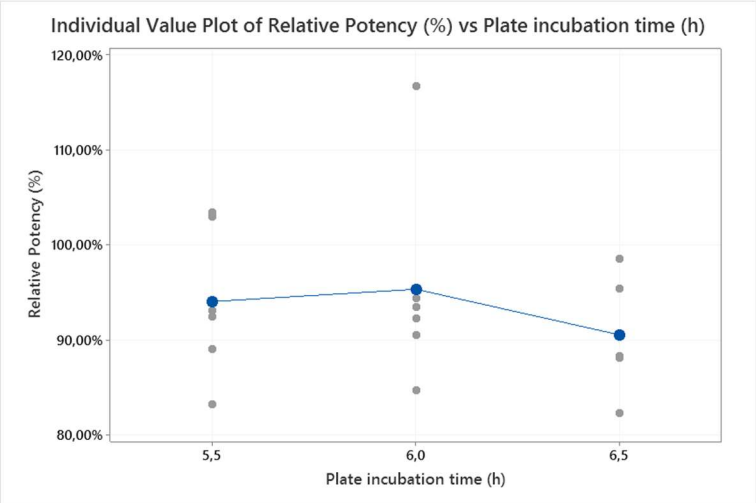

Figure 61: Reporter gene assay validation. Results distribution for the different incubation times of the plates after the application of the stimuli.

The p-value resulting from the ANOVA analysis of the results obtained when incubating the plates 5.5 h; 6.0 h or 6.5 h after the application of the stimuli was 0.610, showing with a 95% confidence that there were no significant differences between the three incubation times, since $p > 0.05$. Additionally, no tendency in the distribution of the results was observed for the 3 incubation times.

To determine if any differences were observed between the results obtained when incubating the plates with for the Bio-Glo™ Luciferase Assay System reagent for 10 min or for 25 min the % RSD between the results obtained for each plate at the 2 incubation times was calculated (Table 40). Additionally, an ANOVA was performed to determine that there were not significant differences between the 2 incubation times.

Table 40: Reporter gene assay validation. Robustness results for the Bio-Glo™ Luciferase Assay System reagent incubation time.

Plate Id	Bio-Glo incubation time (min)	Relative potency (%)	Average (%)	SD (%)	% RSD
Plate 34	10	89%	91%	2%	2%
Plate 34	25	92%			
Plate 35	10	117%	106%	11%	11%
Plate 35	25	94%			
Plate 36	10	95%	97%	2%	2%
Plate 36	25	99%			
Plate 37	10	103%	98%	5%	5%
Plate 37	25	93%			
Plate 38	10	92%	88%	4%	4%
Plate 38	25	85%			
Plate 39	10	88%	89%	1%	1%
Plate 39	25	90%			
Plate 40	10	83%	93%	10%	11%
Plate 40	25	103%			
Plate 41	10	93%	92%	1%	2%
Plate 41	25	90%			
Plate 42	10	82%	85%	3%	3%
Plate 42	25	88%			

The analysis of the results showed that there were no major changes in the results due to alterations in the incubation time with Bio-Glo™ Luciferase Assay System between 10 and 25 minutes, as a p-value of 0.835 was obtained. Apart from that, a p-value of 0.835 was obtained for the ANOVA analysis comparing the two groups, showing with a 95% confidence that there were no significant differences between them. Figure 62 shows no tendency in the distribution of the results for any of the incubation times tested.

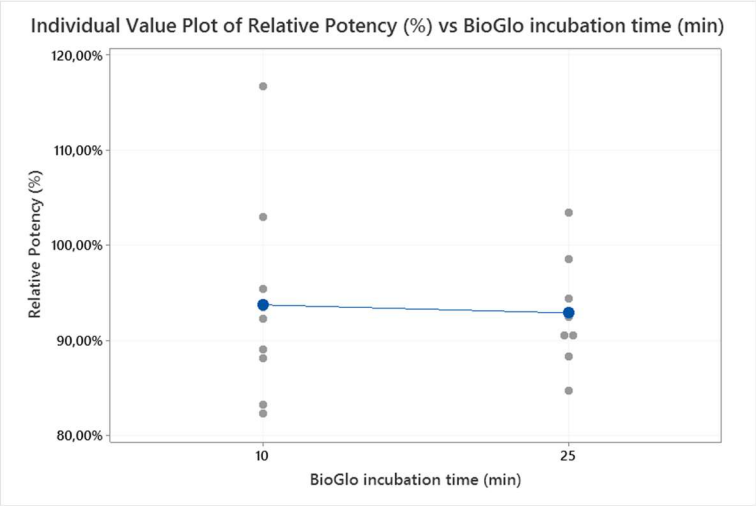

Figure 62: Reporter gene assay validation. Results distribution for the different the Bio-Glo™ Luciferase Assay System incubation times.

Analysed all together, the results presented prove that the assay is robust for plats incubation after the application of the stimuli for 6h ± 30 min and for Bio-Glo™ Luciferase Assay System incubation times between 10 and 25 min.

10.3.5.6. Summary of the reporter gene potency assay validation results

Table 41: Reporter gene assay validation. Results summary.

Parameters	Acceptance criteria	Results		Complies / No Complies
Specificity	No response observed	No response observed		Complies
Linearity	$R^2 \geq 0.95$	$R^2 = 0.98$		Complies
Method Precision	% RSD ≤ 20%	% RSD = 7%		Complies
Intermediate Precision	% RSD ≤ 30%	Analysts	% RSD = 10%	Complies
		Days	% RSD = 4%	Complies
Accuracy	Recovery between 70%-130%	Plate 4	Recovery 87%	Complies
		Plate 5	Recovery 88%	Complies
		Plate 6	Recovery 95%	Complies
		Plate 7	Recovery 101%	Complies
		Plate 8	Recovery 92%	Complies
		Plate 9	Recovery 105%	Complies
		Plate 10	Recovery 106%	Complies
		Plate 11	Recovery 85%	Complies
		Plate 12	Recovery 95%	Complies
Robustness	P-Value > 0.05	Plate incubation time	p = 0.610	Complies
		Bio-Glo incubation time	p = 0.835	Complies

11. DISCUSSION OF CHAPTER 2

Immune Thrombocytopenia is a bleeding disorder, mild or moderated in most of the cases but that can evolve to sever in some patients, associated with low platelet counts in those who suffer from it (83). Even in those individuals exempt from the most severe symptoms, poor life quality is associated with ITP (112).

The association of the existing treatments with severe adverse effects and the failure, in some patients, of the first line treatments (117) (119), together with the discovery and purification of the growth factor thrombopoietin, responsible for increasing the platelet synthesis, motivated the research focused on the development of new alternatives, but the first generation of thrombopoietic drugs, composed by recombined thrombopoietin forms, failed due to the induction, in some of the participants in the clinical trials, of neutralizing antibodies against the pharmaceutical products which cross-reacted with endogenous thrombopoietin, leading to a worsened thrombocytopenia after the treatment (166).

The second generation of thrombopoietic drugs, consisting in TPO receptor agonists, capable of activating TPO-R, but with no sequence similarity with endogenous TPO, achieved more successful results, ending with the FDA approval in 2008 of romiplostim and eltrombopag as second line treatments for ITP (167) (168).

After the success of romiplostim in the market, RJF decided to develop a biosimilar for romiplostim. The development of biosimilar products is a good strategy for pharmaceutical companies, as it represents the reduction of the costs associated with the development of pharmaceutical products, which is especially high for biologics, and it is also advantageous for the society as it increases the accessibility to the novel therapy without a reduction in efficacy and safety (19).

The comparison of 3 batches of the biosimilar DP and 3 batches of the biosimilar DS with 3 batches of the RMP proved similarity in the kinetics of the molecular interaction with the TPO-R, demonstrating that at equal effective sample concentrations, comparable binding with equivalent association and dissociation phases was obtained for the biosimilar DP, biosimilar DS and RMP.

The proving of the similarity between the biosimilar and the RMP in terms of receptor binding allowed the start of a next step in the project, consisting in the development of adequate potency measurement methodology, as evidencing comparable biological activity between the

biosimilar and the RMP is essential for the demonstration of biosimilarity. Additionally, adequate validated procedures for the assessment of the potency of the product are essential for any pharmaceutical formula commercialization.

Two complementary assays have been developed to assess the potency of the product. Both assays are based on modified cell lines which belong to the hematopoietic linage, and which are dependent on hematopoietic growth factors. This is important for mimicking the physiological process as much as possible.

The first assay is a proliferation assay useful for the confirmation of the ability of the biosimilar under development to complete its purpose, which is cell proliferation, for the increasement of the platelet counts in the ITP patients. The main disadvantage of the proliferation assay is that it is time consuming as 72 h are required for the obtention of the result. The second assay consists in a reporter gene-based assay, which is useful to confirm the activation of the receptor and the consequent gene transcription but does not provide evidence about the final response caused by the drug. On the other hand, the reporter gene base assay presents the advantage that it allows for the obtention of results just 6 h after the treatment of the cells, which may be useful for the performance of studies on the product which may require the analysis of many samples in a short period of time.

The decision of working with the two potency assays makes sense during the development of the product, as it allows for the accumulation of more information about the developing product and its mechanism of action. After the accumulation of sufficient data, the evaluation of the necessity of maintaining the two assays for ensuring the quality of the final product will be required.

For both cell lines a confirmation of an adequate receptor expression, a verification of the functionality of the receptors expressed and a parametric definition of all the considerations to be followed for the performance of the assay were made before the definition of a validation plan.

The validation of both potency assays developed demonstrated for the assays to be specific, as no response was shown for the excipients buffer, linear, as the results obtained were directly proportional to the active concentration, accurate, as the calculated result was proximal to the theoretical result, and precise, as acceptable differences were obtained for different assays performed on the same sample.

Apart from that for the proliferation assay, proved to be robust to variations in the incubation time after the application of CCK8 between 3.0 h and 4.0 h, as no significant differences were observed between 3.0 h, 3.5 h and 4.0 h incubation times.

On the other hand, the gene reporter assay proved to be robust to variations in the incubation time of the plates after the application of Bio-Glo™ Luciferase Assay System reagent between 10 and 25 min, as no significant differences where observed between these two incubation times, and also to variations in the incubation time of the plates after the application of the stimuli between 5.5 and 6.5 h, as no significant differences were detected between 5.5 h, 6.0 h and 6.5 h incubation times.

Both assays have been used after its validation for the analysis of the RJF biosimilar products generated from different fabrications and maintained in distinct stability conditions. If adequate results are met for all the parameters described in the quality target product profile, those results will be used for the determination of the commercial pharmaceutical product specifications.

CHAPTER 3: ASSESSMENT OF THE CITOTOXICITY CAUSED BY AN ALREADY COMMERCIAL DISULFIRAM / BENZIL BENZOATE CREAM FOR THE TREATMENT OF SCABIES

12. INTRODUCTION TO CHAPTER 3

12.1. SCABIES

Scabies is a pathology of the human skin caused by the infestation of the epidermis and the dermis layers by the mite *Sarcopters scabiei var. homins* (181). It is strongly associated with poverty and with neglected hygienic conditions, which makes it more prevalent in developing counties, and with overcrowded areas, due to the easy transmissibility of the diseases. Despite this, scabies is a worldwide health issue, with an incidence of approximately 300,000,000 cases per year, which received the World Health Organization designation as a neglected disease in 2009 (182).

The pathology is highly contagious, and the transmission occurs trough skin-to-skin contact or through contact with infected fomites, as the mites can survive for around 48 h separated from the human organism (183). The complete cycle of the mite (Figure 63) occurs on the human host. The infection starts when the pregnant adult female of the mite colonizes the epidermis, digging tunnels in the stratum corneum, and laying 2-3 eggs daily, which hatch 2-3 days after. The larvae develop into nymphs and finally to adult individuals after approximately 21 days after hatching, which mate and proliferate, before dying approximately 60 days after birth (181).

The most common presentation of scabies is classic scabies, where the number of mites infecting an individual is usually reduced to 10-15 mites. Other forms of scabies are the nodular scabies, characterized for the apparition of pruritic nodules caused by a hypersensitivity reaction, usually related with a reinfection, and crusted scabies, characterised by a high density of infecting mites in the individual and usually related with immunodeficiencies (184).

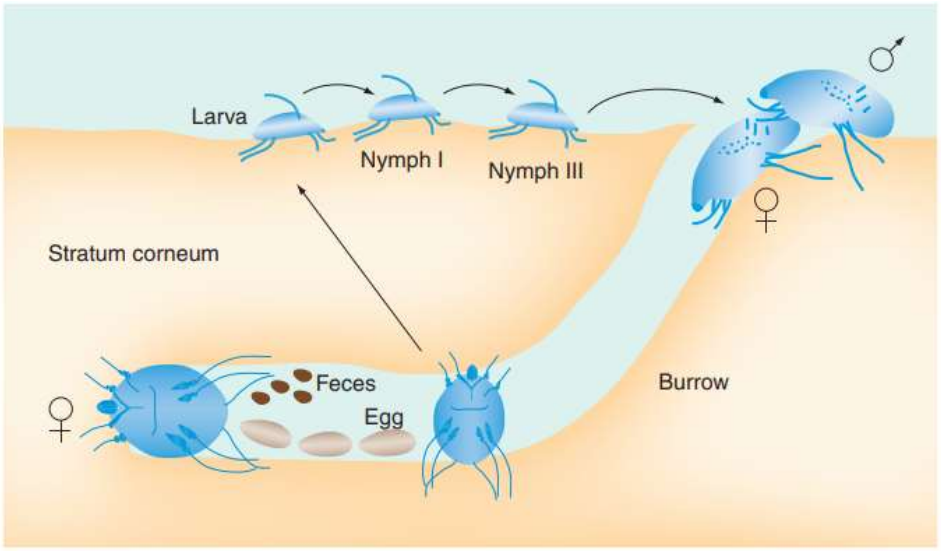

Figure 63: Sarcopters scabiei var. homins life cycle (185).

The symptomatology starts around 3-4 weeks after the first infection, but this time is reduced to 1-2 days in cases of reinfestation. The most characteristic symptom of scabies is a constant itch which worsens at night (184), and it is mainly caused by the inflammatory response generated after the detection of the mite itself and its secretion and excretion products by the immune system cells (186). The skin lesions are produced mainly in the skin folds and are caused by the penetration of the mite in the skin and the secretion of a lytic substance which dissolves the skin tissue allowing the tunnel digging, these lesions are associated with stigmatization of the patients (187). Other symptoms associated with the pathology are the difficulty for sleeping, related with the itching, and debility, because of the incapability to rest (188). All these symptoms conduct to a decreased life quality.

Scabies is usually associated with secondary infections, responsible for complications in the disease, as the mites' secretion products inhibit the complement system, providing a favourable environment for bacterial proliferation (189).

The diagnosis of the disease is usually hard due to the difficulty for the observation of the mite, because of the reduced number of infecting mites per individual. This causes that most of the times the diagnosis is made through the analysis of the skin symptoms together with the patient's medical history. The delay in the apparition of the symptoms after the infection causes that the detection of the pathology occurs too late for the prevention of an outbreak, which makes the treatment of the close contacts essential for the prevention of reinfestation and increases the disease management cost (182,184,190).

12.1.1. Scabies treatment

After the detection of a scabies infection, the pharmacological treatment of the patient and their close contacts is required. Together with the medication of the patients, the decontamination of the beddings and the clothes of the infected individuals, washing them at a temperature superior to 60ºC, is required for the elimination of the potentially infecting fomites (188). Severe outbreaks may require prophylactic population treatment to prevent the reinfestation of the cured patients and to guarantee the outbreak control. The remission of the symptomatology after the end of the treatment may take around 6 weeks (191,192). There are several options with proven effectiveness against scabies. Three of the most used are permethrin, ivermectin and benzyl benzoate.

The first line treatment in many industrialized countries is the application of a topical Permethrin 5% cream covering the complete body surface excluding the head, as this area is usually unaffected in adults (193). The treatment is applied at night and removed in the morning. Permethrin acts through the disruption of the sodium channels in the cells of the nervous system of the mites, causing its death. The treatment presents low toxicology and minimum adverse effects (187,194). Despite this, the use of this treatment has as a negative point that it is not accessible for developing countries, which are the most affected by the pathology, and an increase in the development of resistances.

A second option of treatment is the use of ivermectin 200 µg / kg (188), which causes the death of the parasite by interfering with the normal function of its chloride channels, important for the normal function of the cells of the muscular and the nervous system. One of the advantages of this treatment is that it can be taken orally, which makes its use easier and a good option for prophylactic treatment for close contacts (182).

The third option for scabies treatment consists in the topical application of a benzyl benzoate cream at 10-25 % concentration covering the full body surface, excluding the head, and letting it to act for 24 h (195).

All the treatments have in common that a second application is recommended 1 or 2 weeks after the first application. This is because the treatments are less effective on the eggs, and the second application ensures the elimination of all the infecting individuals.

Bioglan, the Swedish subsidiary of RJF, has a formula, available in the market, composed by a combination of disulfiram (2 %) and benzyl benzoate (22.5 %) for the treatment of scabies, this combination is believed to present an enhancer effect achieving an improved activity compared with a treatment with benzyl benzoate alone. A series of experiments were performed in RJF to gain more information about the pharmaceutical formula cytotoxicity profile.

12.1.1.1. Disulfiram

Disulfiram is mostly known for its use in the treatment of chronic alcoholism dishabituation, as it is an inhibitor of the enzyme aldehyde dehydrogenase, which causes the accumulation in blood of acetaldehyde after alcohol consumption, that produces disconformable effects on the patient (196).

Despite its importance in the treatment of alcoholism, disulfiram initial use was for other purposes. In the early 40s, its use was destined to the vulcanization of rubber in industry, and the first application of the chemical for medical purposes was in 1942, when the efficacy of disulfiram against scabies was firstly reported. After the determination of its ability for the chelation of cooper as the mechanism of action as scabicide, its effectiveness against intestinal warms was also evaluated with positive results (197).

In recent years, the perspective of another repositioning for disulfiram has emerged. In the one hand, the potential of disulfiram for the treatment of cancer is being studied due to its antiproliferative activity and due to its effects on oxidative stress (198–200). On the other hand, its effectiveness as antibiotic and for the treatment of other parasitic infections is also under study (201–203).

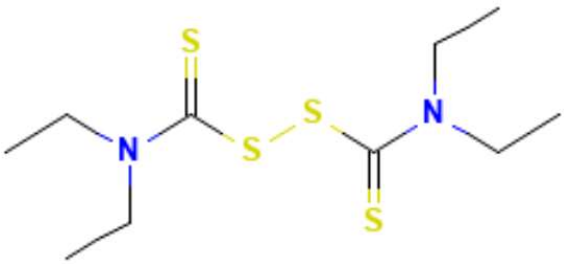

Figure 64: Disulfiram structure (204).

12.1.1.2. Benzyl benzoate

Benzyl benzoate (BB) is an ester derived from benzoic acid and benzyl alcohol (205) and it is one of the oldest options for scabies treatment (206). It is believed to cause the *Sarcopters scabiei var. homins* mite death trough impairment of the correct nervous system functioning by interfering with the ion channels (195).

Even though BB presents better *in-vitro* results against scabies than other treatment options (207,208), the positive results are reduced *in-vivo*, because BB is a potent skin irritant which causes intense skin burning sensation after its application, which have a negative effect on patients' compliance (205).

Although BB mechanism of action lacks complete comprehension and even considering the adverse effects produced by it and the reduced compliance, topical BB application is one of the preferable options for scabies treatment, mainly due to its affordable price, which makes it the best option in developing countries, in which permethrin availability is limited and in which scabies is a major health concern (188).

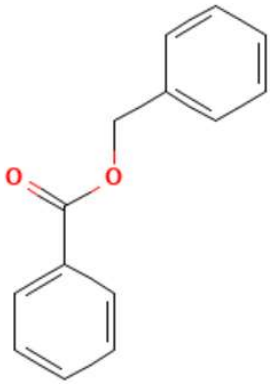

Figure 65: Benzyl benzoate structure (209).

12. RESULTS OF CHAPTER 3

12.1. CYTOTOXICITY ASSAY OF THE D / BB CREAM AND ITS COMPONENTS ON HEK001 CELL LINE

A cytotoxicity assay was performed to determine the response of the cells to the stimulation with the active ingredients of the cream, disulfiram (D) and benzyl benzoate (BB), the D / BB cream and the placebo of the cream, and for the determination of non-cytotoxic threshold for the establishment of the most adequate concentrations to be used in the posterior steps. The results obtained after the 24 h treatment with the active ingredients of D / BB cream are presented in Table 42, and graphically represented in Figure 66 and in Figure 67.

Table 42: Survival rates obtained for the cells after a 24 h exposure to different concentrations of disulfiram and benzyl benzoate.

[D] µM	% Survival
33.36	0.10
22.24	0.19
14.83	1.61
9.88	17.79
6.59	53.36
4.39	89.59
2.93	99.82
1.95	102.95
1.3	100.00
0	100.00

[BB] µM	% Survival
5000	94.23
1666.67	96.47
555.56	93.35
185.19	92.50
61.73	99.98
20.58	98.11
6.86	92.23
2.29	90.11
0.76	87.88
0	100.00

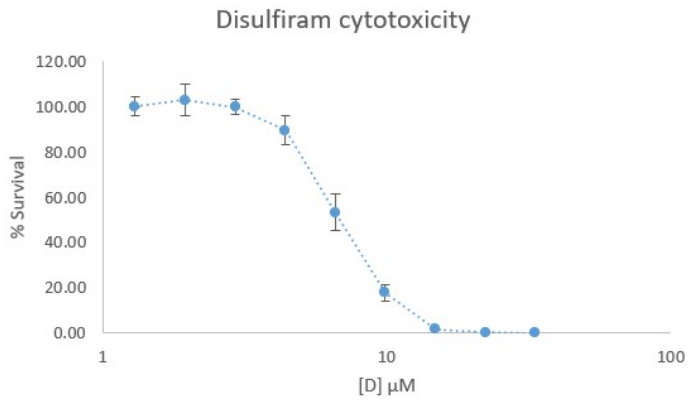

Figure 66: Graphic representation of the cytotoxicity profile of disulfiram.

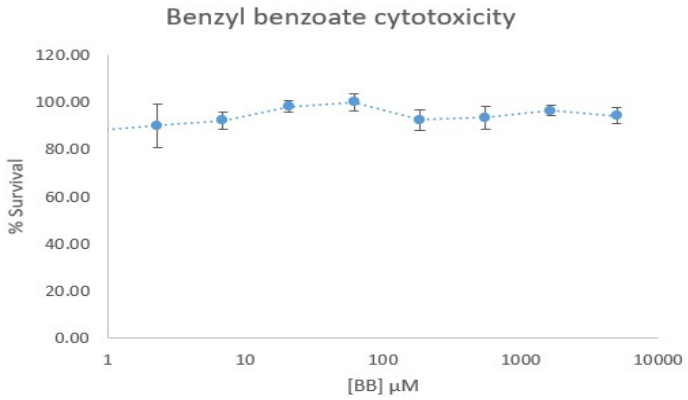

Figure 67: Graphic representation of the cytotoxicity profile of benzyl benzoate.

The analysis of the cytotoxicity produced by the two active ingredients when tested separately illustrated that while D caused a decrease in cell viability starting at the concentration of 6.59 µM, BB was not cytotoxic for keratinocytes, as the highest concentration tested was innocuous for cell viability. These observations led us to think that the cytotoxicity observed for D / BB cream was related with disulfiram and not with benzyl benzoate.

Additionally, to the analysis of the impact in cell viability produced by the two active ingredients, the cytotoxicity of the placebo was also evaluated. The results obtained after the 24 h treatment with different concentration of the placebo are presented in Table 43, and graphically represented in Figure 68. Considering that disulfiram was the active ingredients causing a reduction in cell viability, the results were plotted considering the concentration of D.

Table 43: Survival rates obtained for the cells after a 24 h exposure to different concentrations of the placebo.

[PLACEBO]	% Survival
C1	86.40
C2	100.60
C3	106.04
C4	102.01
C5	113.63
C6	109.71
C7	105.93
C8	112.21
C9	111.38
C10	100.00

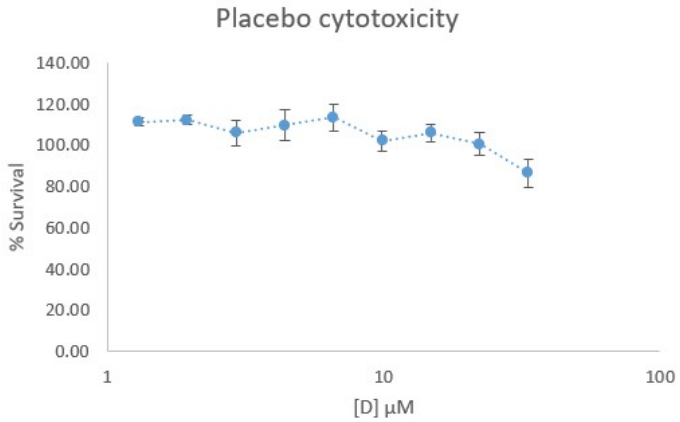

Figure 68: Graphic representation of the cytotoxicity profile of Placebo.

The cytotoxicity results obtained for the placebo showed that a reduction in cell viability should neither be expected for the components of the cream's placebo.

The results obtained after the 24 h treatment with different concentration of the D / BB cream are presented in Table 44, and graphically represented in Figure 68.

Table 44: Survival rates obtained for the cells after a 24 h exposure to different concentrations of the D/BB cream.

[D/BB] µM	% Survival
32.10 / 504.76	0.09
21.40 / 336.51	0.20
14.27 / 224.34	1.33
9.51 / 149.56	6.45
6.34 / 99.76	36.43
4.23 / 66.47	92.51
2.82 / 44.31	99.24
1.88 /29.54	105.71
0.94 / 14.77	107.70
0.00 / 0.00	100.00

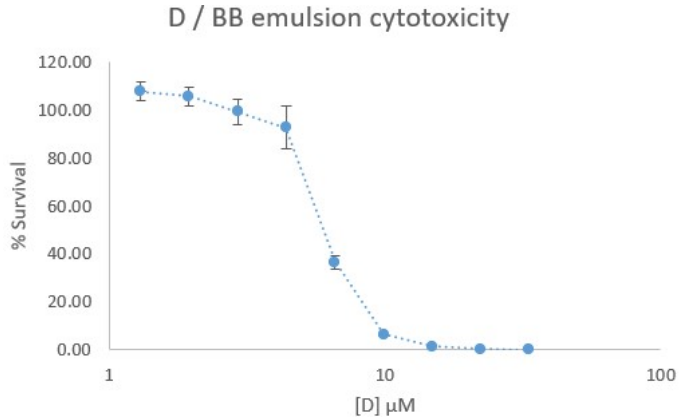

Figure 69: Graphic representation of the cytotoxicity profile of D/BB cream

The results showed that the treatment with the cream caused a reduction in cell viability at concentrations equal or higher than 6.34 µM for D and equal of higher than 99.76 µM for BB, which was consistent with the results obtained for D when assessed separately from the rest of the components. Considering this, together with the fact that none of the other components of the cream showed any cytotoxicity, it can be assumed that the cytotoxicity caused by the D / BB cream is only related with the presence of D in it.

12.2. EVALUATION OF THE IMPACT OF THE TREATMENT WITH THE D / BB CREM ON HEK001 GENE EXPRESSION THROUGH A TRANSCRIPTOMIC MICROARRAY ANALYSIS

To assess the impact of the treatment in gene expression, HEK001 cells were treated for 24 h with the D / BB cream, using a concentration corresponding to a dose of 6.59 µM for D and of 99.77 µM for BB. The selection of the concentration for the treatment was performed based on the results of the cytotoxicity assay.

According to the filtering criteria ($p < 0.05$ and fold change > / < 1.5), 95 genes were identified to present differential expression between the cells treated with the cream compared with the cells without treatment. Those genes were classified in two groups, depending on if they were down-regulated genes (fold change < 1.5, Table 45), or up-regulated genes (Fold change > 1.5, Table 46).

Table 45: Down-regulated genes after the treatment with D / BB cream. The genes were ordered according to their p-value.

Gene Symbol (Name)	p-value	Fold Change	[CTRL] (raw)	[D/BB] (raw)	FUNCTION
AOX1 (Aldehyde Oxidase 1)	7.40E-06	- 1.82	199	110	Important for the **metabolism of drugs** with aromatic residues (210).
IL24 (Interleukin 24)	9.47E-06	- 1.77	572	325	Control of the cell cycle, being able to cause the **cell cycle arrest** and induce cell death after the detection of cell damage (211).
HIST1H2AE (Histone H2A type 1-B/E)	4.06E-05	- 1.68	2028	1208	Component of the nucleosome.
NR1D1 (Nuclear Receptor subfamily 1 group D member 1)	4.58E-05	- 1.60	465	289	Role in the regulation of cytokines and chemokines in **inflammatory response** (212).
KRTAP2-3 (Keratin Associated Protein 2-3)	6.59E-05	- 1.89	484	258	Keratin associated protein. Important for the cytoskeletal functioning (213).
CDC45 (Cell Division Cycle 45)	6.88E-05	- 1.57	447	282	Essential for the initiation of the **DNA replication** (214).
TMEM105 (Transmembrane protein 105)	9.01E-05	- 1.71	79	46	Component of the cell membrane.
HIST2H3A (Histone cluster 2 H3 family member)	1.03E-04	- 1.67	537	321	Component of the nucleosome.
SHCBP1 (SH2 domain-binding protein 1)	1.09E-04	- 1.51	929	612	Important in the downstream signalling pathway of Shc. Plays a role in **cell proliferation and differentiation** (215).
HIST2H3C (Histone H3.2)	1.18E-04	- 1.62	509	313	Component of the nucleosome.

Gene Symbol (Name)	p-value	Fold Change	[CTRL] (raw)	[D/BB] (raw)	FUNCTION
KIAA0101 (PCNA-associated factor)	1.30E-04	- 1.61	332	213	Promoter of the **cell proliferation**. **Regulator of DNA repair** and of the control of centrosome number during **DNA replication** (216).
CSNK1G1 (Casein Kinase 1 Gamma 1)	1.30E-04	- 1.61	332	213	Involved in the Wnt signalling pathway. Important in **cell proliferation** as it has a role in the **cell cycle arrest** after identification of DNA damage and involved in **DNA repair** (217).
RRM2 (Ribonucleotide reductase subunit M2)	1.46E-04	- 1.66	1533	923	Deoxyribonucleotides synthesis catalyser. Essential for the **synthesis of DNA**. Inhibitor of Wnt signalling pathway (218).
CPED1 (Cadherin like and PC-Esterase Domain Containing 1)	1.48E-04	- 1.74	129	78	Expressed in a diversity of tissues but with not known function (219).
CXCL5 (C-X-C Motif Chemokine Ligand 5)	1.95E-04	- 1.50	2006	1359	Chemokine. Participates in **neutrophil requitement and activation**. Involved in angiogenesis and in the generation of connections within the tissues (220).
EXO1 (Exonuclease 1)	2.05E-04	- 1.65	436	265	Involved in **DNA mismatch repair** (221).
RAB33A (Ras-related protein Rab-33A)	2.14E-04	- 1.52	51	34	**Vesicular transport** (222).
FAM111B (FAM111 Trypsin Like Peptidase B)	2.14E-04	- 1.56	564	361	Regulator of the p53 signalling pathway. Regulator of the **cell cycle** and **apoptosis** by controlling the expression of BAG3 and BCL2 (223).

Gene Symbol (Name)	p-value	Fold Change	[CTRL] (raw)	[D/BB] (raw)	FUNCTION
HIST1H2BJ (Histone H2B type 1-J)	2.24E-04	- 1.51	638	423	Component of the nucleosome.
HIST1H2AB (Histone H2A type 1-B/E)	2.24E-04	- 1.71	313	181	Component of the nucleosome.
ESX1 (Homeobox protein ESX1)	2.56E-04	- 1.55	197	128	Regulator of the **cell cycle** trough arrest at phase M by inhibition of cyclin A an B1 degradation (224).
PTGS2 (Prostaglandin-endoperoxide synthase 2)	3.16E-04	- 1.56	1488	984	Involved in the synthesis of prostanoids, important for the **inflammatory response** (225).
IL7R (Interleukin 7 receptor)	4.24E-04	- 1.51	977	662	Critical role in **lymphocytes development** (226).
HIST1H2AM | HIST1H3J (Histone H2A type 1 | Histone H3.1)	6.72E-04	- 1.55	898	578	Component of the nucleosome.
HIST1H2AG (Histone H2A type 1)	7.25E-04	- 1.56	1659	1057	Component of the nucleosome.
HIST1H2BG (Histone H2B type 1-C/E/F/G/I)	8.02E-04	- 1.54	1014	649	Component of the nucleosome.
ADAMTS1 (Metalloproteinase with thrombospondin motifs 1)	8.56E-04	- 1.54	357	245	Association with the **inflammatory response**. Inhibitor of **cell proliferation** and **angiogenesis** (227).
EPHX3 (Epoxide Hydrolase 3)	1.09E-03	- 1.54	120	83	Conversion of epoxides into diols and tiols (228).

Gene Symbol (Name)	p-value	Fold Change	[CTRL] (raw)	[D/BB] (raw)	FUNCTION
CLSPN (Claspin)	1.13E-03	- 1.75	325	205	Sensor of the **integrity of DNA**. Mediator of the **arrest of the cell cycle** (229).
HIST1H1B (Histone H1.5)	1.15E-03	- 1.62	1770	1085	Component of the nucleosome.
HIST1H3B (Histone H3.1)	1.59E-03	- 1.67	189	119	Component of the nucleosome.
KRTAP2-1 (Keratin-Associated Protein 2-1)	1.71E-03	- 1.57	421	277	Important for the cytoskeletal functioning (213).
HIST1H3A (Histone H3.1)	2.46E-03	- 1.75	114	71	Component of the nucleosome.
HIST1H3G (Histone H3.1)	2.65E-03	- 1.56	280	183	Component of the nucleosome.
FYB (FYN Binding Protein)	2.76E-03	- 1.53	439	310	Involved in **T-cells and platelets activation** cascades. Role in **cytoskeleton rearrangement** (230).
HIST1H4A (Histone H4)	3.00E-03	- 1.68	74	40	Component of the nucleosome.
HIST3H2BB (Histone H2B type 3-B)	3.08E-03	- 1.52	194	128	Component of the nucleosome.
HIST1H3H (Histone H3.1)	3.21E-03	- 1.64	127	82	Component of the nucleosome.
HAS2 (Hyaluronan Synthase 2)	3.22E-03	- 1.69	267	152	Essential for the **synthesis of hyaluronan**, important component of the ECM, and a regulator of cells **adhesion, migration, and differentiation** (231).

Gene Symbol (Name)	p-value	Fold Change	[CTRL] (raw)	[D/BB] (raw)	FUNCTION
GINS2 (DNA replication complex GINS protein PSF2)	3.74E-03	- 1.57	302	208	Essential for **DNA replication** (232).
FBXO5 (F-box only protein 5)	4.48E-03	- 1.68	338	222	Regulator of anaphase promoting complex during **cell cycle** (233).
HIST1H2BI (Histone H2B type 1-C/E/F/G/I)	4.63E-03	- 1.62	186	125	Component of the nucleosome.
HIST1H2BM (Histone H2B type 1-M)	4.98E-03	- 1.54	620	344	Component of the nucleosome.
ESAM (Endothelial Cell Adhesion Molecule)	6.14E-03	- 1.57	85	60	Promotes cell to cell interactions and aggregation, important for **endothelial integrity** (234).
YBX1 (Y-Box Binding Protein 1)	2.05E-02	- 1.62	70	49	Participates in DNA and RNA related processes such as **repression, stabilization, splicing and DNA repair** (235).

Table 46: Up-regulated genes after the treatment with D / BB cream. The genes were ordered according to their p-value.

Gene Symbol (Name)	p-value	Fold Change	[CTRL] (raw)	[D/BB] (raw)	FUNCTION
CLU | MIR6843 (Clusterin | MicroRNA 6843)	5.68E-09	5.56	106	564	Involved in cellular processes such as **ubiquitination, apoptosis, cell proliferation and cell death** (236).
AKR1C2 (Aldo-Keto Reductase Family 1 Member C2)	1.48E-06	2.20	172	368	**Detoxification** processes trough the conversion of aldehyde and ketone groups into alcohols using NADP or NADPH (237).

Gene Symbol (Name)	p-value	Fold Change	[CTRL] (raw)	[D/BB] (raw)	FUNCTION
AKR1C1 (Aldo-Keto Reductase Family 1 Member C1)	1.51E-06	2.26	157	342	**Detoxification** processes trough the conversion of aldehyde and ketone groups into alcohols using NADP or NADPH (237).
PHGDH (Phosphoglycerate Dehydrogenase)	2.65E-06	2.04	151	314	Catalyses the reaction for the starting of **L-serine, cysteine,** and **glycine synthesis** (238).
ASNS (Asparagine Synthetase (Glutamine-Hydrolyzing))	4.85E-06	2.46	491	1297	Aspartate and glutamine conversion into **asparagine and glutamate** (239).
MT1F (Metallothionein 1F)	6.21E-06	2.03	2011	3913	Metallothionein. Involved in the **heavy metals' metabolism** and in the protection against the toxicity caused by them (240).
GLS2 (Glutaminase 2)	8.76E-06	1.82	29	55	**Production of glutathione**, which has antioxidant and detoxifying function (241).
SLC7A11 (Solute Carrier Family 7 Member 11)	9.01E-06	1.75	728	1294	Part of a transport system responsible for the exchange of cysteine for glutamate. Important for the correct **cell metabolism** and the progression of the **cell cycle** (242).
PSAT1 (Phosphohydroxy-threonine aminotransferase)	1.12E-05	1.86	1227	2445	Catalyses the **synthesis** of phosphohydroxythreonine and (243).
CHAC1 (ChaC Glutathione Specific Gamma-Glutamylcyclo-transferase 1)	2.03E-05	1.85	252	468	**Pro-apoptotic** factor trough the catalysation of glutathione cleavage (244).

Gene Symbol (Name)	p-value	Fold Change	[CTRL] (raw)	[D/BB] (raw)	FUNCTION
TEF (Thyrotroph Embryonic Factor)	2.94E-05	1.76	65	115	Transcription factor.
SLC6A9 (Solute Carrier Family 6 Member 9)	6.25E-05	1.63	528	851	Regulation of the expression of proteins implicated in **DNA repair** (245).
TCP11L2 (T-Complex 11 like 2)	6.38E-05	1.66	162	284	Promotes muscle-derived satellite cells **differentiation** (246).
TNFSF10 (TNF superfamily member 10)	8.23E-05	1.55	360	553	Cytokine. After binding its receptor induces **apoptosis** (247).
NQO1 (NAD(P)H Quinone Dehydrogenase 1)	1.05E-04	1.54	1174	1781	Cell **detoxification** processes (248).
GABARAPL1 (GABA type A receptor associated protein like 1)	1.20E-04	1.51	450	688	Self-recycling of the endoplasmic reticulum trough the formation of autophagosome vacuoles. Regulation of processes such as **cell death** and **cell proliferation** and migration (249).
TRIB3 (Tribbles Pseudokinase 3)	1.32E-04	1.66	459	754	Participates in the adaptation to different types of stress, acting as a regulator of the **integrated stress response** (250).
EPCAM (Epithelial Cell Adhesion Molecule)	1.48E-04	1.60	223	353	Participates in the induction of **proliferation** in stem cells. Formation of interactions between epithelial cells (251).
NALCN (Sodium Leak Channel, Non-Selective)	1.65E-04	1.52	125	186	Calcium, sodium, and potassium permeable **channel**, responsible for regulating the cell membrane's potential (252).

Gene Symbol (Name)	p-value	Fold Change	[CTRL] (raw)	[D/BB] (raw)	FUNCTION
RASSF6 (Ras Association Domain Family member 6)	1.71E-04	1.59	33	51	**Apoptosis** inducer and **cell cycle** regulator (253).
ERBB3 (Erb-B2 Receptor Tyrosine Kinase 3)	1.75E-04	1.64	64	114	**Cell proliferation and differentiation** regulation (254).
ZSCAN31 (Zinc Finger and SCAN Domain Containing 31)	1.86E-04	1.64	32	54	Transcription factor.
BVES-AS1 (BVES Antisense RNA 1)	2.01E-04	1.60	36	57	**Long noncoding RNA** (255). Its expression reduces the expression of BVES, which is important for the correct formation of junctions in several tissues and participates in the regulation of cAMP, Wnt signalling pathways (256).
GCLC (Glutamate-Cysteine Ligase Catalytic Subunit)	2.23E-04	1.58	504	799	Limiting enzyme for the synthesis of glutathione, and therefore, essential for the **antioxidant and detoxifying** functions in the cell (257).
REPS2 (RALBP1 Associated Eps Domain Containing 2)	2.27E-04	1.63	55	90	Involved in Ral signalling pathway, which makes it an important controller of **cell proliferation and survival** (258).
CPT1A (Carnitine Palmitoyl-transferase 1A)	2.68E-04	1.69	156	270	Fatty acid oxidation, for **energy production**, in the mitochondria (259).
ADPRM (ADP-Ribose/CDP-Alcohol Diphosphatase, Manganese Dependent)	2.99E-04	1.66	42	70	Synthesis of the second messenger ADP-ribose through hydrolysation (260).

Gene Symbol (Name)	p-value	Fold Change	[CTRL] (raw)	[D/BB] (raw)	FUNCTION
EPHX1 (Epoxide Hydrolase 1)	4.10E-04	1.52	236	388	**Metabolism** of endogenous lipids (261).
AKR1C3 (Aldo-Keto Reductase Family 1 Member C3)	8.39E-04	1.53	129	192	**Detoxification** processes trough the conversion of aldehyde and ketone groups into alcohols using NADP or NADPH (237).
UST (Uronyl 2-Sulfotransferase)	8.95E-04	1.52	97	147	Sulfotransferase.
DNASE2 (Deoxyribonuclease 2, Lysosomal)	8.99E-04	1.51	336	483	Responsible for the **DNA degradation** in apoptotic processes (262).
TTLL1 (TTL Family Tubulin Polyglutamylase Complex Subunit L1)	9.08E-04	1.62	68	104	Able to induce the reprograming of somatic cell for **pluripotency induction** (263).
TLR6 (Toll like receptor 6)	1.04E-03	1.69	60	105	Receptor involved in the **innate immunity**. When activated by diacylated or triacylated lipopeptides recognition triggers the inflammatory response trough NF-κβ activation (264).
TP53INP1 (Tumor Protein P53 Inducible Nuclear Protein 1)	1.37E-03	1.50	75	113	In **response to cell stress** inhibits cell proliferation and induces apoptosis (265).
CAT (Catalase)	1.39E-03	1.63	232	349	Give cells protection against **oxidative stress** (266).
IRAK1BP1 (nterleukin 1 Receptor Associated Kinase 1 Binding Protein 1)	1.75E-03	1.62	113	181	Involved in the NF-κβ signalling pathway and essential for **cell survival**. Essential for the prevention of an excessive inflammatory response (267).

Gene Symbol (Name)	p-value	Fold Change	[CTRL] (raw)	[D/BB] (raw)	FUNCTION
FAM129A (Niban Apoptosis Regulator 1)	1.81E-03	1.55	58	92	Regulates other proteins phosphorylation in **response to stress**, protecting the cells from apoptosis (268)**.**
GSTM4 (Glutathione S-Transferase Mu 4)	1.82E-03	1.54	192	291	Catalyser for the transference of glutathionyl group from glutathione, promoting the **detoxifying action** of glutathione (269).
FIG4 (Polyphospho-inositide Phosphatase)	2.34E-03	1.62	97	158	Involved in the activation of PI(3,5)P2, important for lysosomal and **vesicular transport** normal function (270).
CXCL10 (C-X-C Motif Chemokine Ligand 10)	2.43E-03	1.51	129	193	**Pro-inflammatory** chemokine (271).
DENND4C (DENN Domain Containing 4C)	3.04E-03	1.50	251	400	Activates the canonical Wnt signalling pathway, important for the induction of **cell fate specification and cell proliferation and migration** (272).
LRRC8B (Leucine Rich Repeat Containing 8 VRAC Subunit B)	3.24E-03	1.58	79	115	Component of the channel responsible for the maintenance of a content intracellular volume. Alterations in its expression may lead to **apoptosis** (273).
ZNF483 (Zinc Finger Protein 483)	4.10E-03	1.56	46	72	Transcriptional regulator.
DOCK11 (Dedicator of Cytokinesis 11)	4.29E-03	1.56	108	153	Participates in **B-cells development** (274).
UHRF1BP1 (UHRF1 Binding Protein 1)	4.76E-03	1.50	93	139	**Anti-apoptotic** (274).

Gene Symbol (Name)	p-value	Fold Change	[CTRL] (raw)	[D/BB] (raw)	FUNCTION
PER2 (Period Circadian Regulator 2)	4.93E-03	1.50	65	93	**Repressor of the transcription** for the control of the circadian rhythms related metabolic pathways (275).
PIK3C2B (Phosphatidy-linositol-4-Phosphate 3-Kinase Catalytic Subunit Type 2 Beta)	6.23E-03	1.54	50	79	Involved in EGF and PDGF pathways. Induces rearrangements of the cytoskeleton, important for **cell proliferation, survival, and migration** (276).
GRB14 (Growth Factor Receptor Bound Protein 14)	6.96E-03	1.53	40	61	Inhibits a tyrosine kinase receptor involved in **cell growth and in cellular metabolism** (277).
SESN3 (Sestrin 3)	7.62E-03	1.51	297	423	Metabolic regulator involved in several cellular functions, including the **protection against oxidative and genotoxic stress** (278).
MCOLN3 (Mucolipin TRP Cation Channel 3)	2.38E-02	1.83	53	83	Cation channel (279).

The interactions between the genes whose expression was altered by the treatment were explored using the software String , v11.5 (https://string-db.org) and are presented in Figure 70. Several groups can be identified in the image. In the first place, the group marked in red corresponds to genes of response to cell damage, including genes for the adaptation to oxidative stress and pro-apoptotic genes and genes of protection against apoptosis. Secondly, the group marked in yellow includes genes responsible for the detoxification of the cell and for the drug metabolism. Thirdly, the group marked in green is composed by genes implicated in the inflammatory response. Finally, the groups marked in black, and blue correspond to genes important for the cell cycle arrest in response to cell damage. The group marked in black includes genes implicated in the progression of DNA synthesis, while the group marked in blue corresponds to histones, which are important for the cell cycle progression and, as it can be observed, are highly affected for the treatment.

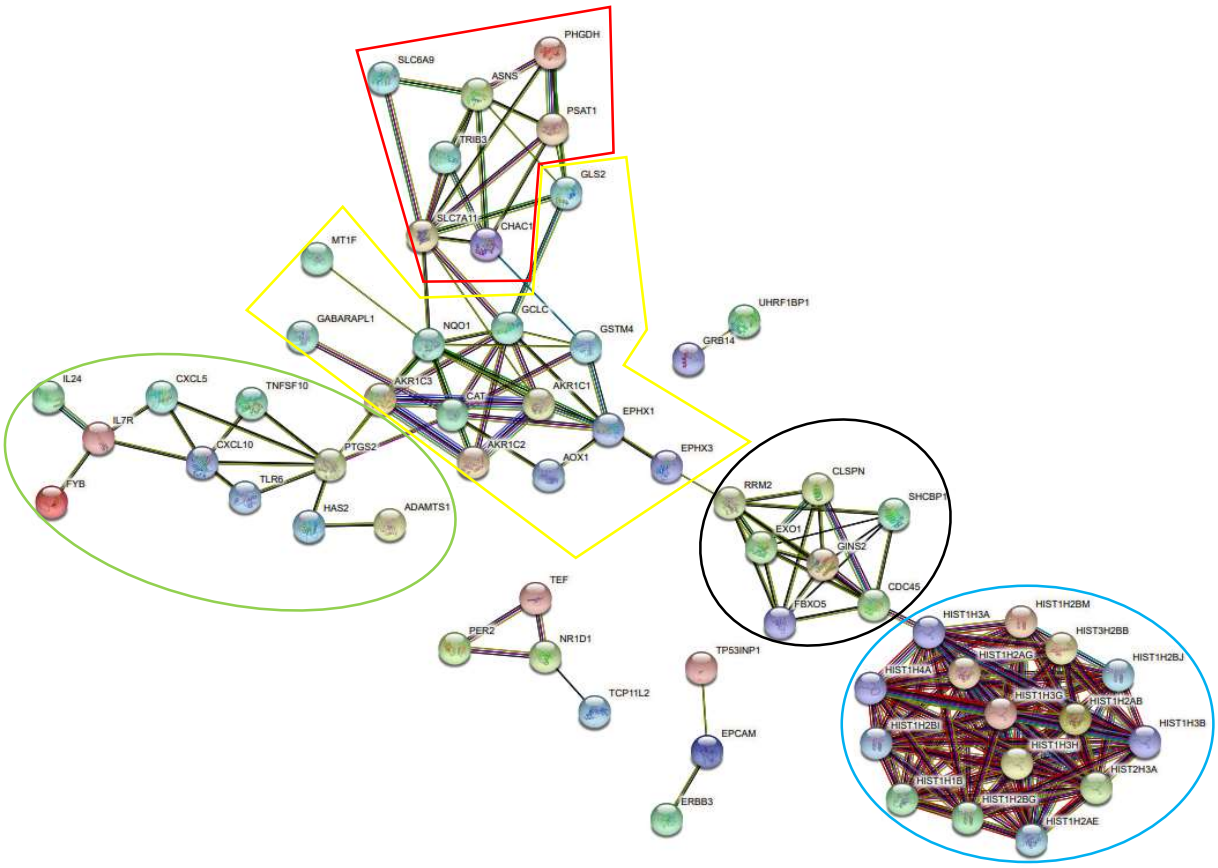

Figure 70: String DB gene interactions representation.

13. DISCUSSION OF CHAPTER 3

The formula available in the market based on disulfiram and benzyl benzoate is one of the treatment options for scabies, a neglected skin disease, highly related with crowded environments and with poverty, which has a high impact in patients life quality (182,187,188). This pharmaceutical product is registered in Sweden and in Iceland, but its use in the rest of the globe has been limited. The recent increase in the scabies incidence in the industrialized countries, probably related with the increase of migration (280), and the apparition of resistances to other scabies treatments (281–284), makes the evaluation of an extension of the geographical area of use of the disulfiram / benzyl benzoate cream interesting, as its limited use, together with the fact that it has more than one active ingredient, offer good perspective in terms of restraining the development of resistances (281).

The analysis of the cytotoxicity caused by the different components of the pharmaceutical formula, when analysed separately, illustrated that neither benzyl benzoate nor the placebo where responsible for the cell death observed for the complete product. On the other hand, disulfiram caused elevated cytotoxicity in keratinocytes at concentrations equal to 6.59 µM or higher. These results lead to the conclusion that disulfiram is the main responsible for the cell cytotoxicity produced by the D / BB. The results presented are representative of the situation that occurs in the patients after the application of the treatment, as the cytotoxicity is evaluated in keratinocytes, which are one of the first cells with which the product comes in contact to, and therefore, those that will be exposed to a highest dose. The cytotoxicity is evaluated at 24 hours, which is the time of exposure to treatment.

The microarrays analysis provided information on the cellular signalling pathways affected after the 24 h treatment with the D / BB cream. This information allows for a better prediction of the adverse effects to be expected and provides clues as to how to prevent them. Most of the pharmaceutical products available in the market present adverse effects, and the important issue is to know them to be able to control them and to make a proper risk assessment for the evaluation of the risk / benefit ratio for informed decision making.

The analysis of the genes whose expression is affected by the treatment shows that the D / BB cream causes an alteration of several pathways important for proper cell functioning. The genes altered can be divided in two groups, in the first place, the genes directly affected by the treatment, which are representative for the cytotoxicity caused in the cell, and, in the second place, the genes responsible for protecting the cell from this cytotoxicity.

The application of the D / BB cream to the cells causes an inflammatory response, illustrated, for example, by the downregulation of NR1D1, associated with an inflammatory phenotype and a reduced cell survival (285), and the upregulation of pro-inflammatory chemokines such as CXCL10.

Additionally, there is a clear induction of apoptosis, represented by the downregulation of interleukin 24, promoting the expression of proapoptotic BCL proteins (286); RAB33, impairing the recycling of damaged or unneeded proteins, promoting their accumulation, and leading to apoptosis (287); and CLSPN (288); and the upregulation of pro-apoptotic genes such as CHAC1, which induces the apoptosis of the cell trough the catalysation of glutathione cleavage (244); BVES-AS1, whose overexpression inhibits cell proliferation while promotes apoptosis (255); TP53INP1, that induces apoptosis in response to stress (265); REPS2, that enhances apoptosis through the NF-κβ signalling pathway inhibition (289); TNSF10, FASSF6 and LRRC8B.

Finally, an alteration in the expression of several genes involved in metal ions metabolism, such as ADAMTS1 or MT1F (227,240), can be observed, probably because of disulfiram's metals chelation properties (197).

As a result of altered gene expression for the genes in the first group, defence mechanisms are activated in the cell to minimize the effects of cytotoxicity. First, there is a cell cycle arrest for the cell to be able to repair the damage suffered before cell division, this cell cycle arrest is mediated through the inhibition of the expression of genes such as CDC45, essential for the initiation of DNA replication (214); GINS2, also required for the DNA replication (232); and SHCBP1, together with and overexpression of several genes which causes the inhibition of proliferation, such as FAM111B (223), among other genes. Additionally, there is an important down regulation of histone genes, whose expression is associated with the S phase of the cell cycle and the increase of its synthesis is essential for the DNA replication and the cell cycle progression, so the reduction of its expression implies the cell cycle arrest (290).

Mechanisms for DNA repair are also activated, promoted by the inhibition of the expression of genes such as EXO1, which is downregulated after the occurrence of double-strand breaks to ensure proper DNA repair (291), and the overexpression of genes such as PHGDH, which improves the response to DNA damage (292); and SLC6A9, the overexpression of which results in an increase of DNA repair proteins (245).

There is also a modulation of the expression of genes to promote cell survival, such as anti-apoptotic genes and genes of protection against oxidative stress, for example CLU, secreted to

prevent apoptosis in a situation of stress, FAM111B, whose downregulation reduces the expression of pro-apoptotic proteins such as BAG3 and BCL2; SLC7A11, that when upregulated confers protection against ferroptosis to the cell; and CAT, FAM129A and SESN3, which conferee protection against oxidative stress (266,268,278).

Finally, the expression of genes for cell detoxification and drug metabolism, such as various AKRs, which are important for the detoxification of numerous carbonyl substrates, with both endogen and exogen origin, through their reduction using NAD(P)H as cofactor (293);EPHX1, which is involved in the detoxification of epoxides (294), alkylating agents that can be related with high toxicity, and finally genes involved in glutathione synthesis, such as GLS2 and GCLC (241,257).

Even though the activation of several cytotoxicity pathways after the application of the D / BB can be a source of concern, an internal study performed in RJF for the analysis of the drug absorption (data not shown) showed diffusion to be the principal drug absorbance mechanism. This study illustrated that BB presents good permeability, but the detection of D was only possible in the most external layers of the skin. These results are positive in the case of scabies treatment, as they guarantee a high concentration of the active ingredient where the parasitic infestation occurs, and a proper elimination of the cream after the accomplishment of its function through washing and skin desquamation, while preventing a systemic accumulation of disulfiram, which is strongly believed to be the responsible of the cytotoxicity observed in the cells and which may be related with adverse effects, as the aldehyde dehydrogenase inhibition can conduct to undesirable events occurring on the dermis, the nervous and the cardiac systems, the liver, and the gastrointestinal tract (295), even though the safety profile of disulfiram is well studied and shows a good tolerability for disulfiram oral consumption for several months or even years (296).

Apart from an extension of the geographical area of use of the D / BB crema, the pharmaceutical product also presents interesting perspectives for drug repositioning, considering the new mechanism of action findings of its active ingredients, especially disulfiram.

As previously mentioned, a topical application of disulfiram containing products is preferable, as several adverse effects might be related with a systemic accumulation of this chemical. Considering this, one of the most promising options for D / BB cream repositioning is the study of its effectiveness in other ectopic parasitic infection with structural and physiological

similarities with *Sarcopters scabiei var. homins*. In fact, its use is already approved for the treatment of head and pubic lices.

Additionally, the D / BB cream might be useful for the treatment of skin bacterial infections, as a potential antimicrobial effect of disulfiram has already been described (201,203,297). The mechanism of action of disulfiram against bacterial infections has not been defined yet, but it might be related with the chelation properties of disulfiram (298), as many bacteria use metals as cofactors in many processes essential for their survival. The effect of disulfiram in the disruption of the bacterial membrane, reducing its flexibility has been also hypothesized (299). Finally, the bacterial growth impairment might be mediated by the inhibition of the membrane channels, having an impact on cell potential, which maintenance is essential for proper bacterial functioning.

In summary, the D / BB cream presents interesting options for both a geographic extend of its use and a drug repositioning to increase its therapeutic uses. Additional studies will be required to gain knowledge on the cytotoxicity of the product and the mechanisms of action for its antibiotic and antiparasitic activities.

14. GENERAL DISCUSSION

Pharmaceutical products are essential for the maintenance of a healthy population, as they are necessary for the prevention and treatment of diseases. Despite this, the discovery and development process of a new pharmaceutical product is highly expensive and time requiring since thousands of compounds need to be tested for one of them to get into the market. Additionally, the insurance of developing high-quality products is also essential to guarantee the safety of the patients under treatment, which makes the establishment of severe quality controls through the whole discovery, development, and manufacturing process of pharmaceuticals, mandatory.

The limitations of chemical synthesis products in the treatment of multiple medical conditions have favoured an increase in recent years in the development of products based on biologics as active ingredients, which provide with many new treatment possibilities but also present a much more complex manufacturing, purification, and characterization process, which represents an even greater increase in their discovery and development cost.

The development of generic or biosimilar products to an innovator is a good alternative, which implies benefits for both the pharmaceutical company, which profits with a cheapest and fastest new pharmaceutical product production, and the patients, as it implies a reduction in the cost of the treatments, but the requirements of time and money to develop this type of product is still very high.

In any case, for the generation new pharmaceutical products to be profitable for the pharmaceutical companies, it is essential to stablish control mechanisms in all the steps of the development process to be able to detect, as soon as possible, that a new candidate is not suitable for its intended purpose and, therefore, stop investing money on it. Considering that it is inevitable to test a big number of compounds for the selection of the final candidate, failing fast and cheap is the best option for companies.

The increase in the complexity of the new molecules being used as active ingredients and the increment of the regulatory authorities' requirements in terms of providing information about the new product mechanism of action for characterization and quality controls, before being able to bring a new product to market, the development of more complex assays, additional to the traditional physicochemical tests, has become necessary.

Cell-based bioassays are an excellent tool for the obtention of information of the biological activity of the pharmaceutical products, and their use in the evaluation of pharmaceuticals has become more important with the increase of the complexity of the molecules to be evaluated.

Cell-based bioassays are important for the determination of the characteristics of new drug candidates and for the selection of the best candidate for its progression in the development of the final drug product. The importance of the cell-based bioassays in the first steps of new products discovery and development has been evidenced through the evaluation of the anti-inflammatory potential of several plant extracts, which were candidates for the development of a cream for the treatment of acne outbreaks. The cell-based assays used were useful both for the characterization of the cell line in terms of receptor expression in the cell membrane and for the assessment of the plant extracts characteristics, for the selection of the best candidate.

After the selection of the lead, the availability of a validated cell-based bioassay with demonstrated linearity, precision, accuracy, selectivity, and robustness is essential for the progression of the development process of many pharmaceutical products. This cell-based bioassay is going to ensure that that the final drug product elicits the desired biological activity and to demonstrate batch-to-batch comparability and the stability of the product's potency through its whole self-life. As exemplified in this dissertation, the development of adequate analytical methods for the determination of the potency of a new product is a complex process which requires for the characterization of the cell line that is going to be used in the assay, to prove its suitability for the mimicking of the desired biological response, the optimization of the assay method that allows, for the obtention of the most reliable results with the minimum time and economic expenses, and finally, the demonstration, through the generation of documented results during the methods validation, of the adequacy of the method for all the required parameters to ensure the obtention of reliable results in the drug substance, the drug product and the intermediate samples generated during the manufacturing process.

Once the product has got into the market, additional studies might be performed to generate more information about the product, which can be useful to explore new possibilities for the pharmaceutical of for its active ingredients. Drug repositioning is another alternative to the long and expensive development of the new product and may help to increase the commercial benefits obtained from a product. An example of the possibilities offered by the continuation of the analysis of a product after the obtention of its authorization into the market is discussed through the evaluation of the cytotoxicity elicited by an already commercial cream based on disulfiram and benzyl benzoate as active ingredients, that allowed to determine the most

probable component of the cream to be responsible for the cytotoxicity observed in keratinocytes, which is disulfiram, and to hypothesize about the mechanisms through which this cytotoxicity occurs. The information obtained will be useful to discuss in the future the adequacy of an extension of the geographical area of use of the cream or the extension of its use for the treatment of other pathologies.

In summary, the cell-based bioassays are an essential tool for pharmaceutical companies not only during the discovery and development of new compounds, but also, for the quality controls essential for the release of new batches and for the performance of additional studies once the product is in the market. The importance of the cell-based bioassays through the whole lifespan of pharmaceutical products is expected to rise even more in the future, as the complexity of the new molecular candidates for the development of new products is also increasing. Therefore, the capability of the pharmaceutical companies to efficiently and parametrically develop methods to test this new compound is essential.

15. CONCLUSIONS

- Cell-based assays are essential in the pharmaceutical industry in all the drug development phases, as they are necessary to ensure a complete characterization of the products and for a proper potency determination.

- The infection of HaCaT cells with heat inactivated *C. acnes* causes the increase of the expression in the cell membrane of the toll like receptors 2 and 4, induces the expression of the inflammatory mediators IL-8, TNFα and CXCL1 and causes the migration of the NF-κβ transcription factor to the cell nucleus.

- The treatment of the cells with a *Camellia sinensis* plant extract, a *Mornida citrifolia* plant extract or a combination of both, after the infection of HaCaT cells with heat inactivated *C. acnes* causes a reduction of the expression of the inflammatory mediators IL-8, TNFα and CXCL1 and decreases the migration of the NF-κβ transcription factor to the cell nucleus.

- The potency assay developed based on cell proliferation for the determination of the late response generated by the RJF TPO-RA biosimilar for the evaluation of its biological activity, is linear, precise, accurate, selective, and robust.

- The potency assay developed based on a reporter gene for the determination of the early response generated by the RJF TPO-RA biosimilar for the evaluation of its biological activity, is linear, precise, accurate, selective, and robust.

- Disulfiram is the component of the already commercial disulfiram / benzyl benzoate cream responsible for the cytotoxicity observed in keratinocytes after the treatment.

- The treatment of keratinocytes with the disulfiram / benzyl benzoate cream causes the activation in the cells of cytotoxicity pathways, related with the inflammatory response and the induction of apoptosis, and protection pathways, related with a cell cycle arrest, DNA repair, protection against apoptosis and oxidative stress and detoxification and drugs metabolism.

-

16. REFERENCES

1. Laboratorios Reig Jofre [Internet]. [cited 2022 Jun 7]. Available from: https://reigjofre.com/en/about-us/reig-jofre-in-brief/
2. FDA Glossary of Terms [Internet]. [cited 2022 Jun 7]. Available from: https://www.accessdata.fda.gov/scripts/cder/daf/index.cfm?event=glossary.pa%20ge
3. U.S. FDA Drug Definitions [Internet]. [cited 2022 Jun 7]. Available from: https://www.registrarcorp.com/definitions/
4. Preziosi P. Drug development. In: Comprehensive medicinal chemistry II. In: Taylor J, Triggle D, editors. Oxford: Elsevier; 2007. p. 173–202.
5. Kaitin KI. Deconstructing the drug development process: The new face of innovation. *Clin Pharmacol Ther*. 2010;87(3):356–61.
6. Dimasi JA, Grabowski HG. The cost of biopharmaceutical R&D: Is biotech different? *Manage Decis Econ*. 2007;28(4–5):469–79.
7. Gallego V, Naveiro R, Roca C, Ríos Insua D, Campillo NE. AI in drug development: a multidisciplinary perspective. *Mol Divers*. 2021;25(3):1461–79.
8. Sinha S, Vohora D. Drug discovery and development: An Overview. In: Pharmaceutical Medicine and Translational Clinical Research. Elsevier Inc.; 2017. p. 19–32.
9. Brodniewicz T, Grynkiewicz G. Origin of new structures for DDD. *Acta Pol Pharm*. 2010;67(6):579–86.
10. Hughes JP, Rees SS, Kalindjian SB, Philpott KL. Principles of early drug discovery. *Br J Pharmacol*. 2011;162(6):1239–49.
11. Federsel HJ. Chemical process research and development in the 21st century: Challenges, strategies, and solutions from a pharmaceutical industry perspective. *Acc Chem Res*. 2009;42(5):671–80.
12. Beninger P. Pharmacovigilance: An overview. *Clin Ther*. 2018;40(12):1991–2004.
13. Berdigaliyev N, Aljofan M. An overview of drug discovery and development. *Future Med Chem*. 2020;12(10):939–47.
14. Overington JP, Al-Lazikani B, Hopkins AL. How many drug targets are there? *Nat Rev Drug Discov*. 2006;5(12):993–6.
15. Biologics and Biosimilars. [Internet]. [cited 2022 Jun 13]. Available from: https://badgut.org/information-centre/a-z-digestive-topics/biosimilars-pamphlet/
16. FDA. What Are “Biologics” Questions and Answers. [Internet]. [cited 2022 Jun 13]. Available from: https://www.fda.gov/about-fda/center-biologics-evaluation-and-research-cber/what-are-biologics-questions-and-answers

17. EMA. Generic and hybrid medicines. [Internet]. [cited 2022 Jun 13]. Available from: https://www.ema.europa.eu/en/human-regulatory/marketing-authorisation/generic-hybrid-medicines

18. CHMP. Committee for Medicinal Products for Human Use (CHMP) Guideline on similar biological medicinal products [Internet]. [cited 2022 Jun 13]. Available from: www.ema.europa.eu/contact

19. dos Reis C, Teixo R, Mendes F, Cruz RS. Biosimilar medicines - Review. *Int J Risk Saf Med*. 2016;28(1):45–60.

20. Quality considerations in demonstrating biosimilarity of a therapeutic protein product to a reference product guidance for industry [Internet]. [cited 2022 Jun 13]. Available from: http://www.fda.gov/Drugs/GuidanceComplianceRegulatoryInformation/Guidances/default.htmand/orhttp://www.fda.gov/BiologicsBloodVaccines/GuidanceComplianceRegulatoryInformation/Guidances/default.htm

21. Medicines Agency E. Committee for Medicinal Products for Human Use (CHMP) Guideline on similar biological medicinal products containing biotechnology-derived proteins as active substance: quality issues (revision 1) [Internet]. [cited 2022 Jun 13]. Available from: www.ema.europa.eu

22. Jin G, Wong STC. Toward better drug repositioning: Prioritizing and integrating existing methods into efficient pipelines. *Drug Discov Today*. 2014;19(5):637–44.

23. Ashburn TT, Thor KB. Drug repositioning: Identifying and developing new uses for existing drugs. *Nat Rev Drug Discov*. 2004;3(8):673–83.

24. Current Good Manufacturing Practice (CGMP) Regulations [Internet]. [cited 2022 Jun 11]. Available from: https://www.fda.gov/drugs/pharmaceutical-quality-resources/current-good-manufacturing-practice-cgmp-regulations

25. Good Manufacturing Practice. European Medicines Agency. [Internet]. [cited 2022 Jun 11]. Available from: https://www.ema.europa.eu/en/human-regulatory/research-development/compliance/good-manufacturing-practice

26. International Council for Harmonisation of Technical Requirements for Pharmaceuticals for Human Use. [Internet]. [cited 2022 Jun 11]. Available from: https://www.ich.org/page/ich-guidelines

27. ICH Topic Q 5 D. Quality of Biotechnological Products: Derivation and characterisation of cell substrates used for production of biotechnological/biological products. Available from: http://www.emea.eu.int

28. Cell Counting Kit-8 Technical Manual Cell Proliferation Assay and Cytotoxicity Assay [Internet]. [cited 2022 Jun 8]. Available from: http://www.dojindo.eu.com/

29. Council of Europe. Statistical analysis of results of biological assays and tests. In: European Pharmacopoeia. 6th ed. Strasbourg: Council of Europe; 2008. p. 571–600.

30. USP_1032. Design and development of biological assays. [cited 2022 Jul 2]; Available from: https://www.ipqpubs.com/wp-content/uploads/2010/06/USP_1032.pdf

31. Luciferase Assay System [Internet]. [cited 2022 Jun 8]. Available from: www.promega.com

32. CellTiter-Glo® reagent mechanism of action [Internet]. [cited 2022 Jun 8]. Available from: http://www.bjlalb.com.cn/news_view.aspx?TypeId=4&Id=441&Fid=t2:4:2

33. Grice EA, Segre JA. The skin microbiome. *Nat Rev Microbiol*. 2011;9(4):244–53.

34. Boniol M, Verriest JP, Pedeux R, Doré JF. Proportion of skin surface area of children and young adults from 2 to 18 years old. *J Invest Dermatol*. 2008;128(2):461–4.

35. Gallo RL, Nakatsuji T. Microbial symbiosis with the innate immune defense system of the skin. *J Invest Dermatol*. 2011;131(10):1974–80.

36. Grice EA, Kong HH, Renaud G, Young AC, Bouffard GG, Blakesley RW, et al. A diversity profile of the human skin microbiota. *Genome Res*. 2008;18(7):1043–50.

37. Cogen AL, Nizet V, Gallo RL. Skin microbiota: A source of disease or defence? *Br J Dermatol*. 2008;158(3):442–55.

38. Hsieh MF, Chen CH. Review: Delivery of pharmaceutical agents to treat acne vulgaris: Current status and perspectives. *J Med Biol Eng*. 2012;32(4):215–24.

39. Suh DH, Kwon HH. What's new in the physiopathology of acne? *Br J Dermatol*. 2015;172(S1):13–9.

40. Williams HC, Dellavalle RP, Garner S. Acne vulgaris. *Lancet*. 2012;379:361–72.

41. Beylot C, Auffret N, Poli F, Claudel JP, Leccia MT, del Giudice P, et al. *Propionibacterium acnes*: An update on its role in the pathogenesis of acne. *J Eur Acad Dermatol Venereol*. 2014;28(3):271–8.

42. Lavers I. Diagnosis and management of acne vulgaris. *Nurse Prescribing*. 2014;12(7):330–6.

43. Gollnick H, Cunliffe W, Berson D, Dreno B, Finlay A, Leyden JJ, et al. Management of acne: A report from a global alliance to improve outcomes in acne. *J Am Acad Dermatol*. 2003;49(1 SUPPL.):S1-37.

44. Webster GF. Acne. *Curr Probl Dermatol*. 1996;8(6):240–62.

45. Fox L, Csongradi C, Aucamp M, du Plessis J, Gerber M. Treatment modalities for acne. Molecules. 2016;21(8):1063.

46. Brüggemann H, Henne A, Hoster F, Liesegang H, Wiezer A, Strittmatter A, et al. The complete genome sequence of *Propionibacterium acnes*, a commensal of human skin. *Science (1979)*. 2004;305(5684):671–3.

47. Elias PM. The skin barrier as an innate immune element. *Semin Immunopathol*. 2007;29(1):3–14.

48. Köllisch G, Kalali BN, Voelcker V, Wallich R, Behrendt H, Ring J, et al. Various members of the Toll-like receptor family contribute to the innate immune response of human epidermal keratinocytes. *Immunology*. 2005;114(4):531–41.

49. Ljashimoto C, Hudson KL, Anderson K v. The Toll gene of Drosophila, required for Dorsal-Ventral embryonic polarity, appears to encode a transmembrane protein. *Cell*. 1988;52:269–79.

50. Rock FL, Hardiman G, Timans JC, Kastelein RA, Fernando Bazan J. A family of human receptors structurally related to Drosophila Toll. *Dev Biol*. 1998;95:588–93.

51. Medzhitov R, Preston-Hurlburt P, Janeway CA. A human homologue of the Drosophila Toll protein signals activation of adaptive immunity. *Nature*. 1997;388:394–7.

52. Medzhitov R. Toll-Like receptors and innate immunity. *Nat Rev*. 2001;1:135–45.

53. Kim J, Ochoa MT, Krutzik SR, Takeuchi O, Uematsu S, Legaspi AJ, et al. Activation of Toll-Like receptor 2 in acne triggers inflammatory cytokine responses. *J Immunol*. 2002;169(3):1535–41.

54. Pivarcsi A, Bodai L, Réthi B, Kenderessy-Szabó A, Koreck A, Széll M, et al. Expression and function of Toll-like receptors 2 and 4 in human keratinocytes. *Int Immunol*. 2003;15(6):721–30.

55. Cong TX, Hao D, Wen X, Li XH, He G, Jiang X. From pathogenesis of acne vulgaris to anti-acne agents. *Arch Dermatol Res*. 2019;311(5):337–49.

56. Medzhitov R, Preston-Hurlburt P, Kopp E, Stadlen A, Chen C, Ghosh S, et al. MyD88 is an adaptor protein in the hToll/IL-1 receptor family signaling pathways. *Mol Cell*. 1998;2:253–8.

57. Medzhitov R, Janeway CJ. The Toll receptor family and microbial recognition. *Trends Microbiol*. 2000;8(10):452–6.

58. Zhang B, Choi YM, Lee J, An IS, Li L, He C, et al. Toll-like receptor 2 plays a critical role in pathogenesis of acne vulgaris. *Biomed dermatol*. 2019;3(1):https://doi.org/10.1186/s41702-019-0042-2.

59. Hayden MS, West AP, Ghosh S. NF-κB and the immune response. *Oncogene*. 2006;25(51):6758–80.

60. Gilmore TD. Introduction to NF-κB: Players, pathways, perspectives. *Oncogene*. 2006;25(51):6680–4.

61. Karin M, Greten FR. NF-κB: Linking inflammation and immunity to cancer development and progression. *Nat Rev Immunol*. 2005;5(10):749–59.

62. Sweeney TE, Suliman HB, Hollingsworth JW, Welty-Wolf KE, Piantadosi CA. A toll-like receptor 2 pathway regulates the Ppargc1a/b metabolic co-activators in mice with Staphylococcal aureus sepsis. *PLoS ONE*. 2011;6(9).

63. Graham HN. Green tea composition, consumption, and polyphenol chemistry. *Prev Med*. 1992;21:334–50.

64. Gardner EJ, Ruxton CHS, Leeds AR. Black tea - Helpful or harmful? A review of the evidence. *Eur J Clin Nutr*. 2007;61(1):3–18.

65. Vuong Q v. Epidemiological evidence linking tea consumption to human health: A review. *Crit Rev Food Sci Nutr*. 2014;54(4):523–36.

66. Prasanth MI, Sivamaruthi BS, Chaiyasut C, Tencomnao T. A review of the role of green tea (*camellia sinensis*) in antiphotoaging, stress resistance, neuroprotection, and autophagy. *Nutrients*. 2019;11(2):474.

67. Abe K, Ijiri M, Suzuki T, Taguchi K, Koyama Y, Isemura M. Green tea with a high catechin content suppresses inflammatory cytokine ex-pression in the galactosamine-injured rat liver. *Biomed Res*. 2005;26(5):187–92.

68. Hayakawa S, Ohishi T, Miyoshi N, Oishi Y, Nakamura Y, Isemura M. Anti-cancer effects of green tea epigallocatchin-3- gallate and coffee chlorogenic acid. *Molecules*. 2020;25(19):4553.

69. Suzuki Y, Miyoshi N, Isemura M. Health-promoting effects of green tea. *Proc Jpn Acad Ser B*. 2012;88(3):88–101.

70. Hamilton-Miller JMT. Antimicrobial properties of tea (*Camellia sinensis L.*). *Antimicrob Agents Chemother*. 1995;39(11):2375–7.

71. Wang MY, West BJ, Jensen CJ, Nowicki D, Su C, Palu AK, et al. *Morinda citrifolia* (Noni): A literature review and recent advances in Noni research. *Acta Pharmacol Sin*. 2002;23(12):1127–41.

72. Brown AC. Anticancer activity of *Morinda citrifolia* (noni) fruit: A review. *Phytother Res*. 2012;26(10):1427–40.

73. Dussossoy E, Brat P, Bony E, Boudard F, Poucheret P, Mertz C, et al. Characterization, anti-oxidative and anti-inflammatory effects of Costa Rican noni juice (*Morinda citrifolia L.*). *J Ethnopharmacol*. 2011;133(1):108–15.

74. Afzan A, Zaidan MRS, Rain N, Badrul AR, Adlin A, Zakiah &. In vitro screening of five local medicinal plants for antibacterial activity using disc diffusion method diffusion method. *Trop Biomed*. 2005;22(2):165–70.

75. Govindan R, Chackaravarthi G, Ramachandran G, Chelliah CK, Muthuchamy M, Quero F, et al. Effective removal of biofilm formation in *Acinetobacter baumannii* using chitosan nanoparticles loaded plant essential oils. *J King Saud Univ Sci*. 2022;34(3): https://doi.org/10.1016/j.jksus.2022.101845.

76. Halim AM, Lee PP, Chang ZW, Chang CC. The hot-water extract of leaves of noni, *Morinda citrifolia*, promotes the immunocompetence of giant freshwater prawn, *Macrobrachium rosenbergii*. *Fish Shellfish Immunol*. 2017;64:457–68.

77. Erdei L, Bolla BS, Bozó R, Tax G, Urbán E, Kemény L, et al. TNIP1 regulates *Cutibacterium acnes*-induced innate immune functions in epidermal keratinocytes. *Front Immunol*. 2018;9:2155.

78. Picot J, Guerin CL, le Van Kim C, Boulanger CM. Flow cytometry: Retrospective, fundamentals and recent instrumentation. *Cytotechnology*. 2012;64(2):109–30.

79. Medzhitov R. Inflammation 2010: New adventures of an old flame. *Cell*. 2010;140(6):771–6.

80. Lanas A. A review of the gastrointestinal safety data- a gastroenterologist's perspective. *Rheumatology*. 2010;49(SUPL 2):3–10.

81. Morgan MJ, Liu ZG. Crosstalk of reactive oxygen species and NF-κB signaling. *Cell Res*. 2011;21(1):103–15.

82. Lambert MP, Gernsheimer TB. Clinical updates in adult immune thrombocytopenia. *Blood*. 2017;129(21):2829–35.

83. Rodeghiero F, Stasi R, Gernsheimer T, Michel M, Provan D, Arnold DM, et al. Standardization of terminology, definitions and outcome criteria in immune thrombocytopenic purpura of adults and children: Report from an international working group. *Blood*. 2009;113(11):2386–93.

84. Schulze H, Gaedicke G. Immune thrombocytopenia in children and adults: What's the same, what's different? *Haematologica*. 2011;96(12):1739–41.

85. Schoonen WM, Kucera G, Coalson J, Li L, Rutstein M, Mowat F, et al. Epidemiology of immune thrombocytopenic purpura in the general practice research database. *Br J Haematol*. 2009;145(2):235–44.

86. Fogarty PF. Chronic immune thrombocytopenia in adults: Epidemiology and clinical presentation. *Hematol Oncol Clin North Am*. 2009;23(6):1213–21.

87. Moulis G, Palmaro A, Montastruc JL, Godeau B, Lapeyre-Mestre M, Sailler L. Epidemiology of incident immune thrombocytopenia: a nationwide population-based study in France. *Blood*. 2014;124(22):3308–15.

88. Shulman NR, Marder VJ, Weinrach RS. Similarities between known antiplatelet antibodies and the factor responsible for thrombocytopenia in idiopathic purpura. Physiologic, serologic and isotopic studies. *Ann N Y Acad Sci*. 1965;124(2):499–542.

89. Audia S, Mahévas M, Samson M, Godeau B, Bonnotte B. Pathogenesis of immune thrombocytopenia. Vol. 16, Autoimmunity Reviews. Elsevier B.V.; 2017. p. 620–32.

90. Bakchoul T, Sachs UJ. Platelet destruction in immune thrombocytopenia: Understanding the mechanisms. *Hamostaseologie.* 2015;35(3):187–94.

91. Audia S, Santegoets K, Laarhoven AG, Vidarsson G, Facy O, Ortega-Deballon P, et al. Fcγ receptor expression on splenic macrophages in adult immune thrombocytopenia. *Clin Exp Immunol*. 2017;188(2):275–82.

92. Kuwana M, Okazaki Y, Kaburaki J, Kawakami Y, Ikeda Y. Spleen is a primary site for activation of platelet-reactive T and B cells in patients with immune thrombocytopenic purpura. *J Immunol Res*. 2002;168(7):3675–82.

93. Kuwana M, Kawakami Y, Ikeda Y. Suppression of autoreactive T-cell response to glycoprotein IIb/IIIa by blockade of CD40/CD154 interaction: Implications for treatment of immune thrombocytopenic purpura. *Blood*. 2003;101(2):621–3.

94. Nieswandt B, Bergmeier W, Rackebrandt K, Gessner JE, Zirngibl H. Identification of critical antigen-specific mechanisms in the development of immune thrombocytopenic purpura in mice. *Blood*. 2000;96(7):2520–7.

95. McMillan R, Wang L, Tomer A, Nichol J, Pistillo J. Suppression of in vitro megakaryocyte production by antiplatelet autoantibodies from adult patients with chronic ITP. *Blood*. 2004;103(4):1364–9.

96. Chang M, Nakagawa PA, Williams SA, Schwartz MR, Imfeld KL, Buzby JS, et al. Immune thrombocytopenic purpura (ITP) plasma and purified ITP monoclonal autoantibodies inhibit megakaryocytopoiesis in vitro. *Blood*. 2003;102(3):887–95.

97. Khodadi E, Asnafi AA, Shahrabi S, Shahjahani M, Saki N. Bone marrow niche in immune thrombocytopenia: a focus on megakaryopoiesis. *Ann Hematol*. 2016;95(11):1765–76.

98. Nugent D, McMillan R, Nichol JL, Slichter SJ. Pathogenesis of chronic immune thrombocytopenia: Increased platelet destruction and/or decreased platelet production. *Br J Haematol*. 2009;146(6):585–96.

99. Malara A, Abbonante V, di Buduo CA, Tozzi L, Currao M, Balduini A. The secret life of a megakaryocyte: Emerging roles in bone marrow homeostasis control. *Cell Mol Life Sci*. 2015;72(8):1517–36.

100. Cines DB, Bussel JB, Liebman HA, Luning Prak ET. The ITP syndrome: Pathogenic and clinical diversity. *Blood*. 2009;113(26):6511–21.

101. Schattner A. Consequence or coincidence? The occurrence, pathogenesis and significance of autoimmune manifestations after viral vaccines. *Vaccine*. 2005;23(30):3876–86.

102. Feusner JH, Slichter SJ, Harker LA. Mechanisms of thrombocytopenia in varicella. *Am J Hematol*. 1979;7:255–64.

103. Zucker-Franklin D, Termin CS, Cooper MC. Structural changes in the megakaryocytes of patients infected with the human immune deficiency virus (HIV-1). *Am J Pathol*. 1989;134(6):1295–303.

104. Verdonck LF, van Heugten H, de Gast GC. Delay in platelet recovery after bone marrow transplantation: Impact of cytomegalovirus infection. *Blood*. 1985;66(4):92–3.

105. Praituan W, Rojnuckarin P. Faster platelet recovery by high-dose dexamethasone compared with standard-dose prednisolone in adult immune thrombocytopenia: A prospective randomized trial. *J Thromb Haemost*. 2009;7(6):1036–8.

106. Neunert C, Noroozi N, Norman G, Buchanan GR, Goy J, Nazi I, et al. Severe bleeding events in adults and children with primary immune thrombocytopenia: A systematic review. *J Thromb Haemost*. 2015;13(3):457–64.

107. Neunert CE, Buchanan GR, Imbach P, B Bolton-Maggs PH, Bennett CM, Neufeld E, et al. Bleeding manifestations and management of children with persistent and chronic immune thrombocytopenia: data from the Intercontinental Cooperative ITP Study Group (ICIS). *Blood*. 2013;121(22):4457–62.

108. Hill QA, Newland AC. Fatigue in immune thrombocytopenia. *Br J Haematol*. 2015;170(2):141–9.

109. Ruggeri M, Tosetto A, Palandri F, Polverelli N, Mazzucconi MG, Santoro C, et al. Thrombotic risk in patients with primary immune thrombocytopenia is only mildly increased and explained by personal and treatment-related risk factors. *J Thromb Haemost*. 2014;12(8):1266–73.

110. Thai LH, Mahévas M, Roudot-Thoraval F, Limal N, Languille L, Dumas G, et al. Long-term complications of splenectomy in adult immune thrombocytopenia. *Medicine*. 2016;95(48):e5098.

111. Enger C, Bennett D, Forssen U, Fogarty PF, McAfee AT. Comorbidities in patients with persistent or chronic immune thrombocytopenia. *Int J Hematol*. 2010;92(2):289–95.

112. McMillan R, Bussel JB, George JN, Lalla D, Nichol JL. Self-reported health-related quality of life in adults with chronic immune thrombocytopenic purpura. *Am J Hematol*. 2008;83(2):150–4.

113. Flores A, Klaassen RJ, Buchanan GR, Neunert CE. Patterns and influences in health-related quality of life in children with immune thrombocytopenia: A study from the Dallas ITP Cohort. *Pediatr Blood Cancer*. 2017;64(8).

114. Provan D, Stasi R, Newland AC, Blanchette VS, Bolton-Maggs P, Bussel JB, et al. International consensus report on the investigation and management of primary immune thrombocytopenia. *Blood*. 2010;115(2):168–86.

115. Altintas A, Ozel A, Okur N, Okur N, Cil T, Pasa S, et al. Prevalence and clinical significance of elevated antinuclear antibody test in children and adult patients with idiopathic thrombocytopenic purpura. *J Thromb Thrombolysis*. 2007;24(2):163–8.

116. Cuker A, Cines DB, Neunert CE. Controversies in the treatment of immune thrombocytopenia. *Curr Opin Hematol*. 2016;23(5):479–85.

117. Matschke J, Müller-Beissenhirtz H, Novotny J, Vester I, Hertenstein B, Eisele L, et al. A randomized trial of daily prednisone versus pulsed dexamethasone in treatment-naïve adult patients with immune thrombocytopenia: EIS 2002 study. *Acta Haematol*. 2016;136(2):101–7.

118. Molineux G, Newland A. Development of romiplostim for the treatment of patients with chronic immune thrombocytopenia: From bench to bedside: Review. *Br J Haematol*. 2010;150(1):9–20.

119. Palandri F, Polverelli N, Sollazzo D, Romano M, Catani L, Cavo M, et al. Have splenectomy rate and main outcomes of ITP changed after the introduction of new treatments? A monocentric study in the outpatient setting during 35 years. *Am J Hematol*. 2016;91(4):E267–72.

120. Guan Y, Wang S, Xue F, Liu X, Zhang L, Li H, et al. Long-term results of splenectomy in adult chronic immune thrombocytopenia. *Eur J Haematol*. 2017;98(3):235–41.

121. Din B, Wang X, Shi Y, Li Y. Long-term effect of high-dose dexamethasone with or without low-dose dexamethasone maintenance in untreated immune thrombocytopenia. *Acta Haematol*. 2015;133(1):124–8.

122. Wei Y, Ji XB, Wang YW, Wang JX, Yang EQ, Wang ZC, et al. High-dose dexamethasone vs prednisone for treatment of adult immune thrombocytopenia: a prospective multicenter randomized trial. *Blood*. 2016;127(3):296–302.

123. Gudbrandsdottir S, Birgens HS, Frederiksen H, Jensen BA, Krogh Jensen M, Kjeldsen L, et al. Rituximab and dexamethasone vs dexamethasone monotherapy in newly diagnosed patients with primary immune thrombocytopenia. *Blood*. 2013;121(11):1976–81.

124. Chugh S, Darvish-Kazem S, Lim W, Crowther MA, Ghanima W, Wang G, et al. Rituximab plus standard of care for treatment of primary immune thrombocytopenia: A systematic review and meta-analysis. *Lancet Haematol*. 2015;2(2):e75–81.

125. Kuter DJ, Bussel JB, Lyons RM, Pullarkat V, Gernsheimer TB, Senecal FM, et al. Efficacy of romiplostim in patients with chronic immune thrombocytopenic purpura: a double-blind randomised controlled trial. *Lancet*. 2008;371:395–403.

126. Kelemen E, Cserhati I, Tanos B. Demonstration and some properties of human thrombopoietin in thrombocythaemic sera. *Acta Hematol*. 1958;20:350–5.

127. Bartley TD, Bogenberger J, Hunt P, Li Y s, Lu HS, Martin F, et al. Identification and cloning of a megakaryocyte growth and development factor that is a ligand for the cytokine receptor Mpl. *Cell*. 1994;77:1117–24.

128. Kuter DJ, Beeler DL, Rosenberg RD. The purification of megapoietin: A physiological regulator of megakaryocyte growth and platelet production. *Proc Natl Acad Sci USA*. 1994;91(23):11104–8.

129. Lok S, Kaushansky K, Holly RD, Kuijper JL, Lofton-Day CE, Oort PJ, et al. Cloning and expression of murine thrombopoietin cDNA and stimulation of platelet production in vivo. *Nature*. 1994;369(6481):565–8.

130. de Sauvage FJ, Hass PE, Spencer SD, Malloy BE, Gurney AL, Spencer SA, et al. Stimulation of megakaryocytopoiesis and thrombopoiesis by the c-Mpl ligand. *Nature*. 1994;369:533–8.

131. Sohmaa Y, Akahori H, Sekib N, Horib TA, Ogami K, Katoa T, et al. Cloning and chromosomal localization of the human thrombopoietin gene. *FEBS Lett*. 1994;353:57–61.

132. Kausahansky Kenneth. Thrombopoietin. *N Engl J Med*. 1998;339(11):746–54.

133. Li J, Yang C, Xia Y, Bertino A, Glaspy J, Roberts M, et al. Thrombocytopenia caused by the development of antibodies to thrombopoietin. *Blood*. 2001;98(12):3241–8.

134. Feese MD, Tamada T, Kato Y, Maeda Y, Hirose M, Matsukura Y, et al. Structure of the receptor-binding domain of human thrombopoietin determined by complexation with a neutralizing antibody fragment. *Proc Natl Acad Sci USA*. 2004;101(7):1816–21.

135. Pearce KH, Potts BJ, Presta LG, Bald LN, Fendly BM, Wells JA. Mutational analysis of thrombopoietin for identification of receptor and neutralizing antibody sites. *J Biol Chem*. 1997;272(33):20595–602.

136. Dasouki MJ, Rafi SK, Olm-Shipman AJ, Wilson NR, Abhyankar S, Ganter B, et al. Exome sequencing reveals a thrombopoietin ligand mutation in a Micronesian family with autosomal recessive aplastic anemia. *Blood*. 2013;122(20):3440–9.

137. Broudy VC, Lin NL, Sabath DF, Papayannopoulou T, Kaushansky K. Human platelets display high-affinity receptors for thrombopoietin. *Blood*. 1997;86(6):1896–940.

138. Kato T, Oda A, Inagaki Y, Ohashi H, Matsumoto A, Ozaki K, et al. Thrombin cleaves recombinant human thrombopoietin: One of the proteolytic events that generates truncated forms of thrombopoietin. *Am J Med Sci*. 1997;94:4669–74.

139. Hokom MM, Lacey D, Kinstler OB, Choi E, Kaufman S, Faust J, et al. Pegylated megakaryocyte growth and development factor abrogates the lethal thrombocytopenia associated with carboplatin and irradiation in mice. *Blood*. 1995;86(12):4486–92.

140. Spivak JL. The in vivo metabolism of recombinant human erythropoietin. *Contrib Nephrol*. 1989;76:67–77.

141. Harker LA, Marzec UM, Hunt P, Kelly AB, Tomer A, Cheung E, et al. Dose-response effects of pegylated human megakaryocyte growth and development factor on platelet production and function in nonhuman primates. *Blood*. 1996;88(2):511–21.

142. Linden HM, Kaushansky K. The glycan domain of thrombopoietin enhances its secretion. *Biochemistry*. 2000;39(11):3044–51.

143. Muto T, Feese MD, Shimada Y, Kudou Y, Okamoto T, Ozawa T, et al. Functional analysis of the c-terminal region of recombinant human thrombopoietin. C-terminal region of thrombopoietin is a “shuttle” peptide to help secretion. *J Biol Chem*. 2000;275(16):12090–4.

144. Kato T, Matsumoto A, Ogami K, Tahara T, Morita H, Miyazaki H. Native trombopoietin: structure and function. *Stem Cells*. 1998;16:322–8.

145. Stoffel R, Wiestner A, Skoda RC. Thrombopoietin in thrombocytopenic mice: evidence against regulation at the mRNA level and for a direct regulatory role of platelets. *Blood*. 1996;87(2):567–73.

146. Shinguang Qian, Fumin Fu, Wei Li, Qi Chen, de Sauvage Frederic J. Primary role of the liver in thrombopoietin production shown by tissue-specific knockout. *Blood*. 1998;92(6):2189–91.

147. Chaligné R, Tonetti C, Besancenot R, Roy L, Marty C, Mossuz P, et al. New mutations of MPL in primitive myelofibrosis: Only the MPL W515 mutations promote a G1/S-phase transition. *Leukemia*. 2008;22(8):1557–66.

148. Varghese LN, Defour JP, Pecquet C, Constantinescu SN. The thrombopoietin receptor: Structural basis of traffic and activation by ligand, mutations, agonists, and mutated calreticulin. *Front Endocrinol*. 2017;8(59):doi: 10.3389/fendo.2017.00059.

149. Bazan JF. Structural design and molecular evolution of a cytokine receptor superfamily. *Proc Natl* Acad Sci USA. 1990;87:6934–8.

150. Deane CM, Kroemer RT, Richards WG. A structural model of the human thrombopoietin receptor complex. *J Mol Graph Model*. 1997;15(3):170–88.

151. Matthews EE, Thévenin D, Rogers JM, Gotow L, Lira PD, Reiter LA, et al. Thrombopoietin receptor activation: transmembrane helix dimerization, rotation, and allosteric modulation. *FASEB J*. 2011;25(7):2234–44.

152. Staerk J, Lacout C, Sato T, Smith SO, Vainchenker W, Constantinescu SN. An amphipathic motif at the transmembrane-cytoplasmic junction prevents autonomous activation of the thrombopoietin receptor. *Blood*. 2006;107(5):1864–71.

153. Leroy E, Defour JP, Sato T, Dass S, Gryshkova V, Shwe MM, et al. His499 regulates dimerization and prevents oncogenic activation by asparagine mutations of the human thrombopoietin receptor. *J Biol Chem*. 2016;291(6):2974–87.

154. Tong W, Sulahian R, Gross AW, Hendon N, Lodish HF, Huang LJS. The membrane-proximal region of the thrombopoietin receptor confers its high surface expression by JAK2-dependent and -independent mechanisms. *J Biol Chem*. 2006;281(50):38930–40.

155. Drachman JG, Kaushansky K. Dissecting the thrombopoietin receptor: Functional elements of the Mpl cytoplasmic domain. *Proc Natl Acad Sci USA*. 1997;94:2350–5.

156. Hitchcock IS, Chen MM, King JR, Kaushansky K. YRRL motifs in the cytoplasmic domain of the thrombopoietin receptor regulate receptor internalization and degradation. *Blood*. 2008;112(6):2222–31.

157. Saur SJ, Sangkhae V, Geddis AE, Kaushansky K, Hitchcock IS. Ubiquitination and degradation of the thrombopoietin receptor c-Mpl. *Blood*. 2010;115:1254–63.

158. Nagata Y, Todokoro K. Thrombopoietin induces activation of at least two distinct signaling pathways. *FEBS Lett*. 1995;377:497–501.

159. Alexander WS, Maurer AB, Novak U, Harrison-Smith M. Tyrosine-599 of the c-Mpl receptor is required for Shc phosphorylation and the induction of cellular differentiation. *EMBO J*. 1996;15(23):6531–40.

160. Hitchcock IS, Kaushansky K. Thrombopoietin from beginning to end. *Br J Haematol*. 2014;165(2):259–68.

161. Bacon CM, Tortolani"' PJ, Shimosaka A, Rees RC, Longo DL, O'shea JJ. Thrombopoietin (TPO) induces tyrosine phosphorylation and activation of STAT5 and STAT3. *FEBS Lett*. 1995;370:63–8.

162. Kuter DJ. Biology and chemistry of thrombopoietic agents. *Semin Hematol*. 2010;47(3):243–8.

163. Kuter DJ. The biology of thrombopoietin and thrombopoietin receptor agonists. *Int J Hematol*. 2013;98(1):10–23.

164. Machlus KR, Italiano JE. The incredible journey: From megakaryocyte development to platelet formation. *J Cell Biol*. 2013;201(6):785–96.

165. Cantor AB. Thrombocytopoiesis. In: Hematology: Basic Principles and Practice. Elsevier Inc.; 2018. p. 334–49.

166. Kuter DJ, Bain B, Mufti G, Bagg A, Hasserjian RP. Bone marrow fibrosis: Pathophysiology and clinical significance of increased bone marrow stromal fibres. *Br J Haematol*. 2007;139(3):351–62.

167. Yang BB, Doshi S, Arkam K, Franklin J, Chow AT. Development of romiplostim for treatment of primary immune thrombocytopenia from a pharmacokinetic and pharmacodynamic perspective. *Clin Pharmacokinet*. 2016;55(9):1045–58.

168. Bussel JB, Pinheiro MP. Eltrombopag. *Cancer Res Treat*. 2011;157:289–303.

169. Cwirla SE, Balasubramanian P, Duffin DJ, Wagstrom CR, Gates CM, Singer SC, et al. Peptide agonist of the thrombopoietin receptor as potent as the natural cytokine. *Science (1979)*. 1997;276(5319):1696–9.

170. Broudy VC, Lin NL. AMG531 stimulates megakaryopoiesis in vitro by binding to Mpl. *Cytokine*. 2004;25(2):52–60.

171. Amgen. Highlights of prescribing information [Internet]. Available from: www.fda.gov/medwatch.

172. Jawa V, Hokom M, Hu Z, El-Abaadi N, Zhuang Y, Berger D, et al. Assessment of immunogenicity of romiplostim in clinical studies with ITP subjects. *Ann Hematol*. 2010;89(SUPPL 1):75–85.

173. Saroha D, Mazza AO. Surface plasmon resonance. *Appl Biochem Biotechnol*. 2005;126:79–92.

174. Jason-Moller L, Murphy M, Bruno J. Overview of Biacore Systems and Their Applications. *Curr Protoc Protein Sci*. 2006;Chapter 19(Unit 19.13).

175. Shankaran DR, Gobi KV, Miura N. Recent advancements in surface plasmon resonance immunosensors for detection of small molecules of biomedical, food and environmental interest. *Sens Actuators B Chem*. 2007;121(1):158–77.

176. Patching SG. Surface plasmon resonance spectroscopy for characterisation of membrane protein–ligand interactions and its potential for drug discovery. *Biochim Biophys Acta*. 2014;1838(1 Pt A):43–55.

177. ICH harmonized tripartite guideline. Specifications: test procedures and acceptance criteria for biotechnological / biological products Q6B [Internet]. [cited 2022 Jul 4]. Available from: https://www.ema.europa.eu/en/documents/scientific-guideline/ich-q-6-b-test-procedures-acceptance-criteria-biotechnological/biological-products-step-5_en.pdf

178. Thurner M, Asim F, Garczarczyk-Asim D, Janke K, Deutsch M, Margreiter E, et al. Development of an in vitro potency assay for human skeletal muscle derived cells. *PLoS ONE*. 2018;13(3):e0194561.

179. Moore M, Ferguson J, Burns C. Applications of cell-based bioassays measuring the induced expression of endogenous genes. *Bioanalysis*. 2014;6(11):1563–74.

180. ICH Topic Q 2 (R1). Validation of Analytical Procedures: Text and Methodology [Internet]. [cited 2022 Jul 4]. Available from: https://www.ema.europa.eu/en/documents/scientific-guideline/ich-q-2-r1-validation-analytical-procedures-text-methodology-step-5_en.pdf

181. Micali G, Lacarrubba F, Verzì AE, Chosidow O, Schwartz RA. Scabies: Advances in noninvasive diagnosis. *PLOS Negl Trop Dis*. 2016;10(6):e0004691.

182. Anderson KL, Strowd LC. Epidemiology, diagnosis, and treatment of scabies in a dermatology office. *J Am Board Fam Med*. 2017;30(1):78–84.

183. Arlian LG, Runyan RA, Achar S, Estes SA. Survival and infestivity of *Sarcoptes scabiei vat. canis* and *vat. hominis*. *J Am Acad Dermatol*. 1984;11(2 Pt 1):210–5.

184. Gilson RL, Crane JS. Scabies [Internet]. [cited 2022 Jul 4]. Available from: https://www.ncbi.nlm.nih.gov/books/NBK544306/?report=printable

185. Mumcuoglu KY, Gilead L, Ingber A. New insights in pediculosis and scabies. *Expert Rev Dermatol*. 2009;4(3):285–302.

186. Garcovich S, Maurelli M, Gisondi P, Peris K, Yosipovitch G, Girolomoni G. Pruritus as a distinctive feature of type 2 inflammation. *Vaccines (Basel)*. 2021;9(3):303.

187. Motswaledi HM, Motswaledi H. Clinical diagnosis and treatment of scabies, a neglected tropical disease. *S Afr Fam Pract*. 2021;63(1):e1–6.

188. Chandler DJ, Fuller LC. A Review of Scabies: An Infestation More than Skin Deep. *Dermatology*. 2019;235(2):79–80.

189. Swe PM, Christian LD, Lu HC, Sriprakash KS, Fischer K. Complement inhibition by *Sarcoptes scabiei* protects *Streptococcus pyogenes* - An in vitro study to unravel the molecular mechanisms behind the poorly understood predilection of *S. pyogenes* to infect mite-induced skin lesions. *PLOS Negl Trop Dis*. 2017;11(3):e0005437.

190. Karimkhani C, Colombara D v., Drucker AM, Norton SA, Hay R, Engelman D, et al. The global burden of scabies: a cross-sectional analysis from the global burden of disease study 2015. *Lancet Infect Dis*. 2017;17(12):1247–54.

191. Arlian LG, Morgan MS, Rider SD. *Sarcoptes scabiei*: Genomics to proteomics to biology. *Parasites Vectors*. 2016;9(1):380.

192. Mahmood W, Viberg LT, Fischer K, Walton SF, Holt DC. An aspartic protease of the scabies mite *Sarcoptes scabiei* is involved in the digestion of host skin and blood macromolecules. *PLOS Negl Trop Dis*. 2013;7(11):e2525.

193. Gunning K, Kiral B, Pippitt K. Lice and scabies: Treatment update. *Am Fam Physician*. 2019;99(10):635–42.

194. Heukelbach J, Feldmeier H. Scabies. *Lancet*. 2006;367:1767–74.

195. Alberici F, Pagani L, Ratti G, Viale P. Ivermectin alone or in combination with benzyl benzoate in the treatment of human immunodeficiency virus-associated scabies. *Br J Dermatol*. 2000;142:969–72.

196. Karamanakos PN, Pappas P, Boumba VA, Thomas C, Malamas M, Vougiouklakis T, et al. Pharmaceutical agents known to produce disulfiram-like reaction: Effects on hepatic ethanol metabolism and brain monoamines. *Int J Toxicol*. 2007;26(5):423–32.

197. Kragh H. From disulfiram to Antabuse: The invention of a drug. *Bull Hist Chem*. 2008;33(2):82–8.

198. Skrott Z, Mistrik M, Andersen KK, Friis S, Majera D, Gursky J, et al. Alcohol-abuse drug disulfiram targets cancer via p97 segregase adaptor NPL4. *Nature*. 2017;552(7684):194–9.

199. Viola-Rhenals M, Patel KR, Jaimes-Santamaria L, Wu G, Liu J, Dou QP. Recent advances in Antabuse (Disulfiram): The importance of its metal-binding ability to its anticancer activity. *Curr Med Chem*. 2018;25(4):506–24.

200. Kast RE, Boockvar JA, Brüning A, Cappello F, Chang WW, Cvek B, et al. A conceptually new treatment approach for relapsed glioblastoma: Coordinated undermining of survival paths with nine repurposed drugs (CUSP9) by the International Initiative for accelerated improvement of glioblastoma care. *Oncotarget*. 2013;4:503.

201. Long TE. Repurposing thiram and disulfiram as antibacterial agents for multidrug-resistant *Staphylococcus aureus* infections. *Antimicrob Agents Chemother*. 2017;61(9):e00898.

202. Scheibel LW, Adler A, Trager W. Tetraethylthiuram disulfide (Antabuse) inhibits the human malaria parasite *Plasmodium falciparum*. *Proc Natl Acad Sci USA*. 1979;76(10):5303–7.

203. Horita Y, Takii T, Yagi T, Ogawa K, Fujiwara N, Inagaki E, et al. Antitubercular activity of disulfiram, an antialcoholism drug, against multidrug- and extensively drug-resistant *Mycobacterium tuberculosis* isolates. *Antimicrob Agents Chemother*. 2012;56(8):4140–5.

204. PubChem. Disulfiram (Compound) [Internet]. [cited 2022 Jun 8]. Available from: https://pubchem.ncbi.nlm.nih.gov/compound/3117

205. Sharma G, Dhankar G, Thakur K, Raza K, Katare OP. Benzyl benzoate-loaded microemulsion for topical applications: Enhanced dermatokinetic profile and better delivery promises. *AAPS PharmSciTech*. 2016;17(5):1221–31.

206. Bachewar NP, Thawani VR, Mali SN, Gharpure KJ, Shingade VP, Dakhale GN. Comparison of safety, efficacy, and cost effectiveness of benzyl benzoate, permethrin, and ivermectin in patients of scabies. *Indian J Pharmacol*. 2009;41(1):9–14.

207. Currie BJ, Harumal P, Mckinnon M, Walton SF. First documentation of *In Vivo* and *In Vitro* ivermectin resistance in Sarcoptes scabiei. Clin Infect Dis. 2004;39(1):e8-12.

208. Walton SF, Myerscough MR, Currie BJ. Studies in vitro on the relative efficacy of current acaricides for *Sarcoptes scabiei var. hominis*. *Trans R Soc Trop Med Hyg*. 2000;94(1):92–6.

209. PubChem. Benzyl-benzoate [Internet]. [cited 2022 Jun 8]. Available from: https://pubchem.ncbi.nlm.nih.gov/compound/Benzyl-benzoate

210. Sigruener A, Buechler C, Orsó E, Hartmann A, Wild PJ, Terracciano L, et al. Human aldehyde oxidase 1 interacts with ATP-binding cassette transporter-1 and modulates its activity in hepatocytes. *Horm Metab Res*. 2007;39(11):781–9.

211. Whitaker EL, Filippov VA, Duerksen-Hughes PJ. Interleukin 24: Mechanisms and therapeutic potential of an anti-cancer gene. *Cytokine Growth Factor Rev*. 2012;23(6):323–31.

212. Duez H, Staels B. Nuclear receptors linking circadian rhythms and cardiometabolic control. *Arterioscler Thromb Vasc Biol*. 2010 Aug;30(8):1529–34.

213. Chang TH, Huang H da, Ong WK, Fu YJ, Lee OK, Chien S, et al. The effects of actin cytoskeleton perturbation on keratin intermediate filament formation in mesenchymal stem/stromal cells. *Biomaterials*. 2014;35(13):3934–44.

214. Leatherwood J. Emerging mechanisms of eukaryotic DNA replication initiation. *Curr Opin Cell Biol*. 1998;10(6):742–8.

215. Peng C, Zhao H, Chen W, Song Y, Wang X, Li J, et al. Identification of SHCBP1 as a novel downstream target gene of SS18-SSX1 and its functional analysis in progression of synovial sarcoma. *Oncotarget*. 2016;7(41):66822–34.

216. Simpson F, Lammerts Van Bueren K, Butterfield N, Bennetts JS, Bowles J, Adolphe C, et al. The PCNA-associated factor KIAA0101/p15PAF binds the potential tumor suppressor product p33ING1b. *Exp Cell Res*. 2006;312(1):73–85.

217. Davidson G, Wu W, Shen J, Bilic J, Fenger U, Stannek P, et al. Casein kinase 1γ couples Wnt receptor activation to cytoplasmic signal transduction. *Nature*. 2005;438(7069):867–72.

218. Rahman MA, Amin ARMR, Wang D, Koenig L, Nannapaneni S, Chen Z, et al. RRM2 regulates Bcl-2 in head and neck and lung cancers: A potential target for cancer therapy. *Clin Cancer Res*. 2013;19(13):3416–28.

219. Maynard RD, Godfrey DA, Medina-Gomez C, Ackert-Bicknell CL. Characterization of expression and alternative splicing of the gene cadherin-like and PC esterase domain containing 1 (Cped1). *Gene*. 2018;674:127–33.

220. Fang ZA, He Y, Sun C, Zhan L, Zhou G, Wei B, et al. Expression and potential role of CXCL5 in the pathogenesis of intrauterine adhesions. *Int J Med Res*. 2021;49(3):300060521997718.

221. Sertic S, Quadri R, Lazzaro F, Muzi-Falconi M. EXO1: A tightly regulated nuclease. *DNA Repair (Amst)*. 2020;93:102929.

222. Cheng E, Trombetta SE, Kovacs D, Beech RD, Ariyan S, Reyes-Mugica M, et al. Rab33A: Characterization, expression, and suppression by epigenetic modification. *J Invest Dermatol*. 2006;126(10):2257–71.

223. Sun H, Liu K, Huang J, Sun Q, Shao C, Luo J, et al. FAM111B, a direct target of p53, promotes the malignant process of lung adenocarcinoma. *Onco Targets Ther*. 2019;12:2829–42.

224. Ozawa H, Ashizawa S, Naito M, Yanagihara M, Ohnishi N, Maeda T, et al. Paired-like homeodomain protein ESXR1 possesses a cleavable C-terminal region that inhibits cyclin degradation. *Oncogene*. 2004;23(39):6590–602.

225. Jaén RI, Prieto P, Casado M, Martín-Sanz P, Boscá L. Post-translational modifications of prostaglandin-endoperoxide synthase 2 in colorectal cancer: An update. *World J Gastroenterol*. 2018;24(48):5454–61.

226. Zenatti PP, Ribeiro D, Li W, Zuurbier L, Silva MC, Paganin M, et al. Oncogenic IL7R gain-of-function mutations in childhood T-cell acute lymphoblastic leukemia. *Nat Genet*. 2011;43(10):932–41.

227. Luque A, Carpizo DR, Iruela-Arispe ML. ADAMTS1/METH1 inhibits endothelial cell proliferation by direct binding and sequestration of VEGF165. *J Biol Chem*. 2003;278(26):23656–65.

228. Edin ML, Yamanashi H, Boeglin WE, Graves JP, DeGraff LM, Lih FB, et al. Epoxide hydrolase 3 (Ephx3) gene disruption reduces ceramide linoleate epoxide hydrolysis and impairs skin barrier function. *J Biol Chem*. 2021;296:doi: 10.1074/jbc.RA120.016570.

229. Azenha D, Hernandez-Perez S, Martin Y, Viegas MS, Martins A, Lopes MC, et al. Implications of clspn variants in cellular function and susceptibility to cancer. *Cancers (Basel)*. 2020;12(9):doi: 10.3390/cancers12092396.

230. Krause M, Sechi AS, Konradt M, Monner D, Gertler FB, Wehland JFyn-binding protein (Fyb)/SLP-76-associated protein (SLAP), Ena/vasodilator-stimulated phosphoprotein (VASP) proteins and the Arp2/3 complex link T cell receptor (TCR) signaling to the actin cytoskeleton. *J Cell Biol*. 2000;149(1):181–4.

231. Sheng Y, Cao M, Liu Y, He Y, Zhang G, Du Y, et al. Hyaluronan synthase 2 (HAS2) regulates cell phenotype and invadopodia formation in luminal-like breast cancer cells. *Mol Cell Biochem*. 2021;476(9):3383–91.

232. Zhang X, Zhong L, Liu BZ, Gao YJ, Gao YM, Hu XX. Effect of GINS2 on proliferation and apoptosis in Leukemic cell line. *Int J Med Sci*. 2013;10(12):1795–804.

233. Hornsveld M, Feringa FM, Krenning L, van den Berg J, Smits LMM, Nguyen NBT, et al. A FOXO-dependent replication checkpoint restricts proliferation of damaged cells. *Cell Rep*. 2021;34(4): doi: 10.1016/j.celrep.2020.108675.

234. Kacso IM, Kacso G. Endothelial cell-selective adhesion molecule in diabetic nephropathy. *Eur J Clin Invest*. 2012;42(11):1227–34.

235. Lyabin DN, Eliseeva IA, Ovchinnikov LP. YB-1 protein: Functions and regulation. *Wiley Interdiscip Rev RNA*. 2014;5(1):95–110.

236. Wyatt AR, Yerbury JJ, Berghofer P, Greguric I, Katsifis A, Dobson CM, et al. Clusterin facilitates in vivo clearance of extracellular misfolded proteins. *Cell Mol Life Sci*. 2011;68(23):3919–31.

237. Jin Y, Duan L, Lee SH, Kloosterboer HJ, Blair IA, Penning TM. Human cytosolic hydroxysteroid dehydrogenases of the aldo-ketoreductase superfamily catalyze reduction of conjugated steroids: Implications for phase I and phase II steroid hormone metabolism. *J Biol Chem*. 2009;284(15):10013–22.

238. Yamasaki M, Yamada K, Furuya S, Mitoma J, Hirabayashi Y, Watanabe M. 3-phosphoglycerate dehydrogenase, a key enzyme for L-serine biosynthesis, is preferentially expressed in the radial glia/astrocyte lineage and olfactory ensheathing glia in the mouse brain. *J Neurosci*. 2001;21(19):7691–704.

239. Lomelino CL, Andring JT, McKenna R, Kilberg MS. Asparagine synthetase: Function, structure, and role in disease. *J Biol Chem*. 2017;292(49):19952–8.

240. Karin M, Eddyt RL, Henryt WM, Haleyt LL, Byerst MG, Showst TB. Human metallothionein genes are clustered on chromosome 16. *Genetics*. 1984;81:5494–8.

241. Zhang C, Liu J, Zhao Y, Yue X, Zhu Y, Wang X, et al. Glutaminase 2 is a novel negative regulator of small GTPase Rac1 and mediates p53 function in suppressing metastasis. *Elife*. 2016;5:e10727.

242. Lin W, Wang C, Liu G, Bi C, Wang X, Zhou Q, et al. SLC7A11 / xCT in cancer: biological functions and therapeutic implications. *Am J Cancer Res*. 2020;10(10):3106–26.

243. Choi BH, Rawat V, Högström J, Burns PA, Conger KO, Ozgurses ME, et al. Lineage-specific silencing of PSAT1 induces serine auxotrophy and sensitivity to dietary serine starvation in luminal breast tumors. *Cell Rep*. 2022;38(3):110278.

244. Chen MS, Wang SF, Hsu CY, Yin PH, Yeh TS, Lee HC, et al. CHAC1 degradation of glutathione enhances cystine-starvation-induced necroptosis and ferroptosis in human triple negative breast cancer cells via the GCN2-eIF2α-ATF4 pathway. *Oncotarget*. 2017;8(70):114588–602.

245. Xiang C, Zhang ML, Zhao QZ, Xie QP, Yan HC, Yu X, et al. LncRNA-SLC6A9-5:2: A potent sensitizer in 131 I-resistant papillary thyroid carcinoma with PARP-1 induction. *Oncotarget*. 2017;8(14):22954–67.

246. Li S, Wang Z, Tong H, Li S, Yan Y. TCP11L2 promotes bovine skeletal muscle-derived satellite cell migration and differentiation via FMNL2. *J Cell Physiol*. 2020;235(10):7183–93.

247. He W, Wang Q, Xu J, Xu X, Padilla MT, Ren G, et al. Attenuation of TNFSF10/TRAIL-induced apoptosis by an autophagic survival pathway involving TRAF2- And RIPK1/RIP1-mediated MAPK8/JNK activation. *Autophagy*. 2012;8(12):1811–21.

248. Zhang K, Chen D, Ma K, Wu X, Hao H, Jiang S. NAD(P)H:Quinone oxidoreductase 1 (NQO1) as a therapeutic and diagnostic target in cancer. *J Med Chem*. 2018;61(16):6983–7003.

249. Jacquet M, Hervouet E, Baudu T, Herfs M, Parratte C, Feugeas JP, et al. GABARAPL1 inhibits EMT signaling through SMAD-tageted negative feedback. *Biology (Basel)*. 2021;10(10):956.

250. Bhattacharya B, Xiao S, Chatterjee S, Urbanowski M, Ordonez A, Ihms EA, et al. The integrated stress response mediates necrosis in murine *Mycobacterium tuberculosis* granulomas. *J Clin Invest*. 2021;131(3):e130319.

251. Munz M, Baeuerle PA, Gires O. The emerging role of EpCAM in cancer and stem cell signaling. *Cancer Res*. 2009;69(14):5627–9.

252. Chua HC, Wulf M, Weidling C, Rasmussen LP, Pless SA. The NALCN channel complex is voltage sensitive and directly modulated by extracellular calcium. *Sci Adv*. 2020;6(17):eaaz3154.

253. Hossain S, Iwasa H, Sarkar A, Maruyama J, Arimoto-Matsuzaki K, Hata Y. The RASSF6 tumor suppressor protein regulates apoptosis and cell cycle progression via retinoblastoma protein. *Mol Cell Biol*. 2018;38(17):e00046-18.

254. Reif R, Adawy A, Vartak N, Schröder J, Günther G, Ghallab A, et al. Activated ErbB3 translocates to the nucleus via clathrin-independent endocytosis, which is associated with proliferating cells. *J Biol Chem*. 2016;291(8):3837–47.

255. Wen W, Wang H, Xie S, Wu Z, Zhang C. BVES-AS1 inhibits the malignant behaviors of colon adenocarcinoma cells via regulating BVES. *Cell Biol Int*. 2021;45(9):1945–56.

256. Parang B, Thompson JJ, Williams CS. Blood Vessel Epicardial Substance (BVES) in junctional signalling and cancer. *Tissue Barriers*. 2018;6(4):1–12.

257. Lu SC. Glutathione synthesis. *Biochim Biophys Acta Gen Subj*. 2013;1830(5):3143–53.

258. Badway JA, Baleja JD. Reps2: A cellular signalling and molecular trafficking nexus. *Int J Biochem Cell Biol*. 2011;43(12):1660–3.

259. Schlaepfer IR, Joshi M, Professor A. CPT1A-mediated fat oxidation, mechanisms and therapeutic potential. *Endocrinology*. 2020;161(2):bqz046.

260. Baszczyński O, Watt JM, Rozewitz MD, Fliegert R, Guse AH, Potter BVL. Synthesis of phosphonoacetate analogues of the second messenger adenosine 5′-diphosphate ribose (ADPR). *RSC Adv*. 2020;10(3):1776–85.

261. Edin ML, Zeldin DC. Regulation of cardiovascular biology by microsomal epoxide hydrolase. *Toxicol Res*. 2021;37(3):285–92.

262. Keyel PA. DNAses in health and disease. *Dev Biol*. 2017;429(1):1–11.

263. Ye B, Liu B, Hao L, Zhu X, Yang L, Wang S, et al. Klf4 glutamylation is required for cell reprogramming and early embryonic development in mice. *Nat Commun*. 2018;9(1):1261.

264. Takeda K, Akira S. Toll-Like receptors. In: Current Protocols in Immunology. Blackwell Publishing Inc.; 2015. p. doi:10.1002/0471142735.im1412s77.

265. Saadi H, Seillier M, Carrier A. The stress protein TP53INP1 plays a tumor suppressive role by regulating metabolic homeostasis. *Biochimie*. 2015;118:44–50.

266. Glorieux C, Calderon PB. Catalase, a remarkable enzyme: Targeting the oldest antioxidant enzyme to find a new cancer treatment approach. *Biol Chem*. 2017;398(10):1095–108.

267. Ge H, Wang G, Zhang L, Wang S, Zou Z, Yan S, et al. Characterization of interleukin-1 receptor-associated kinase 1 binding protein 1 gene in small abalone *Haliotis diversicolor*. *Gene*. 2012;506(2):417–22.

268. Evstafieva AG, Kovaleva IE, Shoshinova MS, Budanov A v., Chumakov PM. Implication of KRT16, FAM129A and HKDC1 genes as ATF4 regulated components of the integrated stress response. *PLoS ONE*. 2018;13(2):e0191107.

269. Liloglou T, Walters M, Maloney P, Youngson J, Field JK. A T2517C polymorphism in the GSTM4 gene is associated with risk of developing lung cancer. *Lung cancer*. 2002;37(2):143–6.

270. Dyson JM, Fedele CG, Davies EM, Mitchell CA. Phosphoinositide phosphatases: Just as important as the kinases. *Subcell Biochem*. 2015;58:215–79.

271. Lee EY, Lee ZH, Song YW. The interaction between CXCL10 and cytokines in chronic inflammatory arthritis. *Autoimmun Rev*. 2013 Mar;12(5):554–7.

272. Liu X, Yang L, Jiang D, Lu W, Zhang Y. Circ-DENND4C up-regulates TCF4 expression to modulate hepatocellular carcinoma cell proliferation and apoptosis via activating Wnt/β-catenin signal pathway. *Cancer Cell Int*. 2020;20:295.

273. Wilczyński B, Dąbrowska A, Saczko J, Kulbacka J. The role of chloride channels in the multidrug resistance. *Membranes (Basel)*. 2022;12(1):38.

274. Sugiyama Y, Fujiwara M, Sakamoto A, Tsushima H, Nishikimi A, Maruyama M. The immunosenescence-related factor DOCK11 is involved in secondary immune responses of B cells. *Immun Ageing*. 2022;19(1):2.

275. Redondo JA, Bibes R, Drubbel AV, Dassy B, Bisteau X, Maury E, et al. Per2 circadian oscillation sensitizes esophageal cancer cells to chemotherapy. *Biology (Basel)*. 2021;10(4):266.

276. Katso RM, Pardo OE, Palamidessi A, Franz CM, Marinov M, de Laurentiis A, et al. Phosphoinositide 3-kinase C2β regulates cytoskeletal organization and cell migration via Rac-dependent mechanisms. *Mol Biol Cell*. 2006;17(9):3729–44.

277. Desbuquois B, Carré N, Burnol AF. Regulation of insulin and type 1 insulin-like growth factor signalling and action by the Grb10/14 and SH2B1/B2 adaptor proteins. *FEBS J*. 2013;280(3):794–816.

278. Sun W, Wang Y, Zheng Y, Quan N. The emerging role of sestrin2 in cell metabolism, and cardiovascular and age-related diseases. *Aging Dis*. 2020;11(1):154–63.

279. Kim SW, Kim DH, Park KS, Kim MK, Park YM, Muallem S, et al. Palmitoylation controls trafficking of the intracellular Ca2+ channel MCOLN3/TRPML3 to regulate autophagy. *Autophagy*. 2019;15(2):327–40.

280. Kühne A, Gilsdorf A. Infectious disease outbreaks in centralized homes for asylum seekers in Germany from 2004–2014. *Bundesgesundheitsblatt Gesundheitsforschung Gesundheitsschutz*. 2016;59(5):570–7.

281. Soerensen C, Pallesen K, Munk N, Vestergaard C. Eleven Danish patients diagnosed with Scabies and treated with Tenutex. *Clin Case Rep*. 2021;9(3):1688–90.

282. Elsner E, Uhlmann T, Krause S, Hartmann R. Increase of scabies and therapy resistance among German military personnel: An 8-year follow-up study in the Department of Dermatology of the Armed Forces Hospital Berlin, Germany (2012–2019). *Hautarzt*. 2020;71(6):447–54.

283. Mang R, Kremer A, Lehmann P, Assmann T. Scabies—clinical resistance to permethrin therapy: Case reports and a critical discussion of current treatment recommendations. *Hautarzt*. 2021;72(7):595–9.

284. Meyersburg D, Kaiser A, Bauer JW. Loss of efficacy of topical 5% permethrin for treating scabies: an Austrian single-center study. *J Dermatol Treat*. 2022;33(2):774–7.

285. Killoy KM, Harlan BA, Pehar M, Vargas MR. NR1D1 downregulation in astrocytes induces a phenotype that is detrimental to cocultured motor neurons. *FASEB J*. 2022;36(4):e22262.

286. Lacey A, Hedrick E, Cheng Y, Mohankumar K, Warren M, Safe S. Interleukin-24 (IL24) is suppressed by PAX3-FOXO1 and is a novel therapy for rhabdomyosarcoma. *Mol Cancer Ther*. 2018;17(12):2756–66.

287. Itoh T, Fujita N, Kanno E, Yamamoto A, Yoshimori T, Fukuda M. Golgi-resident small GTPase Rab33B interacts with Atg16L and modulates autophagosome formation. *Mol Biol Cell*. 2008;19(7):2916–25.

288. Semple JI, Smits VAJ, Fernaud JR, Mamely I, Freire R. Cleavage and degradation of Claspin during apoptosis by caspases and the proteasome. *Cell Death Differ*. 2007;14(8):1433–42.

289. Penninkhof F, Grootegoed JA, Blok LJ. Identification of REPS2 as a putative modulator of NF-κB activity in prostate cancer cells. *Oncogene*. 2004;23(33):5607–15.

290. Stein GS, Stein J 1, van Wijnen AJ, Lian JB. Regulation of histone gene expression. *Curr Opin Cell Biol*. 1992;4:166–73.

291. Tomimatsu N, Mukherjee B, Harris JL, Boffo FL, Hardebeck MC, Potts PR, et al. DNA-damage-induced degradation of EXO1 exonuclease limits DNA end resection to ensure accurate DNA repair. *J Biol Chem*. 2017;292(26):10779–90.

292. Rathore R, Schutt CR, van Tine BA. PHGDH as a mechanism for resistance in metabolically-driven cancers. *Cancer Drug Resist*. 2020;3(4):762–74.

293. Penning TM. The aldo-keto reductases (AKRs): Overview. *Chem Biol Interact*. 2015;234:236–46.

294. Decker M, Arand M, Cronin A. Mammalian epoxide hydrolases in xenobiotic metabolism and signalling. *Arch Toxicol*. 2009;83(4):297–318.

295. Qian L, Cantrell FL. Disulfiram. In: Encyclopedia of Toxicology: Third Edition. Elsevier; 2014. p. 208–9.

296. Shirley DA, Sharma I, Warren CA, Moonah S. Drug repurposing of the alcohol abuse medication disulfiram as an anti-parasitic agent. *Front Cell Infect Microbiol*. 2021;11:633194.

297. Sheppard JG, Frazier KR, Saralkar P, Hossain MF, Geldenhuys WJ, Long TE. Disulfiram-based disulfides as narrow-spectrum antibacterial agents. *Bioorganic Med Chem Lett*. 2018;28(8):1298–302.

298. Barth KS, Malcolm RJ. Disulfiram: An old therapeutic with new applications. *CNS Neurol Disord Drug Targets*. 2010;9(1):5–12.

299. Liegner KB. Disulfiram (Tetraethylthiuram disulfide) in the treatment of lyme disease and babesiosis: Report of experience in three cases. *Antibiotics*. 2019;8(2):doi: 10.3390/antibiotics8020072.

ANNEX I: Human Thrombopoietin Receptor gene sequence

ATGCCCTCCTGGGCCCTCTTCATGGTCACCTCCTGCCTCCTCCTGGCCCCTCAAAACCTGGCCCAAGTCA
GCAGCCAAGATGTCTCCTTGCTGGCATCAGACTCAGAGCCCCTGAAGTGTTTCTCCCGAACATTTGAGG
ACCTCACTTGCTTCTGGGATGAGGAAGAGGCAGCGCCCAGTGGGACATACCAGCTGCTGTATGCCTAC
CCGCGGGAGAAGCCCCGTGCTTGCCCCCTGAGTTCCCAGAGCATGCCCCACTTTGGAACCCGATACGTG
TGCCAGTTTCCAGACCAGGAGGAAGTGCGTCTCTTCTTTCCGCTGCACCTCTGGGTGAAGAATGTGTTC
CTAAACCAGACTCGGACTCAGCGAGTCCTCTTTGTGGACAGTGTAGGCCTGCCGGCTCCCCCCAGTATC
ATCAAGGCCATGGGTGGGAGCCAGCCAGGGGAACTTCAGATCAGCTGGGAGGAGCCAGCTCCAGAAA
TCAGTGATTTCCTGAGGTACGAACTCCGCTATGGCCCCAGAGATCCCAAGAACTCCACTGGTCCCACGG
TCATACAGCTGATTGCCACAGAAACCTGCTGCCCTGCTCTGCAGAGGCCTCACTCAGCCTCTGCTCTGG
ACCAGTCTCCATGTGCTCAGCCCACAATGCCCTGGCAAGATGGACCAAAGCAGACCTCCCCAAGTAGA
GAAGCTTCAGCTCTGACAGCAGAGGGTGGAAGCTGCCTCATCTCAGGACTCCAGCCTGGCAACTCCTA
CTGGCTGCAGCTGCGCAGCGAACCTGATGGGATCTCCCTCGGTGGCTCCTGGGGATCCTGGTCCCTCCC
TGTGACTGTGGACCTGCCTGGAGATGCAGTGGCACTTGGACTGCAATGCTTTACCTTGGACCTGAAGA
ATGTTACCTGTCAATGGCAGCAACAGGACCATGCTAGCTCCCAAGGCTTCTTCTACCACAGCAGGGCAC
GGTGCTGCCCCAGAGACAGGTACCCCATCTGGGAGAACTGCGAAGAGGAAGAGAAAACAAATCGAAG
AGAAAACAAATCCAGGACTACAGACCCCACAGTTCTCTCGCTGCCACTTCAAGTCACGAAATGACAGCA
GGACTACAGACCCCACAGTTCTCTCGCTGCCACTTCAAGTCACGAAATGACAGCATTATTCACATCCTTG
TGGAGGTGACCACAGCCCCGGGTACTGTTCACAGCTACCTGGGCTCCCCTTTCTGGCATTATTCACATCC
TTGTGGAGGTGACCACAGCCCCGGGTACTGTTCACAGCTACCTGGGCTCCCCTTTCTGGATCCACCAGG
CTGTGCGCCTCCCCACCCCAAACTTGCACTGGAGGGAGATCTCCAGTGGGCATCTGGAATTGATCCACC
AGGCTGTGCGCCTCCCCACCCCAAACTTGCACTGGAGGGAGATCTCCAGTGGGCATCTGGAATTGGAG
TGGCAGCACCCATCGTCCTGGGCAGCCCAAGAGACCTGTTATCAACTCCGATAGAGTGGCAGCACCCA
TCGTCCTGGGCAGCCCAAGAGACCTGTTATCAACTCCGATACACAGGAGAAGGCCATCACAGGAGAAG
GCCATCAGGACTGGAAGGTGCTGGAGCCGCCTCTCGGGGCCCGAGGAGGGACCCTGGAGCTGCGCCC
GCGATCTCGCAGGACTGGAAGGTGCTGGAGCCGCCTCTCGGGGCCCGAGGAGGGACCCTGGAGCTGC
GCCCGCGATCTCGCTACCGTTTACAGCTGCGCGCCAGGCTCAACGGCCCCACCTACCAAGGTCCCTGGA
GCTCGTGGTCGGACCCCTACCGTTTACAGCTGCGCGCCAGGCTCAACGGCCCCACCTACCAAGGTCCCT
GGAGCTCGTGGTCGGACCCAACTAGGGTGGAGACCGCCACCGAGACCGCCTGGATCTCCTTGGTGACC
GCTCTGCATCTAGTGCTGGGCCTAACTAGGGTGGAGACCGCCACCGAGACCGCCTGGATCTCCTTGGT
GACCGCTCTGCATCTAGTGCTGGGCCTCAGCGCCGTCCTGGGCCTGCTGCTGCAGCGCCGTCCTGGGCC
TGCTGCTGCTGAGGTGGCAGTTTCCTGCACACTACAGGAGACTGAGGCATGCCCTCTGAGGTGGCAGT
TTCCTGCACACTACAGGAGACTGAGGCATGCCCTGTGGCCCTCACTTCCAGACCTGCACCGGGTCCTAG

GCCAGTACCTTAGGGACACTGCAGCCCTGAGCCCGCCGTGGCCCTCACTTCCAGACCTGCACCGGGTCC

TAGGCCAGTACCTTAGGGACACTGCAGCCCTGAGCCCGCCCAAGGCCACAGTCTCAGATACCTGTGAA

GAAGTGGAACCCAGCCTCCTTGAAATCCTCCCCAAGTCCTCAGACAAGGCCACAGTCTCAGATACCTGT

GAAGAAGTGGAACCCAGCCTCCTTGAAATCCTCCCCAAGTCCTCAGAGAGGACTCCTTTGCCCCTGTGT

TCCTCCCAGGCCCAGATGGACTACCGAAGATTGCAGCCTTCTTGAGGACTCCTTTGCCCCTGTGTTCCTC

CCAGGCCCAGATGGACTACCGAAGATTGCAGCCTTCTTGCCTGGGGGCCTGGGGACCATGCCCCTGTC

TGTGTGCCCACCCATGGCTGAGTCAGGGTCCTGCTGTACCACCCACATTGCCAACCATTACCATGCCCCT

GTCTGTGTGCCCACCCATGGCTGAGTCAGGGTCCTGCTGTACCACCCACATTGCCAACCATTCCTACCTA

CCACTAAGCTATTGGCAGCAGCCTTGACCTACCTACCACTAAGCTATTGGCAGCAGCCTTGA

ANNEX II: The efficacy and biopharmaceutical properties of a fixed-dose combination of disulfiram and benzyl benzoate (Submitted to International Journal of Molecular Sciences)

Article

The efficacy and biopharmaceutical properties of a fixed-dose combination of disulfiram and benzyl benzoate

Maria Lajarin-Reinares [1,2], Elia Martinez Esteve [2], Eloy Pena-Rodríguez [2], Mariona Cañellas-Santos [3], Sanja Bulutd, Kostas Karabelas [4], Adam Clauss [4], Carles Nieto [2], Mireia Mallandrich [5], and Francisco Fernandez-Camposb [2,*]

Citation: Lastname, F.; Lastname, F.; Lastname, F. Title. *Int. J. Mol. Sci.* **2022**, *23*, x. https://doi.org/10.3390/xxxx

Academic Editor: Firstname Lastname

Received: date
Accepted: date
Published: date

Publisher's Note: MDPI stays neutral with regard to jurisdictional claims in published maps and institutional affiliations.

[1] Department of Genetics and Microbiology, Campus Microbiology Unit, Autonomous Barcelona University, Barcelona Spain
[2] Topical & Oral development R+D Reig Jofre Laboratories, Barcelona, Spain
[3] Biotechnology Department R+D Reig Jofre Laboratories, Barcelona, Spain
[4] Department of Product Development, Bioglan AB, Malmö, Sweden.
[5] Department of Pharmacy, Pharmaceutical Technology and Physical Chemistry, School of Pharmacy and Food Sciences, University of Barcelona, Barcelona, Spain.
* Correspondence: ffernandez@reigjofre.com; Tel.: (+34-935-507-718)

Abstract: Scabies and hair lice are parasitic diseases that affect human skin and hair, respectively. The incidence of infections is increasing, as well as the number of reported cases of resistance to current treatments such as permethrin. Tenutex®, a fixed-dose combination of disulfiram and benzyl benzoate emulsion, is available on the market in some European countries and is an interesting alternative to standard insecticides due to its unique combination of two active ingredients, providing a chance to avoid or delay resistance to treatment. Although the product has been available for many years, transdermal absorption and in vitro efficacy have not been reported previously. The dermal absorption of the emulsion active ingredients was evaluated, and only benzyl benzoate was found in the receptor compartment. An ex vivo anti scabies study demonstrated that exposure for 6 or 24 h completely eradicated the parasite. The in vitro pediculicidal activity showed superior efficacy against double-resistant (permethrin and malathion) strains. The positive results obtained here suggest that Tenutex® is a good treatment option, especially in situations where drug resistance has been encountered with other drugs.

Keywords: disulfiram; benzyl benzoate; skin permeation; topical medication; antiparasitic agents; scabies; lice.

1. Introduction

Scabies is a superficial skin disease caused by *Sarcoptes scabiei* mites. It is a world-wide infection, estimated to affect from 130 million [1] to 300 million [2] people per year. Other authors estimated the global prevalence at 0.2–70%, depending on the geographical location [3]. It spreads easily in crowded areas (including elderly care homes and military environment) and those with poor sanitation; due to migration pressure, cases are increasing in developed countries [4]. The parasites produce tunnels under the skin with erythematous and pruritic lesions, which could present as pustules, vesicles, and nodules. Furthermore, scratching of pruritic lesions can lead to bacterial infection (*Staphylococcus aureus* and *Streptococcus pyogenes*), which further worsens the pathology [3]. Skin symptoms usually appear four weeks after the primary infection, together with unspecific signs (discomfort, eruptions, eczema, etc.), common to other skin diseases. Furthermore, the frequent low number of adult parasites present on the skin makes diagnosis difficult; microscopic observation of parasite eggs and/or feces is usually required [5]. *Sarcoptes* are usually observed in skin folds (i.e., fingers, arms, wrist, genital area, axillae) and around the trunk in general. The neck and face are not usually affected in adults but could be affected in infants [6]. The entire life cycle of the mite occurs in humans. Adult individuals' mate on the skin surface and females lay their eggs in skin burrows within the stratum corneum. After 2–3 weeks, eggs hatch into larvae that after several days transform into nymphs (with two developmental stages, the protonymph and tritonymph) that will eventually become adults. The development time from egg to adult can be up to 21 days, and the adult life span ranges from 26 to 40 days [7].

Several hygiene measures should be considered to reduce the recurrence and spread of the infection, e.g., the treatment of sexual partners and washing clothes and bedsheets at high temperatures [6]. Apart from these precautions, there are several pharmacological treatments to eradicate mites, generally insecticides that are given either topically or orally. Recommended treatments, according to the European Academy of Dermatology and Venereology [8], include topical permethrin (5% cream) or benzyl benzoate lotion (10–25%), or oral treatment with ivermectin. As an alternative treatment, the topical administration of malathion, ivermectin, sulfur, or synergized pyrethrin has been suggested. Other remedies to treat scabies include topical treatment with crotamiton, monosulfiram, and lindane. The more severe form of infestation, crusted scabies, occurring mainly in immune-compromised patients, requires a combination of topical scabicides and oral ivermectin. The gold standard of pharmacological treatment of scabies is topical 5% permethrin. Treatment usually consists of a single dose, covering the entire body surface except the face. It is a multidose regimen, i.e., one dose per day for five days, or two single doses separated by one week, obtaining, in most cases, the complete eradication of the disease and very good tolerance [3].

Drug resistance has not been widely studied; however, it has been described in literature [7]. There is increasing evidence of drug resistance and several case studies report lower-than-expected topical permethrin effectiveness [9-13]. Thus, the availability of alternative treatments is of increasing concern.

Pediculus humanus var. *capitis*, commonly known as hair lice, is an ectoparasite that infests the human scalp. It feeds from blood from the infestation site. Female lice produce eggs that attach to the hair and hatch in approximately one week. Within 7–10 days after hatching, the nymph

becomes an adult that can live up to approximately 30 days [14]. Pediculosis, or infestation by *Pediculus humanus*, usually affects up to 13% of children 5–13 years old. Although it is not a severe disease, it is bothersome and can cause irritation, itching, social rejection, school access limitations, and a secondary skin infection due to scratching—for example, pyoderma by *Streptococcus* or *Staphylococcus spp* [15)]. The main principles for the treatment of head lice include the use of noninsecticide agents, insecticide agents, and wet combing. In many European countries, the use of noninsecticide agents has become the treatment of choice and has overtaken insecticide-based products, probably due to safety concerns and increasing drug resistance [16]. Noninsecticide pediculicides have a physical mode of action, coating the lice and causing them to die by suffocation and/or dehydration. Most noninsecticide products contain either synthetic silicon oils such as dimeticones, or isopropyl myristate or 1,2-octanediol as active ingredients.

The heavy use of neurotoxic insecticides as pediculicides has led to the emergence and spread of drug resistance in many parts of the world [17]. For example, resistance to permethrin has been reported, and the success rate of permethrin as a pediculicide in some parts of the UK is only 30–40%. The reported frequency of permethrin-resistant head lice is extremely high in Denmark [18, 19]. Resistance to malathion has been reported in Denmark, France, the UK, and Australia, although resistance to malathion seems to be less common compared to pyrethroids [19-22]. Double resistance to permethrin and malathion in head lice has also been documented among school children in the UK [21]. Resistance to lindane is well known from many countries and has been reported for many years [23, 24]. Resistance to insecticides is linked to a reduction in the sensitivity of drugs due to genetic mutations in the target genes, P-glycoprotein mediated efflux, and the increased metabolic activities of enzymes such as esterases, cytochrome P450, and glutathione S-transferase [25].

Tenutex® is a cutaneous emulsion consisting of a combination of benzyl benzoate (BB) (22.5%) and disulfiram (D) (2.0%) that has been registered in Sweden since 1982 and in Iceland since 1997 for the treatment of scabies and pediculosis (head lice, crab lice) in adults and children [26, 27]. Thus, the use of this product is geographically restricted today. Both active substances in Tenutex®, benzyl benzoate and disulfiram, have been used individually to treat lice and scabies. Benzyl benzoate is a well-known antiparasitic agent used in many countries to treat lice and scabies, and it is one of the recommended treatments in the European guidelines for the management of scabies [8]. Disulfiram was the active compound in Tenurid, a historical product that was registered in Sweden until 1957 for the treatment of lice and scabies [28]. Disulfiram has been classically used orally as an aldehyde dehydrogenase inhibitor to support alcoholism dishabituation because it produces an increase of acetaldehyde in the blood, leading to patient discomfort, known as the antabuse reaction [29]. In addition, disulfiram exhibits another mechanism of action, as a chelating agent, with alteration of the cell redox profile and antiproliferative activity, and potential indications as an antimicrobial [30, 31] or anticancer [32, 33] agent.

The geographically restricted use of Tenutex® and the fact that the product contains two active ingredients may be opportunities to avoid or delay resistance to treatment [13]. Although Tenutex® is a well-established drug in Sweden, its biopharmaceutical properties such as skin absorption and its in vitro effects on scabies have yet to be described in the literature,

while in vitro effects on human head lice were reported in the early 1980s [34].

The aim of this study is to characterize the skin absorption profile of Tenutex® cutaneous emulsion and to study its in vitro efficacy against scabies and human head lice resistant to common insecticides. Since human scabies mites are not easily accessed, tests were performed using sheep scabies (*Psoroptes ovis*) mites as proxy. In addition, the effect of emulsion exposure time on scabies was tested.

2. Results and Discussion

2.1. Analytical method validation

A high-performance liquid chromatography (HPLC) method for the simultaneous analysis of D and BB in samples from the in vitro permeation test was validated according to the ICH Q2 guidelines. Figure 1 is a representative chromatogram of an analytical standard in the receptor medium at a concentration of 31.7 µg/mL for D and 356.5 µg/mL for BB. The method's specificity was confirmed by the lack of an interfering peak at the retention times of both drug standards (diluted in mobile phase) after the injection of a receptor medium blank and excipients of BB/D emulsion (diluted in mobile phase and in the receptor medium). The stability of the drug solution in the HPLC injector was evaluated for 48 h at 25 ºC, being the difference in peak area between the two time points; if it is below 2%, then samples are considered stable for this period.

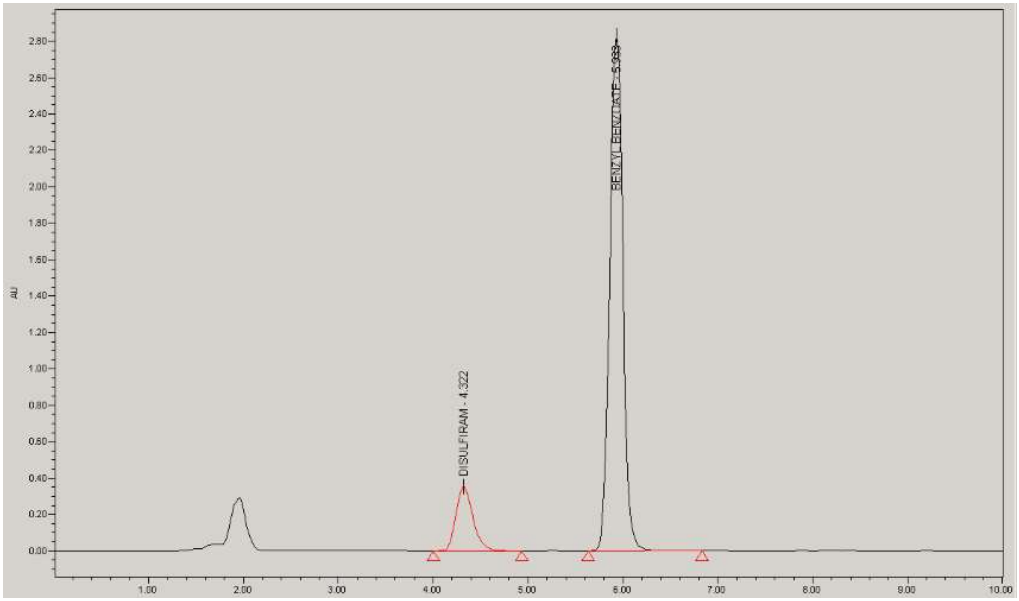

Figure 71: Chromatogram of an analytical standard in the receptor medium at a concentration of 31.7 µg/mL for D and 356.5 µg/mL for BB.

Linearity was assured at the analytical range, with an regression coefficient (r^2) value higher than 0.990. An acceptable coefficient of variation (CV) of response factor (relationship between response and concentration) was obtained (<10%) considering the high concentration range (3–4 log between the lower and higher concentration). There was a lack of tendency in residual plots. Finally, a significantly slope was found for the p-value of regression for both drugs (meaning the slope is significantly different from zero), with a nonsignificant p-value for the BB intercept (no statistical

difference between zero and the intercept) but a significant one with a borderline value of D (Table 1).

Table 47: Regression line for D and BB, range, slope, intercept, coefficient of variation (CV) of response factor, residual plot tendency, and regression coefficient. The distribution was assessed by an equal variance test, Levene's test ($\alpha = 0.05$).

Parameter		D	BB	Specification
Range		0.08–15.70 μg/mL	0.90–182.70 μg/mL	-
Linearity	**Slope**	137,322.71 ($p < 0.05$)	84,127.02 ($p < 0.05$)	$p < 0.05$
	Intercept	–7049.71 ($p = 0.04$)	–16,389.67 ($p > 0.05$)	$p > 0.05$
R^2		0.99980	0.99997	>0.990
CV response factor		8.71%	0.71%	<10%
Homoskedasticity (Levene's test)		$p = 0.31$	$p = 0.83$	$p > 0.05$
Residual plot		No tendency	No tendency	No tendency

Intermediate precision (Table 2 for D and Table 3 for BB) was used as a precision parameter since it had the highest variability (two different analyses on two different days), obtaining global mean values of 104.60% and 95.87% with variation coefficients of 2.61% and 4.01% for D and BB, respectively. Considering a threshold CV value of 6.71%, the method is deemed precise.

Table 48: Results of intermediate precision for disulfiram at three different concentration levels. Mean and CV values are reported.

Concentration level	Sample ID	Disulfiram		
0.08 μg/mL	Analyst 1 day 1	Mean: 101.20% CV = 2.52%	Mean: 103.12% CV = 3.03%	Mean: 104.60% CV: 2.61%
	Analyst 2 day 2	Mean:105.00% CV = 2.54%		
0.38 μg/mL	Analyst 1 day 1	Mean:104.20% CV = 1.92%	Mean: 103.95% CV = 1.37%	
	Analyst 2 day 2	Mean: 103.70% CV = 0.94%		
6.35 μg/mL	Analyst 1 day 1	Mean: 104.80% CV = 0.27%	Mean: 106.62% CV = 2.19%	
	Analyst 2 day 2	Mean: 108.40% CV = 1.84%		

Table 49: Results of intermediate precision for benzyl benzoate.

Concentration level	Sample Id.	Benzyl Benzoate		
0.89 μg/mL	Analyst 1 day 1 Analyst 2 day 2	Mean: 91.70% CV = 1.98% Mean: 90.30% CV = 1.81%	Mean: 91.02% CV = 1.88%	Mean: 95.80% CV = 4.01%
3.57 μg/mL	Analyst 1 day 1 Analyst 2 day 2	Mean: 96.30% CV = 0.37% Mean: 97.60% CV = 0.49%	Mean: 98.90% CV = 0.59%	
71.42 μg/mL	Analyst 1 day 1 Analyst 2 day 2	Mean: 104.80% CV = 0.27% Mean: 108.40% CV = 1.84%	Mean: 100.10% CV = 0.86%	

To calculate the accuracy, results from analysis 1 on day 1 were used (Tables 2 and 3). Global mean values of 103.40% for D and 95.60% for BB, with CV = 2.25% and 3.47% for D and BB, were obtained. Levene's test was carried out to confirm that no statistical differences were found between the concentration levels ($p > 0.05$ for D and BB), and the confidence interval of global percentage recovery was, in both cases, within the 90.0–110.0% range, showing that the method is accurate between the assayed concentration values.

Finally, the limit of quantification (LOQ) value was established at a concentration of 0.080 μg/mL for D and 0.8997 μg/mL for BB.

The analytical method could be considered successfully validated for the analysis of both drug substances in permeation experiments.

2.2. Human skin permeation

An ex vivo permeation experiment with dermatomed human skin (two different skin donors) was used to characterize the skin absorption profile of D and BB in vertical diffusion Franz cells. Before and after the experiment, the skin integrity was evaluated by measuring the transepidermal water loss (TEWL) value, in all samples and at both testing times; a value below 15 g/m^2h indicates that the skin maintains integrity. The drug dose evaluated corresponds to the prescribed therapeutic dose (approximately 3.65 mg/cm^2). According to the technical information available on Tenutex®, 60 g of the product should be applied to the entire body surface except the head, which is approximately 16,340 cm^2 [35]. The results are shown in Figure 2. Only BB was able to penetrate the skin; D was not detected in the chromatogram in any replicate at any time. The permeation parameters are listed in Table 4.

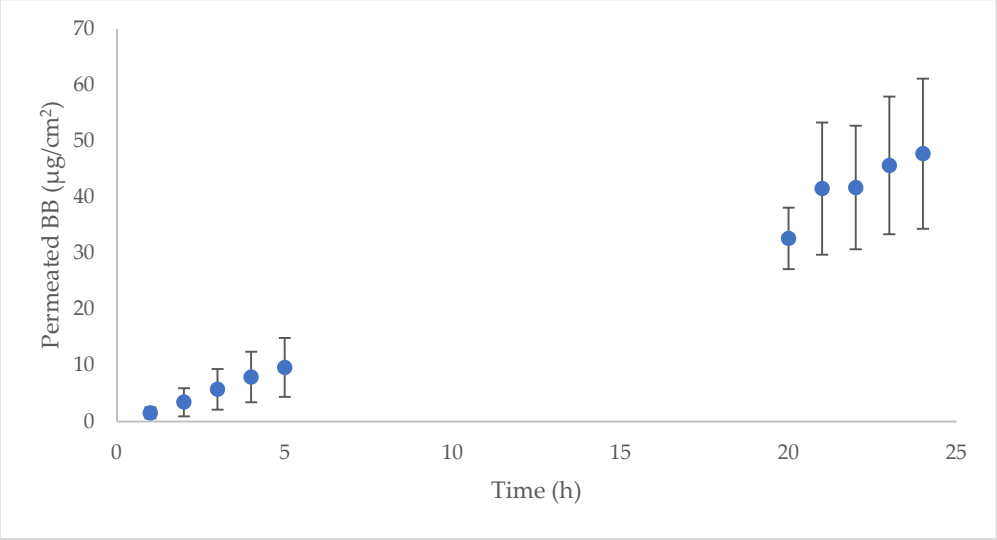

Figure 72: Permeation profile of BB in human skin (n = 9) after administration of 3.65 mg/cm² emulsion.

Table 50: Permeation parameters of benzyl benzoate in human skin.

	Mean	SD
Jsup (µg/h*cm²)	1.3014	0.3366
R^2	0.9963	0.0067
Kp (cm/h)	5.78E-06	1.50E-06
Tlag (h)	0.7755	0.7059
P (cm/h²)	3.5978E-05	1.3657E-05
Dif (1/h)	0.1252	0.0183

BB had a very good permeation profile, achieving steady state within the first hour after administration. This skin absorption is probably caused by the favorable physicochemical properties of the compound, according to the Lipinski rule of five [36]: low molecular weight (212.24 Da), logP value 3.9, low melting point (21 ºC), and fewer than five hydrogen bond donor and acceptors [37]. The high diffusion coefficient (Dif) revealed that drug diffusivity is the main absorption mechanism, and confirmed the permeability of BB. As previously described, BB has been classically used as a scabicide and was reported to have a good safety profile in its clinical use [5]. In addition, BB is a common ingredient in fragrances, and its safety was previously evaluated [38] and confirmed. Two previous studies [39, 40] studied the BB transdermal absorption (in a set of experiments to evaluate the transdermal absorption of compounds used in fragrances), but none of them studied the percutaneous kinetics or the transdermal flux. In addition, the different methodological approaches (dose applied, different vehicles, the use of occlusive material, in vitro or in vivo studies, etc.) in each study make it difficult to compare the results. Although D had good potential permeability, a molecular weight of 296 Da, log P of 3.88, melting point under 200 ºC (71.5 ºC), and fewer than five hydrogen bond donor and acceptors [41], there was no peak observed in any of the permeation samples' chromatograms. This may be due to the relatively low concentration of D in the emulsion (2%) compared with 22.5% BB.

Considering that D could cause several adverse effects if it is systemically available after oral administration (such as dermatological, neurological, hepatic, gastrointestinal, cardiac, and psychiatric events), mainly due to the inhibition of aldehyde dehydrogenase and dopamine beta hydroxylase [42], the lack of permeability is an advantageous property in terms of treatment safety. D would only be available on the outermost skin layer to develop its antiparasitic effect.

2.3. In vitro cytotoxicity evaluation

According to the human skin permeation results, BB was the only component that permeated. The first cells that would come in contact with BB would be skin keratinocytes, so cytotoxicity was tested in human-transformed keratinocyte (HEK001) cells. The concentration tested ranged between 0.305 and 5000 µM, which correspond to 0.647 and 1060 µg/mL, respectively. Seventy-two hours posttreatment, BB had no cytotoxic effect at any concentration (Figure 3).

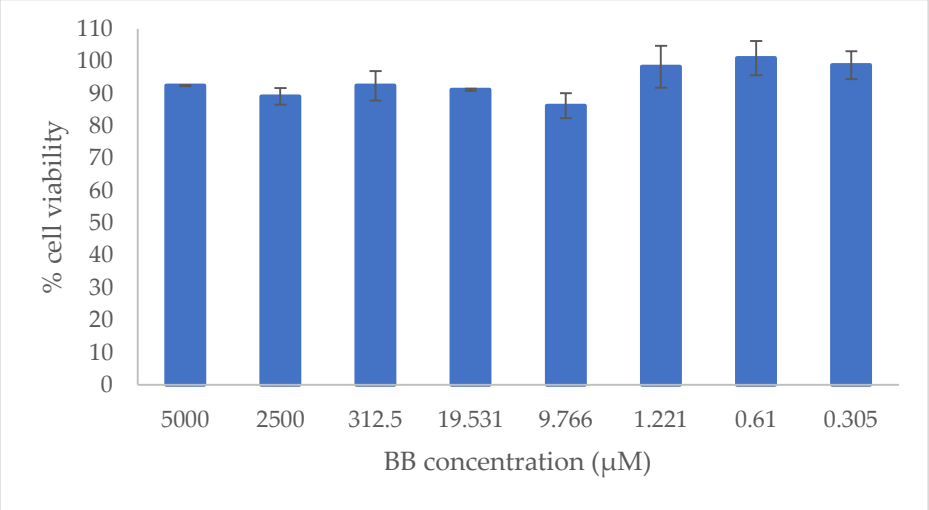

Figure 73: Cell viability 72 h posttreatment with BB. Results show the mean value ± standard deviation (SE).

In the range of concentrations tested, the cell viability was over 85%, with low variability (CV = 5.58%). Luminometric assay determined the number of viable cells in culture based on quantitation of the ATP present, which signals the presence of metabolically active cells [43].

2.4. In vitro and ex vivo efficacy against scabies.

Tenutex®, consisting of a BB/D emulsion (22.5% BB/2.0% D), was tested for acaricidal activity in sheep scabies mites in vitro, by exposing the mites directly to the drug emulsion, and via an indirect assay using skin sections excised from sheep. Thus, excised skin sections from sheep were exposed to the emulsion for different lengths of time and then washed off, followed by placing the mites on the skin sections; after incubation, the acaricidal activity was assessed. This ex vivo assay was considered to better mimic exposure to the drug after treatment in humans than the direct in vitro test on scabies mites, and it was used to compare with the current prescribed treatment of Tenutex®, which states that the emulsion should be applied to the skin for 24 h before rinsing it off [26].

In vitro study (Table 5). The mites exposed to the negative control were unaffected, with a 100% survival rate 24 h post-exposure. Mites exposed to the test product showed mortality rates of 100% at 1 h in both the thin- and thick-layer treatment.

Table 51: Mean percentage mortality across three replicates following exposure to Tenutex® emulsion or placebo. With incubation at 28 ºC with 75% relative humidity for 0, 1, 8, and 24 h.

Test solution	Mean % mortality			
	0 h	1 h	8 h	24 h
Placebo—thin layer (N = 91 mites)	0	0	0	0
Placebo—thick layer (N = 88 mites)	0	0	0	0
Tenutex emulsion—thin layer (N = 91 mites)	0	100	100	100
Tenutex emulsion—thick layer (N = 90 mites)	0	100	100	100

Ex vivo study. The efficacy of the Tenutex® emulsion after a 24-h exposure was demonstrated based on clinical evidence [27]. This long period of time with no possibility of rinsing could be inconvenient for the patient. In addition, sweat could remove some of the product. To test if a reduced exposure time is sufficient to obtain the desired efficacy, the pharmaceutical product was washed from the ex vivo skin surface after 10 min, 60 min, or 6 h after application.

Skin mites exposed to the test product for 10 min before washing showed an initially high level of mean mortality/unresponsiveness of 93.6% 1 h post-exposure. However, mites showed recovery at 8 hours and 24 hours post-exposure (34.2% and 5.8% mean mortality/unresponsiveness, respectively). The final 24-h mean mite mortality for the 10-min treatment was not significantly different to the mean mite mortality of the negative control ($p = 1.000$). A similar trend was observed in mites that had been exposed to skin sections that were treated for 60 min before washing. A mean mortality/unresponsiveness of 89.9% was observed 1 h postexposure; followed by 40.6% and 14.7% mean mortality/unresponsiveness at 8 and 24 h, respectively. The final 24-h mean mite mortality for the 1-h treatment was not significantly different from the mean mite mortality of the negative control ($x^2 = 0.410$, $df = 1$, $p = 0.529$) (Figure 4).

Mites exposed to skin sections treated for 6 h prior to washing showed 100% mean mortality/unresponsiveness at 1 h and 8 h post-exposure, and 98.8% mean mortality/unresponsiveness at 24 h post-exposure. The final 24-h mean mite mortality for the 6-h treatment was significantly different from the mean mite mortality of the negative control ($x^2 = 77.687$, $df = 1$, $p < 0.001$) (Figure 4).

The negative control (on skin section) showed mean mortalities/levels of unresponsiveness of 7.9%, 7.0%, 7.3%, and 8.3% at 1 h, 8 h, 24 h and 30 h post-exposure, respectively. The positive control on the skin showed 100% mean mortality/unresponsiveness at all time points (Fig. 4).

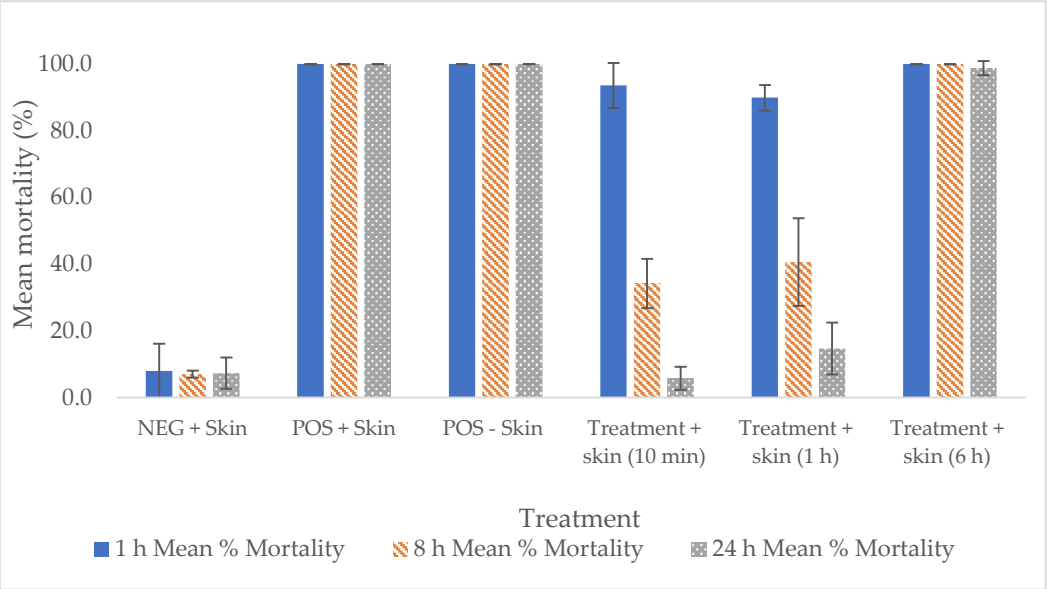

Figure 74: Mean (±S.E.) mortality/unresponsiveness of *P. ovis* mites exposed to the test compound in vitro ('–skin') or ex vivo ('+skin'), expressed as a percentage (%) of mites exposed (*n* = 3 replicates per treatment; *n* = 2 replicates per control). All treatments were incubated at 28 ºC and 75% HR at checked at 1, 8, and 24 h post-exposure. 'NEG + skin' = negative control on the skin section (*n* = 47–51 mites per replicate); 'POS + Skin' = positive control on skin section (*n* = 50–55 mites per replicate); 'POS – Skin = positive control on petri dish only (*n* = 50–53 mites per replicate); 'Treated + Skin (10 min)'= test compound in skin washed after 10 min (*n* = 47–52 mites per replicate); 'Treated + Skin (1 h)' = test compound on skin washed after 60 min (*n* = 46–52 mites per replicate); 'Treated + Skin (6 h)' = test compound in skin washed after 6 h (*n* = 46–56 mites per replicate).

Mites may need a minimum contact of 6 h with the product on the skin in order for us to obtain complete mortality. This fact could potentially be evaluated in a future clinical trial, but it is a promising result, and could facilitate patient compliance. For example, patients could apply the product at night before going to sleep, and on the following morning they could have a shower.

2.5. In vitro efficacy against adults and eggs of the human BH-RL strain of lice, resistant to both permethrin and malathion

Adulticidal efficacy: Following an 8-h incubation, BB/D emulsion resulted in an average mortality response (Figure 5) of 74% 10 min after the rinsing procedure; after 15 h, the value increased to 86% but the difference was not significant (t-test, $p < 0.05$).

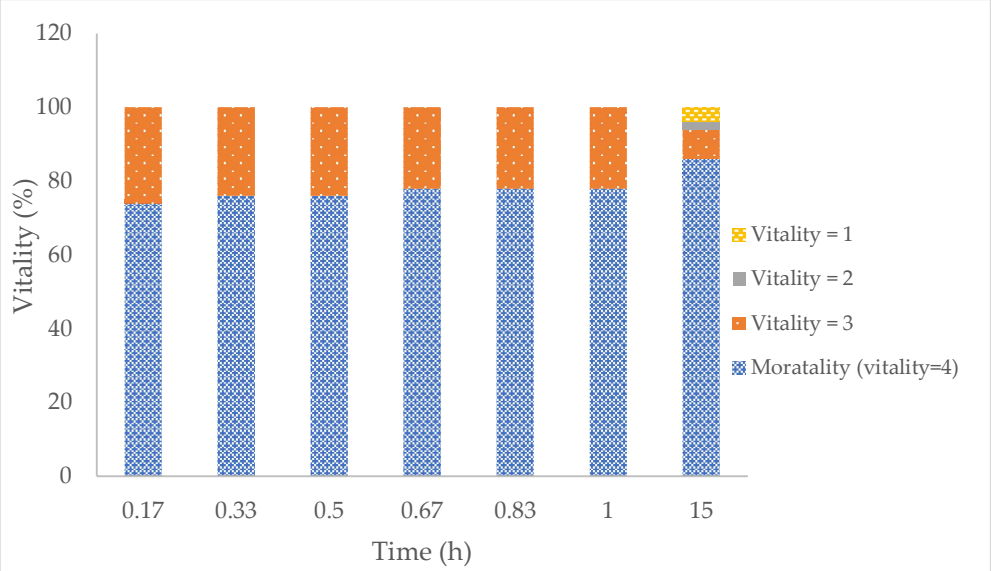

Figure 75: Percentage of young adults observed at a specific vitality classification after 8 h of incubation with Tenutex® emulsion. The treatment was replicated a total of five times, with five males and five females per replication (n = 10).

To show that the lice were resistant to permethrin, the same procedure was carried out with a commercial 1% permethrin product (Nix®) (Fig. 6). Ten minutes post-rinse, a 12% mortality response was obtained, and it remained the same for the following 7 h. After 10 h, there was a significant mortality increase, up to 55% ($p < 0.05$), and after 23 h the mortality response was 60%—not significant compared to the 10-h response. The vitality result for permethrin treatment showed a significantly lower pediculicidal effect compared to the BB/D treatment.

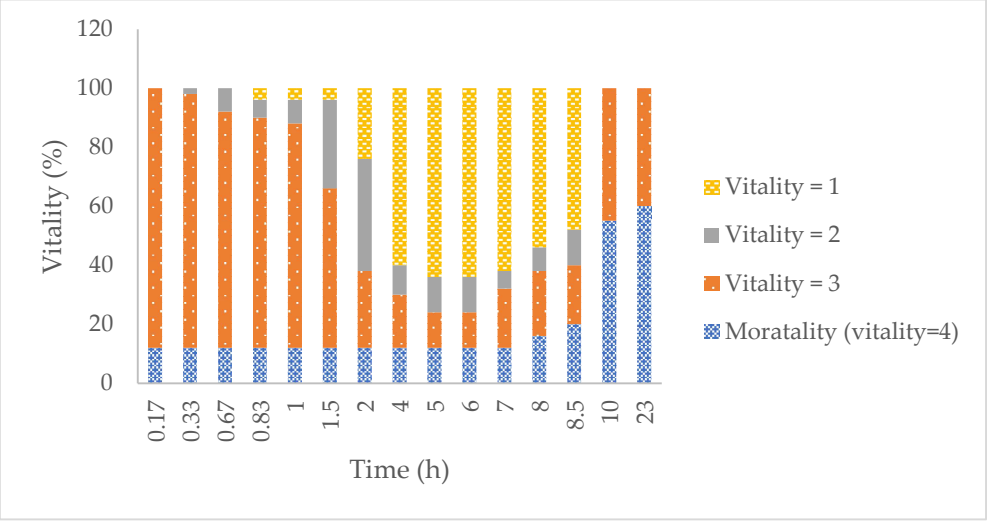

Figure 76: Percentage of young adults observed at specific vitality classification after 10 min of incubation with Nix®. Treatment was replicated a total of five times, with five males and five females per replicate (n = 10).

Finally, the negative control (distilled water) did not show mortality after 15 h and the mortality response increased to 2% after 23 h. This was significantly different from the Tenutex® and Nix® results. Under the

experimental conditions, the Tenutex® emulsion was significantly more toxic than Nix®.

Ovicidal efficacy: Table 6 shows the cumulative hatch rate after treatment with Tenutex® and the negative control (distilled water (ddH_2O)). Exposure to the test product for 1 h was not enough to obtain an adequate mortality rate (around 14–15% hatch after five days of follow-up). However, a single exposure to Tenutex® for 8 h produced a cumulative hatch rate of 0.2% (corresponding to only one hatch). Finally, exposure to the test product for 24 h achieved complete egg eradication. The egg hatch of the negative control was higher than 98% after exposure to water for 1 or 8 h. The survival of the negative control exposed for 24 h was 87%.

Table 52: Average % hatchability with standard deviation of eggs for three replicates following tuft submersion in either Tenutex or distilled water (the negative control) for 1, 8, or 24

	Average % Hatchability ± SD
Tenutex, 1 h	15 ± 18
ddH_2O, 1 h	96 ± 2
Tenutex, 8 h	0.2 ± 0.4
ddH_2O, 8 h	98 ± 1
Tenutex, 24 h	0 ± 0
ddH_2O, 24 h	87 ± 4

3. Materials and Methods

3.1. Materials

The Tenutex® emulsion, placebo, and drug substances (disulfiram and benzyl benzoate) were kindly gifted by Bioglan AB (Malmö, Sweden). Standard of disulfiram and benzyl benzoate (Sigma-Aldrich, Burlington, MA, USA) were used for validation of the analytical method. Methanol and KH_2PO_4 (Scharlab, S.L., Sentmenat, Spain) were used for the mobile phase. Phosphate-buffered saline (PBS) (Sigma-Aldrich) and hydroxypropyl–beta-cyclodextrin (HPCD) (Pracofar, S.L., Martorell, Spain) were used for the preparation of the receptor medium. Dimethyl sulfoxide (DMSO) (Sigma-Aldrich), Gibco keratinocyte medium with L-glutamine, and epidermal growth factor (EGF) (Thermo Fisher Scientific, Barcelona, Spain) were used for the cytotoxic evaluation.

3.2. *High-performance liquid chromatography quantification and validation of disulfiram and benzyl benzoate*

The simultaneous quantification of disulfiram and benzyl benzoate was carried out with HPLC-UV equipment (Water Alliance 2695, Cerdanyola del Vallès, Spain). Mobile phase (KH_2PO_4 1.7 mg/mL, pH 5.5: methanol (30:70 v/v)) flowed isocratically at 1.2 mL/min through a C18 column (4.6 x 150 mm, 3 μm, Thermo Scientific, Barcelona, Spain) kept at 30 ºC. The injection volume was 40 μL. The method validation was carried out according to the ICH Q2 guidelines. The analytical range was set from 0.080 to 15.85 μg/mL for D and from 0.0899 to 71.97 μg/mL for BB. The linearity, intermediate precision, and accuracy were studied within this range. In addition, the LOQ and solution stability in the HPLC autosampler were determined.

3.3. Ex vivo skin absorption experiment with human skin

Dermatomed human skin (approximately 0.5 mm thick), used in the ex vivo permeation test, was obtained from the abdominal region of two different woman during plastic surgery (Condalab, Madrid, Spain). Written consent was obtained from the skin donors. Permeation studies were performed in vertical Franz diffusion cells (VidraFoc, Barcelona, Spain) with a permeation area of 1.54 cm^2. BB/D emulsion (Tenutex®) was dosed in the donor compartment at an equivalent prescription dose (approximately 3.65 mg/cm^2). Skin was kept frozen at –20 ºC until use (six months maximum storage period). At the day of the experiment, skin was thawed at room temperature, and placed between the donor and receptor compartment of Franz cells. A 15% w/w HPCD solution in PBS (pH 5.5) was used as the receptor medium; to maintain sink conditions during the experiment, the temperature was kept at 32 ± 1 ºC, with continuous stirring at 700 rpm. Skin integrity was evaluated at the beginning and end of the experiment by TEWL measurement (Delfin Technologies, Kuopio, Finland). Samples from the receptor compartment (300 µL) were taken at regular time intervals up to 24 h and replenished with the same volume of fresh receptor medium. Samples were analyzed and quantified using the method described in the previous section.

After drug quantification, the following permeation parameters were calculated: the transdermal flux (J, $\mu g/cm^2h$) (Equation (1)), permeability coefficient (Kp, cm/h) (Equation (2)), lag time (tlag, h) (obtained by linear extrapolation of the x-axis of the points at steady state), diffusion parameter (Dif, 1/h) (Equation (3)) and partitioning parameter (P, cm/h^2) (Equation (4)).

$$J = \frac{dQ}{(dT \cdot S)}, \quad (1)$$

where J is the transdermal flux, dQ is the permeated amount differential, dT is the time differential, and S is the membrane diffusion surface.

$$Kp = \frac{J}{C_d}, \quad (2)$$

where Cd (µg/mL) is the concentration of the drug in the donor compartment.

$$Dif = \frac{1}{6T_{lag}}, \quad (3)$$

$$P = \frac{Kp}{D}, \quad (4)$$

3.4. In vitro cytotoxicity evaluation

Cell treatments (n = 6): human-transformed keratinocyte (CRL2404, ATCC, Manassas, VA, USA) cells were seeded in 96-well plates at 10,000 cells/well in 50 µL of medium (keratinocyte serum-free medium, supplemented with 2 mM L-glutamine and 5 ng/mL Epidermal Growth Factor (hEGF)). The cells were incubated at 37 ºC in a 5% CO_2, 95% air-humidified atmosphere for 24 h. After 24 h of incubation, the cells were treated with increasing doses of BB (0.305 to 5000 µM; a stock solution was prepared in DMSO and the final concentration of DMSO in the wells was below 1%). A medium with DMSO at 1%, sodium dodecyl sulfate at 10%, and a cell culture medium were used as the experimental control. The exposure period was 72 h.

At the end of the incubation time, cytotoxicity was evaluated using the CellTiter-Glo® Luminescent Cell Viability Assay (Dojindo Molecular

Technologies, Rockville, MD, USA). One hundred microliters of CellTiter-Glo® reagent were added directly to every well plate, cultured in serum-free medium and incubated for 10 min. The luminescence was measured immediately by a Victor X3 luminometer (Perkin Elmer, Waltham, MA, USA).

3.5. In vitro and ex vivo efficacy against scabies

To evaluate the in vitro and ex vivo efficacy of BB/D emulsion against scabies, *Psoroptes ovis* mites (sheep scabies) were selected as the model, since the ethical sourcing of human scabies is almost impossible.

One-year-old Scotch Mule lambs (n = 3) were infested with *P. ovis* mites and housed indoors for a period of six weeks. After that time, animals were sacrificed via an anesthetic overdose. The study protocol (1258/CC1406) was approved by the London School of Hygiene and Tropical Medicine ethics committee (reference 2020-07A, approval date: 26 May 2020). Skin sections (5 cm x 5 cm) were taken with a scalpel and deposited in a petri dish at room temperature to harvest live mobile mites. Once obtained, mites were washed with purified water on a 63-µm filter and dried with blotting paper and stored in an Eppendorf tube until the study (within 2 h).

In vitro study. Petri dishes were coated with a thin or thick layer of BB/D emulsion or the placebo. Collected mites were placed on corresponding dishes (20–30 mites per replicate and three replicates per condition) and incubated at 28 ºC/75% relative humidity (HR) for 1, 8, and 24 h. After this period, acaricidal activity was assessed by stereomicroscopic examination (mites were considered viable if any movement was observed).

Ex vivo study. Single sheep scab naïve was sacrificed and skin sections (4 cm x 4 cm) were excised with a scalpel and placed on a petri dish. Adult female mites were obtained from the collected mites previously described. Around 50 *P. ovis* mites were immediately applied to ex vivo skin sections (positive and negative control and test samples) and incubated at 28 ºC/75% HR. Two positive controls were used: product on petri dish (not washed off) with mites applied directly to the product, and product on skin (not washed off) with mites applied directly to the skin. The negative control was the skin with no product and mites applied directly to the skin. In the experimental condition, a thin layer of emulsion was applied to the skin and washed with purified water after 10 min, 1 h and 6 h after exposure. Acaricidal activity was assessed by microscopic examination after 1, 8, and 24 h.

3.6. In vitro efficacy against permethrin-resistant head lice and its eggs

To evaluate the efficacy of the BB/D emulsion against lice adults and eggs, permethrin- and malathion-resistant human head lice (*Pediculus humanis capitis*, BR-HL strain) were used [44, 45].

Blood-fed adults, half or fully engorged (n = 10; 5 males and 5 females), were transferred to hair tufts. Five milliliters of BB/D emulsion or distilled water (used as a negative control) were gently rubbed for 60 s and incubated at room temperature for 8 h. Then the tuft was washed with a commercial shampoo diluted at 5% (w/w) in distilled water for 60 s to remove the excess product and subsequently rinsed carefully with distilled water so as not to detach the adult lice. Finally, the hair was allowed to dry on filter paper and lice were examined for viability at different time points. A total of five replicates were carried out for each condition. Lice were classified as: 1 (living lice with no change in activity or behavior), 2 (lice with

minor changes in vital signs), 3 (lice with major changes in vital signs, i.e., not walking but gut, leg, and/or antennae movement present) and 4 (no vital signs at all). To validate that the lice were resistant to permethrin, the same study was conducted with a permethrin 1% commercial product (Nix ®) with observation for up to 23 h.

Eggs were obtained from female adults that were placed on a tuft of human hair and left until approximately 50 eggs were laid per hair tuft. Then the adults were removed. BB/D emulsion or distilled water (5 mL) was applied as previously described in the adult experiment. Incubation was carried out at room temperature in a dark fume hood for 1, 8, and 24 h. Then the hair tuft with the eggs was washed and rinsed as previously described. Dried tufts with the eggs were placed in a Petri dish and incubated at 31 ºC and 70–80% relative humidity. Egg viability (%hatchability) was evaluated for 11 days, according to (Equation 5). A total of three replicates was carried out.

% Hatchability = Number eggs hatched/total eggs oviposited * 100 (5)

3.7. Statistical analysis

To assess the in vitro efficacy against scabies, a survival curve analysis was performed on data using STATA (version 15.1) with a log rank (Mantel–Cox) test applied to compare survival curves.

To test ex vivo efficacy, a Chi-square test (or Fisher's exact test) was performed in R studio to compare the mean proportion of the negative control against each washing interval treatment after conducting a test of homogeneity between replicates.

4. Conclusions

An analytical method validation was successfully developed for the quantification of D and BB permeation studies and is fit for purpose. The permeation profiles for dermatomed human skin revealed fast permeation of BB and nonpermeation of D. Moreover, the cytotoxicity assay showed the noncytotoxic effect of BB and confirmed the safe topical use of this compound, together with the low adverse effects reported in the literature for this treatment.

The results of in vitro and ex vivo efficacy demonstrated that Tenutex® had a strong knockdown effect on P. ovis within 1 h of exposure on all the skin sections treated. However, on the skin sections treated for the shortest periods of time, mite recovery was observed over time. In contrast, mites exposed to the skin sections treated for 6 h before washing showed almost 100% mean mortality/unresponsiveness across all time points.

The in vitro efficacy studies against the adults and eggs of human lice showed that Tenutex was substantially adulticidal on the permethrin-resistant BR-HL strain following an 8-h exposure. Moreover, the product was 100% ovicidal following a 24-h exposure. The BB/D emulsion killed almost all of the lice eggs after an 8-h exposure (99.8%).

This study has provided more information on the efficacy, biopharmaceutical properties, and safety of Tenutex®, a cutaneous emulsion containing a fixed-dose combination of the active ingredients benzyl benzoate and disulfiram and used for the topical treatment of human scabies and lice. The balance of properties of this unique combination makes

Tenutex® a good treatment option, especially in situations where resistance to other drugs has been encountered.

Author Contributions: Conceptualization, E.M-E. and M.M; methodology, E.P.-R., F.F.-C and M.L.-R.; validation, F.F.-C.; formal analysis, E.P.-R and M.L.-R.; investigation, M.C-S, M.L.-R. and E.M.-E; resources, S.B, K.K. and M.M.; data curation, C.N.; writing—original draft preparation, M.L.-R and F.F.-C; writing—review and editing, A.C., K.K; visualization, M.L.-R; supervision, C.N. and K.K; project administration, F.F.-C. All authors have read and agreed to the published version of the manuscript.

Funding: This research received no external funding.

Institutional Review Board Statement: The animal study protocol (1258/CC1406) was approved by the London School of Hygiene and Tropical Medicine ethics committee (reference 2020-07A, approval date: 26 May 2020).

Informed Consent Statement: Not applicable.

Data Availability Statement: Not applicable.

Acknowledgments: Assistance provided by by Mari Carmen Moreno from Reig Jofre was greatly appreciated.

Conflicts of Interest: F.F.-C, E.P.-R, E.M.-E, M.C.-S and C.N are employees of Reig Jofre. A.C, K.K. and S.B., are employees of Bioglan AB. The authors are not involved in any commercial or marketing activities of the developed product.

References

1. Dressler, C., Rosumeck, S., Werner, R. N. & Nast, A. M E D I C I N E The Treatment of Scabies A Systematic Review of Randomized Controlled Trials. doi:10.3238/arztebl.2016.0757.
2. Fitzgerald, D., Grainger, R. J. & Reid, A. Interventions for preventing the spread of infestation in close contacts of people with scabies. Cochrane Database Syst. Rev. 2014, (2014).
3. Rosumeck, S., Nast, A. & Dressler, C. Ivermectin and permethrin for treating scabies. Cochrane Database Syst. Rev. 2018, (2018).
4. Kühne, A. & Gilsdorf, A. Infectious disease outbreaks in centralized homes for asylum seekers in Germany from 2004–2014. Bundesgesundheitsblatt - Gesundheitsforsch. - Gesundheitsschutz 59, 570–577 (2016).
5. Strong, M., Johnstone, P. & Group, C. I. D. Interventions for treating scabies. Cochrane Database Syst. Rev. 2007, (2007).
6. Gunning, K., College, U. & City, S. L. AAFP: Lice and Scabies. Am. Fam. Physician website 635–642 (2019).
7. Arlian, L. G. & Morgan, M. S. A review of Sarcoptes scabiei: past, present and future. Parasites Vectors 2017 101 10, 1–22 (2017).
8. Salavastru, C. M., Chosidow, O., Boffa, M. J., Janier, M. & Tiplica, G. S. European guideline for the management of scabies. J. Eur. Acad. Dermatology Venereol. 31, 1248–1253 (2017).
9. Mang, R., Kremer, A., Lehmann, P. & Assmann, T. Scabies—clinical resistance to permethrin therapy: Case reports and a critical discussion of current treatment recommendations. Hautarzt 72, 595–599 (2021).
10. Meyersburg, D., Kaiser, A. & Bauer, J. W. 'Loss of efficacy of topical 5% permethrin for treating scabies: an Austrian single-center study'. https://doi.org/10.1080/09546634.2020.1774489 (2020) doi:10.1080/09546634.2020.1774489.
11. Elsner, E., Uhlmann, T., Krause, S. & Hartmann, R. Increase of scabies and therapy resistance among German military personnel: An 8-year follow-up study in the Department of Dermatology of the Armed Forces Hospital Berlin, Germany (2012–2019). Hautarzt 71, 447–454 (2020).
12. Zargari, O., Aghazadeh, N. & Moeineddin, F. Clinical applications of topical ivermectin in dermatology. Dermatol. Online J. 22, (2016).
13. Soerensen, C. A. S., Pallesen, K. A. U., Munk, N. T. & Vestergaard, C. Eleven Danish patients diagnosed with Scabies and treated with Tenutex®. Clin. Case Reports 9, 1688–1690 (2021).
14. Pablo Màrquez, B. Actualización en pediculosis capitis. Med. Fam. Semer. 45, 128–133 (2019).
15. Leung, A. K. C., Fong, J. H. S. & Pinto-Rojas, A. Pediculosis capitis. J. Pediatr. Heal. Care 19, 369–373 (2005).
16. Salavastru, C. M., Chosidow, O., Janier, M. & Tiplica, G. S. European guideline for the management of pediculosis pubis. Journal of the European Academy of Dermatology and Venereology vol. 31 1425–1428 (2017).
17. Durand, R. et al. Insecticide resistance in head lice: clinical, parasitological and genetic aspects. Clin. Microbiol. Infect. 18, 338–344 (2012).
18. Burgess, I. F., Kay, K., Burgess, N. A. & Brunton, E. R. Soya oil-based shampoo superior to 0.5% permethrin lotion for head louse infestation. Med. Devices Evid. Res. 4, 35–42 (2011).
19. Kristensen, M., Knorr, M., Rasmussen, A.-M. & Jespersen, J. B. Survey of Permethrin and Malathion Resistance in Human Head Lice Populations from Denmark. J. Med. Entomol. 43, 533–538 (2006).
20. Izri, M. A. & Brière, C. Premiers cas de résistance de Pediculus capitis Linné 1758 au malathion en France. Presse médicale (Paris, France : 1983) vol. 24 1444 (1995).
21. Downs, A. M. R., Stafford, K. A., Harvey, I. & Coles, G. C. Evidence for double resistance to permethrin and malathion in head lice. Br. J. Dermatol. 141, 508–511 (1999).
22. Hunter, J. A. & Barker, S. C. Susceptibility of head lice (Pediculus humanus capitis) to pediculicides in Australia. Parasitol. Res. 90, 476–478 (2003).
23. Kucirka, S. A., Parish, L. C. & Witkowski, J. A. The Story of Lindane Resistance and Head Lice. Int. J. Dermatol. 22, 551–555 (1983).

24. Burgess, I. F., Brown, C. M., Peock, S. & Kaufman, J. Head lice resistant to pyrethroid insecticides in Britain. BMJ vol. 311 752 (1995).
25. Soderlund, D. M. & Knipple, D. C. The molecular biology of knockdown resistance to pyrethroid insecticides. Insect Biochemistry and Molecular Biology vol. 33 563–577 (2003).
26. Tenutex® - FASS Allmänhet.
27. Landegren, J., Borglund, E. & Storgards, K. Treatment of scabies with disulfiram and benzyl benzoate emulsion: a controlled study. Acta Derm. Venereol. 59, 274–276 (1979).
28. Tenurid - FASS Allmänhet.
29. Karamanakos, P. N. et al. Pharmaceutical agents known to produce disulfiram-like reaction: Effects on hepatic ethanol metabolism and brain monoamines. Int. J. Toxicol. 26, 423–432 (2007).
30. Frazier, K. R., Moore, J. A. & Long, T. E. Antibacterial activity of disulfiram and its metabolites. J. Appl. Microbiol. 126, 79–86 (2019).
31. Das, S., Garg, T., Chopra, S. & Dasgupta, A. Repurposing disulfiram to target infections caused by non-tuberculous mycobacteria. J. Antimicrob. Chemother. 74, 1317–1322 (2019).
32. Li, H. et al. The combination of disulfiram and copper for cancer treatment. Drug Discov. Today 25, 1099–1108 (2020).
33. Ekinci, E., Rohondia, S., Khan, R. & Dou, Q. P. Repurposing Disulfiram as An Anti-Cancer Agent: Updated Review on Literature and Patents. Recent Pat. Anticancer. Drug Discov. 14, 113–132 (2019).
34. Brinck-Lindroth, G., Lundqvist, L. & Nilsson, A. Control of the human head louse with disulfiram and benzyl benzoate emulsions. Acta Derm. Venereol. 64, 325–330 (1984).
35. SCCS Scientific committee on Consumer Safety. the Sccs Notes of Guidance for the Testing of Cosmetic Ingredients and Their Safety Evaluation 10 Th Revision - Sccs/1602/18. (2018).
36. Lipinski, C. A. Drug-like properties and the causes of poor solubility and poor permeability. J. Pharmacol. Toxicol. Methods 44, 235–249 (2000).
37. National Center for Biotechnology Information. Benzyl benzoate. PubChem Compound Summary for CID 2345 (2022).
38. Johnson, W. et al. Safety Assessment of Benzyl Alcohol, Benzoic Acid and its Salts, and Benzyl Benzoate. Int. J. Toxicol. 36, 5S–30S (2017).
39. Jimbo, Y. Penetration of fragrance compounds through human epidermis. J. Dermatol. 10, 229–239 (1983).
40. Bronaugh, R. L., Wester, R. C., Bucks, D., Maibach, H. I. & Sarason, R. In vivo percutaneous absorption of fragrance ingredients in rhesus monkeys and humans. Food Chem. Toxicol. 28, 369–373 (1990).
41. National Center for Biotechnology Information. Disulfiram: Chemical and physical properties. PubChem Compd. Summ. CID 3117 (2022).
42. Qian, L. & Cantrell, F. L. Disulfiram. Encycl. Toxicol. Third Ed. 208–209 (2014) doi:10.1016/B978-0-12-386454-3.00725-9.
43. Niles, A. L., Moravec, R. A. & Riss, T. L. In Vitro Viability and Cytotoxicity Testing and Same-Well Multi-Parametric Combinations for High Throughput Screening. Curr. Chem. Genomics 3, 33 (2009).
44. Yoon, K. S. et al. An improved in vitro rearing system for the human head louse allows the determination of resistance to formulated pediculicides. Pestic. Biochem. Physiol. 86, 195–202 (2006).
45. Gao, J. R., Yoon, K. S., Frisbie, R. K., Coles, G. C. & Clark, J. M. Esterase-mediated malathion resistance in the human head louse, Pediculus capitis (Anoplura: Pediculidae). Pestic. Biochem. Physiol. 85, 28–37 (2006).